"AN ANALYTICAL APPROACH TO THE DESIGN OF PILLARS IN COAL"

Part 2: Application of the Model to Case Histories

FINAL REPORT, PHASE 2
BY

K. Barron

Work on this project was carried out under the auspices of the Canada Centre for Mineral and Energy Technology, Energy, Mines and Resources, Canada

D.S.S. File # 18 SQ 23440-0-9106

D.S.S. Contract Serial # ISQ 80 - 00161

Canmet Project # 334-101

Canmet Scientific Authority: Dr. D.F.G. Hedley

March 1983

220 pp

MICROMEDIA
OCT 20 1983

SUMMARY

In the Phase 1 report an analytical model was developed to determine the development of fracture zones in coal pillars, the stress distribution across pillars and the strength of coal pillars. This report considers the experimental data in the literature on coal pillars and attempts to use the model to "predict" these experimental results.

It is shown that the analytical model will give a good fit to the results of all, except one, of the fourteen case histories considered from the literature provided that a judicous choice is made for the values of the input parameters for the solid and broken coal properties. Unfortunately the case histories did not give sufficient data to adequately define these required input properties, hence "typical" estimated values had to be used for some of these properties. In these circumstances therefore, although the model may give a good "prediction" of the field data, some doubt must remain as to the validity of the model because of this use of "typical" estimated rather than actual properties.

Very strong indirect evidence was obtained to indicate that the proposed brittle/pseudo-ductile failure theory developed in the Phase 1 report is applicable both to coal specimens and to coal pillars within the stress ranges normally encountered in coal mines. The evidence is, however, indirect and it is recommended that a "Phase 3" study be carried out; this would comprise a comprehensive specimen testing program aimed at giving direct proof of the validity of this failure theory. In addition such a testing program would give answers to some outstanding questions on size effects on various parameters.

Some modifications to the analytic model are recommended in order to improve the accuracy of the determination of the transition point for those cases where sufficient data is available.

It may therefore be concluded that the analytic model gives a good qualitative and quantitative description of coal pillar behaviour but its' total verification still requires further work as recommended.

TABLE OF CONTENTS

1. INTRODUCTION

2. DISCUSSION OF THE REQUIRED INPUT PARAMETERS FOR THE COAL STRENGTH PROGRAM

2.1 Analytical Expressions for Specimen Strength

2.2 Cube Strength-Size Relationships

2.3 Strength-Shape Relationships

  2.3.1 For specimens, as predicted by the analytical equations

  2.3.2 Comparison of the analytical results with the Hustrulid and Holland/Gaddy equations

  2.3.3 Conclusions with respect to strength/shape effects for specimens

2.4 Conclusions with Respect to Input Strengths for the Model

2.5 Input Values for μ_B, ϕ_B, and P_B

3. CASE HISTORIES OF RELEVANCE TO THE BRITTLE/PSEUDO-DUCTILE TRANSITION POINT

3.1 Case History #1: Peak and Post Peak (residual) Strengths of Pittsburgh Coal Specimens

  3.1.1 Case Background

  3.1.2 Mohr envelope in Balmer's parametric form

  3.1.3 Determination of the transition point

  3.1.4 Conclusions with respect to the transition point

  3.1.5 Notes on the residual stress envelope

  3.1.6 Determination of the coefficient of sliding friction, using the residual stress envelope

  3.1.7 Conclusions with respect to the residual stress envelope

  3.1.8 Errors caused by assuming a single parameter parabolic Mohr envelope

3.2 Case History #2: Strength Characteristics of Some Other U.S. Coals
  3.2.1 Case Background
  3.2.2 Case study results
  3.2.3 Discussion
  3.2.4 Conclusions

3.3 Case History #3: Strength Characteristics of a U.K. Muddy Siltstone
  3.3.1 Case Background
  3.3.2 Case study results
  3.3.3 Discussion
  3.3.4 Conclusion

3.4 Case History #4: Specimens that "Did Not Fail Abruptly"
  3.4.1 Case Background
  3.4.2 Critical $({}^{B}/{}_{H}) = \gamma_c$ ratio
  3.4.3 Calculations
  3.4.4 Conclusions

3.5 Conclusions with Respect to Brittle/Pseudo-Ductile Transition Point

3.6 Recommendations

4. CASE HISTORIES OF RELEVANCE TO THE STRESS DISTRIBUTION ACROSS PILLARS

4.1 Case History #5: Stress Measurements in Coal Pillars
  4.1.1 Case Background
  4.1.2 Elastic Solutions
  4.1.3 Pillar model solutions
  4.1.4 Discussion and conclusions

4.2 Case History #6: Stress Measurements in Coal Pillars
  4.2.1 Case Background
  4.2.2 Results
  4.2.3 Comparison of model solution with normal borehole results
  4.2.4 Conclusion
4.3 Conclusions with Respect to Case Histories for Pillar Stress Distribution

5. CASE HISTORIES OF RELEVANCE TO PILLAR STRENGTH FORMULAE
5.1 Case History #7: Salamon and Munro's Pillar Strength Formula
  5.1.1 Case Background
  5.1.2 Results
  5.1.3 Discussion
  5.1.4 Summary of the pillar strength formulae derived from the analytical model
  5.1.5 Comparison of the analytical pillar strength formulae with that of Salamon and Munro
5.2 Case History #8: Bieniawski's Strength Formula
  5.2.1 Case Background
  5.2.2 Comparison with the Analytical Model

5.3 Case History #9: The Holland/Gaddy Pillar Strength Formula
  5.3.1 Case Background
  5.3.2 Comparison with the analytic model

5.4 Case History #10: Wagner's Pillar Strength Formula
  5.4.1 Case Background
  5.4.2 Comparison with the analytic model

5.5 Discussion and Conclusions

6. CASE HISTORIES OF RELEVANCE TO FRACTURE ZONE DEVELOPMENT IN PILLARS

6.1 Case Background

6.2 Case History #11: Fracture Zone in a Pillar at Canmore Mine, Wilson Seam

6.3 Case History #12: Fracture Zone in Three Pillars at McIntyre #2 Mine, #4 Seam

6.4 Conclusions

7. CASE HISTORIES OF RELEVANCE TO PILLAR YIELDING

7.1 Case History #13: A Coal Pillar Strength Determination

- 7.1.1 Case Background
- 7.1.2 Discussion
- 7.1.3 Model Solution
- 7.1.4 Discussion and Conclusions

7.2 Case History #14: Stress Measurements in Coal Pillars

- 7.2.1 Case Background
- 7.2.2 Model Solution

7.3 Conclusions

8. CONCLUSIONS AND RECOMMENDATIONS

8.1 Conclusions

- 8.1.1 With respect to the input parameters
- 8.1.2 With respect to brittle/pseudo-ductile transition
- 8.1.3 Field case histories related to stress distribution across pillars
- 8.1.4 Field case histories related to pillar strength formulae
- 8.1.5 Field case histories related to fracture zone development in pillars

8.1.6 Field case histories related to pillar yielding
8.2 Recommendations

9. REFERENCES

10. ACKNOWLEDGEMENTS

APPENDICES

APPENDIX A: ERRATA AND CHANGES TO THE PART I REPORT

APPENDIX B: SIZE/SHAPE RELATIONSHIPS FOR THE UNIAXIAL COMPRESSIVE STRENGTH OF COAL SPECIMENS

B1: Size/Strength Relationships for Cubical Test Specimens
B.1.1: Review of Previous Work

B2: Shape/Strength Relationships for Prismatic Test Specimens
B.2.1 Review of Previous Work
B.2.2 Summary and Discussion of Strength/Shape Relationships

B3 Evaluation of the "General Form" of Size/Shape Relationships
B.3.1 Statistical analyses
B.3.2 Summary and Conclusions

B4 Comparison of Three Strength/Shape Relationships for a Typical Pillar Size
B5 Conclusion
References for Appendix B

APPENDIX C: VALUES FOR THE ANGLE OF FRICTION OF BROKEN COAL AND FOR THE UNIAXIAL COMPRESSIVE STRENGTH OF BROKEN COAL

C1: For a Selection of Western Canadian Coals

C2: For Canmore Coal

C3: For U.K. Coals

C4: For U.S. Coals

C5: Discussion

C6: Conclusions

References for Appendix C

APPENDIX D: BALMER'S GENERAL ANALYTIC SOLUTION FOR MOHR'S ENVELOPE

D1: The Mohr Diagram

D2: Application to a Curved Envelope

D3: Application to Triaxial Data for Coal

D4: References for Appendix D

APPENDIX E: A PROPOSED COAL TESTING PROGRAM

E1: Introduction

E2: Unanswered Questions

E3: Phase 3 - Study Proposal

E.3.1 Objectives
E.3.2 Proposed Approach

E4 Detailed Coal Testing Program

E.4.1 Group A - Uniaxial Tests on solid coal specimens
E.4.2 Group B - Triaxial Tests on solid coal specimens
E.4.3 Group C - Triaxial Tests on recompacted broken coal
E.4.4 Group D - Shear box tests - cut coal specimens
E.4.5 Group E - Uniaxial model pillars ($^{H}/_{B} < 1$)

FIGURES

Figure 1: Example Analysis of Pillar Stability and Stress Distributions

Figure 2: Comparison of Different Strength/Shape Relationships for Specimens (H = 2 inches)

Figure 3: Comparison of Different Strength/Shape Relationships for Specimens (H = 4 inches)

Figure 4: Post-Peak Behaviour of Pittsburgh Coal

Figure 5: Balmer Envelopes for Peak and Residual Stresses

Figure 6: Intersection of the Peak and Residual Stress Mohr Envelopes

Figure 7: Transition Point from the Peak and Residual σ_1 vs σ_3 relationship

Figure 8: Straight Line Approximation of the Residual Stress Envelope

Figure 9: Peak Stress Envelope in the Single Parameter Parabolic Form

Figure 10: Transition Point using the Single Parameter Parabolic Mohr Envelope

Figure 11: p-q Diagram

Figure 12: p-q Diagrams for Some U.S. Coals (8)

Figure 13: (a) Peak Stress Envelope for Muddy Siltstone
(b) Slip Test Envelope for Muddy Siltstone

Figure 14: Transition Point for Muddy Siltstone

Figure 15: Results Obtained from Borehole No. 1 in Pillar X

Figure 16: Results Obtained from Borehole No. 3 in Pillary Y

Figure 17: Elastic Solutions

Figure 18: Model Solution

Figure 19: Test Site at Witbank, Wolvekrans Section, No. 2 Seam

Figure 20: Enlarged Plan View of the Two Test Pillars

Figure 21: Results - Normal Boreholes - Pillar A

Figure 22: Results - Normal Boreholes - Pillar B

Figure 23: Results - Diagonal Boreholes - Pillar A

Figure 24: Results - Diagonal Boreholes - Pillar B

Figure 25: Comparison of Normal Borehole Results with Elastic Solutions

Figure 26: Pillar Strength Calculations

Figure 27: Comparison of the Salamon/Munro Strength Equation with Model Results

Figure 28: Comparison of Bieniawski's Strength Equation with Model Results

Figure 29: Comparison of the Holland/Gaddy Strength Equation with Model Results

Figure 30: Pillar Strength as a Function of Width to Height Ratio and Number of Jacks (After Wagner (23))

Figure 31: Comparison of the Wagner Strength Equation with the Model Results

Figure 32: Comparison of Pillar Strength Variations with Pillar Width for a 10ft. High Pillar - For all Formulae

Figure 33: Idealized Fracture Zone and Pillar Core Regions

Figure 34: Test Pillar Location, Wilson Seam, Canmore Mine

Figure 35: Fracture Index across Pillar #1, Canmore, Wilson Seam

Figure 36: Comparison of Fracture Index Distribution with Analytically Determined Stress Distribution

Figure 37: Location of the Test Pillars, #2 Mine, #4 Seam, McIntyre Mines

Figure 38: Fracture Index Distribution Across Pillars, A, B, and C

Figure 39: Comparison of Fracture Index Distribution and Stress Distribution across Pillar A

Figure 40: Comparison of Fracture Index Distribution and Stress Distribution across Pillar B

Figure 41: Comparison of Fracture Index Distribution and Stress Distribution across Pillar C

Figure 42: Mining Sequence when Reducing Test Pillar Size

Figure 43: Stress Changes in Test Pillars as Size is Reduced

Figure 44: Model Stress Distributions in the Test Pillar at Different Sizes

Figure 45: Comparison of Various Pillar Strength vs $^B/H$ relationships

Figure 46: Specimen Strength/Shape Results for Case History #14

Figure 47: Average Stress Profile of a Coal Pillar Subjected to 1000 psi Overburden Stress During Initial and Secondary Mining

Figure 48: Model Stress Distribution for Case History #14

APPENDIX FIGURES

Figure A1: Flow Diagram for Revised Failure Criteria

Figure B1: Uniaxial Compressive Strength Correlations - U.K. Coals
Figure B2: Uniaxial Compressive Strength Correlations - U.S. Coals
Figure B3: Uniaxial Compressive Strength Correlations - S. African coals
Figure B4: Uniaxial Compressive Strength Correlations - all coals - all data
Figure B5: Uniaxial Compressive Strength Correlations - all coals - prisms only
Figure B6: Correlations - all coals when $H > 0.5$ inches
Figure B7: Correlations - all coals in inverse $(H/\sqrt{B})$ form $(\sqrt{B}/H < 1.4)$
Figure B8: 3 Forms of Strength Shape Relationships for Specimens of Pillar Size

Figure D1: Mohr's Diagram
Figure D2 to D 19: Mohr Envelopes in Balmers Form for a Range of U.K. Coals

Figure E1: Possible Size Effects on Mohr Envelopes
Figure E2: Stress/Strain Curves for Triaxial Tests - Varying Confining Pressure
Figure E3: Stress/Deformation Curves for Slip Tests on Broken Specimens
Figure E4: Possible Estimate of Transition Point by Differences Between Peak and Residual Stresses

TABLES

1. Comparison of small specimen size/shape effects
2. Typical k and A values for various coals
3. Triaxial test data for Pittsburgh coal (6)
4. Balmer's solution for peak and residual stress envelopes
5. Determination of the coefficient of sliding friction from the residual stress envelope
6. Table of correlation coefficient R
7. Table of results for linear fit of data
8. Triaxial strengths for solid and broken muddy siltstone (9)
9. Summary of specimens that did not fail abruptly
10. Calculations using brittle/pseudo-ductile failure theory to explain Holland's results
11. Model solutions for Case History #5
12. Comparison of coal strength data for collieries representing all major coal fields in South Africa
13. Pillar strength work sheet
14. Model results for Canmore test pillar
15. Model results for McIntyre test pillars
16. Model solutions for Case History #13
17. Model solutions for Case History #14

APPENDIX TABLES

Table B1: U.K. Coal Data

Table B2: U.S. Coal Data

Table B3: S. African Coal Data

Table B4: Miscellaneous Coal Data

Table B5: Comparison of Shape Relationships for H = 120 in., σ_c (1 inch cube) = 6000 psi

Table D1: Triaxial Fracture Strength Data for Coals (From Hobbs (D2))

1. INTRODUCTION

The ability to design pillars for underground coal mining operations is of prime importance in room and pillar mining during both the development and extraction phases, and in longwall mining to control entries between panels, etc. Pillar failure during mining represents a major potential safety hazard and is generally avoided in practice by overdesigning the pillar using large safety factors, however, this may result in reduced extraction ratios and in loss of reserves. It is also essential to be able to design stable barrier pillars between mining panels, not only for structural stability but also to prevent ventilation leakage between mined out areas which could cause spontaneous combustion and mines fires.

Although much past rock mechanics research has been devoted to assessing pillar loads and pillar strengths, no one approach to pillar design has been completely satisfactory, and pillar design still owes much to trial and error procedures during actual mining operations. A satisfactory analytical design method for determining stable pillar dimensions, whilst not eliminating the necessity for design adjustments made on the basis of site experience, would contribute significantly to safety and underground strata control.

With these overall objectives in mind CMRC proposed a two part contract research study to D.S.S. (CANMET) in 1980. This contract was awarded and work commenced in February 1981. The progress of this work is summarized below.

The objectives of this contract were as follows:-

Phase 1: To develop an analytical approach to define coal pillar stability and lead to the evaluation of optimum pillar dimensions.

Phase 2: To evaluate the applicability of this analytical approach to pillar design by testing it using experimental data extracted from the extensive literature on the subject.

Phase 1 of the work has been completed and the report was submitted in January 1982.(1) In Phase 1, as planned, the Centre developed a new computer based approach to the analysis of the stability of pillars in coal mines. In this analytical approach the mean vertical stress acting on the pillar is calculated using either tributary area theory or Coates' modified pillar loading hypothesis; the initial vertical elastic stress distribution across the pillar is then approximated. The pillar is split into narrow vertical slices and the stresses acting on each slice, starting at the pillar edge, are calculated and compared to the failure criteria. If the slice fails, the residual stress capacity of the slice is determined and the difference between this stress and the initial stress is shed onto the remaining, as yet unfailed, slices. Successive analysis of each slice in turn allows the depth of the failed zone, the vertical stress distribution in the failed zone and the elastic core of the pillar, and the confining stress build up in the failed zone to be calculated.

The failure criteria used in this analysis are based on Mohr theory as defined by a parabolic (or a general curvilinear) Mohr envelope. At low confining stresses brittle fracture occurs; at high confining stresses a pseudo-ductile failure mechanism is invoked which allows a slice to yield. The brittle/pseudo-ductile transition point is defined as the point on the Mohr envelope where the shear resistance to sliding exceeds the shear resistance to fracture. Consequently the failed zone may comprise only a fracture zone or a fracture zone plus a yield zone; likewise the pillar may fail by brittle fracture or by yielding.

Pillar strength has been defined as the mean pillar stress required to just extend the failed zone to the centre of the pillar. This strength can be determined by either the above slice by slice analysis or from deterministic equations which have been evolved by integrating over the pillar width.

Figure 1 illustrates the results of an application of the program to the analysis of the stability of rib pillars in a hypothetical cross section of a mine using typical coal parameters. A wide range of hypothetical analyses were performed in Phase 1 which revealed a number of important conclusions:-

(i) There is a minimum pillar stress below which fracture cannot initiate in the pillar; hence there is a minimum pillar strength.

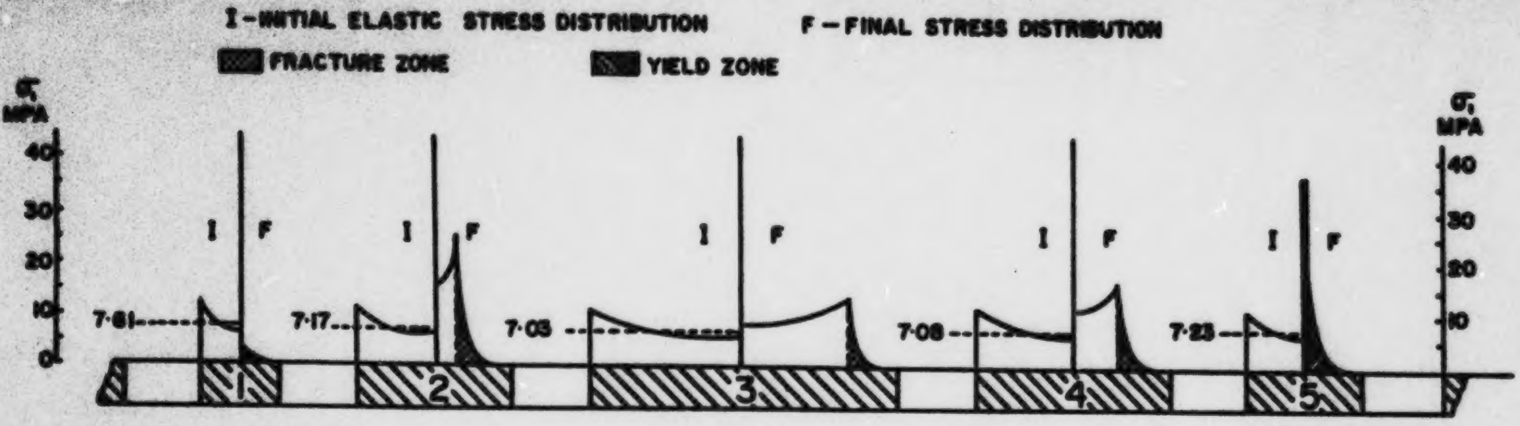
I - INITIAL ELASTIC STRESS DISTRIBUTION
F - FINAL STRESS DISTRIBUTION
FRACTURE ZONE
YIELD ZONE
σ₁ MPA
40
30
20
10
0
I
F
7·61
7·17
7·03
7·08
7·23
1
2
3
4
5

PILLAR NO.	1	2	3	4	5
HEIGHT - m.	3	3	3	3	3
WIDTH - m.	6	12	24	15	9
MEAN STRESS-MPA	7·61	7·17	7·03	7·08	7·23
STRENGTH-MPA	3·79	9·39	16·78	12·35	4·46
SAFETY FACTOR	0·50	1·31	2·39	1·75	0·62
FAILURE MODE	CAT. FRACTURE	STABLE	STABLE	STABLE	YIELD
DEPTH OF FRACTURE ZONE	3 (TO CENTRE)	4·21	3·9	4·1	4·21
DEPTH OF YIELD ZONE - m.	-	-	-	-	4·5 (TO CENTRE)
SHED LOAD - MN	22·94	-	-	-	25·02
CRITICAL WIDTH TO AVOID: CATASTROPHIC FAILURE - m.	8·66	8·72	8·72	8·72	8·70
ULTIMATE FAILURE - m.	9·52	10·44	10·34	10·38	10·48

FIGURE 1: EXAMPLE ANALYSIS OF PILLAR STABILITY AND STRESS DISTRIBUTIONS

(ii) In specific circumstances, once fracture initiates at the pillar edge the failed zone must propogate immediately to the centre of the pillar. This unstable situation has been called "catastrophic failure" and could be regarded as a model of a "pillar burst". The critical pillar dimensions to avoid such catastrophic failure can be calculated.

(iii) In more normal circumstances, there is a failed zone at the periphery of the pillar with a central elastic core. As the pillar loading increases the failed zone gradually extends into the pillar until it reaches the centre when the pillar is deemed to have failed. This failure is called "ultimate failure"; the critical pillar dimensions to avoid ultimate failure can be calculated, as can the residual load capacity of the failed pillar.

From these phase 1 results it would appear that this analytical model does give a qualitative approximation of the observed behaviour of coal pillars. This leads naturally into Phase 2 of this contract in which the object is to "verify" the model by using it to predict the results of a number of experimental case histories reported in the literature. This report gives the results of Phase 2 of this study.

Note: A number of minor typographical, drafting and computer program errors inadvertently were included in the phase 1 report. Appendix A lists these errata.

2. DISCUSSION OF THE REQUIRED INPUT PARAMETERS FOR COAL STRENGTH PROGRAM

2.1 Analytical Expression for Specimen Strength

The analytically derived pillar strength formulae can be used to examine the strength/size and strength/shape relationships for test specimens under uniform loading. (eg. specimens in a testing machine and/or specimens cut in-situ in the mine and loaded uniformly by jacks). For such specimens the "pillar stress concentration", $\bar{Y}$, must be equal to unity since the load is directly applied to the specimen cross section. Further, since the specimens in such tests are uniformly loaded then $Y_{mm} = \bar{Y}$.

Let us therefore re-express the analytically derived pillar strength equations as they would apply to uniformly loaded specimens. Let us also introduce the size/shape factor, γ, but putting $\gamma = (b/h)$. The three analytical equations for strength developed in the phase 1 report can then, for specimens, be expressed as follows:-

(i) Minimum pillar strength

$$\bar{\sigma}_{s\,min} = \frac{\bar{Y}}{Y_{mm}} \cdot 2A \text{ but for uniformly loaded specimens } \bar{Y} = Y_{mm} = 1$$

$$\text{therefore } \bar{\sigma}_{s\,min} = 2A \qquad (1)$$

where A is the "Mohr constant" defined in the phase 1 report.

(ii) when ${}^{d}T/_{b} > 1$, then the pillar (specimen) fails by fracture and the strength is given by:-

$$\bar{\sigma}_{SF} = \frac{P_B\,(1-\sin\phi_B)}{2\sin\phi_B}\left[\frac{1}{\gamma\tan\phi_B}\left\{e^{\tan\phi_B\left(\frac{1+\sin\phi_B}{1-\sin\phi_B}\right)\gamma} - 1\right\} - 1\right] \qquad (2)$$

(iii) when ${}^{d}T/_{b} < 1$, then the pillar (specimen) fails by pseudo-ductile yield and the strength is given by:-

$$\bar{\sigma}_{sy} = \frac{P_B\ (1-\mathrm{Sin}\phi_B)}{2\ \mathrm{Sin}\phi_B}\left[\frac{1}{\gamma\ \tan\phi_B}\left\{e^{\tan\phi_B\left\{\frac{(1+\mathrm{Sin}\phi_B)}{(1-\mathrm{Sin}\phi_B)}\right\}\left\{\frac{d_T}{b}\right\}\gamma} - 1\right\} - \left(\frac{d_T}{b}\right)\right] + \left(1-\frac{d_T}{b}\right)\ P_{1T} \tag{3}$$

where

$$\left(\frac{d_T}{b}\right) = \frac{(1-\mathrm{Sin}\phi_B)}{(1+\mathrm{Sin}\phi_B)} \cdot \frac{1}{\gamma\ \tan\phi_B}\ \mathrm{Log}_e\left\{\frac{2\ P_{1T}\ \mathrm{Sin}\phi_B}{P_B\ (1+\mathrm{Sin}\phi_B)} + \frac{(1-\mathrm{Sin}\phi_B)}{(1+\mathrm{Sin}\phi_B)}\right\} \tag{4}$$

and

$$P_{1T} = \frac{A}{2} + \frac{A}{2\mu_B^2}\left\{1+(1+\mu_B^2)^{½}\right\} + \left\{\frac{A^2}{2} + \frac{A^2}{2\mu_B^2}\left[1 + (1+\mu_B^2)^{½}\right]\right\}^{½} \tag{5}$$

where d_T is the depth of the transition point, b is the semi-pillar (specimen) width, ϕ_B is the angle of internal friction for broken coal, μ_B is the coefficient of sliding friction for coal on coal, P_{1T} is the major principal stress at the transition point.

It is seen from the above equation that P_{1T} and $\bar{\sigma}_{s\ min}$ are dependent only on material properties (A and μ_B) and are independent of the specimen width/height ratio γ. d_T the depth of the transition point is inversely proportional to γ.

$\overline{\sigma}_{SF}$ and $\overline{\sigma}_{sy}$ are also dependent on γ.

2.2 Cube Strength - Size Relationships

Consider the above relationships when applied to cubical coal specimens, ie. $\gamma = 1$.

When $\gamma = 1$:-

(i) The ratio ($^{d}T/b$) is dependent only on the material properties P_B, ϕ_B, A and μ_B. ie. this ratio is the same for a cube of any size.

(ii) From equations (2) and (3), putting $\gamma = 1$ it is seen that according to these analytical expressions the cube strength for cubes of different side lengths will all be the same.

ie. the analytical equations predict no change of strength with variation of cube size. Yet, of course there is ample evidence in the literature (see Appendix B section B.1) to show that cube strength does vary, very significantly with cube size.

If the analytical approach is correct then it must follow that any variation of cube strength with cube size must be due to variations of the material properties with size. Now both P_B and ϕ_B are properties of crushed, broken, coal and it would therefore seem unlikely that they would vary with size. Likewise, μ_B is the coefficient of sliding friction between coal surfaces and should also be relatively size independent. This leaves only A as the variable that must be size dependent (remembering that A is the so called "Mohr constant" and theoretically $2A = \sigma_c$ where σ_c is the uniaxial compressive strength). It follows therefore that the variation of A with size must reflect the variation of σ_c with size. i.e. it must reflect the difference between the compressive strength of a small specimen and the "mass" strength.

It is therefore exceedingly important to define how A will vary with cube size since this is one of the prime input parameters into the analysis. Clearly the value derived from small specimen tests (which is often the only strength data available) will not be the value of A to be used in the large specimen (pillar) analysis due to this size effect.

Appendix B gives a comprehensive review of past work on cube size/strength relationships. The consensus of this work is that the cube size effect may be expressed by:-

$$\sigma_c = \frac{k}{\sqrt{D}}$$

where k is numerically (but not dimensionally) equal to the strength of a 1 inch cube in psi and D is the cube edge length in inches.

Hustrulid (2) indicates that the cube strength becomes constant when D >36 inches, given by $\sigma_c = k/\sqrt{36} = 0.167$ k. Whereas Bieniawski (3) and Barron (Appendix B) suggest that σ_c becomes a constant when D >64 inches, and equal to $k/\sqrt{64} = 0.125$ k. Depending which value of the upper limit of size effect is considered there will be an approximate 30% difference in the value of σ_c. The upper size limit of 64 inches will be assumed in this paper since Bieniawski's work shows clearly that there is a continuing size effect at greater than the 36 inches given by Hustrulid.

Hence we can take into account the size effect in the analytical approach if the input value for A to be used in the analysis is given by:-

$$A = \frac{\sigma_c}{2} = \frac{k}{2\sqrt{D}} \quad \text{when } D < 64 \text{ inches}$$

$$\text{and } A = \frac{\sigma_c}{2} = \frac{k}{2}(0.125) \quad \text{when } D > 64 \text{ inches}$$

It will be arbitrarily assumed, and discussed in the next section, that the value of A to be used as input into the pillar strength equations for non-cubic (rectangular) specimens is that determined from a cube of strength equal to the specimen (pillar) height.

$$\text{i.e.} \quad A = \frac{\sigma_c}{2} = \frac{k}{2\sqrt{H}} \quad \text{when } H < 64 \text{ inches} \qquad (6)$$

$$\text{and } A = \frac{\sigma_c}{2} = \frac{k}{2}(0.125) \quad \text{when } H > 64 \text{ inches} \qquad (7)$$

For example,

Suppose the only information we know is that the cube strength of a 3 inch cube is 3000 psi. Then k for a 1 inch cube is given by:-

$$k = 3000\sqrt{3} = 5196$$

Then the input value of A for pillar (specimens) of height 2", 10", 30", 100", 120" is given below:-

k 1 inch cube	Specimen (pillar) height-inches	Strength of a cube of side equal to specimen height $\sigma_c = k/\sqrt{H}$	$A = \sigma_c/2$
	2	3674	1837
5196	10	1643	821
	30	948	474
	100	649*	325
	120	649*	325

*$H > 60'' \therefore A = \text{constant} = k/2\,(0.125)$

2.3 Strength - Shape Relationships

2.3.1 For specimens, as predicted by the analytical equations

From equations 2 and 3 it is seen that the analytical expressions for prism strength are a complex function of γ, the (b/h) shape ratio; but if equation 1 applies then the specimen has a constant strength.

If we want to consider these equations in nomalized form, i.e. σ_p/σ_c ratio form, then we can have several combinations depending on the mode of failure for the prism and for the cube. To examine these effects let us consider two examples; firstly when $H = 2$ inches and secondly when $H = 4$ inches. The strength calculations and the σ_p/σ_c ratios for these examples are given in Table 1 assuming "typical" coal parameters of $k = 5000$, $\mu_B = \tan^{-1} \phi_B = 0.577$, $\phi_B = 30^\circ$ and $P_B = 25$ psi.

2.3.2 Comparison of analytical results with the Hustrulid and Holland/Gaddy equations.

Table 1 also gives the prism strengths, for a prism of the defined height, and the σ_p/σ_c ratios as calculated using, firstly the Hustrulid (2) form of equation where:-

$$\sigma_c = \frac{k}{\sqrt{H}}$$

and $$\frac{\sigma_p}{\sigma_c} = 0.778 + 0.222 \left(\frac{B}{H}\right)$$

and secondly, using the Holland-Gaddy equation (with limits as imposed by Barron (see Appendix B)):-

$$\sigma_p = k \frac{\sqrt{B}}{H}$$

and $$\sigma_c = \frac{k}{\sqrt{H}}$$

i.e. $$\frac{\sigma_p}{\sigma_c} = = \sqrt{\frac{B}{H}} \text{ for constant H}$$

TABLE 1: COMPARISON OF SMALL SPECIMEN SIZE SHAPE EFFECTS

CASE A: $H = 2$ inches $k = 5000$ $\mu_B = \tan^{-1}\phi_B = .577$ $\phi_B = 30^\circ$ $P_B = 25$ psi $A = \frac{5000}{2\sqrt{2}} = 1767$

$P_{1T} = 10{,}009$ psi $\sigma_{p\,min} = 2A = 3534$

Y	b inches	k inches	From Analytical Eq. $\bar{\sigma}_p$ - psi	$\frac{\sigma_p}{\sigma_c}$	FROM HUSTRULID σ_p psi	$\frac{\sigma_p}{\sigma_c}$	FROM HOLLAND/GADDY (BARRON'S LIMITS) $\sqrt{\frac{b}{H}}$	σ_p psi	$\frac{\sigma_p}{\sigma_c}$
.25	.25	1	3534*	1	2946	.833	.353	1765	.50
.5	.5	1	3534*	1	3142	.889	.50	2500	.707
.75	.75	1	3534*	1	3338	.944	.61	3050	.862
1.0	1.0	1	3534*	1	3535	1.0	.707	3535	1.0
2.0	2.0	1	3534*	1	4312	1.22	1.0	5000	1.41
3.0	3.0	1	3850	1.089	5090	1.44	1.22	6100	1.725
4.0	4.0	1	6228	1.76	5868	1.66	1.41**	7000	1.98

* $\sigma_{p\,min} > \bar{\sigma}_p$

** Limit Value $\sqrt{\frac{b}{H}} > 1.41$

1. ANALYTICAL RESULTS CORRELATED IN HUSTRULID'S FORM GIVES:-

$\frac{\sigma_p}{\sigma_c} = 0.859 + 0.159\left(\frac{b}{H}\right)$, $r = 0.795$ c.f. Hustrulid $\frac{\sigma_p}{\sigma_c} = 0.778 + .222\left(\frac{b}{H}\right)$

2. ANALYTICAL RESULTS CORRELATED IN HOLLAND/GADDY FORM GIVES:-

$\frac{\sigma_p}{\sigma_c} = 0.96\sqrt{\frac{b}{H}}$ c.f. Holland/Gaddy $\frac{\sigma_p}{\sigma_c} = 1.0\sqrt{\frac{b}{H}}$

CASE B: $H = 4$ inches $k = 5000$ $\mu_B = \tan^{-1}\phi_B = .577$ $\phi_B = 30^\circ$ $P_B = 25$ psi $A = \frac{5000}{2\sqrt{4}} = 1250$

$P_{1T} = 7080$ psi $\sigma_{p\,min} = 2A = 2500$ psi

Y	b inches	k inches	From Analytical Eq. $\bar{\sigma}_p$ - psi	$\frac{\sigma_p}{\sigma_c}$	FROM HUSTRULID σ_p psi	$\frac{\sigma_p}{\sigma_c}$	FROM HOLLAND/GADDY (BARRON'S LIMITS) $\sqrt{\frac{b}{H}}$	σ_p psi	$\frac{\sigma_p}{\sigma_c}$
.25	.25	2	2500*	1	2075	.833	.25	1250	.50
.5	1.0	2	2500*	1	2222	.889	.353	1765	.707
.75	1.5	2	2500*	1	2350	.944	.433	2165	.866
1.0	2	2	2500*	1	2500	1.0	.50	2500	1.0
2.0	4	2	2500*	1	3050	1.22	.707	3535	1.41
3.0	6	2	3850	1.54	3600	1.44	.866	4330	1.732
4.0	8	2	4749	1.90	4150	1.66	1.0	5000	2.0

* $\sigma_{p\,min} > \bar{\sigma}_p$

1. ANALYTICAL RESULTS CORRELATED IN HUSTRULID'S FORM GIVES:-

$\frac{\sigma_p}{\sigma_c} = 0.814 + 0.238\left(\frac{b}{H}\right)$, $r = 0.92$ c.f. Hustrulid $\frac{\sigma_p}{\sigma_c} = 0.778 + 0.222\left(\frac{b}{H}\right)$

2. ANALYTICAL RESULTS CORRELATED IN HOLLAND/GADDY FORM GIVES:-

$\frac{\sigma_p}{\sigma_c} = 1.02\sqrt{\frac{b}{H}}$ c.f. Holland/Gaddy $\frac{\sigma_p}{\sigma_c} = 1.0\sqrt{\frac{b}{H}}$

Figures 2 and 3 give these comparisons in terms of σ_p versus (B/H) and σ_p/σ_c versus (B/H).

It is seen from these figures that:-

(i) The analytical equation results show a constant strength with (B/H) and consequently a constant (σ_p/σ_c) ratio equal to 1 over a considerable range of (B/H) values up to between 2 and 3 in both examples.

(ii) Thereafter the analytical results show a rapid increase of σ_p and σ_p/σ_c with (B/H) when the prism is in the ultimate failure mode, following by a less rapid increase when the prism is in the ultimate yield mode.

(iii) It is clear that these results are very different from those given by the Hustrulid or the Holland/Gaddy forms, which also differ between themselves.

Suppose however the analytical data is treated as "real" data and correlated in the same form as firstly, Hustrulid and secondly, Holland/Gaddy:-

In the Hustrulid form of correlation this leads to:-

Case A (H = 2")
$$\frac{\sigma_p}{\sigma_c} = 0.859 + 0.159 \left(\frac{B}{H}\right), \quad r = 0.795$$

Case B (H = 4")
$$\frac{\sigma_p}{\sigma_c} = 0.814 + 0.238 \left(\frac{B}{H}\right), \quad r = 0.920$$

compared to Hustrulid's equations

$$\frac{\sigma_p}{\sigma_c} = 0.778 + 0.222 \left(\frac{B}{H}\right)$$

These correlations equations are surprisingly close considering the major differences in approach. In the Holland/Gaddy (constant H) form of correlation this leads to:-

Case A (H = 2")
$$\frac{\sigma_p}{\sigma_c} = 0.96\sqrt{\frac{B}{H}}$$

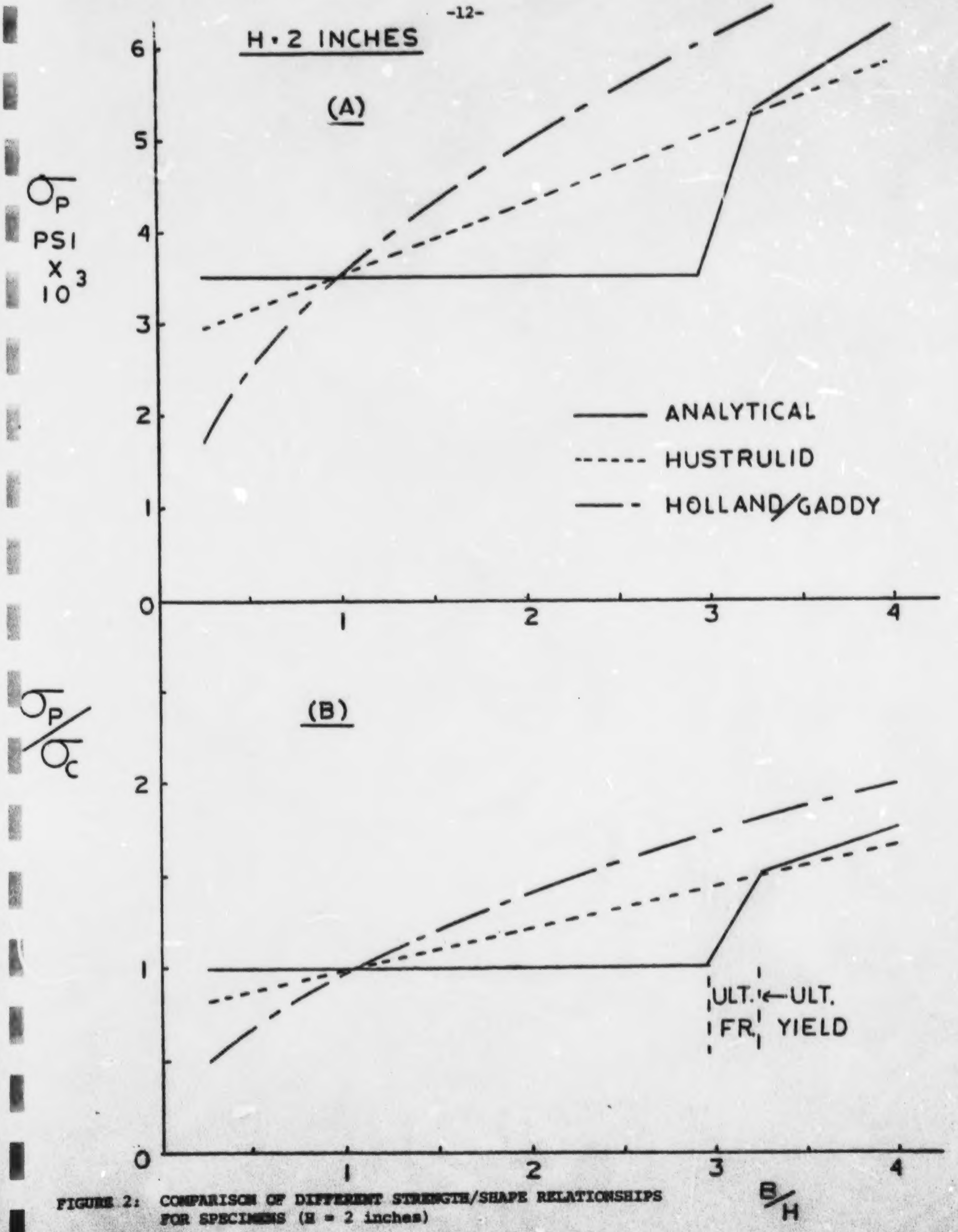

FIGURE 2: COMPARISON OF DIFFERENT STRENGTH/SHAPE RELATIONSHIPS FOR SPECIMENS (H = 2 inches)

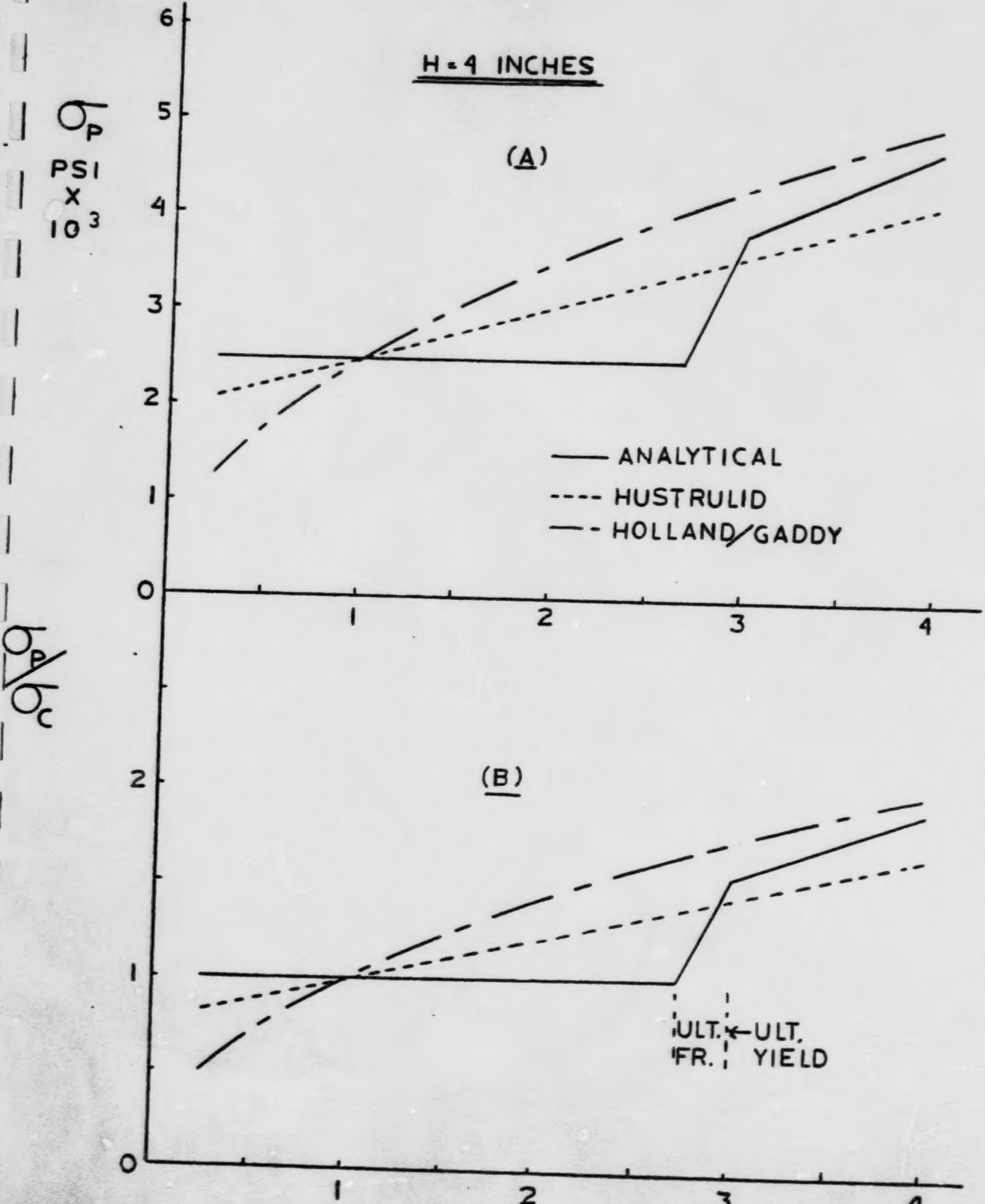

FIGURE 3: COMPARISON OF DIFFERENT STRENGTH/SHAPE RELATIONSHIPS FOR SPECIMENS (H = 4 inches)

Case B (H = 4") $\frac{\sigma_p}{\sigma_c} = 1.02\sqrt{\frac{B}{H}}$

compared to the Holland/Gaddy constant H form of:-

$$\frac{\sigma_p}{\sigma_c} = 1.0\sqrt{\frac{B}{H}}$$

Again these correlations are surprisingly similar.

When viewed in this manner, one possible conclusion is that the scatter in the real data which lead to the establishment of Hustrulids and of the Holland/Gaddy equations is such that it masks the effects brought out by the analytical equations. The analytical equations when correlated in the Hustrulid or the Holland/Gaddy manner then yield similar equations despite the fact that the analytical form is totally different.

Two other aspects bear discussion. Firstly none of the above forms consider the "end effects" during specimen testing. To what extent the empirically derived data, which form the basis for both the Hustrulid and Holland/Gaddy expressions, has been affected by "end effects" cannot be assessed since they are based on multi data sources for which undoubtedly the testing conditions and end effects varied from data source to data source. Secondly, bearing the above in mind, the empirically derived forms all show a reducing strength of prism (with constant height) continuing below $(^B/_H)$ ratios of 0.75 ⟶ 0.25. Inuitively the author feels that for such tall/thin specimens the uniaxial strengths would more likely be a constant (as indicated by the analytical approach) and that, perhaps, the changes in strength observed in this range at least might be attributed to "end effects". This however is pure speculation and cannot be settled on the basis of the evidence available.

2.3.3 Conclusions with respect to strength/shape effects for specimens

(i) The application of the analytical equations to small specimens does take into account the shape effects on strength, in so far as γ is an influencing parameter.

(ii) The form of the change of prism strength with γ is very different from that derived by other workers such as Hustrulid or Holland/Gaddy.

(iii) Nonetheless the analytical data could be treated in the same manner as the Hustrulid and Holland/Gaddy forms of expressions and coincidentally yields quite similar correlations. Thus, the analytical results are compatible with the previous work to some extent.

(iv) Clearly much more needs to be done with respect to defining adequately the size/shape relationships as none of the forms are totally compatible with each other. In particular what, if any, affect the specimen end effects may have had on reported data in impossible to assess.

2.4 Conclusions with Respect to Input Strengths for the Model

(i) The value of A to be input in the model should be that determined from the cube strength, σ_C, of a cube equal to the specimen (pillar) height, given by:-

$$A = \frac{\sigma_c}{2} = \frac{k}{2\sqrt{H}} \quad \text{when } H < 64 \text{ inches}$$

$$\text{and} \quad A = \frac{\sigma_c}{2} = \frac{k}{2}\,(0.125) \quad \text{when } H > 64 \text{ inches}$$

when k is numerically (but not dimensionally) equal to the 1 inch cube strength in p.s.i.

(ii) The model equations do take into account shape effects which are not totally incompatible with other work (but neither are they satisfactorily confirmed). Thus no modification should be made to the A input value to take into account shape effects; these effects will be taking into account automatically by the model.

(iii) Table 2 gives a range of typical k values and the resulting A values (for $H >$ 64 inches) for a range of coals from different areas of the world. (derived from data in Appendix B). This table will be used as a source of "typical" A values for later case histories where the actual site data is not available.

TABLE 2: TYPICAL k AND A VALUES FOR VARIOUS COALS

COAL	k (range)	A (when H > 64 inches) psi
U.K. COALS		
Oakdale	890-1150	55-72
Pentremahr	5280-5550	330-350
Deep Duffryn	2350	150
Cymtillery	1750-2630	110-165
Barnsley Hards	4940-8078	310-500
Barnsley Brights	3810-5290	240-330
Markham	4760	300
Linby	4150-7960	260-500
U.S. COALS		
Pittsburgh	6216-7000	390-440
Pocohontos	2300-3000	145-190
Clintwood	3850	240
Harlan	9100	570
Marker	9900	620
Pittsburgh #8 Seam	2900	180
S. AFRICA		
Witbank (Wolverkrans #4 Seam)	5090	320
Natal (Durban Navigation)	6100	380
New Largo	5628	350
CANADA		
Star-Key (Clover bar seam)	4250	265
Mean	4770	300
Standard Deviation	2370	150
Range	890-9900	55-620

(iv) The value of k can be determined from standard small specimen laboratory tests on cubes of a convenient size and hence the value of A for the appropriate pillar or specimen height can be determined from small specimen tests.

2.5 Input Values for μ_B ϕ_B and P_B.

Appendix C summarises results of triaxial tests conducted on specimens of re-compacted crushed coal, and on failed solid coal specimens by various authors. The following conclusions are drawn:-

(i) There is no evidence, positive or negative, to suggest whether or not ϕ_B the angle of friction for broken coal is the same as the angle of friction for coal surfaces sliding on each other.

ie. whether or not $\mu_B = \tan \phi_B$

This relationship will be assumed to be true, unless stated otherwise, in the case histories considered later. Clearly there is a need for a testing program to evaluate this.

(ii) All the tests on the re-compacted and broken coal specimens yielded Mohr envelopes which are very closely filled by a straight line, within the range of confining pressures tested. Hence the assumption in the model that μ_B is constant is a reasonable first approximation. However, it should be remembered (see note, page 68, Phase 1 Report) that there is evidence in the literature to suggest that μ_B might vary with normal stress at high confining pressures.

(iii) The angle of friction, ϕ_B, for broken coal can vary significantly from one coal to the next. Measurements given in Appendix C cover a range from 23° to 45°. A typical "mean value" for coal might be around 30°.

(iv) When ϕ_B is unknown, but the angle of internal friction of solid coal, ϕ_s, is known then ϕ_B appears to be approximated by putting $\phi_B = 0.8\ \phi_s$.

(However the determination of ϕ_s demands a linear envelope of failure. This paper suggests that the failure envelope is non-linear. Hence ϕ_s in this case refers to that determined from the approximate linear envelope which will be obtained from relatively low confining pressure tests prior to non-linearity being seen).

(v) The determination of the cohesion, and hence of the uniaxial compressive strength, P_B, of broken coal is unsatisfactory. At best the results give a maximum possible value. In reality a value of perhaps $^1/_{10}$ th of this maximum value is probably more realistic; this would suggest that P_B lies within a 1-200 psi range for most coals.

It is unfortunate that the model results are quite sensitive to the value of P_B. In practice it may be better to "back analyse" field results to determine the effective P_B for any particular mine site, for further application in that mine.

(vi) There is no indication in the literature as to whether, P_B, ϕ_B and μ_B are influenced by size effects. Intuitively the author believes that their values should be relatively size independent, but this should be an area of further investigation. For this study of case histories it will be assumed that they are size independent.

3. CASE HISTORIES OF RELEVANCE TO THE BRITTLE/PSEUDO-DUCTILE TRANSITION POINT

The failure criterion developed in Phase 1 of the study and used in the model defines a brittle/pseudo-ductile transition point as being that point on the Mohr envelope where the shear resistance to sliding exceeds the shear resistance to fracture. This failure criterion has been used successfully (4, 5) to predict hard rock behaviour at exceptionally high confining pressures; it has not previously been applied to coal or at such relatively low confining pressures. At least one reputable reviewer has questioned the application of this failure criterion to coal at the relatively low stress levels experienced in coal pillars. The coal specimen testing literature has therefore been examined with the object of seeking evidence to support or deny this failure criterion. A basic requirement is that the literature contain triaxial data on both the peak and residual stresses at and following failure. Unfortunately there are only a limited number of papers in which such data is available in sufficient detail for this examination.

3.1 Case History #1: Peak and Post Peak (Residual) Strengths of Pittsburgh Coal Specimens.

3.1.1 Case Background

Kripakov (6) in his finite element study of pillar stability in pitching seams gives a suite of triaxial test data for Pittsburgh coal showing that there is a peak stress at failure and a "post peak" or residual stress after failure. Figure 4 reproduces these triaxial test results reported by Kripakov. This data can be used as a means of determining if it is possible for a "transition point" to exist and, if so, to determine the stress conditions at this transition point. Table 3 gives the stress data derived from the graphs given in Figure 4.

3.1.2 Mohr envelopes in Balmer's parametric form

It is shown in Appendix D that a much better curvilinear fit of the Mohr envelope can be obtained by expressing it in Balmer's parametric form (7) rather than in the parabolic form developed in the Phase 1 Report. For this case history only therefore this improved form of envelope will be used, but the differences between

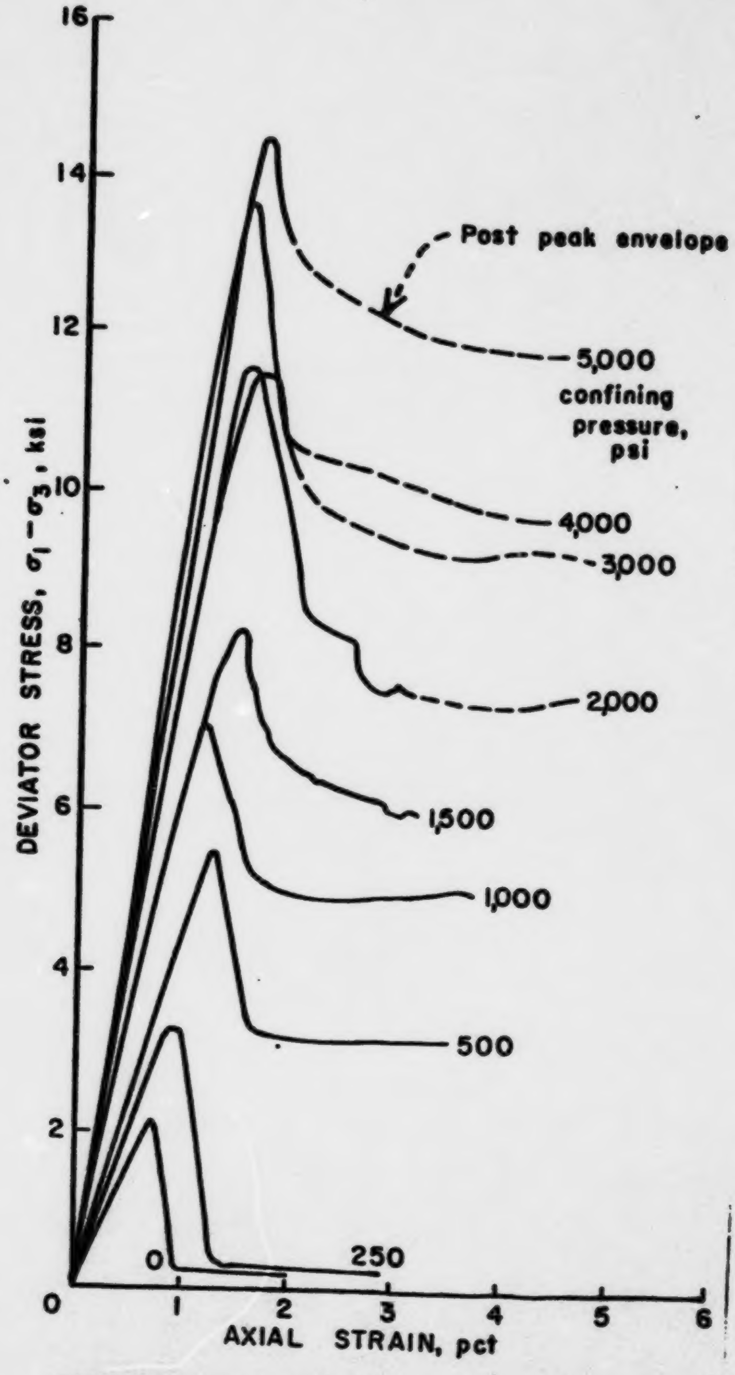

FIGURE 4 - Post-peak behavior of Pittsburgh coal.

TABLE 3: TRIAXIAL TEST DATA FOR PITTSBURGH COAL (6)

				A	B
σ_3 psi	$\sigma_1-\sigma_3$ Peak-psi	$\sigma_1-\sigma_3$ Residual-psi	σ_1 Peak σ_1 Resi. psi	σ_1 Peak psi	σ_1 Residual psi
0	2074	170	1904	2074	170
250	3300	296	3004	3550	546
500	5460	3090	2370	5960	3590
1000	7025	4910	2115	8025	5910
1500	8300	6010	2290	9800	7510
2000	11600	7320	4280	13600	9320
3000	11430	9140	2290	14430	12140
4000	13670	9735	3935	17670	13735
5000	14560	11809	2751	19560	16809

this and the parabolic form will also be addressed.

The parametric form of the Mohr's envelope derived by Balmer can be expressed by the following equations:-

$$\sigma_3 = a + b\,\sigma_1^{\,c} \qquad (8)$$

$$\sigma = \left\{\frac{b\,(c+1)\,\sigma_1^{\,c}}{1 + bc\,\sigma_1^{\,c-1}}\right\} + a \qquad (9)$$

$$\tau = \left\{\frac{\sigma_1 - a - b\sigma_1^{\,c}}{1 + bc\,\sigma_1^{\,c-1}}\right\} \cdot \sqrt{bc\,\sigma_1^{\,c-1}} \qquad (10)$$

and the slope of the Mohr envelope, α, is given by:-

$$\tan^{-1} \alpha = \frac{\partial\tau}{\partial\sigma_1} = \left\{\frac{1 - bc\,\sigma_1^{\,c-1}}{2\sqrt{bc\,\sigma_1^{\,c-1}}}\right\} \qquad (11)$$

Table 4 gives the parameters a, b and c for the best fit solutions in Balmers form for the peak and residual stress data for Pittsburgh coal given in Table 3. Figures 5A and 5B shows the results in graphical form.

The two envelopes, for peak and residual stresses respectively, can be surperimposed on the same graph as shown in Figure 6.

It is seen from Figure 6 that these two envelopes intersect at τ = 7650 psi, σ = 11,150 psi. However, this is not the transition point. The peak stress envelope plots the shear stress and the normal stress at failure, acting on the failure plane; whereas, the residual stress envelope plots the shear and normal stresses acting on a different plane. This can be demonstrated by calculating α using equation (iii) and remembering that $2\theta = 90 + \alpha$ where θ is the angle of the plane of maximum shear stress with the horizontal:-

TABLE 4: BALMERS SOLUTION FOR PEAK AND RESIDUAL ENVELOPES

	Peak Stress - A	Residual Stresses - B
$\sigma_3 =$	$0.000247\,\sigma_1^{1.70} - 124.65$	$0.1585\,\sigma_1^{1.06} - 305.7$

$$\sigma_N = \frac{b\,(c+1)\,\sigma_1^{\,c}}{1 + bc\,\sigma_1^{\,c-1}} + a$$

$$\tau = \left\{\frac{\sigma_1 - a - b\,\sigma_1^{\,c}}{1 + bc\,\sigma_1^{\,c-1}}\right\}\sqrt{bc\,\sigma_1^{\,c-1}}$$

	A	B
a =	-124.65	-305.74
b =	0.000247	0.1585
c =	1.70	1.06

σ_1	σ_3	σ_N	τ	σ_3	σ_N	τ
2500	23	237	713	327	723	887
5000	355	988	1612	1015	1820	1647
7500	831	1996	2551	1724	2944	2403
10,000	1433	3201	3485	2448	4086	3158
12,500	2152	4570	4396	3183	5241	3910
15,000	2980	6076	5274	3927	6406	4661
17,500	3910	7702	6112	4679	7581	5411
20,000	4938	9433	6907	5437	8763	6159
25,000	7274	13166	8364	6969	11148	7653
30,000	9963	17205	9639	8520	13554	9143
35,000	12985	21501	10732	10087	15978	10630

GRAPHIC SOLUTION OF MOHRS ENVELOPE

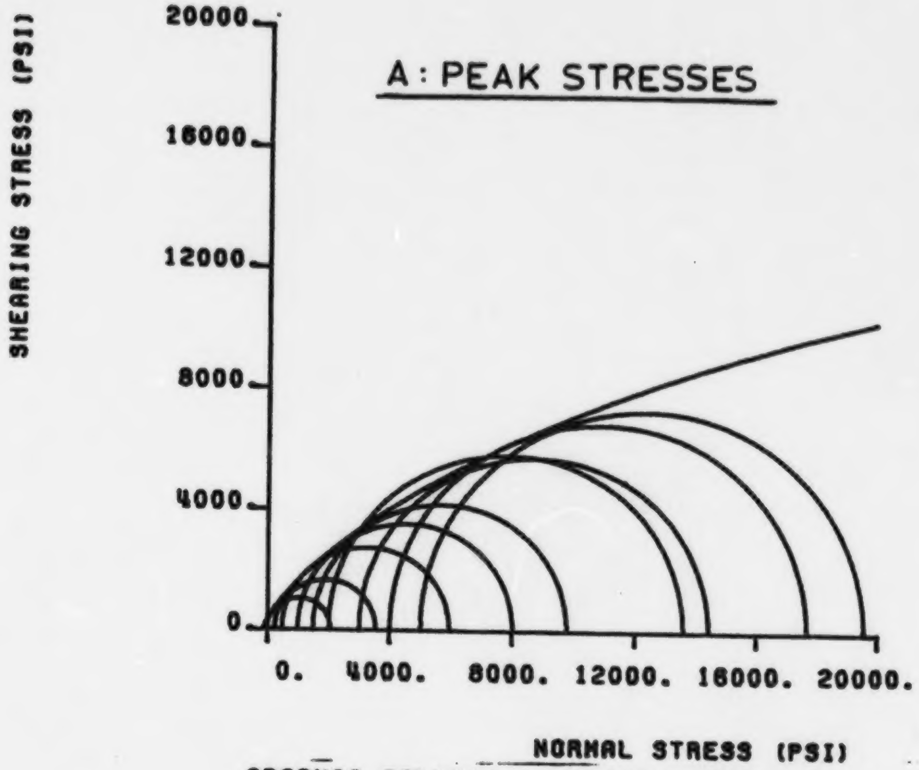

GRAPHIC SOLUTION OF MOHRS ENVELOPE

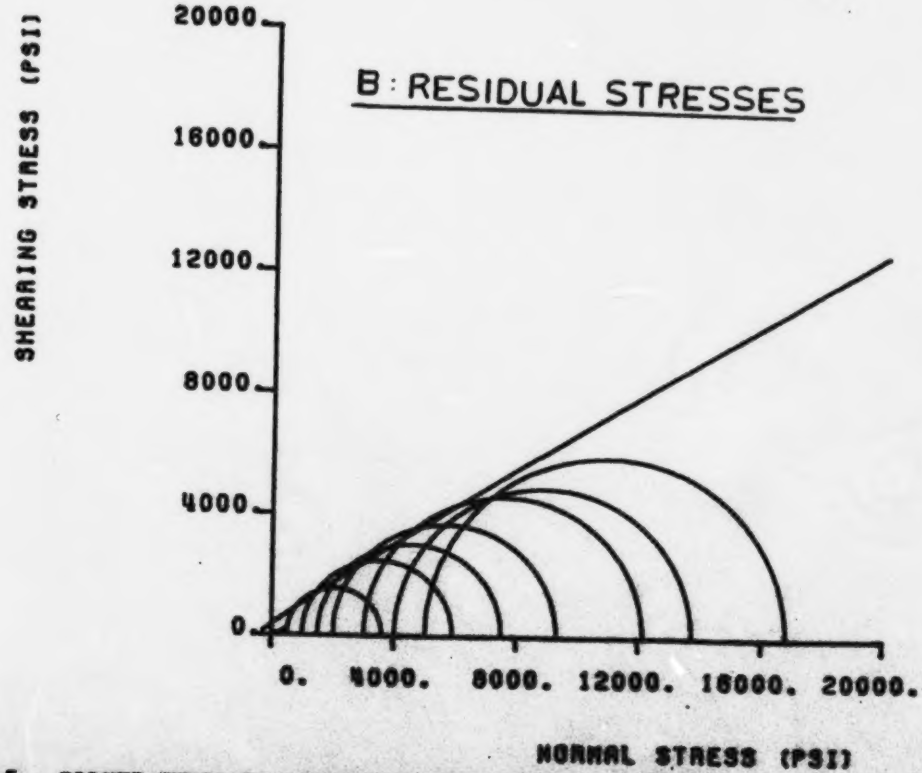

FIGURE 5: BALMER ENVELOPES FOR PEAK AND RESIDUAL STRESSES

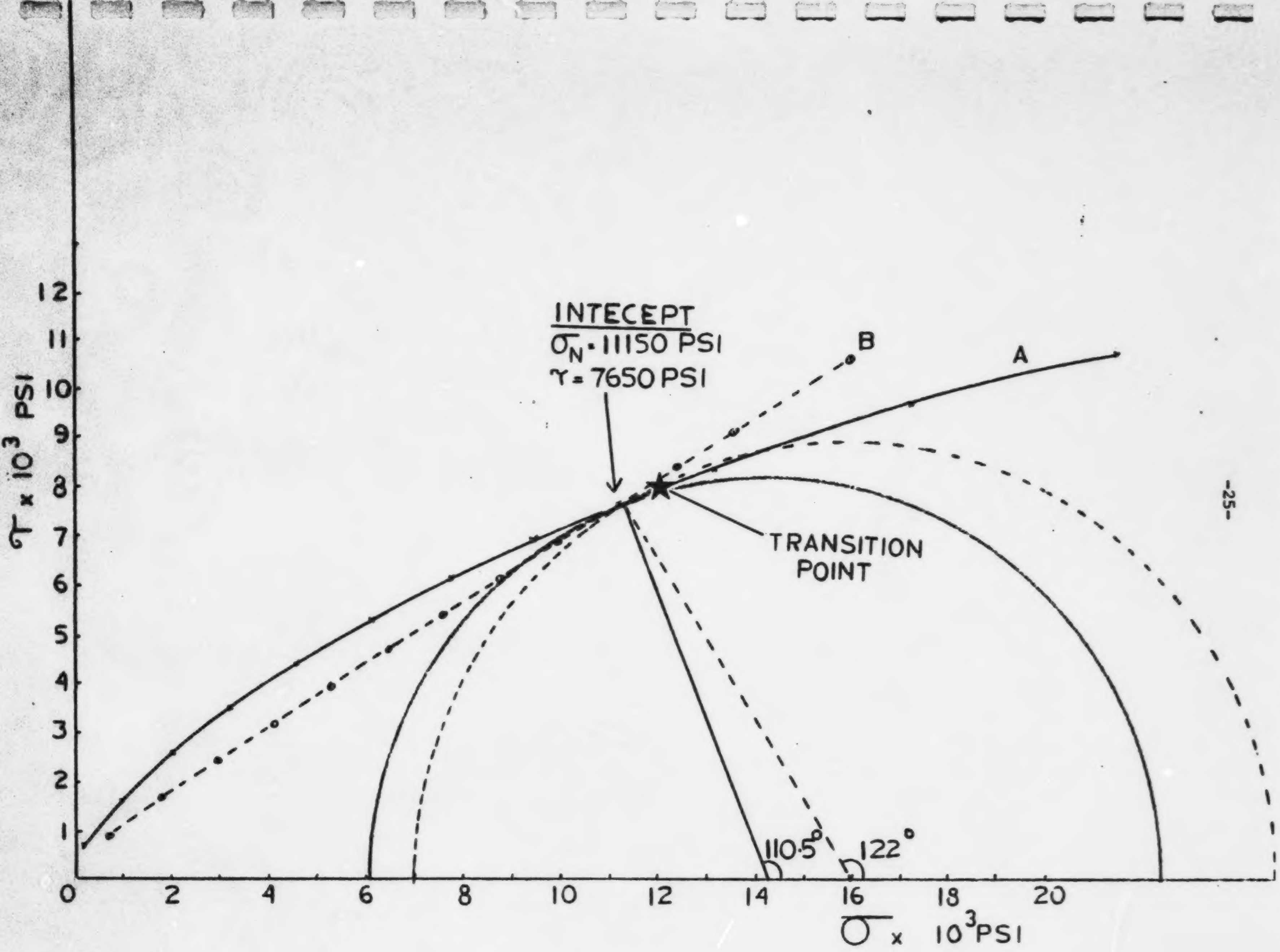

FIGURE 6: INTERSECTION OF THE PEAK AND RESIDUAL STRESS MOHR ENVELOPES

	A. Peak Stress Failure Plane	B Residual Stress Plane
α	20.6°	32.0°
$2\theta = 90 + \alpha$	110.6°	122°
θ	55.3°	61°

This is also illustrated in Figure 6 by drawing the Mohr's circles for each curve at the point of intersection. It is clearly seen that these circles represent different stress conditions acting on the specimen. Hence this point of intersection cannot be the transition point.

3.1.3 Determination of the transition point

Before determining the transition point let us first re-state the definition of the transition point given in the Phase 1 Report. The brittle/pseudo-ductile transition point is defined as the point on the Mohr envelope of failure (peak stress envelope) where the shear resistance to sliding on the failure plane equals the shear resistance to fracture on that plane.

Consequently the σ_1 and σ_3 values for fracture along that plane must be equal to the σ_1 and σ_3 values for sliding on that plane. i.e. the transition point will occur at the position where the two σ_1 versus σ_3 graphs intersect, as shown in Figure 7. From equation (8) this will occur when:-

$$a_1 + b_1 \sigma_1^{c_1} = a_2 + b_2 \sigma_1^{c_2} \qquad (12)$$

where a_1, b_1, c_1, and a_2, b_2, and c_2 are the Balmer parameters for the peak and residual stress envelopes respectively.

For this particular data set, using the a, b and c values given in Table 4, this equation yields:-

$$\sigma_1 = 23{,}337 \text{ psi}$$

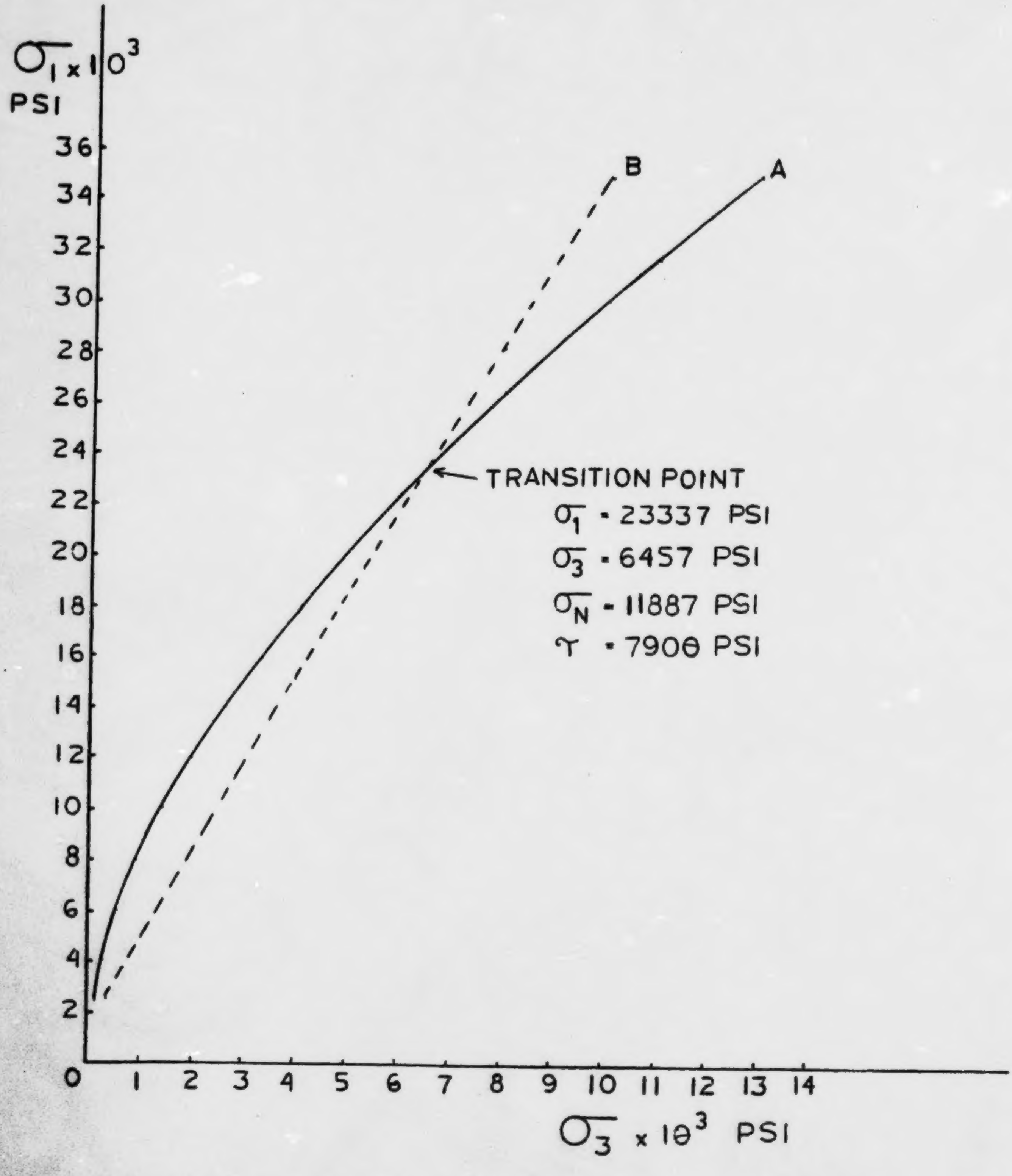

FIGURE 7: TRANSITION POINT FOR THE PEAK AND RESIDUAL σ_1 vs σ_3 RELATIONSHIP

and substituting this value of σ_1 into equation (8) gives:-

$$\sigma_3 = 6457 \text{ psi}$$

Further, substituting the value of σ_1 into the parametric form of the peak stress envelope (a_1, b_1, c_1) gives the normal stress σ, and the shear stress τ at the transition point, on the failure plane as:-

$$\sigma = 11{,}887 \text{ psi}$$
$$\tau = 7{,}900 \text{ psi}$$

This transition point has also been indicated on Figure 6 - reconfirming that the point of intersection of the peak and residual stress envelopes is close to, but not exactly at, the transition point.

3.1.4 Conclusions with respect to the transition point

(i) The analysis of this data for Pittsburgh coal indicates that the transition point exists and that it can be obtained from triaxial peak and residual stress data.

(ii) For this specific coal, it would be expected that at confining pressures greater than σ_3 = 6460 psi the coal specimens would have yielded, with no difference between the peak and residual stresses at failure. Unfortunately the experimental data was only obtained up to a confining pressure of 5000 psi.

It is strongly recommended therefore that when carrying out triaxial tests on coal the confining pressure should be taken to as high a level as the apparatus permits, which often is up to 10,000 psi with standard modern equipment.

(iii) The Mohr envelope for failure (peak stress) is strongly curvilinear ($c = 1.7$) and a very good fit to the data is obtained using the Balmer form of the Mohr envelope.

(iv) The Mohr envelope for the residual stress data is almost a straight line ($c = 1.06$) this will be discussed further in the next section.

(v) Above all, the fact that the transition point does exist for this coal means that a change in the mode of failure must occur beyond the transition point. This is taken as very strong evidence that the proposed failure criterion does in fact apply to at least this coal.

3.1.5 Notes on the residual stress envelope

It is seen from Figure 5B that the Mohr envelope for the residual stress data is almost a straight line (c = 1.06). If c = 1.0 then the Balmer form of envelope reduces to a straight line. For practical purposes, within the limits of experimental error, any envelope with c < 1.1 for the range of data considered can probably be approximated by a straight line over this range of data. However care should be taken not to extend this line much beyond the range of data considered.

Since in this case c = 1.06, then a straight line approximation is acceptable. This approximation has been made for this case and Figure 8 shows the resulting straight line envelope and the principal stresses are related by:-

$$\sigma_3 = -368.75 + 0.2947\,\sigma_1$$

$$\text{i.e.}\quad \sigma_1 = 1251.3 + 3.39\,\sigma_3$$

and the Mohr envelope by:-

$$\tau = 1251.3 + 0.649\,\sigma$$

3.1.6 Determination of the coefficient of sliding friction, using the residual stress envelope

Consider the physical meaning of the residual stress envelope. It describes the shear and normal stresses acting on a plane described by the angle:-

$$\alpha = \tan^{-1} 0.649 = 33^{\circ} \qquad (\theta = 61.5^{\circ})$$

when slip is occuring on the fracture plane which is at an angle given by:-

$$\alpha = 20.6^{\circ} \qquad (\theta = 55.3^{\circ})$$

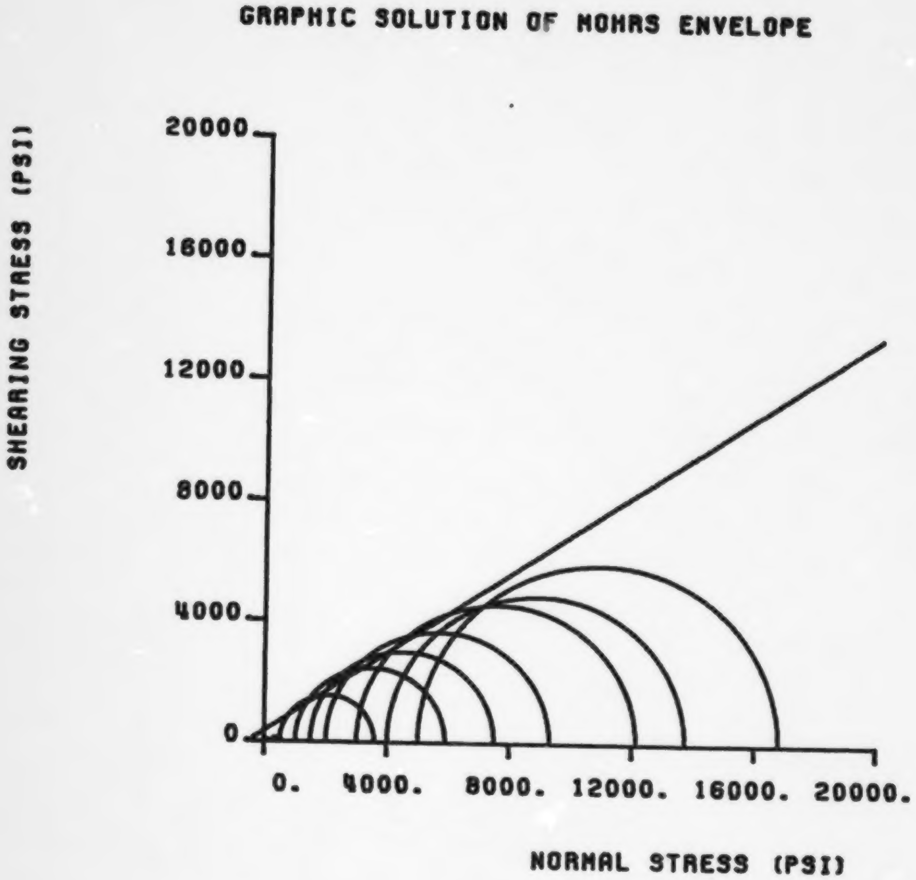

FIGURE 8: STRAIGHT LINE APPROXIMATION OF THE RESIDUAL STRESS ENVELOPE

Thus 0.649 is not the coefficient of friction for sliding on the fracture plane.

However, the coefficient of friction for sliding on the fracture plane can be determined by firstly, calculating the angle of the fracture plane with the horizontal (θ_p) from the peak stress envelope, then determining the residual major principle stress σ_{1R} for the same confining pressure $\sigma_{3p} = \sigma_{3R}$ and finally resolving τ_R and σ_{NR} acting on the failure plane at angle θ_p. The slope of the τ_R, σ_R curve will be the coefficient of sliding friction.

These calculations have been performed for this example and are given in Table 5. From these calculations it is seen that the τ_R, σ_R relationship is given by:-

$$\tau_R = 348.25 + 0.6346\ \sigma_R$$

and thus $\mu = 0.6346$ and the angle of friction $\phi_B = \tan^{-1} 0.6346 = \underline{32.4^o}$

It is noted that this angle 32.4^o is quite close to the 33^o angle obtained had we not performed this correction to account for the different planes. In practice it would therefore seem likely that, within the limits of experimental occuracy, it is probably unnecessary to perform this correction and that the slope of the residual stress envelope gives a good approximation to the coefficient of sliding friction.

3.1.7 Conclusions with respect to the residual stress envelope

(i) For this data set, the residual stress envelope can be approximated by a straight line.

(ii) If the Balmer parameter c is < 1.1 it is safe to make such approximation.

(iii) The slope of the straight line residual stress envelope is not the coefficient of sliding friction because sliding is not taking place on the plane described by this envelope.

(iv) The residual stress data can however be used to calculate the residual normal and shear stresses acting on the failure plane during sliding on this failure plane. This relationship will also be a straight line if the residual stress envelope is a straight line. The slope of this τ_R, σ_R line will be the coefficient of sliding friction. i.e. for this data set:-

TABLE 5: DETERMINATION OF THE COEFFICIENT OF SLIDING FRICTION FROM THE RESIDUAL STRESS ENVELOPE

From the Peak Stress Envelope			From Residual Stress Envelope		τ_R for slip on failure plane	σ_{NR} for slip on failure plane
σ_{1P}	σ_{3P}	$2\theta^o_p$	σ_{3R}	σ_{1R} (for slip on failure plane)	$\frac{\sigma_{1R}-\sigma_{3R}}{2}\ \mathrm{Sin}\theta_p$	$\frac{\sigma_{1R}+\sigma_{3R}}{2} + \frac{\sigma_{1R}-\sigma_{3R}}{2}\ \mathrm{Cos}\ 2\theta_p$
2500	23	1448	23	1329	376	142
5000	355	136	355	2454	729	649
7500	831	130.8	831	4068	1225	1392
10,000	1433	125.5	1433	6109	1903	2413
12,500	2152	121.8	2152	8546	2717	3664
15,000	2980	118.6	2980	11353	3675	5162
17,500	3910	115.8	3910	14506	4769	6902
20,000	4938	113.46	4938	17991	5987	8866
23,337	6457	110.6	6457	23140	7808	11863

$\sigma_{1R} = 1251.3 + 3.39\ \sigma_{3R}$

$\tau_R = 348.25 + 0.6346\ \sigma_R \quad (r = 0.999)$

$\mu = 0.6346 \quad \tan^{-1}\mu = 32.4^o$

$$\mu_B = 0.6346, \qquad \phi_B = 32.4^{\circ}$$

(whereas, if we had incorrectly assumed that the slope of the residual stress envelope gave this coefficient then we would have obtained $\mu = 0.649$, $\phi_B = 33^{\circ}$).

(v) In practice, it would appear that the difference between the values of ϕ_B obtained correctly and incorrectly are probably with the limits of experimental accuracy. Thus an approximation assuming that the slope of the residual stress envelope is equal to the coefficient of sliding friction, whilst not strictly true, probably yields a value within the limits of experimental accuracy.

3.1.8 Errors caused by assuming a single parameter parabolic Mohr envelope

As noted in Section 3.1.2 the preceeding case history has made use of the much superior Balmer form of Mohr envelope. However, the model developed in the Phase 1 Report uses the single parameter parabolic Mohr envelope of the form

$$\tau^2 = A\sigma + A^2/4$$

Although deemed acceptable at the time of the model development, this form does not give the best of fits to the triaxial data. For example, Figure 9 gives the peak stress envelope determined for this Pittsburgh coal data in this form. The equation is:-

$$\tau^2 = 3302\,\sigma + (3302^2/4)$$

Comparing this envelope with the Balmer form (Figure 5A) clearly shows the Balmer envelope to be much the better fit to the data. Consequently the equations given for the failure criteria in the model ought to be re-written, and the program modified, to allow the use of this superior form of envelope. This could be easily done but has not been done at this stage due to time limitations composed by the contract; whilst the use of the Balmer envelope will result in a refined and more accurate model, it does not affect any of the basic principles involved in the overall model development.

The single parameter form of Mohr envelope can also be very useful as a first approximation if a full set of triaxial data for the coal is unavailable. In many cases in the literature only the uniaxial strength, σ_c, is given. Consequently the Balmer form of envelope cannot be derived whereas, since $A = \sigma_c/2$, the less satisfactory parabolic form can be determined and may be used as a first approximation.

It will therefore be interesting to examine the magnitude of errors introduced in the determination of the transition point by using the single parameter parabolic envelope with, for example, this Pittsburgh coal data. (Note that the residual stress envelope will still be kept in the parametric form given earlier in order to ensure that the comparison is only influenced by the change in form of the peak stress envelope).

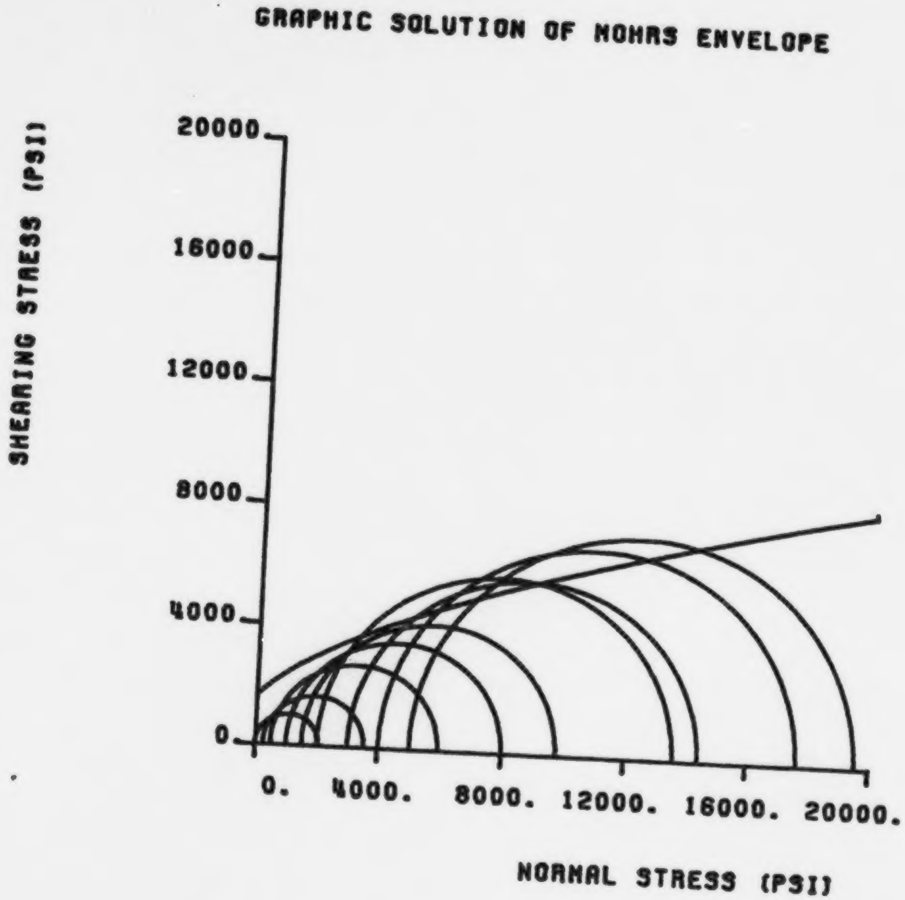

FIGURE 9: PEAK STRESS ENVELOPE IN THE SINGLE PARAMETER PARABOLIC FORM

For failure (peak stress envelope):

$$\tau^2 = A\sigma + \frac{A^2}{4}$$

and the σ_1, σ_3 relationship at failure is given by:-

$$\left\{\frac{\sigma_1 - \sigma_3}{2}\right\}^2 = A\left\{\frac{\sigma_1 + \sigma_3}{2}\right\} \qquad \text{(equation I.1, Phase 1 Report)}$$

and, for the residual stress data (in parametric form)

$$\sigma_{3R} = a_2 + b_2\sigma_{1R}{}^{c_2}$$

The transition point will occur when $\sigma_3 = \sigma_{3_R}$, i.e. when the following equation is satisfied:-

$$\left\{\frac{\sigma_1 - (a_2 + b_2\,\sigma_1{}^{c_2})}{A}\right\}^2 - A\left\{\frac{\sigma_1 \quad (a_2 + b_2\,\sigma_1{}^{c_2})}{A}\right\}^2 = 0$$

This may be solved by successive approximation for σ_1, and then σ_3, τ and σ at the transition point can be calculated.

Using the Pittsburgh data values $a_2 = -305.7$, $b_2 = 0.1585$, $c_2 = 1.06$ and $A = 3302$, then solving gives the transition point as defined below and shown in Figure 10; this is also compared with that determined previously from the parametric envelope:-

Transition Point Stress Conditions	Using the Parabolic Envelope psi	Using the Balmer Envelope, psi	% Difference
σ_1	15338	23337	34.2%
σ_3	4029	6457	37.6%
σ	8032	11887	32.4%
τ	5408	7900	31.5%
2θ	118.86°	110.6	7.5%

It is quite clear from this comparison that there is a significant difference (> 30%) in the stress conditions at the transition point determined by these two methods.

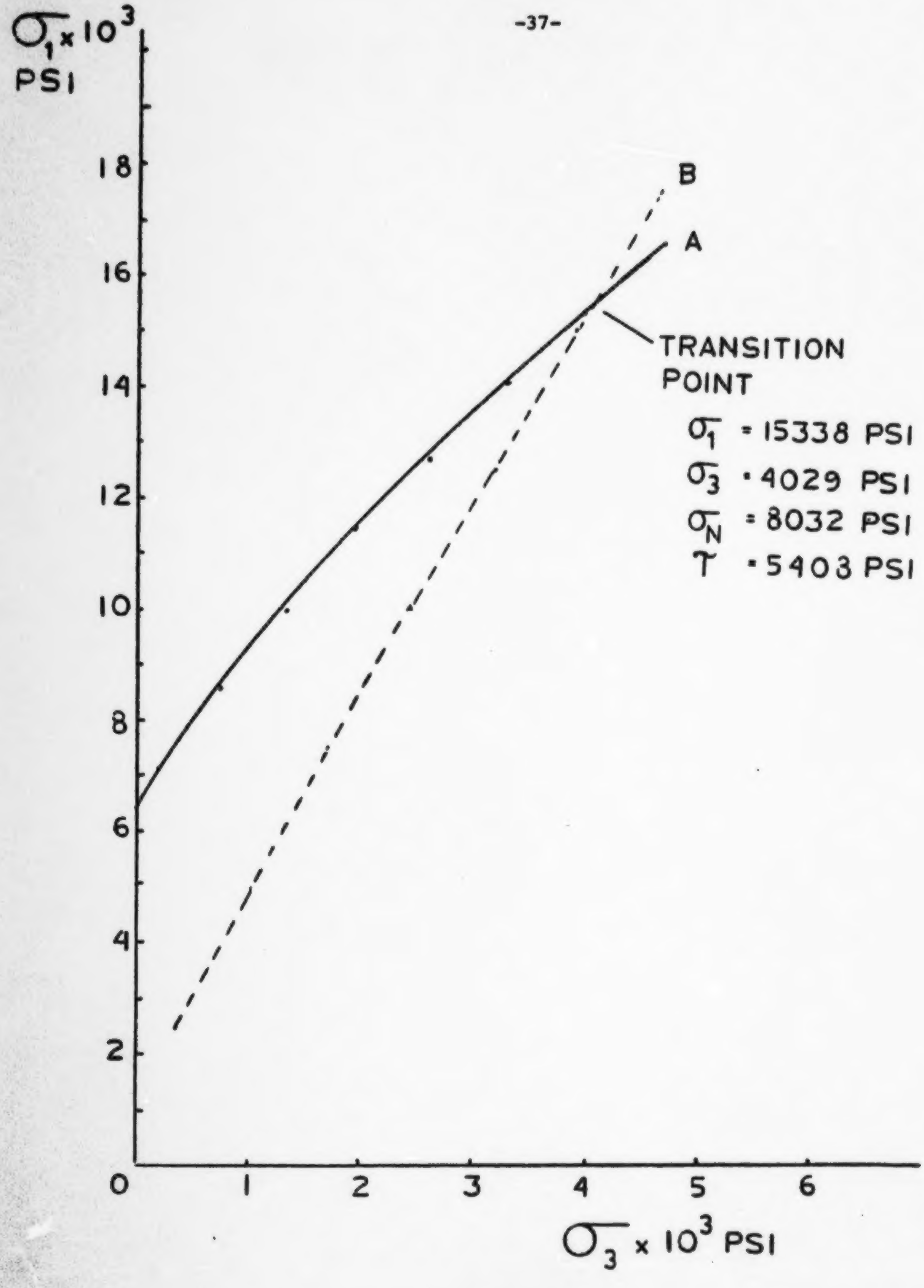

FIGURE 10: TRANSITION POINT USING THE SINGLE PARAMETER PARABOLIC MOHR ENVELOPE

This re-confirms the conclusion drawn above in so far as it is preferable to use the Balmer form of Mohr envelope rather than the single parameter parabolic form, if sufficient data is available.

3.2 Case History #2: Strength Characteristics of Some Other U.S. Coals

3.2.1 Case background

Atkinson and Ko (8) carried out triaxial tests to obtain peak and post-peak (residual) stress data on a number of U.S. Coals. Five of the six coals tested used NX diameter samples (2.157 in.) while the other was EX diameter (0.875 in.). A stiff testing machine was used with four of these coals; this allowed the test to be continued until the post-peak or residual stress plateau was established. The confining pressure, σ_3, ranged from zero to a maximum of 1500 psi.

The failure data for the peak and residual stress conditions for each coal were analysed using "p-q" diagrams. i.e. Rather than representing the failure condition by a Mohr circle, the stress point represented by:-

$$p = \frac{\sigma_1 + \sigma_3}{2} \quad \text{and} \quad q = \frac{\sigma_1 + \sigma_3}{2}$$

was used. This is equivalent to plotting the top point of the Mohr circle and is sufficient to uniquely define the circle, as illustrated in Figure 11.

The plotted stress points define the failure condition for the material, which for a linear case can be represented by the intercept a' and the slope angle α. The angle of internal friction, ϕ, and the cohesion, S_o, of the conventional Mohr analysis are then given by:-

$$\sin\phi = \tan\alpha \qquad \text{and} \qquad S_o = \frac{a}{\cos\phi}$$

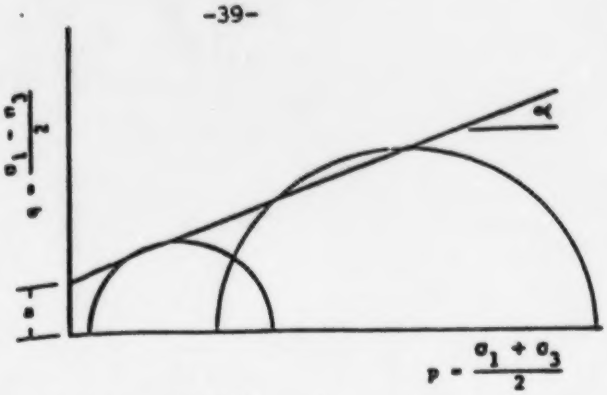
$q = \frac{\sigma_1 - \sigma_3}{2}$
α
a
$p = \frac{\sigma_1 + \sigma_3}{2}$

FIGURE 11: p-q DIAGRAM

TABLE 6: Table of Correlation Coefficient, R

Coal		No. of Data Points	Correlation of Coefficient (Degree of Regression) 4	3	2	1
Beehive	- Peak	35	.971	.969	.964	.961
	- Residual	19	.957	.946	.942	.939
Bruceton	- Peak	15	.984	.983	.982	.980
	- Residual	14	.998	.997	.996	.994
Decker	- Peak	11	.951	.950	.949	.939
	- Residual	10	.995	.994	.993	.987
Federal No. 2	- Peak	20	.969	.968	.968	.967
	- Residual	20	.947	.944	.936	.934
Hanna	- Peak	36	.996	.996	.995	.995
York Canyon	- Peak	56	.990	.989	.988	.987

TABLE 7: Results for Linear Fit of Data

Coal		No. of Data Points	Intercept, psi		Slope Angle, α		R	Cohesion, psi		Angle of Friction, deg.	
			a	Standard Error of a	Tan α	Standard Error of Tan α		c	Standard Error of c	ϕ	Standard Error of ϕ
Beehive	- Peak	35	304.	105.	.7334	.0365	.961	447.	155.	47.2	2.1
	- Residual	19	213.	109.	.6246	.0553	.939	273.	140.	38.7	3.2
Bruceton	- Peak	15	213.	182.	.8037	.0457	.980	358.	306.	53.5	2.6
	- Residual	14	177.	51.	.6789	.0207	.994	298	86.	42.8	1.2
Decker	- Peak	11	739.	151.	.5332	.0653	.939	1242.	254.	32.2	3.7
	- Residual	10	372.	55.	.4749	.0289	.987	625.	92.	28.4	1.7
Federal No. 2	- Peak	20	314.	168.	.7357	.0459	.967	464.	248.	47.4	2.6
	- Residual	20	325.	141.	.6137	.0555	.934	412.	179.	37.9	3.2
Hanna	- Peak	36	141.	40.	.7657	.0133	.995	219.	62.	50.0	0.8
York Canyon	- Peak	56	39.	30.	.8362	.0181	.988	71.	55.	56.7	1.0

3.2.2 Case study results

The p-q failure data from each test series were analysed using a two sample polynomial regression analysis employing a least squares fit. Each set of data was subjected to regression from degree 1 (linear) to degree 4. A measure of the accuracy of a polynomial in fitting the experimental data is given by the correlation coefficient R.

Table 6 lists this correlation coefficient for each degree of regression for all the peak and residual stress data for the six coals. It is seen from this table that very little increase in accuracy is gained by increasing the degree of the fitted polynomial curve beyond the linear curve.
i.e. all data sets are effectively linear over the range of confining pressures considered

The results of the tests on the six coals tested are plotted in Figure 12 and Table 7 presents the results for a linear fit of each data series.

3.2.3 Discussion

The fact that this comprehensive and well documented study shows that for these coals the peak stress envelope is linear can be interpreted as an indication that the failure criterion proposed in the Phase 1 Report is invalid since it requires a curvilinear envelope. However, it should be borne in mind that these tests were limited to relatively low maximum confining pressures not exceeding 1500 psi. It is suggested by the author, but cannot be proved from this data, that had the tests been carried out to higher confining pressures then it is likely that the peak stress envelope would have become non-linear thus allowing an intersection with the residual stress data.

These authors also noted that for the Decker solid coal data the cohesion was considerably higher and the angle of friction lower than for the other coals. They postulated two possible explanations. Firstly that by using EX specimens rather than NX specimens the total volume was reduced by 6 times; thus there may be some size effect in action. If so, this is the first occasion on which data has been

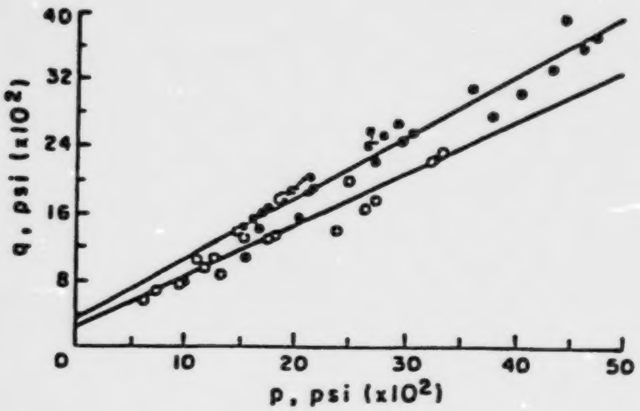

Peak and Residual Strength Data,
Beehive Mine

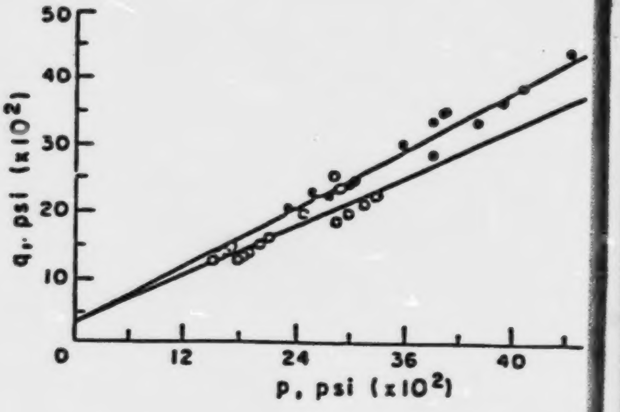

Peak and Residual Strength Data,
Federal No. 2 Mine.

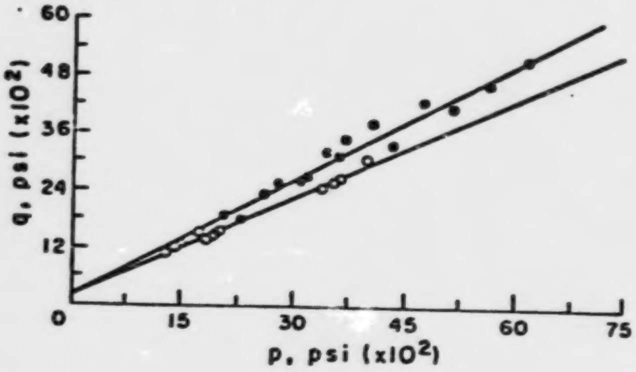

Peak and Residual Strength Data,
Bruceton Mine.

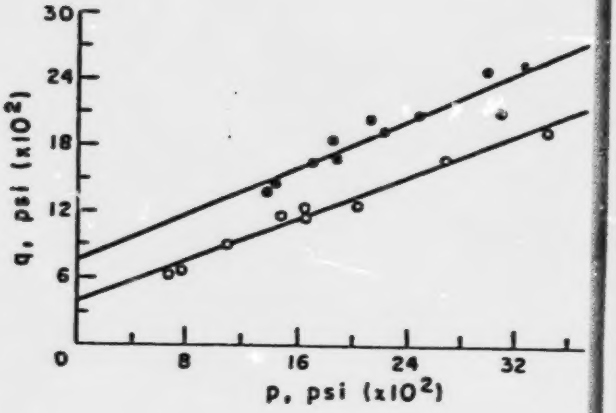

Peak Strength Data, Hanna Site

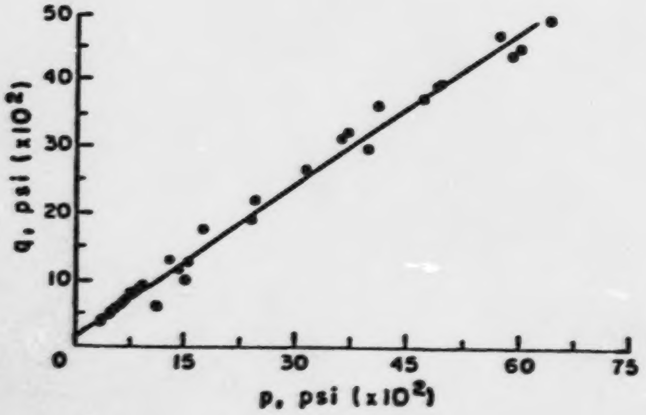

Peak Strength Data, Decker Mine.

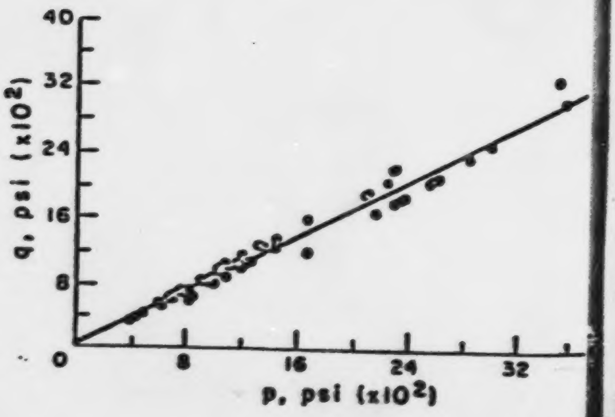

Peak and Residual Strength Data,
York Canyon Mine.

FIGURE 12; p-q DIAGRAMS FOR SOME U.S. COALS (8) recorded which may indicate a size effect on the angle of friction. Their second possible explanation was that this coal is the lowest rank material tested and has the highest moisture content; hence as one descends down the coal rank scale one might expect a reduction in the angle of internal friction.

3.2.4 Conclusion

(i) The results obtained from this study do not back up the concepts of the failure criteria developed in the Phase 1 Report.

(ii) In the authors' opinion this is probably due to not taking the tests to a sufficiently high confining pressure. However, the author cannot prove this from this data.

(iii) These authors suggest the possibility that the angle of internal friction may also be sensitive to specimen size. If so, this would have great significance to the model developed. It is clear that, at some stage, a test program should be carried out to investigate whether or not this is true.

3.3 Case History #3: Strength Characteristics of a U.K. Muddy Siltstone

3.3.1 Case Background

Hobbs (9) carried out triaxial tests on a muddy siltstone determining variation of peak stress with confining pressure for solid specimens and then carrying out "slip tests" under varying confining pressure on the resulting failed specimens. The specimens were 2 inches high by 1 inch diameter. Confining pressures ranged from 0 to 4000 psi.

3.3.2 Case study results

Table 8 gives the results reported by Hobbs. These have been interpreted by the author as follows:-

(i) The Balmer form of Mohr envelope was determined for both the peak stress and broken (slip test) specimen data. These two envelopes are shown in Figure 13A and B.

(ii) Figure 14 shows the intercept given by the σ_1 vs σ_3 relationships for peak stresses at failure and for slip on the fracture surface.

The equations for the σ_1 vs σ_3 relationships are also given in Table 8.

3.3.3 Discussion

(i) It is seen that in this case the peak stress envelope and the slip test envelope are both non-linear, but an intercept still occurs. i.e. transition point exists.

(ii) Hobbs data shows that the slip test envelope has a marked curvature at low levels of confining pressure leading to a cohesion intercept of almost zero. This indicates that these tests show that there is some charge in the coefficient of sliding friction with normal stress at low confining pressures at least; and that the determination of P_B from such tests cannot be relied upon (as discussed previously).

(iii) If the slip test data is treated as linear, then the correlation coefficient is quite good, however this leads to a distinctly different intercept for the transition point, as shown in Figure 14.

TABLE 8: TRIAXIAL STRENGTHS FOR SOLID AND BROKEN MUDDY SILTSTONE (9)

Confining Pressure σ_3 psi	Peak Stress (Solid) σ_1 psi	Stress at Slip (Broken Specimen) σ_1 psi
0	5690+1200	-
50	-	1030+100
100	0	1450+100
250	-	2410+120
500	10,790+1080	3550+140
1000	15,870+1080	5580+180
2000	15,900+1020	8910+240
3000	17,500+2210	-
4000	-	14,410+320

Peak Stress Relationships (Balmer envelope)

$$\sigma_3 = 17.91 + .7269 \times 10^{-17} \sigma_1^{4.849}$$

Broken Specimen Relationship (Balmer envelope)

$$\sigma_3 = -.2296 + .2286 \times 10^{-2} \sigma_1^{1.502}$$

if broken specimen relationship considered linear then

$$\sigma_3 = -445 + .295 \sigma_1 \qquad r = .993$$

GRAPHIC SOLUTION OF MOHRS ENVELOPE

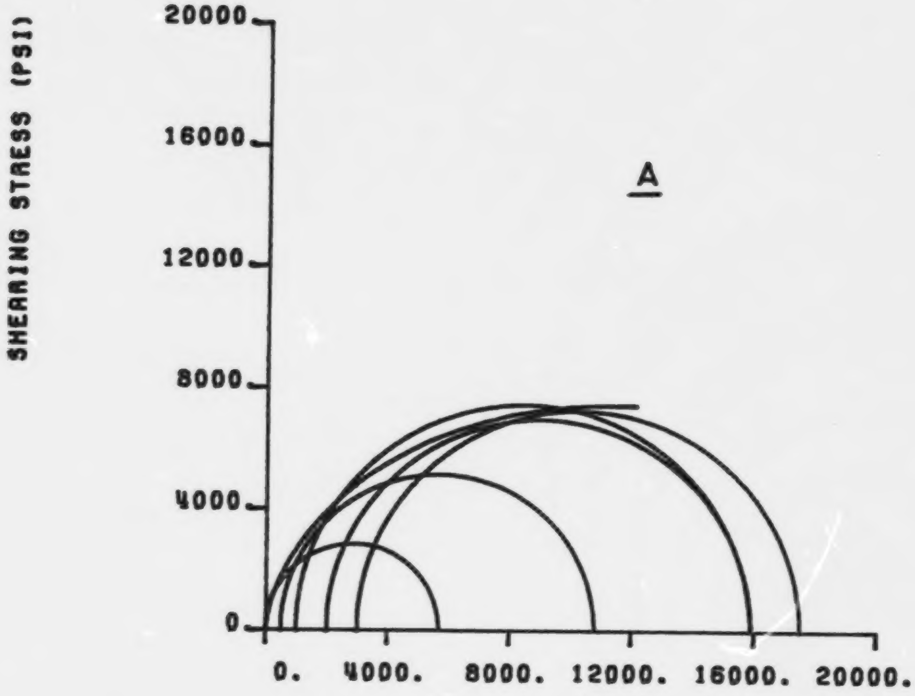

FIGURE 13a: PEAK STRESS ENVELOPE FOR MUDDY SILTSTONE

NORMAL STRESS (PSI)

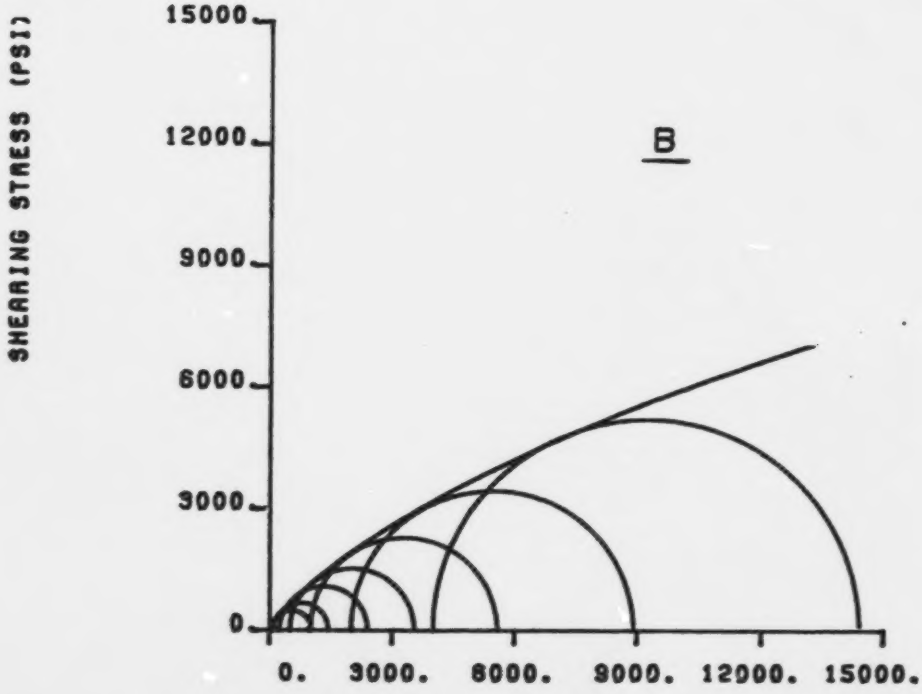

FIGURE 13b: SLIP TEST ENVELOPE FOR MUDDY SILTSTONE

NORMAL STRESS (PSI)

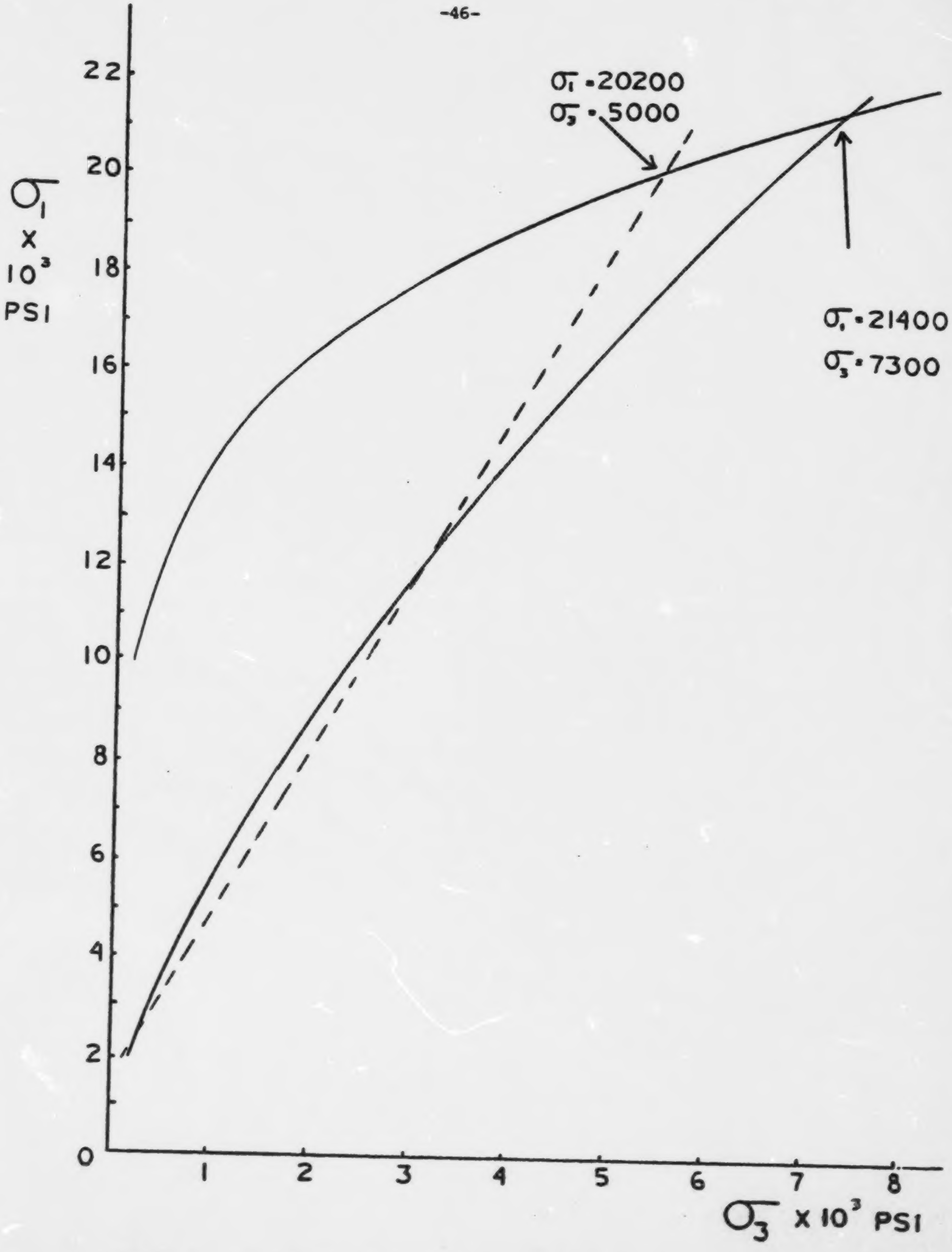

FIGURE 14: TRANSITION POINT FOR MUDDY SILTSTONE

3.3.4 Conclusion

(i) Hobbs data shows that a transition point will occur at relatively low confining pressures (5000-7000 psi) for at least one "coal measure" rock, not just for coal.

(ii) Hobbs range of confining pressures (up to 4000 psi) approached closely the transition point resulting in a large curvature in the peak failure envelope.

(iii) Further work needs to be done to examine whether or not the angle of friction for broken specimens changes with normal stress.

3.4 Case History #4: Specimens That "Did Not Fail Abruptly"

3.4.1 Case Background

Lowall and Holland (10) investigated the effect of varying coal specimens height while the lateral dimensions were held nearly constant at 3 inches on each side. They showed that the results fitted the relationship:-

$$\frac{\sigma_p}{\sigma_c} = 0.70 + 0.30 \left(\frac{B}{H}\right)$$

very well for (B/H) ratios up to about 8, for these specimens that failed abruptly.

However, Holland (11, 12) commenting on these results reported that some of the specimens having a (B/H) ratio of 4.9 or higher did not fail abruptly. Table 9 gives the particulars of these tests together with Hollands footnotes on these specimens.

Holland observed that "While probably it would be incorrect to say that the specimens did not fail, yet there was no point during the application of load when it could be stated definitely that failure occured. The bending of tool steel bearing plates, denting of soft steel bearing plates, and distinct imprint of the round holes on the coal specimen suggest that the coal was forced into a plastic state. Whenever these specimens were examined after loading they were intact (except around the edges) but were rather fragile. When the specimen was broken, shear surfaces apparently could be seen, but they were very smooth and polished (slickensided)".

With respect to the individual specimens Holland noted "the Beckley coal, having a crushing strength as a three inch cube of 1163 psi was forced into gradual failure at a (B/H) ratio of less than 4.9 and greater than 2.87. The Island creek coal, having a crushing strength of 4725 psi (3 inch cube), failed abruptly when the (B/H) ratio was as high as 6.7, but was forced into gradual failure at a (B/H) ratio of 6.8. The Hernshaw coal, having a crushing strength of 4727 psi failed abruptly at a (B/H) ratio of 6.85 but did not fail abruptly when the (B/H) ratio was raised at 9.61. The Coalburg coal having a crushing strength of 6861 psi, failed abruptly when the (B/H) ratio was 7.82 but when the value of this ratio was increased to 12 the

TABLE 9: SUMMARY OF SPECIMENS THAT DID NOT FAIL ABRUPTLY

Coal	B/H for Specimen	Highest (B/H) for Sudden Failure	3" cube Strength psi	B Inches	H Inches	Maximumum Load lbs	Maximum Stress psi
Beckley[a]	4.9	2.87	1163	2.75	0.561	200,000	26,500 (7936?)[a]
Island Creek[b]	6.8	6.7	4725	3.0	0.441	194.250	21,600
Island Creek[c]	12.0	6.7	4725	3.0	0.250	353,000	39,200
Coalburg[d]	11.5	6.9	6861	2.93	0.256	400,000	46,300
Hernshaw[e]	9.6	7.8	4727	3.0	0.313	201,000	22,300

a. This specimen never completely failed in the sense that it stopped taking weight; at a load of 60,000 lbs (on 7.56 sq. inches) it apparently took load more slowly; compact when taken out of the testing machine, but very fragile. Test discontinued because bearing plate failed. (if we assume "yielding" took place at 60,000 lbs. - the maximum stress on pillar is reduced to 7936 psi)

b. This specimen did not completely fail but bearing plate failed. Area 9 sq. inches.

c. Bearing plate bent but coal still intact. Area 9 sq. inches.

d. Coal did not fail in the sense that it stopped taking load or in that there was a noticeably abrupt change in the rate of taking load. Tool-steel bearing plate bent. Dimension of specimen before testing, ¼ by 2 7/8 by 3 inches; ater testing 3 3/8 by 3¼ by approximately ¼ inch.

e. Coal did not fail in the sense that it stopped taking load or abruptly changed its rate of taking load, but the coal acted to shove 3/8 inch thick bearing plate into 1 inch hole in head of testing machine. The imprint of this hole was clearly visible on the coal specimen.

specimen was forced into gradual failure".

Holland also stated that "The factor that causes the increase in strength as the $(^B/_H)$ ratio increases must be the effect of confining pressure due to friction between the faces of the coal specimen and the bearing blocks of the testing machine".

In the authors' opinion, although the friction between the specimen and the machine undoubtedly effects the results, it is believed that what Holland observed in these tests genuine pseudo-ductile behaviour of the specimens and that this type of yielding failure reported by Holland for specimens with large $(^B/_H)$ ratios is precisely what would be expected from the failure theory developed in the Phase 1 Report. Abrupt failure in the specimen is identical to "catastrophic failure" as defined in the report. It will be demonstrated below that these results reported by Holland can be totally explained by the brittle/pseudo-ductile failure theory.

3.4.2 Critical (B/H) = γ_c ratio

According to the equations developed in the Phase 1 Report, the transition between abrupt (catastrophic) failure and yielding (pseudo-ductile) failure will occur when the depth of the transition point, d_T, just reaches the pillar centre. (i.e. when $^{d_T}/b = 1$)

Now, from equation 86 (Phase 1 Report):-

$$d_T = \left(\frac{1-\mathrm{Sin}\phi_B}{1+\mathrm{Sin}\phi_B}\right) \frac{h}{\tan\phi_B} \quad \log_e \left\{\frac{2\,P_{1T}\,\mathrm{Sin}\phi_B}{P_B\,(1+\mathrm{Sin}\phi_B)} + \frac{(1-\mathrm{Sin}\phi_B)}{(1+\mathrm{Sin}\phi_B)}\right\}$$

Hence the transition between abrupt and yielding behaviours occurs when:-

$$\frac{d_T}{b} = 1 = \left(\frac{(1-\mathrm{Sin}\phi_B)}{(1+\mathrm{Sin}\phi_B)}\right) \frac{1}{\gamma_c} \frac{1}{\tan\phi_B} \quad \log_e \left\{\frac{2\,P_{1T}\,\mathrm{Sin}\phi_B}{P_B\,(1+\mathrm{Sin}\phi_B)} + \frac{(1-\mathrm{Sin}\phi_B)}{(1+\mathrm{Sin}\phi_B)}\right\}$$

i.e. where

γ_c = critical $(\frac{b}{h})$ ratio at transition =

$$\left\{\frac{1-\mathrm{Sin}\phi_B}{1+\mathrm{Sin}\phi_B}\right\}\frac{1}{\tan\phi_B}\quad\log_e\left\{\frac{2\,P_{1T}\,\mathrm{Sin}\phi_B}{P_B\,(1+\mathrm{Sin}\phi_B)}+\frac{(1-\mathrm{Sin}\phi_B)}{(1+\mathrm{Sin}\phi_B)}\right\}$$

where

$$P_{1T}=\frac{A}{2}+\frac{A}{2\mu_B^2}\left\{1+(1+\mu_B^2)^{1/2}\right\}+\left\{\frac{A^2}{2}+\frac{A^2}{2\mu_B^2}\left[1+(1+\mu_B^2)^{1/2}\right]\right\}^{1/2}$$

and $A = \sigma_H/2$ where σ_H = cube strength for a specimen of edge length equal to the height H, and if, k = cube strength of a 1 inch cube, then:-

$\sigma_H = \frac{k}{\sqrt{H}}$, (however this relationship breaksdown for cubes whose height is les than 0.51 inches (see Appendix B). For some specimens H is < 0.51 and in these cases it will be assumed that $\sigma_H = 1.4k$

3.4.3 Calculations

The following series of calculation have been made using Hollands' data and the analytical model equations. Firstly the cube strength for a cube of height equal to the specimen height was calculated. From this value of the cube strength the Mohr constant A was determined. Values for ϕ_B, μ_B (= $\tan^{-1}\phi_B$), and P_B were then assumed and the critical (B/H) ratio = γ_c was determined, as was the P_{1T} value. Finally the specimen strength, $\bar{\sigma}_{PRY}$, for the specimens of the given dimensions was calculated from:-

$$\sigma_{PRY}=\frac{P_B\,(1-\mathrm{Sin}\phi_B)}{2\,b\,\mathrm{Sin}\phi_B}\left[\frac{h}{\tan\phi_B}\left\{e^{\tan\phi_B\left\{\frac{1-\mathrm{Sin}\phi_B}{1+\mathrm{Sin}\phi_B}\right\}\frac{d_T}{h}}-1\right\}-d_T\right]+\left(\frac{b-d_T}{b}\right)P_{1T}$$

Various values of μ_B, ϕ_B, and P_B were tried until a combination was obtained such that simultaneously the critical value γ_c lay between the ranges specified by

Hollands experiments and the final yield strength, $\bar{\sigma}_{PRY}$, was close to that obtained in Hollands experiments. Table 10 tabulates these results with the values of μ_B, P_B, and ϕ_B which satisfied both these requirements.

For example: Using $\phi_B = 28^o$, $\mu_B = \tan \phi_B = 0.5317$ and $P_B = 2$ psi for Island Creek coal we obtain $\gamma_c = 6.82$ and $P_{1T} = 72625$ psi. The value of γ_c is very close to that obtained by Holland's first Island Creek specimen. Calculating the specimen strength of this first specimen yields $\bar{\sigma}_{PRY} = 19{,}415$ psi which is very close (within 5.8%) to the maximum strength obtained experimentally by Holland of 21,600 psi.

If we now apply these same parameters to the second Island Creek specimen we again obtain $\gamma_c = 6.82$ (which falls with Hollands observed range of 6.7 to 12.0) and gives $\bar{\sigma}_{PRY} = 42{,}700$ psi which is within 8.2% of Hollands experimental value for the maximum strength of 39,200 psi.

The same applies for all the tests using the parameters given in Table 10. Note should however be taken of the Beckley coal results. It was not possible to fit these results using realistic input parameters and obtain a maximum strength of 26,500 psi as reported by Holland. However, if we note Hollands footnote "a" (table 9) and assume that yielding occurred when the specimen "took load more slowly", then the experimentally derived strength is reduced to 7936 psi which can be fitted, as shown in Table 10, almost exactly using the assumed parameters listed.

3.4.4 Conclusion

1. All of Hollands experimental data on "specimen which did not fail abruptly" can be explained by the specimen (pillar) strength formulae developed in this study using the brittle/pseudo-ductile failure theory, provided that a judicous choice is made for the input coal parameters μ_B, ϕ_B and P_B.

2. Although an estimate can be made of the Mohr constant A for Hollands cube strength data, we have no data on μ_B, ϕ_B and P_B for these coals. Consequently we must assume arbitary values for these parameters in order to fit the results. Thus this exercise does not "prove" the validity of the formulae derived or of the failure theory. Nonetheless, the fact that the use

TABLE 10: CALCULATIONS USING BRITTLE/PSEUDO-DUCTILE FAILURE THEORY TO EXPLAIN HOLLAND'S RESULTS

Coal	k - 1" cube $k = \sigma_c \sqrt{D}$ psi	H inches	Cube Strength, σ_H for Cube of Height equal to H $\sigma_H = \frac{k}{\sqrt{H}}$ *	"Mohr" Constant $A = \frac{\sigma_H}{2}$	Assumed Coal Properties			Calculated		b inches	h inches	Strength at yield σ_p psi
					μ_B	ϕ_B	P_B psi	Critical $\frac{B}{H}$ $= \gamma$	P_{1T} psi			
Beckley	2014	.561	2688	1344	.404	22°	170	4.19	12,750	1.375	.2805	7934
Island Creek	8183	.441	11458 *	5729	.5317	28°	2	6.82	72,625	1.5	.2205	19415
Island Creek	8183	.250	11458 *	5729	.5317	28°	2	6.82	72,625	1.5	.125	42697
Coalburg	11883	.256	16639 *	8319	.404	22°	75	7.15	78,922	1.465	.128	46560
Bernshaw	8187	.313	6619 *	3309	.325	18°	170	7.82	44,380	1.5	.1565	22035

* **Note:** for these specimens, the height is < 0.51 inches which, it will be remembered, is when $\sqrt{\frac{B}{H}}$ relationship breaksdown for cubes. In this case σ_H is assumed $= \frac{k}{\sqrt{0.51}}$. i.e. it is assumed $\sigma_H = 1.4k$ for a cubes of height <0.51 inches. (See Appendix B)

of values for these input parameters which fall within the range of values derived from other coal tests (and hence are possible) allows the Holland results to be closely fitted is regarded an encouraging and is considered to be very strong indirect evidence as to the validity of these concepts.

3. It should be noted that this is the first rational analytical explanation of Holland's results for specimens which did not fail abruptly. Furthermore the physical descriptions by Holland of the manner in which failure of these specimens took place and of the specimens after failure, closely resemble what would be anticipated from pseudo-ductile yield of the specimens.

3.5 Conclusions with Respect to the Brittle/Pseudo-Ductile Transition Point

The following summarises the conclusions to be drawn from the four case histories on specimen testing reported in this chapter.

1. Kripokov's results for Pittsburgh coal, and Hobb's results for a muddy siltstone cleary show that the brittle-ductile transition point does exist, at least for some rocks, within the stress ranges that can be expected to occur in pillars. This is not confirmed by Atkinson and Ko's work due, it is believed, to their tests being restricted to a too low a range of confining pressures.

2. The fact that the transition point does exist, at least for some rocks, means that a change in the mode of failure beyond this point must occur. This is taken as very strong indirect evidence that the proposed failure theory does apply for at least some rocks.

3. The fact that Holland's work shows there is a critical $(^{B}/H)$ ratio beyond which a specimen ceases to fail abruptly and fails gradually is in complete accordance with brittle/pseudo-ductile failure theory. Furthermore, if a judicous choice for the unknown input parameters is made, Hollands results can be totally explained by the specimen (pillar) model developed in the Phase 1 Report, including not only the value of the critical $(^{B}/H)$ ratio but also the value of the ultimate yield strength.

4. In addition, the physical description given by Holland of the manner and mode of failure of his wide/short specimens and of the appearance of these specimens after failure is in complete accord with what would be anticipated from the model in the Phase 1 Report.

5. The above four major conclusions add up to very strong indirect evidence that the postulated mode of failure and model apply to coal specimens. However, this evidence is all indirect and these postulates cannot have been said to have been proven.

There are also a number of unknown or doubtfull points which require further investigation:-

1. The coefficient of sliding friction, determined either from the residual stress envelope or from the slip test envelope appears to be reasonably constant over a range of medium confining pressures. However, at low confining pressures and at high confining pressures it may vary with normal stress. Further work is needed to examine this point.

2. It is assumed that $\mu_B = \tan^{-1} \phi_B$. The data from the literature neither confirms nor denies this assumption. Further work is needed to clarify this point.

3. Atkinson and Ko raise the possibility that μ_B may also be size affected. There is no clear evidence either way. Further work should be done to examine this point.

Each of the above points with respect to μ_B and ϕ_B when clarified will modify exactly how the transition point is accurately determined; however it will change none of the principles of the mechanisms postulated.

Likewise it has been shown that the use of Balmer form parametric Mohr envelopes gives a much better description of the failure envelope then does the single parameter parabolic form of envelope. Hence, if sufficient triaxial data is available, the Balmer form of Mohr envelope should be used. This will necessitate the re-stating of the failure equations at transition and the re-writing of a portion of the model computer program. On the other hand, if the only strength data available is the uniaxial compressive strength, then the single parameter parabolic form of envelope can be used as a first approximation but it will lead to errors in the exact determination of the transition point.

3.6 Recommendations

The following recommendations are made with respect to future work (not part of this contract).

1. A coal specimen testing program should be carried out that is specifically designed to:-
   a) Obtain direct as opposed to indirect evidence for the proposed failure theory.
   b) Investigate whether
      (i) $\mu_B = \tan \phi_B$ is a reasonable assumption
      (ii) whether μ_B and or ϕ_B is affected by specimen size and by normal stress on the failure plane.
   c) Investigate whether the uniaxial size effects discussed in Section 2 are directly applicable under triaxial conditions.

Appendix E outlines the basic principles for such a testing program.

4. CASE HISTORIES OF RELEVANCE TO THE STRESS DISTRIBUTIONS ACROSS PILLARS

4.1 Case History #5: Stress Measurements in Coal Pillars

4.1.1 Case Background

Leeman and van Heerden (13) carried out a series of stress measurements in pillars in a S. African coal mine. The tests were conducted in three coal pillars which were located in the centre of a large mined out area approximately 480 ft. below surface. The pillars were normally 50 ft. square, separated by bords (rooms) 20 ft. wide. This corresponded to approximately 50% extraction. The coal seam was approximately 24 ft. thick of which 10 ft. was being mined leaving 14 ft. of coal in the roof. The seam was approximately horizontal in the test area.

The stress determination in two of the pillars (pillar X and pillar Y) were made by overcoring borehole deformation meters. Figure 15 shows the results obtained from borehole #1 in pillar X. This borehole was at the mid height of the pillar. (a second borehole below this centre line has been ignored in this exercise). Figure 16 shows the results obtained from borehole #3 at the mid-height of the pillar Y. In addition a slotting technique was used in pillar Z to determine the pillar stresses; however this only yielded one data point on the axis of interest to us. i.e. on the mid height, centre of the pillar section.

Since these pillars are all under the same stress concentration, at the same depth, and are the same size, the author has re-plotted this data on Figure 17, which shows the measurements of the vertical stresses measured across the mid height of a pillar on one half of the pillar width. (i.e. symmetry is assumed and the Y data is assumed to be a "mirror" image around the centre, thus allowing all data to be plotted on one side of the centre line).

4.1.2 Elastic Solutions

Leeman and van Heerden assumed that the vertical normal stress (S_V) in the virgin ground at depth Z (ft) below the surface was given by:-

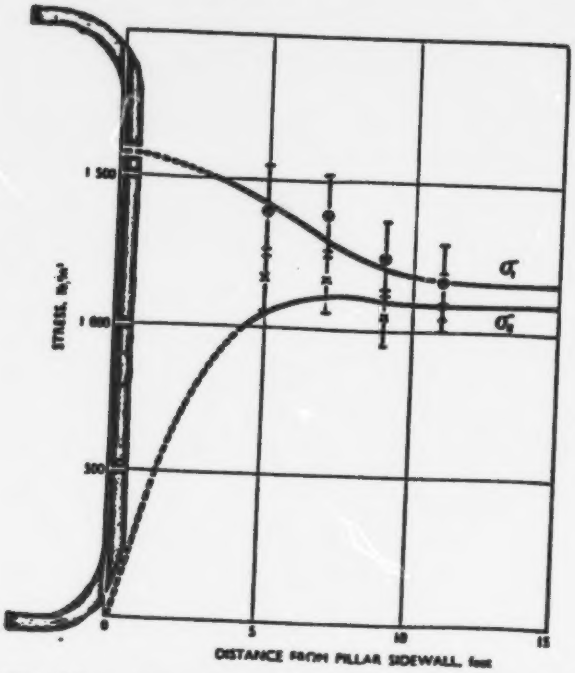

FIGURE 15: RESULTS OBTAINED FROM BOREHOLE NO. 1 IN PILLAR X

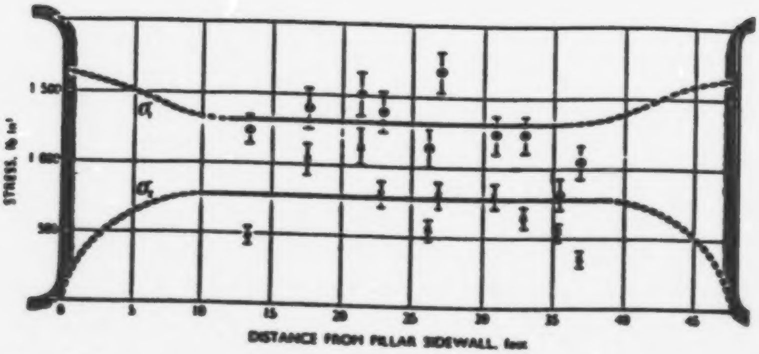

FIGURE 16: RESULTS OBTAINED FROM BOREHOLE NO. 3 IN PILLAR Y

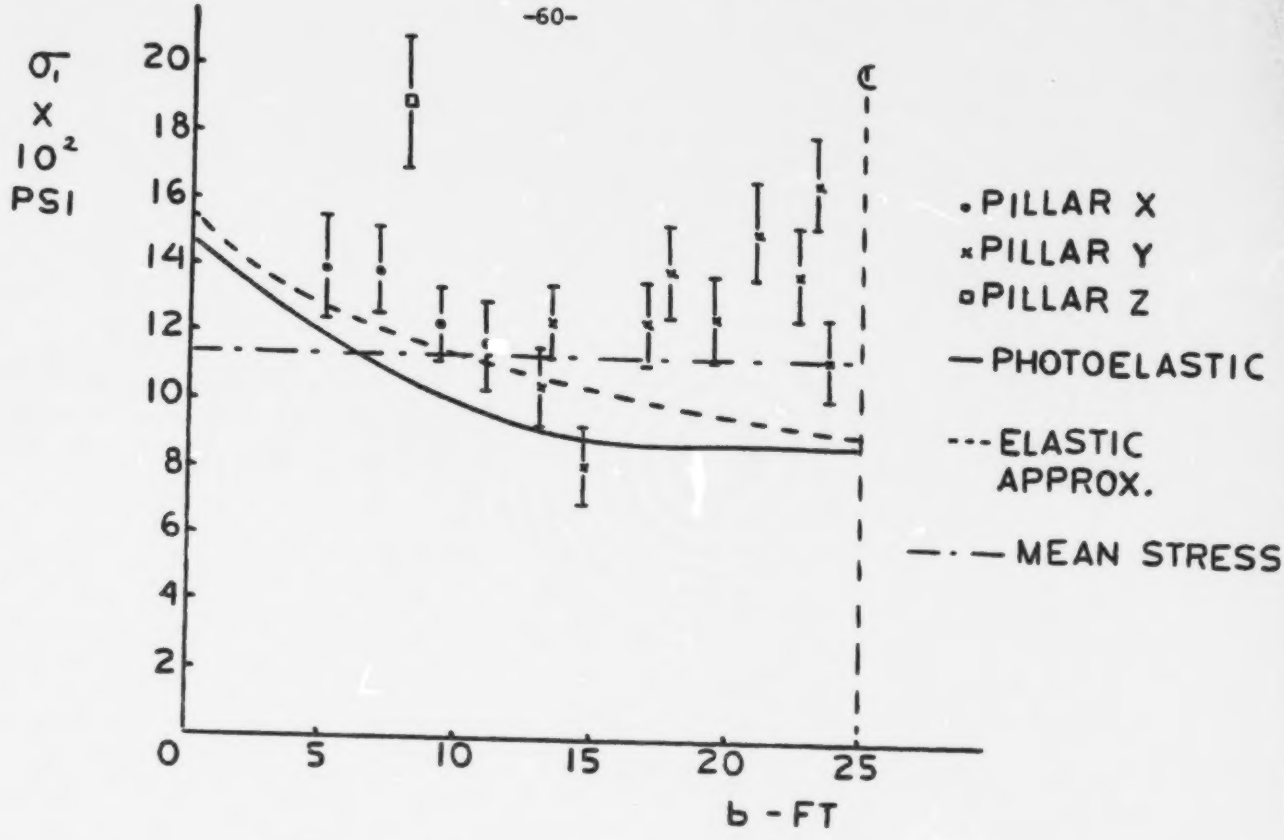

FIGURE 17: ELASTIC SOLUTIONS

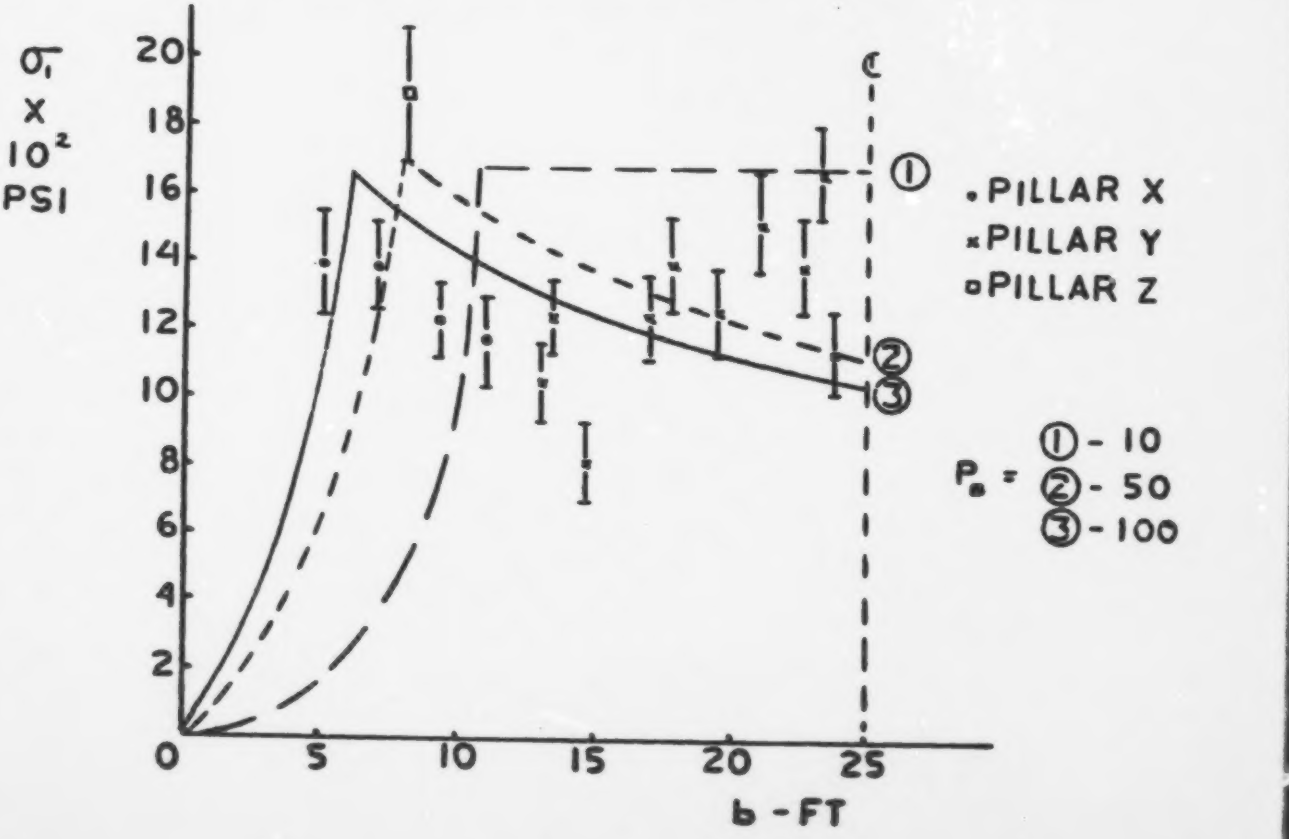

FIGURE 18: MODEL SOLUTION

$$S_v = 1.2 \times Z$$

Thus for this site $S_v = 1.2 \times 480 = 576$ psi

and, since the extraction ratio was 50%, then from tributary area theory, the mean stress acting on the pillar was:-

$$\sigma_p = 1152 \text{ psi}$$

Using this value for σ_p and a photoelastic stress solution for the stress distribution across the pillar, Leeman and van Heerden plotted the vertical stress distribution across the pillar. This solution is shown as the solid line in Figure 17.

The author has also estimated an elastic solution using the approximation method given in the Phase 1 Report (Chapter 4) assuming a rectangular opening (w = 10 ft.), opening height 10 ft. (h = 5 ft.), b = semi pillar width of 25 ft., stress ratio k = 0. This yields a maximum stress concentration at the mid height on the pillar boundary, $Y_{mm} = 2.53$ and the mean stress concentration $\bar{Y} = 1.96$.

The approximate elastic stress concentration distribution across the pillar is given by:-

$$Y = \frac{k_1}{(k_2 + x)} + k_3$$

and, using the above boundary limits, the constants in this equation are determined as:-

$k_1 = 5.8684$, $k_2 = 1.8280$ and $k_3 = 0.5192$

and, assuming as did Leeman and van Heerden, that $S_v = 576$ psi. This yields the approximate elastic stress distribution across the pillar given by the dotted line in Figure 17. It is seen that this approximate solution is in reasonably close agreement with the photoelastic solution.

In comparing the experimental measurements with the photoelastic solution, Leeman and van Heerden concluded that:-

(i) The order of magnitude of the results agree quite satisfactorily

and (ii) If it is accepted that the measuring techniques are sound, then the stresses in the pillars confirm to theoretical predictions.

The author does not fully agree with these conclusions; clearly the results of the elastic and experimental measurements are of the same order of magnitude although the significance of this is not of great importance. However, in the authors opinion, the experimental results do not conform particularly well with the theoretical elastic solutions. In particular, the stresses at the centre of the pillar are all greater than the mean stress, as indeed are almost all the measurements. This suggests that perhaps some fracturing has taken place at the pillar edge, causing load to be shed into the pillar core. This possibility will be examined using the pillar model developed in the Phase 1 Report.

4.1.3 Pillar Model Solution

The main pillar program developed in the Phase 1 Report was used to analyse the stress distribution across the pillar. The analytical route used in the model was the one in which the mean pillar stress concentration was input directly.

The following coal properties were assumed.
Uniaxial cube strength for this S. African coal = k = 5600 psi. (mean for 3 S. African coals listed in Table 2).

Hence uniaxial compressive strength of a cube of height equal to the pillar height of 120 inches = $5600/\sqrt{64}$ = 700 psi.

Hence A = $\sigma_c/2$ = 350 psi. In addition it was assumed for this S. African coal that $\mu_B = \tan \phi_B = 0.65$ ($\phi_B = 33^o$). P_B was varied to obtain the solution which gave the best fit by eye to the experimental data; values of P_B = 10, 50, and 100 psi were used.

It should be noted that the stress at the mid height of the boundary of the pillar = $Y_{mm} \times S_v = 2.53 \times 576 = 1457$ psi which is $> \sigma_c$ (700 psi). Hence fracture must have initiated in the pillar.

Table 11 lists the input data and the results. The resulting stress distribution curve is given in Figure 18.

4.1.4 Discussion and Conclusions

It is seen from Figure 18 that when $P_B = 10$ psi the pillar has yielded and the analytical results do not fit the experimental data. However both the solution when $P_B = 50$ and $P_B = 100$ psi appear to give a reasonable fit to the experimental results. Certainly these two latter solutions give a better fit to the results than did the elastic solutions.

It may be concluded that the analytical method goes give a better fit to the experimental results than do the elastic solutions. The analysis can, with a judicous choice of coal properties, give a better explanation than previously of these results. (Note, however, other combinations of P_B and ϕ_B may also give as good or better solutions).

①

```
CALCULATION FOR RECTANGULAR OPENING

VIRGIN STRESS= 576.0          EXTRACTION RATIO=0.0
LENGTH OF SPAN=    0.0        SEMI-WIDTH OF PILLAR= 25.0
SEMI-HEIGHT OF PILLAR= 5.0  OVERBURDEN DEPTH=  480
DISTANCE "E"=  0.0              SEMI-ROOM WIDTH= 10.0
RATIO "SH/SV"=0.0             NUMBER OF PILLARS IN SPAN= 0
COMPRESSIVE STRENGTH OF BROKEN COAL= 10
MOHR CONSTANT "A"=  350.00
ANGLE OF INTERNAL FRICTION OF BROKEN COAL=33.
POISSONS RATIO FOR SURROUNDING ROCK=0.0
POISSONS RATIO FOR PILLAR ROCK=0.0
COEFFICIENT OF SLIDING FRICTION FOR BROKEN COAL=0.65
YOUNGS MODULAS FOR SURROUNDING ROCK=        0
YOUNGS MODULAS FOR PILLAR ROCK=        0
STRESS REDISTRIBUTION COEFFICIENT=0.50
TOTAL NUMBER OF SLICES=   200
SLICE INTERVAL IN PRINTOUT=   4

THE RESULTS ARE

MEAN STRESS CONCENTRATION=1.960
MEAN PILLAR STRESS:LMS=1128.
MAXIMUM STRESS CONCENTRATION=    2.53
THE PILLAR HAS YIELDED
THE LOAD SHED        =    309.33
THE PILLAR STRENGTH =   1112.00
THE SAFETY FACTOR    =       0.99
THE CRITICAL PILLAR DIMENSION TO AVOID
      A) CATASTROPHIC YIELD IS  12.08
      B) ULTIMATE YIELD IS  35.70
             K1=              5.6744
             K2=              1.8218
             K3=              0.5300

  SLICE    (90-0I)  TAUS/F    TAU      STATUS      PONE   PTHREE ACCUM STRESS
  -----    ------   ------    ---      ------      ----   ------ ------------
  1( 0.3)   30.00    303.1   630.0     FAILED       10.8     0.5      0.0
  8( 2.0)   30.00    308.6   783.6     FAILED       38.2     5.9    286.4
 12( 3.0)   30.17    314.1   800.3     FAILED       48.1    11.5    500.6
 16( 4.0)   30.30    322.4   843.6     FAILED       74.0    20.2    635.2
 20( 5.0)   30.47    334.5   883.5     FAILED      117.3    33.7    764.0
 24( 6.0)   30.73    352.1   921.3     FAILED      184.5    54.6    887.9
 28( 7.0)   31.10    378.7   954.6     FAILED      286.0    87.1   1006.3
 32( 8.0)   31.64    410.6   978.2     FAILED      451.2   137.7   1110.4
 36( 9.0)   32.43    468.8   987.1     FAILED      703.9   216.2   1193.3
 40(10.0)   33.90    515.6   963.3     FAILED     1095.2   338.3   1238.1
 44(11.0)   36.75    580.6   894.8    YIELDED     1700.0   472.4   1203.4
 48(12.0)   36.75    580.6   849.2    YIELDED     1700.0   472.4   1128.8
 52(13.0)   36.75    580.6   819.2    YIELDED     1700.0   472.4   1086.2
 56(14.0)   36.75    580.6   796.6    YIELDED     1700.0   472.4   1056.0
 60(15.0)   36.75    580.6   778.0    YIELDED     1700.0   472.4   1033.1
 64(16.0)   36.75    580.6   758.2    YIELDED     1700.0   472.4   1015.2
 68(17.0)   36.75    580.6   744.6    YIELDED     1700.0   472.4   1001.6
 72(18.0)   36.75    580.6   732.5    YIELDED     1700.0   472.4    991.6
 76(19.0)   36.75    580.6   722.4    YIELDED     1700.0   472.4    985.6

 80(20.0)   36.75    580.6   714.0    YIELDED     1700.0   472.4    984.5
 84(21.0)   36.75    580.6   711.3    YIELDED     1700.0   472.4    990.8
 88(22.0)   36.75    580.6   714.3    YIELDED     1700.0   472.4   1010.3
 92(23.0)   36.75    580.6   731.3    YIELDED     1700.0   472.4   1058.6
 96(24.0)   36.75    580.6   793.1    YIELDED     1700.0   472.4   1190.8
100(25.0)   36.75    580.6  1347.7    YIELDED     1700.0   472.4   2260.9

BRITTLE/DUCTILE TRANSITION POINT TAUF=   580.6
FRACTURE ZONE ENDED ON  44TH SLICE AND EXTENDED 11.0 FT INTO THE PILLAR
DEPTH OF FRACTURE ZONE JUST AT FAILURE 10.87
```

②

```
CALCULATION FOR RECTANGULAR OPENING

VIRGIN STRESS= 576.0          EXTRACTION RATIO=0.0
LENGTH OF SPAN=    0.0        SEMI-WIDTH OF PILLAR= 25.0
SEMI-HEIGHT OF PILLAR= 5.0  OVERBURDEN DEPTH=  480
DISTANCE "E"=  0.0              SEMI-ROOM WIDTH= 10.0
RATIO "SH/SV"=0.0             NUMBER OF PILLARS IN SPAN= 0
COMPRESSIVE STRENGTH OF BROKEN COAL= 50
MOHR CONSTANT "A"=   350.00
ANGLE OF INTERNAL FRICTION OF BROKEN COAL=33
POISSONS RATIO FOR SURROUNDING ROCK=0.0
POISSONS RATIO FOR PILLAR ROCK=0.0
COEFFICIENT OF SLIDING FRICTION FOR BROKEN COAL=0.65
YOUNGS MODULAS FOR SURROUNDING ROCK=        0
YOUNGS MODULAS FOR PILLAR ROCK=        0
STRESS REDISTRIBUTION COEFFICIENT=0.50
TOTAL NUMBER OF SLICES=   200
SLICE INTERVAL IN PRINTOUT=   4

THE RESULTS ARE

MEAN STRESS CONCENTRATION=1.960
MEAN PILLAR STRESS:LMS=1128.
MAXIMUM STRESS CONCENTRATION=    2.53
THE PILLAR IS STABLE
THE FAILURE MODE WILL BE ULTIMATE YIELD
THE PILLAR STRENGTH =    1353.16
THE SAFETY FACTOR    =       1.20
THE CRITICAL PILLAR DIMENSION TO AVOID
      A) CATASTROPHIC YIELD IS   7.92
      B) ULTIMATE YIELD IS  15.24
             K1=              5.6744
             K2=              1.8218
             K3=              0.5300

  SLICE    (90-0I)  TAUS/F    TAU      STATUS      PONE   PTHREE ACCUM STRESS
  -----    ------   ------    ---      ------      ----   ------ ------------
  1( 0.3)   30.00    303.1   639.0     FAILED       54.0     3.4      0.0
  8( 2.0)   30.46    329.2   742.4     FAILED      141.1    30.5    337.8
 12( 3.0)   30.87    352.8   777.0     FAILED      230.7    57.5    483.0
 16( 4.0)   31.46    385.1   789.4     FAILED      370.0   100.5    566.0
 20( 5.0)   32.31    428.0   806.0     FAILED      566.4   158.3    643.4
 24( 6.0)   33.58    484.1   782.8     FAILED      882.6   273.0    683.7
 28( 7.0)   35.36    556.1   711.6     FAILED     1445.0   435.7    684.8
 32( 8.0)   36.75    580.6   619.1    YIELDED     1700.0   488.9    575.2
 36( 9.0)   36.75    580.6   573.2  NOT FAILED   1604.6   488.9    503.8
 40(10.0)   36.75    580.6   536.2  NOT FAILED   1611.6   488.9    454.1
 44(11.0)   36.75    580.6   510.6  NOT FAILED   1553.9   488.9    418.3
 48(12.0)   36.75    580.6   487.2  NOT FAILED   1505.1   488.9    390.4
 52(13.0)   36.75    580.6   466.0  NOT FAILED   1462.6   488.9    367.8
 56(14.0)   36.75    580.6   448.7  NOT FAILED   1424.8   488.9    348.8
 60(15.0)   36.75    580.6   432.3  NOT FAILED   1390.6   488.9    332.6
 64(16.0)   36.75    580.6   417.3  NOT FAILED   1359.3   488.9    318.5
 68(17.0)   36.75    580.6   403.5  NOT FAILED   1330.5   488.9    306.1
 72(18.0)   36.75    580.6   390.6  NOT FAILED   1303.7   488.9    295.1
 76(19.0)   36.75    580.6   378.7  NOT FAILED   1278.8   488.9    285.2

 80(20.0)   36.75    580.6   367.5  NOT FAILED   1255.4   488.9    276.3
 84(21.0)   36.75    580.6   356.9  NOT FAILED   1233.4   488.9    268.1
 88(22.0)   36.75    580.6   347.0  NOT FAILED   1212.7   488.9    260.7
 92(23.0)   36.75    580.6   337.6  NOT FAILED   1193.1   488.9    253.8
 96(24.0)   36.75    580.6   328.7  NOT FAILED   1174.4   488.9    247.5
100(25.0)   36.75    580.6   320.2  NOT FAILED   1156.7   488.9    241.6

BRITTLE/DUCTILE TRANSITION POINT:TAUF=   580.6
FRACTURE ZONE ENDED ON  30TH SLICE AND EXTENDED  7.5 FT INTO THE PILLAR.
YEILD ZONE ENDED ON  36TH SLICE AND EXTENDED  8.8 FT INTO THE PILLAR.
DEPTH OF FRACTURE ZONE JUST AT FAILURE  7.24
```

③

```
CALCULATION FOR RECTANGULAR OPENING

VIRGIN STRESS= 576.0          EXTRACTION RATIO=0.0
LENGTH OF SPAN=    0.0        SEMI-WIDTH OF PILLAR= 25.0
SEMI-HEIGHT OF PILLAR= 5.0  OVERBURDEN DEPTH=  480
DISTANCE "E"=  0.0              SEMI-ROOM WIDTH= 10.0
RATIO "SH/SV"=0.0             NUMBER OF PILLARS IN SPAN= 0
COMPRESSIVE STRENGTH OF BROKEN COAL=100
MOHR CONSTANT "A"=  350.00
ANGLE OF INTERNAL FRICTION OF BROKEN COAL=33
POISSONS RATIO FOR SURROUNDING ROCK=0.0
POISSONS RATIO FOR PILLAR ROCK=0.0
COEFFICIENT OF SLIDING FRICTION FOR BROKEN COAL=0.65
YOUNGS MODULAS FOR SURROUNDING ROCK=        0
YOUNGS MODULAS FOR PILLAR ROCK=        0
STRESS REDISTRIBUTION COEFFICIENT=0.50
TOTAL NUMBER OF SLICES=   200
SLICE INTERVAL IN PRINTOUT=   4

THE RESULTS ARE

MEAN STRESS CONCENTRATION=1.960
MEAN PILLAR STRESS:LMS=1128.
MAXIMUM STRESS CONCENTRATION=    2.53
THE PILLAR IS STABLE
THE FAILURE MODE WILL BE ULTIMATE YIELD
THE PILLAR STRENGTH =    1449.23
THE SAFETY FACTOR    =       1.28
THE CRITICAL PILLAR DIMENSION TO AVOID
      A) CATASTROPHIC YIELD IS   5.43
      B) ULTIMATE YIELD IS  11.00
             K1=              5.6744
             K2=              1.8218
             K3=              0.5300

  SLICE    (90-0I)  TAUS/F    TAU      STATUS      PONE   PTHREE ACCUM STRESS
  -----    ------   ------    ---      ------      ----   ------ ------------
  1( 0.3)   30.00    303.1   629.0     FAILED      108.0     4.8      0.0
  8( 2.0)   30.91    352.1   727.8     FAILED      283.1    59.1    314.5
 12( 3.0)   31.72    393.0   745.8     FAILED      461.4   115.0    415.7
 16( 4.0)   32.88    445.6   730.0     FAILED      740.0   201.7    470.4
 20( 5.0)   34.54    512.9   682.5     FAILED     1172.9   336.6    482.6
 24( 6.0)   36.75    580.6   576.2  NOT FAILED   1686.5   484.7    428.4
 28( 7.0)   36.75    580.6   529.5  NOT FAILED   1589.1   484.7    356.3
 32( 8.0)   36.75    580.6   497.8  NOT FAILED   1523.0   484.7    317.9
 36( 9.0)   36.75    580.6   472.5  NOT FAILED   1470.3   484.7    288.6
 40(10.0)   36.75    580.6   451.1  NOT FAILED   1425.6   484.7    268.1
 44(11.0)   36.75    580.6   432.3  NOT FAILED   1386.5   484.7    250.9
 48(12.0)   36.75    580.6   415.5  NOT FAILED   1351.5   484.7    236.7
 52(13.0)   36.75    580.6   400.3  NOT FAILED   1319.7   484.7    224.6
 56(14.0)   36.75    580.6   386.3  NOT FAILED   1290.5   484.7    214.5
 60(15.0)   36.75    580.6   373.4  NOT FAILED   1263.5   484.7    205.5
 64(16.0)   36.75    580.6   361.3  NOT FAILED   1238.4   484.7    197.6
 68(17.0)   36.75    580.6   350.0  NOT FAILED   1214.9   484.7    190.5
 72(18.0)   36.75    580.6   339.5  NOT FAILED   1192.8   484.7    184.2
 76(19.0)   36.75    580.6   329.5  NOT FAILED   1172.0   484.7    178.4

 80(20.0)   36.75    580.6   320.1  NOT FAILED   1152.3   484.7    173.2
 84(21.0)   36.75    580.6   311.1  NOT FAILED   1133.7   484.7    168.4
 88(22.0)   36.75    580.6   302.6  NOT FAILED   1116.0   484.7    164.0
 92(23.0)   36.75    580.6   294.6  NOT FAILED   1099.1   484.7    159.9
 96(24.0)   36.75    580.6   286.9  NOT FAILED   1083.1   484.7    156.1
100(25.0)   36.75    580.6   279.5  NOT FAILED   1067.7   484.7    152.6

BRITTLE/DUCTILE TRANSITION POINT:TAUF=   580.6
FRACTURE ZONE ENDED ON  24TH SLICE AND EXTENDED  6.0 FT INTO THE PILLAR.
DEPTH OF FRACTURE ZONE JUST AT FAILURE  5.80
```

TABLE 11: MODEL SOLUTIONS FOR CASE HISTORY #5

4.2 Case History #6: Stress Measurements in Coal Pillars

4.2.1 Case Background

Van Heerden (14) carried out a series of stress measurements in coal pillars in the #2 seam, Wolverkrans section, Witbank colliery, S. Africa. These measurements were made by overcoring C.S.I.R. strain cells ("doorstoppers"). Figure 19 shows the locations of the two pillars in the mine and Figure 20 shows an enlarged plan view of the two test pillars and the test borehole locations.

The test area was 35.7 m (117 ft.) below surface. The pillars were 6.4 m (21 ft.) square, 2.7 m (8.86 ft.) high and at 12.8 m (42 ft.) centres; thus the rooms were 6.4 m (21 ft.) wide. the extraction ratio is therefore 75% and, using tributary area theory the mean pillar stress concentration factor, $\bar{Y} = 4.0$. The overburden load is taken as 1.1 x 117 = 128 psi given a mean pillar stress of 4 x 128 = 512 psi (or 3.53 MN/m^2, as plotted by van Heerden on his graphs and mislabelled "overburden pressure" - it is in fact the mean stress applied to the pillar - the overburden stress is 0.88 MN/m^2). All of the test holes were located at the mid height of the pillar, holes #1 and 3 (pillar A) and holes #4 and 6 (pillar B) being drilled from the centre of one face of the pillar (normal boreholes) whilst holes #2 (pillar A) and #5 (pillar B) were drilled along the pillar diagonals. (Diagonal boreholes)

4.2.2 Results

Figures 21 to 24 shows the results of the stress measurements reported by van Heerden. In addition, the solid line on these figures is a theoretical solution derived by van Heerden using the method developed by Salamon and Oravecz (15).

It is noted by van Heerden that "the measured values are also in good agreement with the theoretical stress distribution curve except near the pillar faces where the measured results indicate a greater stress concentration then predicted by theory".

He further notes, for the normal boreholes (Figure 21 and 22) "that the measured values are generally lower than the average vertical overburden pressure (mean pillar stress) in the pillar. This is expected because the theoretical distribution

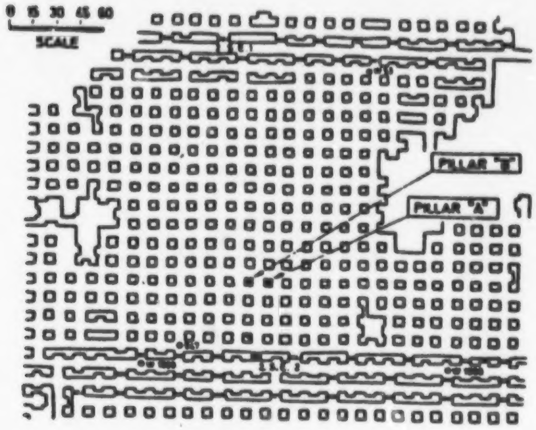
0 15 30 45 60
SCALE
PILLAR "B"
PILLAR "A"

FIGURE 19: TEST SITE AT WITBANK, WOLVEKRANS SECTION NO. 2 SEAM

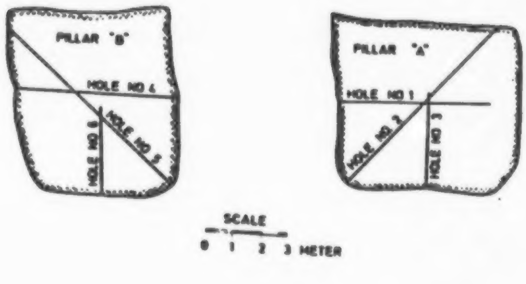
PILLAR "B"
HOLE NO 4
HOLE NO 5
HOLE NO 6
PILLAR "A"
HOLE NO 1
HOLE NO 2
HOLE NO 3
SCALE
0 1 2 3 METER

FIGURE 20: ENLARGED PLAN VIEW OF THE TWO TEST PILLARS

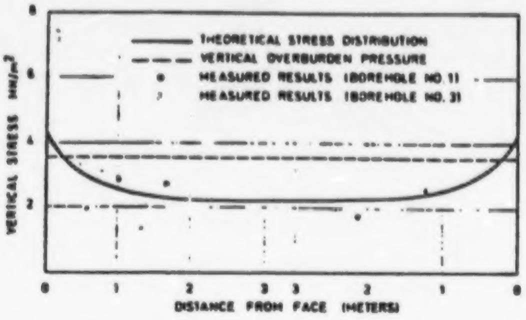

FIGURE 21: RESULTS - NORMAL BOREHOLES - PILLAR A

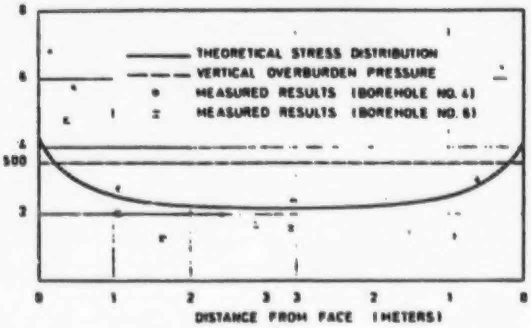

FIGURE 22: RESULTS - NORMAL BOREHOLES - PILLAR B

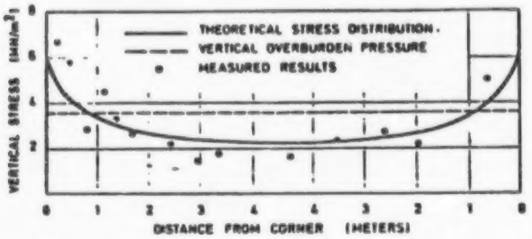

FIGURE 23: RESULTS - DIAGONAL BOREHOLES - PILLAR A

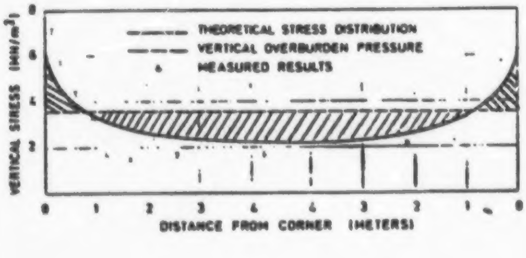

FIGURE 24: RESULTS - DIAGONAL BOREHOLES - PILLAR B

curve also indicates that this should be the case. The reason is that the vertical stress at and near the corners of the pillar is much greater than the stresses at the centre of a pillar face as will be seen from the next two figures" (Figures 23 and 24).

He then considers the diagonal boreholes and concludes that "the measured values are in good agreement with the distribution of vertical stress predicted by theory. Near the pillar corners the measured values are also slightly higher than the theoretical ones. From these curves it can also be deduced that the average measured vertical stress is in good agreement with the average vertical overburden pressure because if the pillar is considered in three dimensions the dotted line indicating the average vertical overburden pressure is exactly the mean value of the theoretical stress distribution in the pillar".

This is all very well, but clearly there is an error somewhere in the presentation of the theoretical results. For compatability of stresses the area of the stress distribution curve under the mean pillar stress line must be equal to the area over this mean stress line. For the normal boreholes this is clearly not the case however that is acceptable, following van Heerden's line of argument, provided that this deficiency is made up from the diagonal boreholes. However it is clearly seen from Figure 23 and 24 that this is not the case. The shaded areas above the line (Figure 24) are clearly much less than the shaded area below the line; likewise with Figure 23. Consequently, somewhere in this presentation there is an error, be it due to miscalculation in the theoretical solution or errors in drafting, which cannot be accounted for.

4.2.3 Comparison of the Model Solution with the Normal Borehole Results

All of the normal borehole results have been replotted in Figure 25, changing to imperial units, as if they applied to one side only of a single pillar. The "theoretical solution" obtained by van Heerden has also been plotted on this Figure. The analytical model will now be used to attempt to reproduce these results.

Now for the Witbank Wolverkrans #2 seam Bieniawski (16) has determined a uniaxial 1 inch cube strength equal to 6200 psi. (i.e. $k = 6200$). Hence the cube

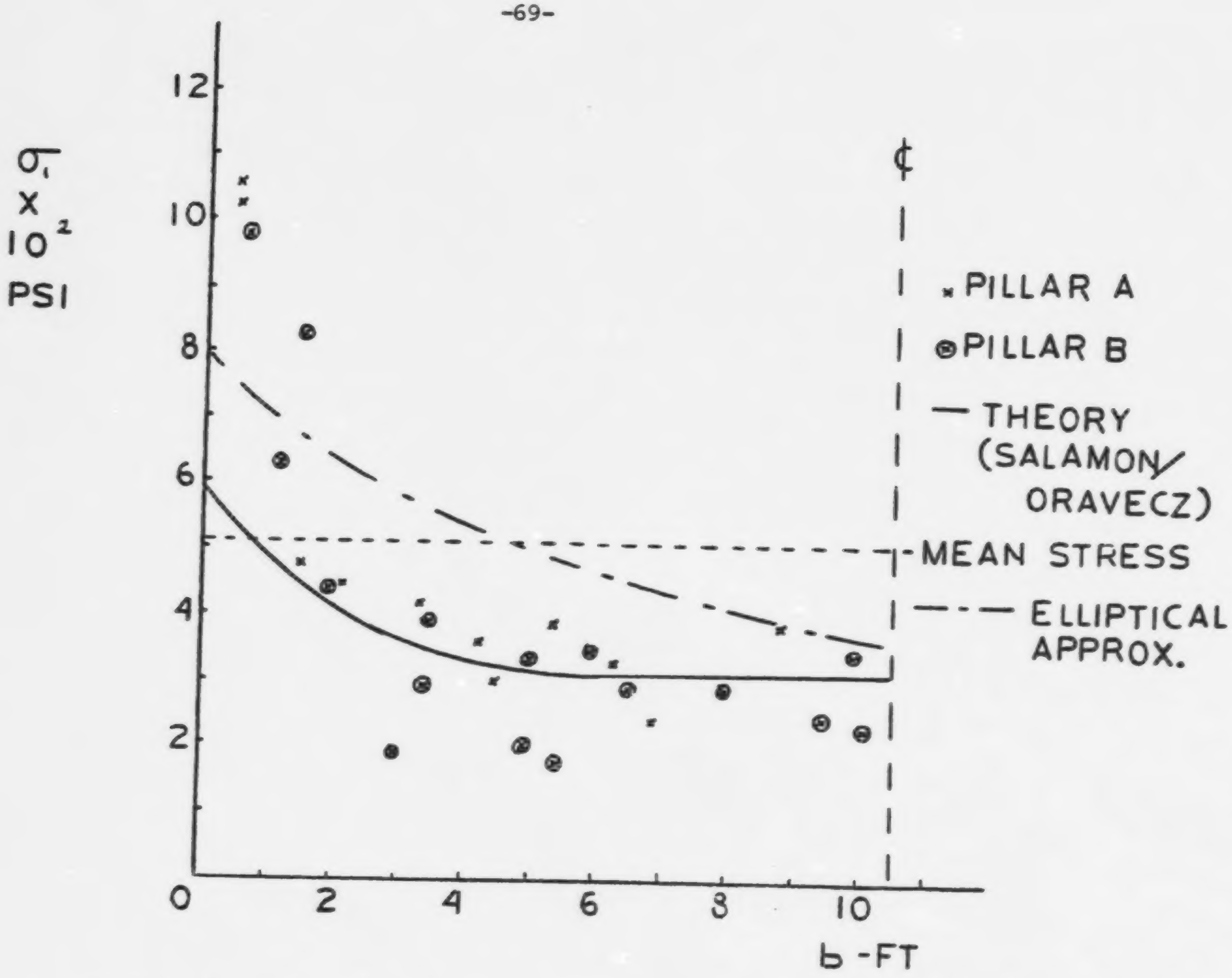

FIGURE 25: COMPARISON OF NORMAL BOREHOLE RESULTS WITH ELASTIC SOLUTIONS

strength for a cube equal to the pillar height H (8.86 ft. = 106 inches, which is > 64 inches) is given by:-

$$\sigma_H = 0.125 \times 6200 = 775$$

i.e. $A = 387 \sim 390$ psi

Now, assuming that the rooms are rectangular, then the maximum stress concentration at the mid height of the side wall is given by equation 21 in the Phase 1 Report as:-

$$Y_{mm} = (2.048 - 0.919k) + 0.572 \log_e (\frac{W}{H}) + 0.09 \left\{(\frac{W}{B} + 1)^2 - 1\right\}$$

which using, stress ratio k = 0, W = 21 ft., H = 8.86 ft. and B = 21 ft. gives:-

$$Y_{mm} = 2.81$$

However, using tributary area theory, with 75% extraction, then the mean pillar stress concentration. $\bar{Y} = 4.0$

i.e. in this case since $\bar{Y} > Y_m$ we must revert to the approximation that $\bar{Y} = Y_{mm} = 4.0$.

i.e. that the stress distribution is approximately uniform and given by:-

$$\sigma_v = 4.0 \times S_v$$
$$\underline{= 4.0 \times 1.1 \times 117 = 515 \text{ psi.}}$$

i.e. the analytic model predicts a uniform stress distribution equal to the mean applied pillar stress. This clearly does not agree in the slightest with van Heerden's measurements.

Further, consider the minimum pillar strength,

$$\sigma_{p\ min} = \frac{\bar{Y}}{Y_{mm}} \cdot 2A$$
$$= 775 \text{ psi} \quad (\text{with } \bar{Y} = Y_{mm})$$

but the mean applied load is only 515 psi. Hence fracture cannot have initiated in the pillar. i.e. the elastic solution (approximation) should apply.

The measured results seem to indicate clearly that the stress distribution is not uniform; the only way that the approximate elastic solution could attempt to fit these results would be to have a situation in which $\bar{Y} < Y_{mm}$. This would only occur if we had a non-rectangular opening. For example: suppose the rooms were elliptical, then for the given dimensions, equation (20), Phase 1 Report, yields $Y_{mm} = 6.12$. Assuming $\bar{Y} = 4.0$.

Then $\sigma_{p\ min} = (4/6.12) \times 775 = 506$ psi

which is approximately equal to the assumed mean applied stress $\sigma_p = 512$ psi. i.e. fracture is on the point of initiating in the pillar. Assuming therefore that it has not just initiated the approximate elastic stress concentration distribution is given by:-

$$Y = \frac{k_1}{(k_2+X)} + k_3$$

when using $Y_{mm} = 6.12$ and $\bar{Y} = 4.0$ yields $k_1 = 3.7447$, $k_2 = -0.32$, and $k_3 = .6132$. The resulting stress distribution is also plotted on Figure 25. This does give a better fit to the results but we have no reason to suppose that the openings in this mine were elliptical in shape. This is therefore not a satisfactory solution.

4.2.4 Conclusion

(i) The analytical model does not fit the measurements given in this paper.

(ii) The only way that an approximate fit can be obtained is to assume that the openings are elliptical rather then rectangular. This does not seem to be a reasonable assumption.

(iii) There would appear to be some error in the theoretical solutions given by van Heerden in this paper. However, assuming that the measurements have been correctly reported, this does not change the conclusion that the analytical model will not describe the results given in this case history.

4.3 Conclusions with Respect to Case Histories for Pillar Stress Distributions

Case History #5 based on Leeman and van Heerden experimental measurements can in fact be better fitted using the analytical model than by using the elastic solution obtained by the original workers. A judicous choice of P_B and ϕ_B allows a reasonable good fit to be obtained. However, other combinations of P_B and ϕ_B may well give equally good or better fits.

Case History #6 based on van Heerden's experimental measurements cannot be fitted by the analytical model. No satisfactory explanation for this lack of fit is available in this case.

5. CASE HISTORIES OF RELEVANCE TO PILLAR STRENGTH FORMULAE

5.1 Case History #7: Salamon and Munros' Pillar Strength Formula

5.1.1 Case Background

Salamon and Munro (17) made an extensive survey of South African coal mines in which the room and pillar mining method was used. From this survey they identified 125 cases comprising 98 stable and 27 collapsed pillars which met the following criteria:-

(i) The mining dimensions in the area of the pillars studied were essentially constant.

(ii) The pillars were approximately square.

(iii) The diameter of the area involved was greater than the depth below surface. i.e. it follows from this that the loads on pillars at the centre of such an area can be closely approximated by tributary area theory. They also assumed that the applied overburden load was given by 1.1 psi/foot of overburden. Hence for square pillars, the mean applied pillar stress, $\bar{\sigma}_p$ is given by:-

$$\underline{\bar{\sigma}_p = \frac{1}{(1-R)} \cdot S_v}$$

where S_v = overburden stress (psi) = 1.1 Z where Z is the overburden depth in feet, and R = extraction ratio = $w\,(w+B)/(w+b)^2$ for square pillars, where w = semi room width, b = semi-room width and B = 2b the pillar width.

(iv) The seams were essentially flat lying with a constant depth of overburden.

It was argued by Salamon and Munro that the ratios of the predicted strengths to the calculated loads at failure, that is, the critical safety factors, form a frequency distribution curve. This distribution is centred around the safety factor of unity. The probability that a pillar will be stable is indicated by the ordinates of the cumulative distribution curve. This assumes that the logarithm of the critical safety factor is normally distributed.

It was assumed that the strength of pillars can be expressed, within the given range of dimensions, as a power function of the height and width of the pillars:-

$$\bar{\sigma}_s = K H^{\gamma} B^{\beta}$$

where H is the pillar height in feet, B is the pillar width in feet, $\bar{\sigma}_s$ is the strength in psi, γ and β are constants and K is the strength of a unit 1 foot cube of coal.

The three values of these unknown constants, γ, β, K were estimated by the method of maximum liklihood. This method also gives an estimate of the logarithmic standard deviation of the distribution. It was shown that the derived strength formula gave a good description of the information obtained from the survey of mining dimensions.

5.1.2 Results

(i) Range of parameters It is important that with such a statistical approach to the pillar strength problem that the derived formula not be extended beyond the range of dimensions considered in the analysis. The table below lists the range of the parameters used in this study for both the stable and collapsed cases.

Range of parameters

Group	Stable	Collapsed
Number of cases in group	98	27
Overburden depth range, Z, feet	65-720	70-630
Range of pillar heights, H, feet	4-16	5-18
Range of pillar widths, B, feet	9-70	11-52
Range of extraction ratios	0.37-0.89	0.45-0.91
Range of width/heights ratios (B/H)	1.2-8.8	0.9-3.6

(ii) Results The values of the parameter K, β and γ derived by Salamon and Munro from this statistical analysis were:-

$$\underline{K = 1322}$$

$$\underline{\beta = 0.46 \pm 0.14}$$

$$\underline{\gamma = -0.66 \pm 0.16}$$

i.e. $$\bar{\sigma}_s = 1322 \, \frac{B^{0.46}}{H^{0.66}}$$

where B and H are given in feet and $\bar{\sigma}_s$ is in lbs/sq. inch.

5.1.3 Discussion

Salamon and Munro argued that since all dimensions were given in feet, the numerical value of K should be taken as the strength of a one foot cube of coal. However, they pointed out that it was unlikely that the obtained value of K would be the actual strength of a one foot cube specimen since this size is well outside the range of dimensions used in the derivation.

Hustrulid (2) pointed out that a in general K will be a constant and have the units of strength only if $\gamma + \beta = 0$. For all other possibilities the units of K would change as B and H change. Thus since $\gamma \neq -\beta$ the units of K are not actually those of strength. Thus the fact that B and H are expressed in feet does not necessarily mean that K is the strength of a unit 1 foot cube.

Bieniawski (16) objected to expressing the strength of coal pillars as a power function of the pillar width and height since this implies that the cube strength (B=H) would continue to decrease indefinitely with increase of side length. This is of course not reasonable but may be possible within the limited range of parameters used in the analysis.

In this analysis it was assumed that the value of K did not vary from coal seam to coal seam. The results of compression tests performed by Bieniawski (17) and by Sowry (19) on 1" cubes from a number of South African coal seams tends to substantiate the validity of this assumption since, with the exception of one locality, the results are all within ± 12.5 per cent range.

Despite the objections raised above, it is clear that the derived equation describes the field data exceptionally well. Further, since this is one of the few attempts that have been made to derive a generalized strength equation based solely on field data and has done so most successfully, it is clear that this study is of prime importance. Consequently it must be a prime study against which the analytical model should be compared.

5.1.4 Summary of the Pillar Strength Formulae derived from the Analytical Model

The analytical approach to coal pillar strengths developed in Part 1 of this study has derived three "pillar strength" formulae which are applicable for different circumstances. These three formulae are:-

$$\bar{\sigma}_{s\,(min)} = \frac{\bar{Y}}{Y_{mm}} \cdot 2A$$

where $\bar{\sigma}_{s\,(min)}$ is the minimum pillar strength possible and is used if $\bar{\sigma}_s$ calculated above is $> \bar{\sigma}_{sF}$ or $> \bar{\sigma}_{sy}$ calculated from the formulae given below. A is the "Mohr constant" for the solid coal, $\bar{Y}$ is the mean pillar stress concentration and Y_{mm} is the maximum stress concentration at the mid height of the side wall of the pillar at its boundary. $\bar{Y}$ is determined from either tributary area theory or Coates pillar formulae and Y_{mm} is determined, for the appropriate shape of adjacent room from equations 18, 20 or 21 in Part I. Note that if Y_{mm} is calculated as $< \bar{Y}$ then Y_{mm} is put equal to $\bar{Y}$ and then $\bar{\sigma}_{s\,(min)} = 2A$.

When $d_T > b$ the pillar fails by brittle fracture and the strength is given by $\bar{\sigma}_{sF}$ as:-

$$\bar{\sigma}_{sF} = \frac{P_B\,(1-\mathrm{Sin}\,\phi_B)}{2b\ \mathrm{Sin}\,\phi_B}\left[\frac{h}{\tan\phi_B}\left\{e^{\tan\phi_B\left\{\frac{1+\mathrm{Sin}\,\phi_B}{1-\mathrm{Sin}\,\phi_B}\right\}\left(\frac{b}{h}\right)} - 1\right\} - b\right]$$

where P_B = uniaxial strength of broken coal

ϕ_B = angle of internal friction of broken coal

h = semi pillar height

b = semi pillar width

d_T = depth of the transition point from brittle to pseudo-ductile yield

where $$d_T = \left\{\frac{1 - \mathrm{Sin}\phi_B}{1 + \mathrm{Sin}\phi_B}\right\} \frac{h}{\tan\phi_B} \mathrm{Log}_e \left\{\frac{2\, P_{1T}\, \mathrm{Sin}\phi_B}{P_B\, (1+\mathrm{Sin}\phi_B)} + \frac{(1 - \mathrm{Sin}\phi_B)}{(1 + \mathrm{Sin}\phi_B)}\right\}$$

where P_{1T} = vertical stress at the transition point between brittle and pseudo-ductile failure and is given by:-

$$P_{1T} = \frac{A}{2} + \frac{A}{2\mu_B^2} \left\{1 + (1 + \mu_B^2)^{1/2}\right\} + \left\{\frac{A^2}{2} + \frac{A^2}{2\mu_B^2} \left[1 + (1 + \mu_B^2)^{1/2}\right]\right\}^{1/2}$$

where A = Mohr constant for the solid coal

μ_B = coefficient of sliding friction of coal on coal

when $d_T < b$ the pillar will fail by pseudo-ductile yield and the strength is given by $\bar{\sigma}_{SY}$ as follows:-

$$\bar{\sigma}_{SY} = \frac{P_B\, (1-\mathrm{Sin}\phi_B)}{2b\, \mathrm{Sin}\phi_B} \left[\frac{h}{\tan\phi_B} \left\{ e^{\tan\phi_B \left\{\frac{1+\mathrm{Sin}\phi_B}{1-\mathrm{Sin}\phi_B}\right\}\left(\frac{d_T}{h}\right)} - 1\right\} - d_T\right] + \left(\frac{b-d_T}{b}\right) \cdot P_{1T}$$

where all the parameters have been defined above.

Figure 26 shows the program logic for determining the pillar strength using these formulae, assuming tributary area theory and rectangular rooms.

5.1.5 Comparison of Analytical Pillar Strength Formulae with that of Salamon and Munro

1. Since the formulae derived from the anlaytical method and that of Salamon and Munro are in totally different forms, a direct comparison is not possible.

2. The only possible method of comparison is therefore to calculate the pillar strengths using the analytical formulae, for parameters within the range given by Salamon and Munro, and then to treat the strengths so calculated as "real data" and correlate this data with B and H in form derived by Salamon and Munro. This will be attempted.

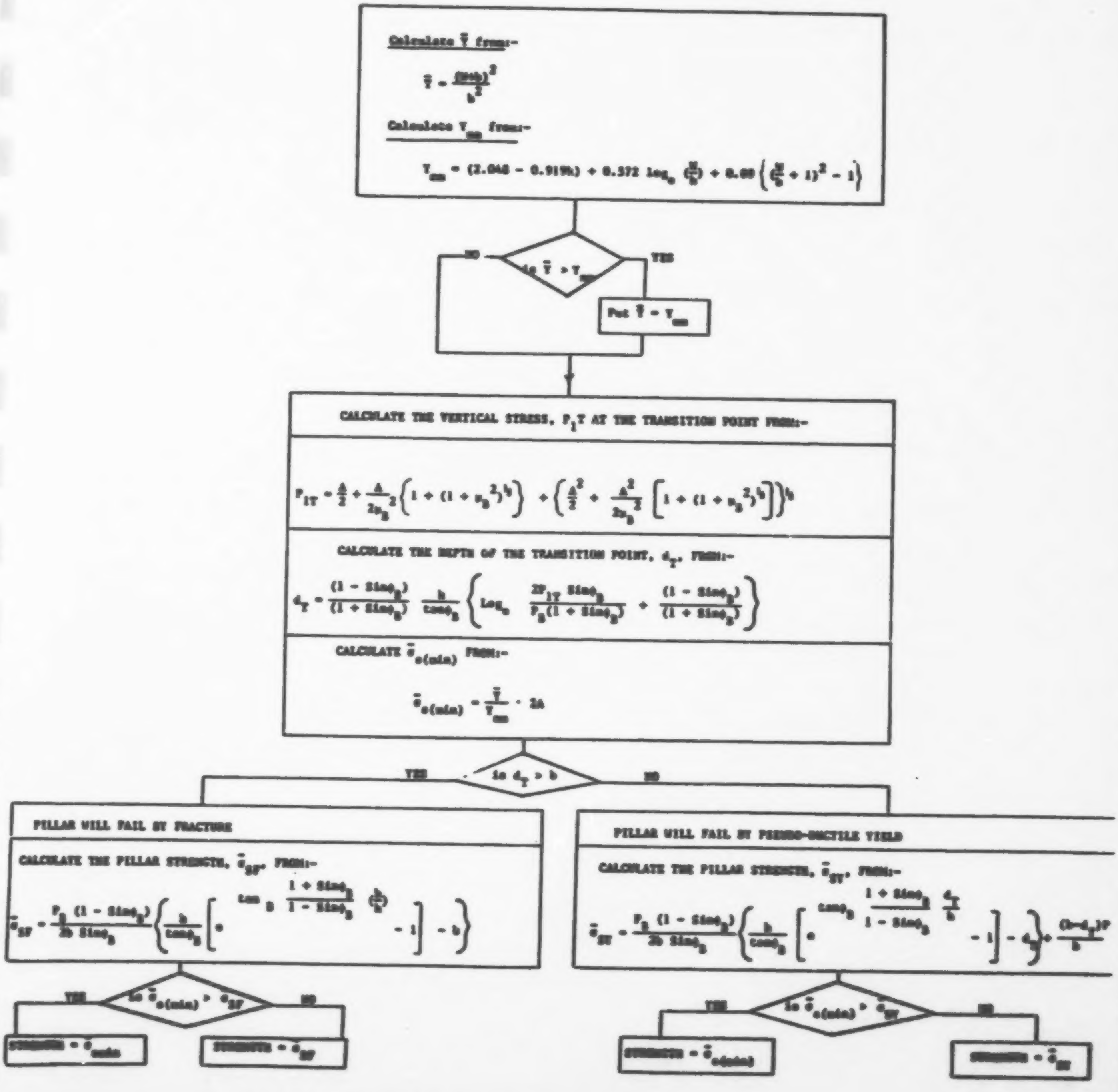
Calculate $\bar{\bar{Y}}$ from:-
$\bar{\bar{Y}} = \frac{(W+b)^2}{b^2}$
Calculate Y_{mm} from:-
$Y_{mm} = (2.048 - 0.919h) + 0.372 \log_e (\frac{W}{b}) + 0.08 \left\{ (\frac{W}{b} + 1)^2 - 1 \right\}$
NO
Is $\bar{\bar{Y}} > Y_{mm}$
YES
Put $\bar{\bar{Y}} = Y_{mm}$
CALCULATE THE VERTICAL STRESS, P_1T AT THE TRANSITION POINT FROM:-
$P_{1T} = \frac{A}{2} + \frac{A}{2n_B{}^2}\left\{1 + (1 + n_B{}^2)^{\frac{1}{2}}\right\} + \left\{\frac{A^2}{2} + \frac{A^2}{2n_B{}^2}\left[1 + (1 + n_B{}^2)^{\frac{1}{2}}\right]\right\}^{\frac{1}{2}}$
CALCULATE THE DEPTH OF THE TRANSITION POINT, d_T, FROM:-
$d_T = \frac{(1 - \sin\phi_B)}{(1 + \sin\phi_B)} \frac{h}{\tan\phi_B} \left\{ \log_e \frac{2P_{1T} \sin\phi_B}{P_B(1 + \sin\phi_B)} + \frac{(1 - \sin\phi_B)}{(1 + \sin\phi_B)} \right\}$
CALCULATE $\bar{\bar{\sigma}}_{s(min)}$ FROM:-
$\bar{\bar{\sigma}}_{s(min)} = \frac{\bar{\bar{Y}}}{Y_{mm}} \cdot 2A$
YES
Is $d_T > b$
NO
PILLAR WILL FAIL BY FRACTURE
CALCULATE THE PILLAR STRENGTH, $\bar{\bar{\sigma}}_{SF}$, FROM:-
$\bar{\bar{\sigma}}_{SF} = \frac{P_B (1 - \sin\phi_B)}{2b \sin\phi_B} \left\{ \frac{h}{\tan\phi_B} \left[e^{\tan_B \frac{1 + \sin\phi_B}{1 - \sin\phi_B} (\frac{b}{h})} - 1 \right] - b \right\}$
YES
Is $\bar{\bar{\sigma}}_{s(min)} > \sigma_{SF}$
NO
STRENGTH = σ_{smin}
STRENGTH = σ_{SF}
PILLAR WILL FAIL BY PSEUDO-DUCTILE YIELD
CALCULATE THE PILLAR STRENGTH, $\bar{\bar{\sigma}}_{SY}$, FROM:-
$\bar{\bar{\sigma}}_{SY} = \frac{P_B (1 - \sin\phi_B)}{2b \sin\phi_B} \left\{ \frac{h}{\tan\phi_B} \left[e^{\tan\phi_B \frac{1 + \sin\phi_B}{1 - \sin\phi_B} \frac{d_T}{h}} - 1 \right] - d_T \right\} + \frac{(b-d_T)P}{b}$
YES
Is $\bar{\bar{\sigma}}_{s(min)} > \bar{\bar{\sigma}}_{SY}$
NO
STRENGTH = $\bar{\bar{\sigma}}_{s(min)}$
STRENGTH = $\bar{\bar{\sigma}}_{SY}$

FIGURE 26: PILLAR STRENGTH CALCULATIONS

3. The pillar height H will be varied from 5-20 ft. (in increments of 5 ft.) and the pillar width will be varied from 10 to 70 ft. (in increments of 10 ft.) These are the approximate ranges for the Salamon/Munro data. However within these unit increments of B and H any cases in which:-

   a) $B/H < 0.9$ will be ignored since they are out of the restricted range and

   b) $R < 0.37$ or > 0.91 will be ignored since these are also out of the restricted range.

4. The following other input parameters are required:-

   $\bar{Y}, Y_{mm}, A, P_B, \phi_B, \mu_B$

   (i) $\bar{Y}$ will be determined, as with Salamon and Munro, assuming tributary area theory:-

$$\text{i.e.}\quad \bar{Y} = \frac{1}{1 - R} = \frac{(w + b)^2}{w^2}$$

where w = semi room width. The room widths will be assumed to be 18 ft.

(ii) Y_{mm} is determined from,

$$Y_{mm} = (2.048-0.919k) + 0.572\ \log_e\left(\frac{W}{h}\right) + 0.09\left\{\left(\frac{W}{b}+1\right)^2 - 1\right\}$$

where the stress ratio k is assumed to be = 0.33

(iii) What value of A should be used?

Bieniawski (16) gives a comparison of coal strength data for S. African coals from all coal fields in S. Africa. These results were all derived from 1" cube specimens. Table 12 lists these results. These results show that the variation is, with the exception of Witbank, Wolverkrans #1 seam, within ± 12.5%. The mean value of the one inch cube strength from this data, 6080 psi.

Thus the cube strength for a cube of height equal to the pillar height is given by:-when $H > 64$ inches $\sigma_H = 0.125 \times k = 760$ psi

and when $H < 64$ inches $\sigma_H = k/\sqrt{H}$

TABLE 12: COMPARISON OF COAL STRENGTH DATA FOR COLLIERIES REPRESENTING ALL MAJOR COAL FIELDS IN SOUTH AFRICA

	Colliery	Locality	Coal density lb/sq ft.	Uniaxial Compressive strength lb/sq in.		Number of specimens	No. of batches	Strength indes
				mean deviation	standard tested per cent			
C	Coalbrook North ...	Second Seam	94.5	5,920	14.1	54	3	103.9
C	Cornelia	Bertha Sect.	89.5	6,350	16.9	60	3	111.5
B	Durban Navigation	Section 5	89.6	5,000	10.0	52	2	87.7
B	Durban Navigation	Section 40	84.6	5,575	16.7	72	3	97.8
A	Kendal ...	-	84.0	6,400	22.6	40	2	112.4
C	Sigma	-	94.7	5,500	14.3	39	2	96.5
D	Springfield	-	91.5	5,875	16.9	100	5	103.0
A	Witbank, Wolvekrans	No. 2 Seam	90.7	5,700	18.1	35	6	100.0
A	Witbank, Wolvekrans	No. 2 Seam	93.1	6,200	27.4	78	9	108.9
A	Witbank, Wolvekrans	No. 1 Seam	92.9	8,200	16.3	49	4	143.9

Note:- (i) All specimens were 1 in. cube in size and were loaded normal to the bedding planes at a constant rate of 100 lb/sq in/sec in a standard laboratory testing machine.

(ii) Coalfields:-
A - Witbank-Breyten Coalfield, Transvaal
B - Klip Rive Coalfield, Natal
C - Vereeniging Coalfield, Orange Free State
D - Balfour Coalfield, Transvaal

Hence for all pillar with height > 64 inches.

$$\sigma_c = 760 \text{ psi}$$

$$\text{i.e.} \quad A = 760/2 = 380 \text{ psi}$$

This value will be used in all the following calculations.

5. (i) The value of P_B was assumed to lie in the range 1 to 200 psi.
   (ii) ϕ_B is assumed = tan μ_B and in the range $20^\circ - 35^\circ$.
   (iii) These values were varied within these ranges to attempt to find as close a fit as possible to Salamon and Munro's results.
   (iv) Table 13 gives the work sheet for this analysis, using $P_B = 100$ psi, and $\phi_B = 22^\circ$.

6. Figure 27 shows the pillar strengths calculated using these model results plotted against $\left\{\frac{B^{0.46}}{H^{0.66}}\right\}$;

correlated in this form the resulting equation is:-

$$\bar{\sigma}_p = 1457 \left\{\frac{B^{0.46}}{B^{0.66}}\right\} - 300$$

with a correlation of 0.956.

i.e. the comparison with Salamon and Munro's formula is surprisingly good when the data is treated in this manner.

TABLE 13: PILLAR STRENGTH WORK SHEET

			MODEL	IN SALAMON'S FORM	IN BIENIAWSKI'S FORM	IN HOLLAND/GADDY FORM	IN WAGNER FORM	STRENGTH FORMULAE			
$\frac{B}{H}$	B FT.	H FT.	$\bar{\sigma}_p$ psi	$\frac{B^{.46}}{H^{.66}}$	$\frac{B}{H}$	$\frac{\sqrt{B}}{H}$ (B & H in inches)	$\sqrt{\frac{B}{H}}$	SALAMON $\bar{\sigma}_p = 1320 \left(\frac{B^{.46}}{H^{.66}}\right)$	BIENIAWSKI $\bar{\sigma}_p = 400+200\left(\frac{B}{H}\right)$	HOLLAND/GADDY $\bar{\sigma}_p = 6080 \left(\frac{\sqrt{B}}{H}\right)$	WAGNER $\bar{\sigma}_p = 1595\sqrt{\frac{B}{H}}$ (A)
2	10	5	760	.997	2	.1826	1.41	1316	840	1110	2248
4	20		1475	1.37	4	.258	2	1810	1280	1568	3190
6	30		2185	1.65	6	.316	2.45	2181	1720	1921	3907
8	40		2540	1.886	8	.365	2.83	2490	2160	2219	4513
10	50		2753	2.09	10	.408	3.16	2759	2600	2480	5040
12	60		2895	2.27	12	.447	3.46	3000	3040	2717	5518
14	70		2996	2.44	14	.483	3.74	3221	3480	2936	5965
1	10	10	760	.631	1	.091	1	832	620	553	1595
2	20		760	.867	2	.129	1.41	1146	840	784	2248
3	30		836	1.046	3	.158	1.732	1380	1060	960	2762
4	40		1475	1.193	4	.183	2	1576	1280	1112	3190
5	50		1901	1.333	5	.204	2.236	1746	1500	1240	3566
6	60		2185	1.438	6	.223	2.449	1899	1720	1356	3906
7	70		2388	1.549	7	.241	2.645	2038	1940	1465	4218
1.33	20	15	760	.664	1.33	.086	1.153	877	692	522	1834
2	30		760	.80	2	.105	1.41	1056	840	638	2248
2.67	40		760	.913	2.67	.122	1.634	1206	987	742	2606
3.33	50		1050	1.012	3.33	.136	1.825	1336	1133	836	2910
4	60		1475	1.10	4	.149	2	1452	1280	906	3190
4.67	70		1779	1.182	4.67	.161	2.16	1560	1427	979	3445
1	20	20	760	.549	1	.065	1	725	620	395	1595
1.5	30		760	.662	1.5	.079	1.22	874	730	480	1945
2	40		760	.756	2	.091	1.41	997	840	553	2248
2.5	50		760	.837	2.5	.102	1.58	1105	950	620	2520
3	60		836	.910	3	.112	1.732	1202	1060	681	2762
3.5	70		1171	.977	3.5	.121	1.870	1290	1170	736	2982
			$A = 380$ $\phi_B = 22^\circ$ $\mu_B = .404$ $P_B = 100$ $P_{1T} = 3605$	a -300 b 1457 r = .956	a = 464 b = 220.5 r = .946	a = 267 b = 6098 r = .924	a -603 b 1033 r = .961				

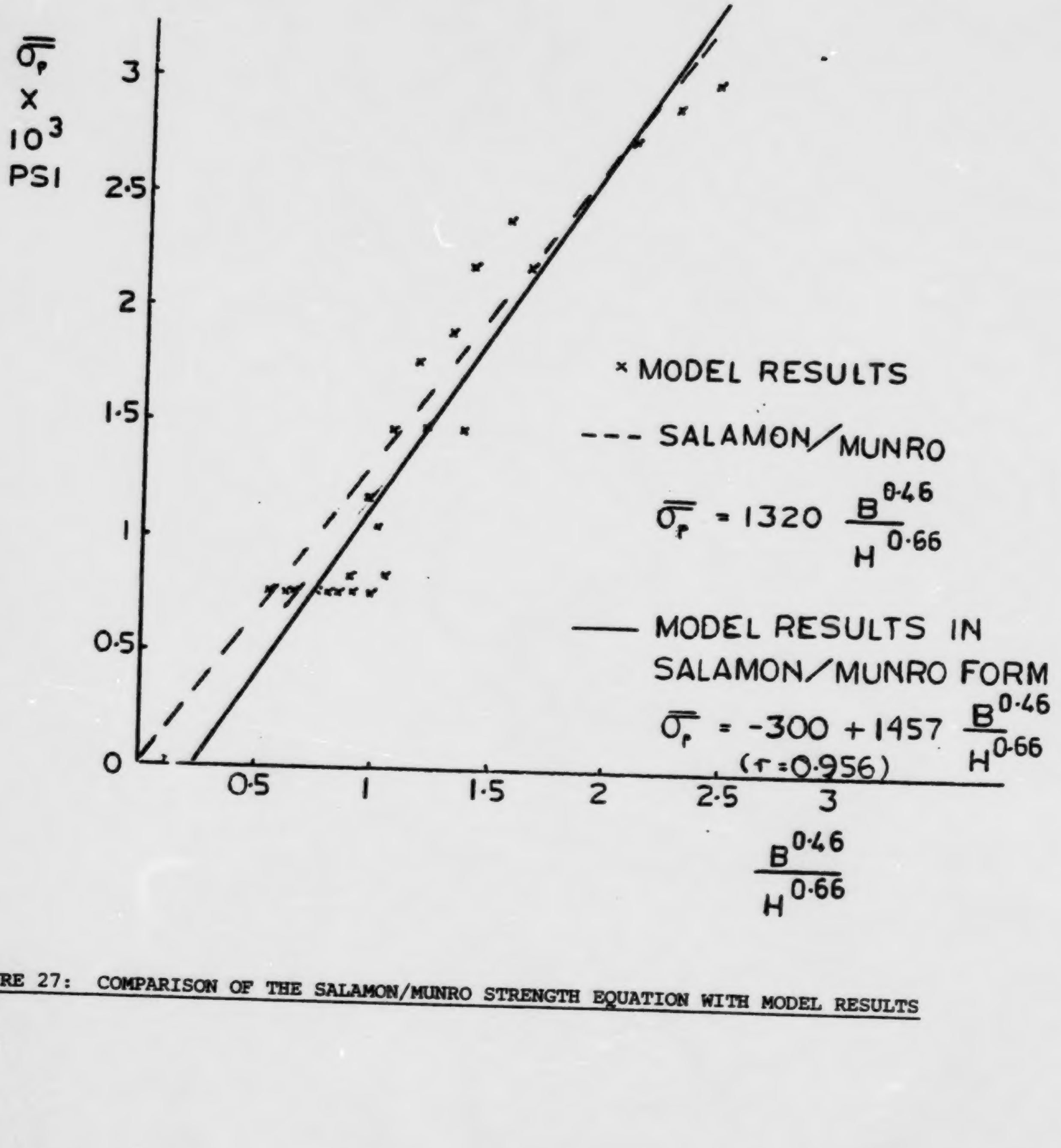

FIGURE 27: COMPARISON OF THE SALAMON/MUNRO STRENGTH EQUATION WITH MODEL RESULTS

5.2 Case History #8: Bieniawski's Strength Formula

5.2.1 Case Background

Bieniawski (20) carried out large scale in situ tests on coal specimens measuring up to 5 ft. by 5 ft. in cross section and up to 5 ft. in height. From this study he examined the size and shape relationships and developed the following pillar strength equation for S. African coals:-

$$\bar{\sigma}_P = 400 + 220 \left(\frac{B}{H}\right)$$

5.2.2 Comparison with the Analytical Model

Since Bieniawski's equation has been developed from a totally different base as the Salamon and Munro formula but is also applied to S. African coals, the same model results used in the preceeding analysis will also be used for comparison with Bieniawski's results. (i.e. $A = 380$, $P_B = 100$, $\mu_B = \tan \phi_B$, $\phi_B = 22^\circ$).

These model results have now been correlated with (B/H) in Bieniawski's form; Table 13 gives the work sheet and Figure 28 plots these results.

When the model results are correlated in this form the following equation is obtained:-

$$\bar{\sigma}_P = 464 + 220.5 \left(\frac{B}{H}\right)$$

with the correlation coefficient $r = 0.946$

It is again seen that the correlation coefficient is quite good and the multiplying constants are reasonably comparable.

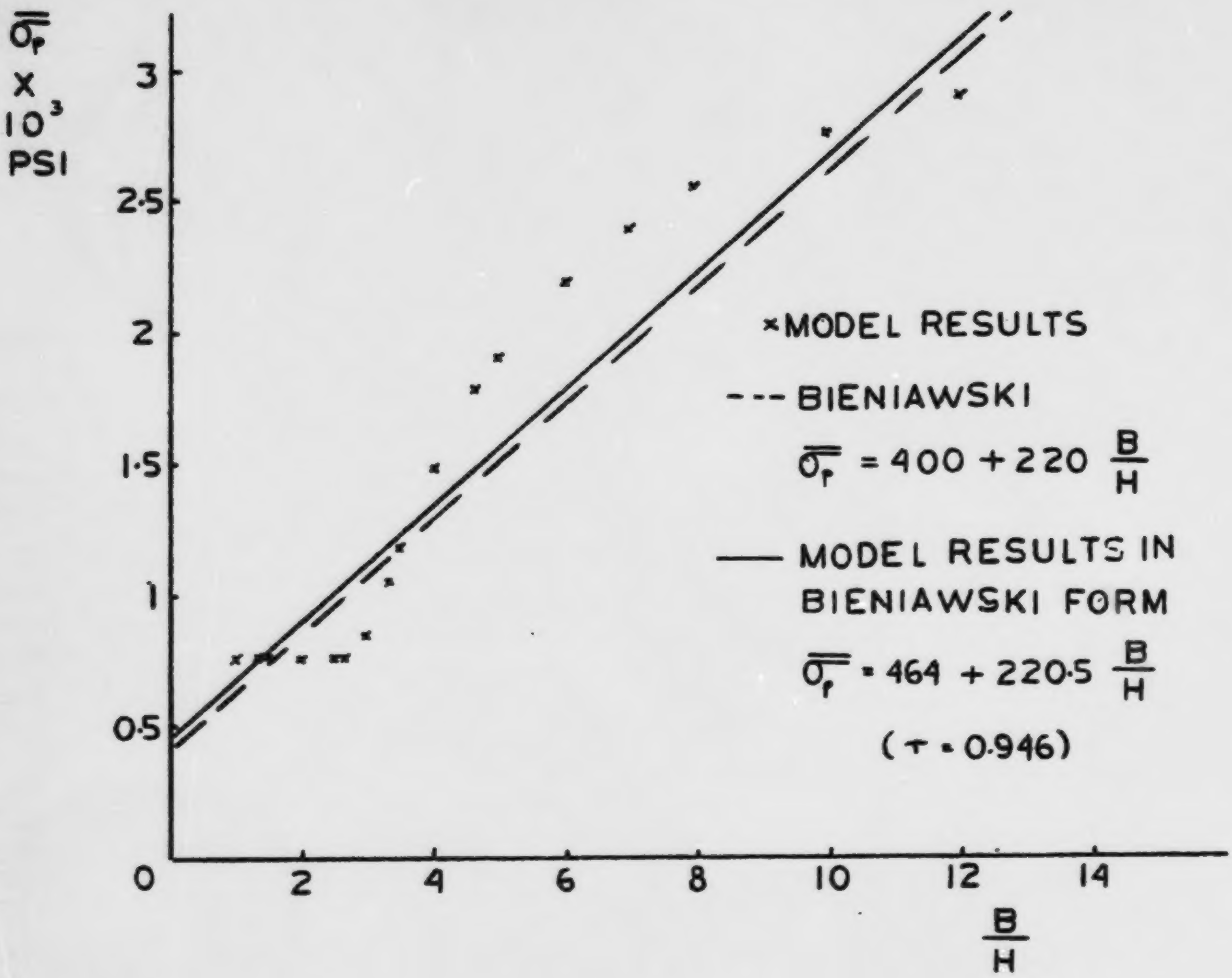

FIGURE 28: COMPARISON OF BIENIAWSKI'S STRENGTH EQUATION WITH MODEL RESULTS

5.3 Case History #9: The Holland/Gaddy Pillar Strength Formula

5.3.1 Case Background

Holland and Gaddy, (21,11) on the basis of coal specimen testing and from Stearts' rules (22) developed the following coal pillar strength formula.

$$\bar{\sigma}_p = k \frac{\sqrt{B}}{H}$$

where k is numerically equal to the uniaxial strength of a 1 inch cube, and B and H are the pillar width and height in inches.

For this exercise, applying this formula to S. African coals, the value k = 6080 will be used, as was used in the model analysis.

i.e. $\bar{\sigma}_p = 6080 \frac{\sqrt{B}}{H}$ for S. African coals

5.3.2 Comparison with the Analytic Model

Once again the same analytically calculated strengths are used for this comparison. ($A = 380$, $P_B = 100$, $\mu_B = \tan \phi_B$, $\phi_B = 22^{\circ}$). The calculations are again given in Table 13 and Figure 29 plots the results against ($\sqrt{B}/H$).

Correlated in this form the analytical data yields the following equation:-

$$\bar{\sigma}_p = 6098 \frac{\sqrt{B}}{H} + 267$$

with a correlation coefficient of $r = 0.924$

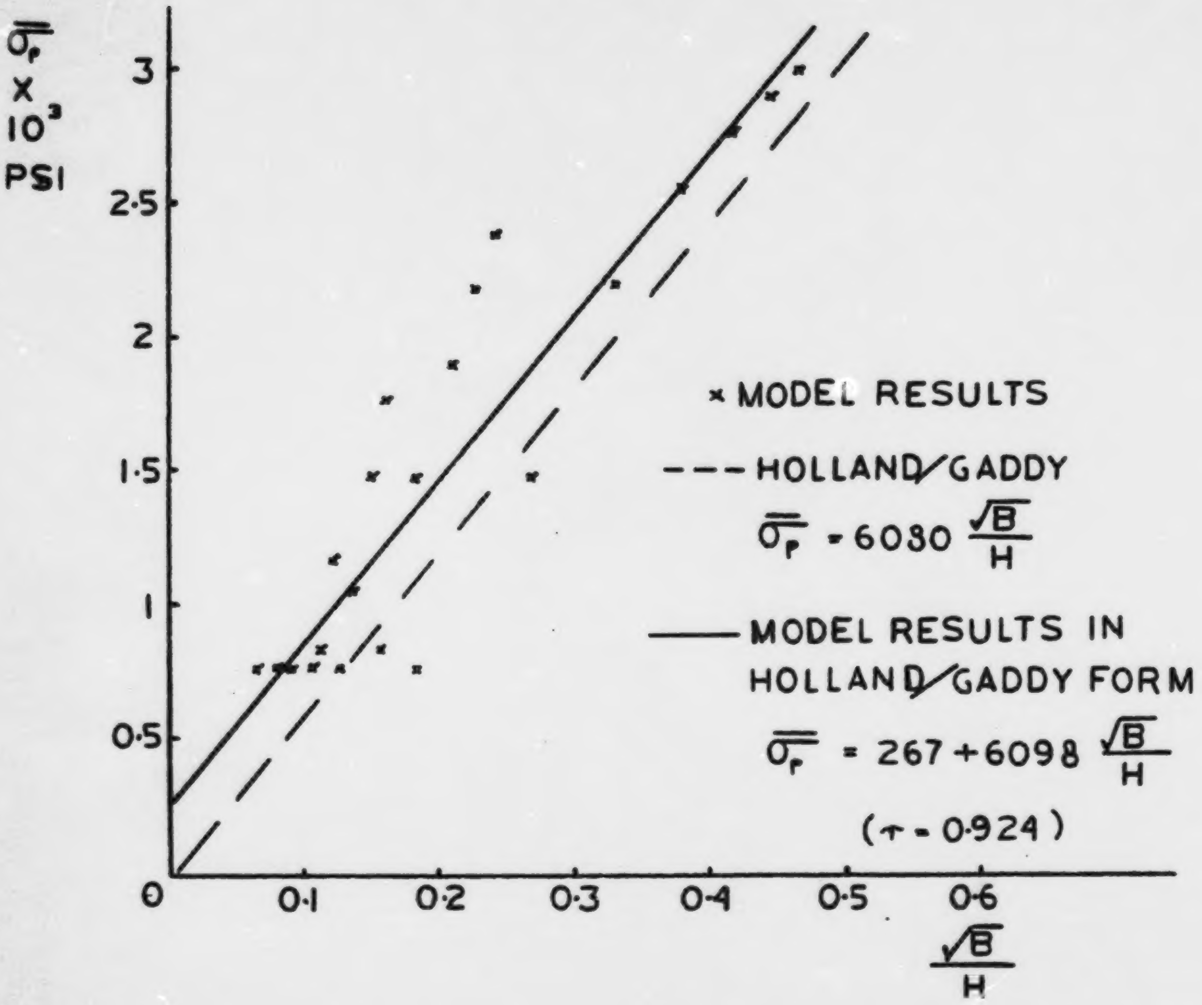

FIGURE 29: COMPARISON OF THE HOLLAND/GADDY STRENGTH EQUATION WITH MODEL RESULTS

5.4 Case History #10: Wagner's Pillar Strength Formula

5.4.1 Case Background

Wagner (23) carried out in situ tests on square and rectangular pillars ranging from 2 ft. to 6.5 ft. side length and width/height, (B/H) ratios from 0.6 to 2.2. These tests differed from all other such in situ tests in so far as, rather than applying uniform loading, the test set up was such that uniform deformation was obtained during loading. This was believed to be more representative of loading that might be applied to a pillar in a mine.

Wagner developed the following pillar strength formula for these tests on S. African coals:-

$$\bar{\sigma}_p = S \left(\frac{W_{eff}}{H}\right)^{½} = 110 \left(\frac{W_{eff}}{H}\right)^{½}$$

when $\bar{\sigma}_p$ and S are in bars.

or $$\bar{\sigma}_p = 1595 \left(\frac{W_{eff}}{H}\right)^{½}$$

when $\bar{\sigma}_p$ and S are in psi.

H is the pillar height and W_{eff} is the "effective pillar width" and is given by:-

$$W_{eff} = \frac{4A_o}{C_o}$$

where A_o = the cross sectional area of the pillar
and C_o = the pillar circumference.

If, as we shall assume, the pillar is square then:-

$$W_{eff} = \frac{4\ B^2}{4\ B} = B$$

i.e. for square pillars this reduces to the equation:-

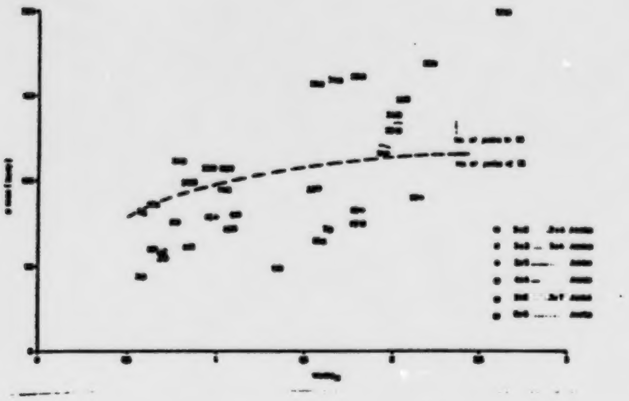

FIGURE 30: PILLAR STRENGTH AS A FUNCTION OF WIDTH TO HEIGHT RATIO AND NUMBER OF JACKS (AFTER WAGNER (23))

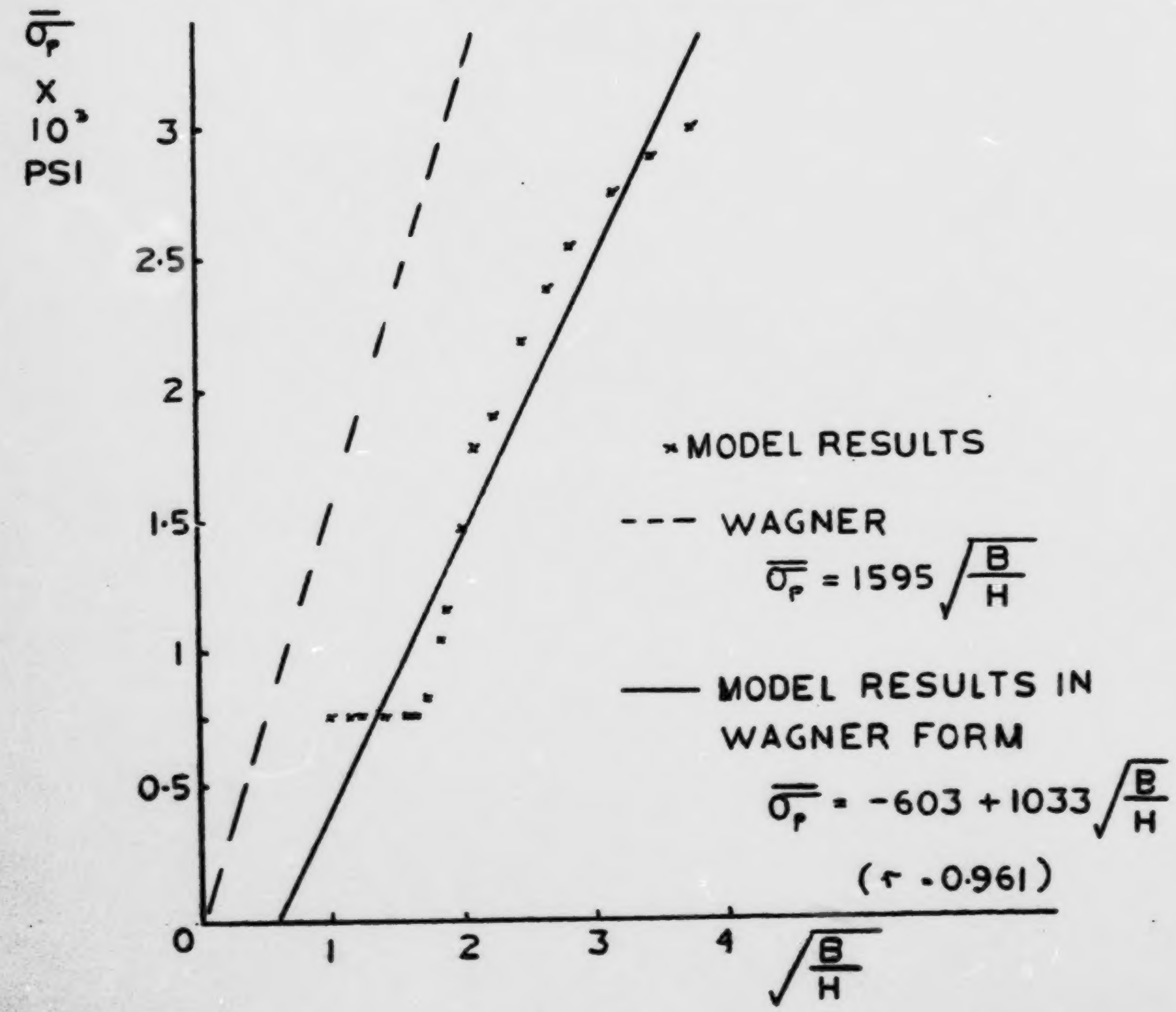

FIGURE 31: COMPARISON OF THE WAGNER STRENGTH EQUATION WITH THE MODEL RESULTS

$$\bar{\sigma}_p = 1595 \sqrt{\frac{B}{H}}$$

Wagner plotted the strength values for all the specimens (pillars) he tested against their width/height ratios, as shown in Figure 30. He noted that "an analysis of this figure shows that the width to height ratio has very little, if any, effect on the strength of small pillars". (those points below the dotted line in Figure 30)

His explanation of this was as follows: "The most likely reason for this observation can be found when comparing the area covered by the circumferential jacks with the total pillar area. In a test pillar in which only 9 jacks were used, the circumferential jacks over 89% of the total area but if 25 jacks are used, this figure drops to 64%".

The author suggests (speculates) that an alternative explanation might be that there is no change in strength with width/height ratio below some critical pillar dimension (as is predicted by the model analysis). i.e. that these results are correct. Unfortunately Wagner does not give the dimensions of the test pillars with the individual results so this speculation cannot be carried further.
i.e. these results might be the first evidence that, as predicted by the model, there is a minimum pillar width (depending on the height) below which the pillar strength remains constant and equal to $\sigma_{p\ min}$. From Figure 30, the mean value of the "constant strengths" below the dotted line is 72 bars with a standard deviation of 15.9 bars.

i.e. 1044 ± 230 psi

From the model analysis, using the same parameters for S. African coal as before:-

$$\bar{\sigma}_{p\ min} = 2A = 760 \text{ psi}$$

which is relatively close to the $\bar{\sigma}_{p\ min}$ obtained by Wagner.

Wagners pillar strength formula given above was derived by analysing only those points above the dotted line in Figure 30. (i.e. the other points were ignored).

5.4.2 Comparison with the Analytical Model

As in the preceeding studies, the same analytically calculated strengths were used and were, this time, correlated against ($\sqrt{B/H}$). Table 13 gives the results which are also plotted in Figure 31.

Correlated in this form the analytical results yielded the following equation:-

$$\bar{\sigma}_p = -603 + 1033\sqrt{\frac{B}{H}}$$

with a correlation coefficient of $r = 0.961$

Comparing this with the Wagner equation we note that the correlation in form (i.e. proportional to $\sqrt{B/H}$) is quite good; but in this case the multiplying parameter is about 35% lower than that given by Wagner.

5.5 Discussion and Conclusions

Figure 32 shows the pillar strength variation predicted by each the preceeding case histories and by the analytical model as the pillar width is varied, for a pillar height 10 ft. This figure illustrates clearly the differences and similarities between these various formulae.

It is clearly seen that:-

(i) The shape or form of the model equations is totally different from the other formulae.

In particular, the model predicts that, for each specific pillar height, there is a minimum pillar width below which the strength remains constant ($\sigma_{p\ min}$) whereas all the other formulae suggest that the strength decreases continuously with decreasing width. Some of Wagners' data tends to confirm that this may be the case, but unfortunately insufficient information is given on the actual pillar sizes (rather than their width height ratios) to establish this as a fact.

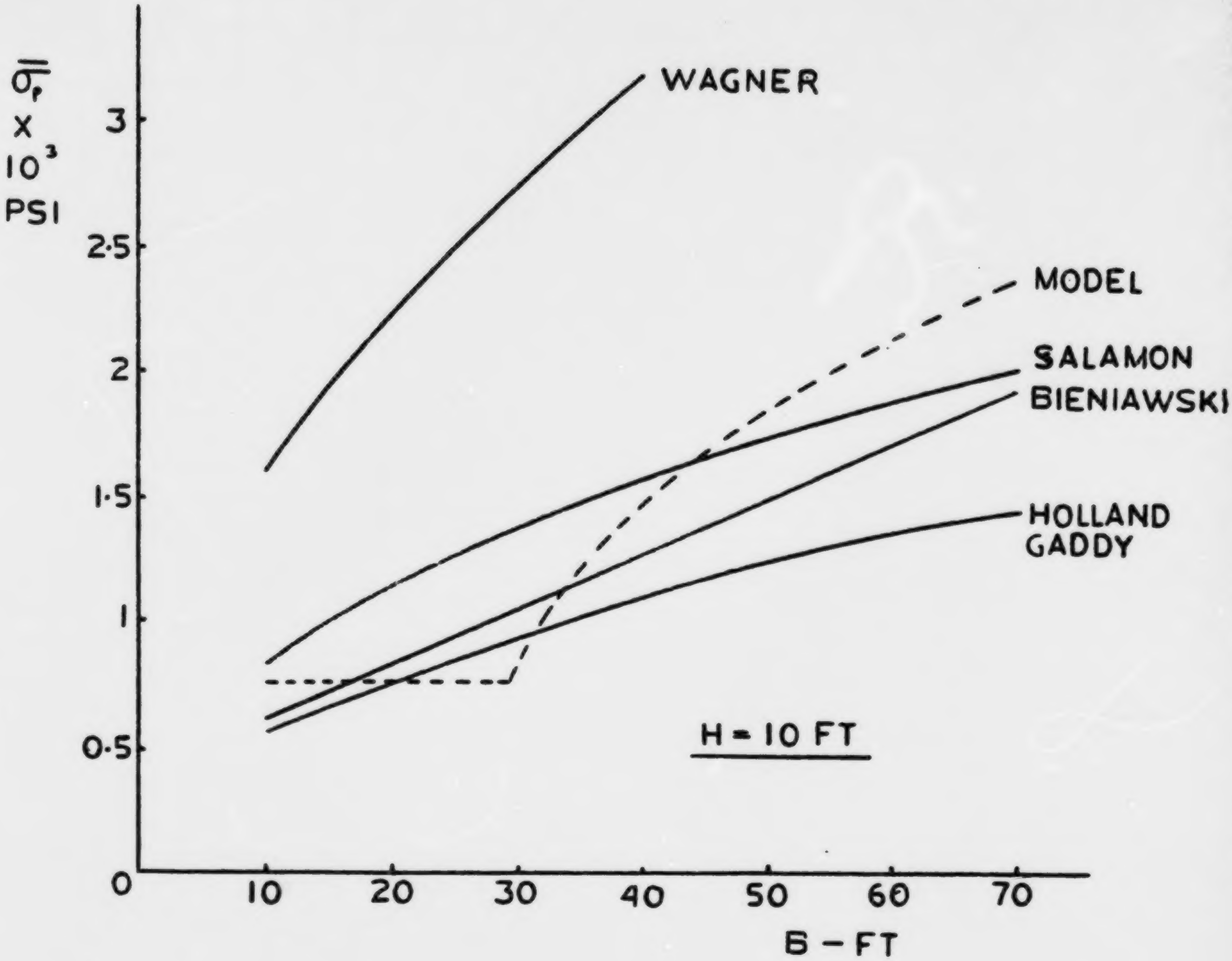

FIGURE 32: COMPARISON OF PILLAR STRENGTH VARIATIONS WITH PILLAR WIDTH FOR A 10 FT. HIGH PILLAR - FOR ALL FORMULAE

(ii) If the analytically derived strengths are treated as "real data" (i.e. as experimental results) then it is shown that they can be correlated to the width and height relationships used by each of the authors with an acceptable correlation coefficient of > 0.9, i.e. in the following forms.

Salamon/Munro $\bar{\sigma}_p \propto \dfrac{B^{0.46}}{H^{0.66}}$

Bieniawski $\bar{\sigma}_p \propto (\frac{B}{H})$

Holland/Gaddy $\bar{\sigma}_p \propto \dfrac{\sqrt{B}}{H}$

Wagner $\bar{\sigma}_p \propto \sqrt{\dfrac{B}{H}}$

When this is done the correlation coefficients are no worse than those obtained by the original workers in establishing their empirical formulae.

Hence it can be concluded that the analytical equations give results which are compatible with all of these previous studies. Clearly this does not prove the validity of the analytical approach but does indicate that the analytical approach gives acceptable strength values.

(iii) To achieve this "level of agreement" between the analytical and experimental results it has been necessary to make a "judicous choice" of the input parameters for the coal properties required by the model. There is no direct means of checking this, other than to say that the values used are within the ranges for coal that were developed in the appendices. (i.e. they are conceivable values).

6. CASE HISTORIES OF RELEVANCE TO FRACTURE ZONE DEVELOPMENT IN PILLARS

6.1 Case Background

Barron (24) developed an air injection technique to investigate the integrity of coal pillars. This test is based on the principal that when pressurized air is injected into coal, the rate of air leakage will be greater in fractured coal than in relatively competent or highly stressed coal. From these tests he calculated a "fracture index", I, which was inversely proportional to the intrinsic permeability of the coal. He showed that the test clearly indicates the peripheral fracture zone around the pillar, the high stress abutment zones in the pillar and the relatively undisturbed zone of coal in the centre of the pillar, as illustrated in idealized form in Figure 33.

It should be noted that it is not known at what value of the fracture index, I, the coal may be considered to be fractured (i.e. greater fracturing than in "undisturbed" coal). Barron assumed an arbitary "cut off" as being when I exceeds the mean of all readings, I mean. i.e. a value of I less than I mean is arbitarily assumed as indicative of fractured coal, whereas larger values of I are interpreted as being due to stress concentrations. Although this cut off was arbitarily chosen, this interpretation appeared to be reasonable since the I values in the central "undisturbed" core portion of the pillar tested appeared to vary about this I mean value.

The results obtained by Barron for a number of pillars will now be examined as case histories for comparison with analytical model solutions.

6.2 Case History #11: Fracture Zones in a Pillar at Canmore Mine, Wilson Seam

Figure 34 shows the location of the test pillars within the Wilson seam, at Canmore, Alberta. Figure 35 shows the fracture indices across the pillar obtained from the air injection tests in this pillar. The pillar is located at approximately 600 ft. below surface; i.e. the overburden stress is approximately, 660 psi. The pillar is approximately 115 ft. square, the room width is 18 ft. Thus assuming

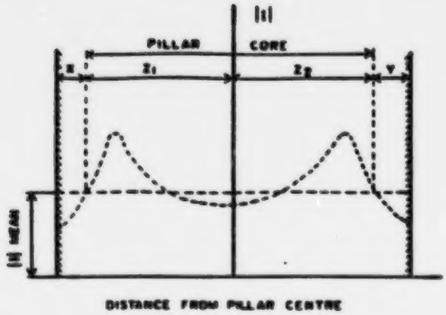
PILLAR
CORE
X
Z1
Z2
Y
DISTANCE FROM PILLAR CENTRE

FIGURE 33: IDEALIZED FRACTURE ZONE AND PILLAR CORE REGIONS

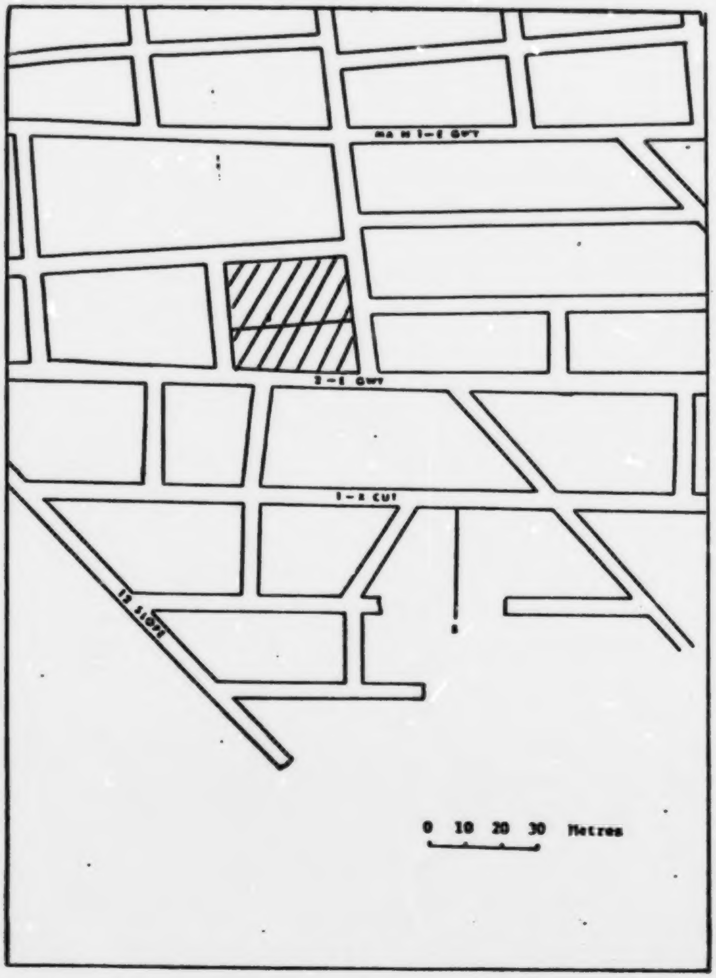
MAIN 1-E GWY
2-E GWY
1-E CUT
12 SLOPE
0 10 20 30 Metres

FIGURE 34: TEST PILLAR LOCATION, WILSON SEAM, CANMORE MINE

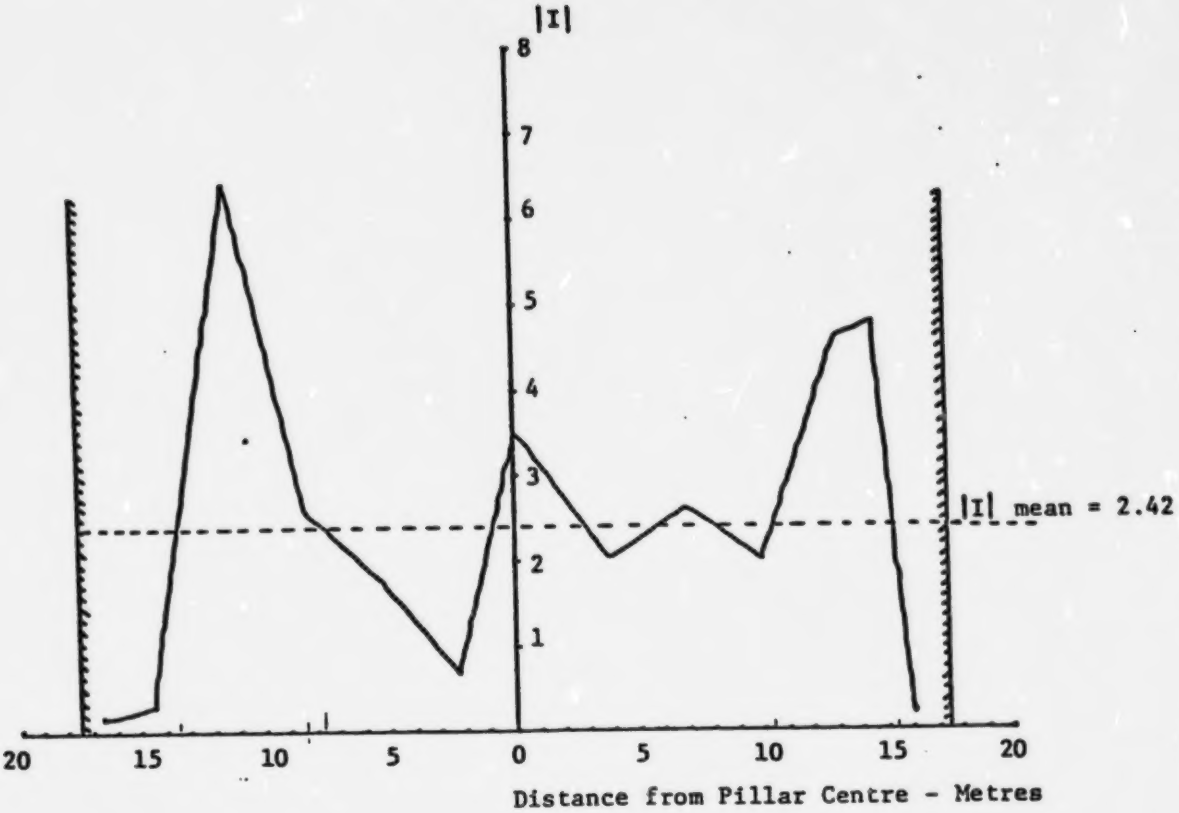

FIGURE 35: FRACTURE INDEX ACROSS PILLAR #1, CANMORE, WILSON SEAM.

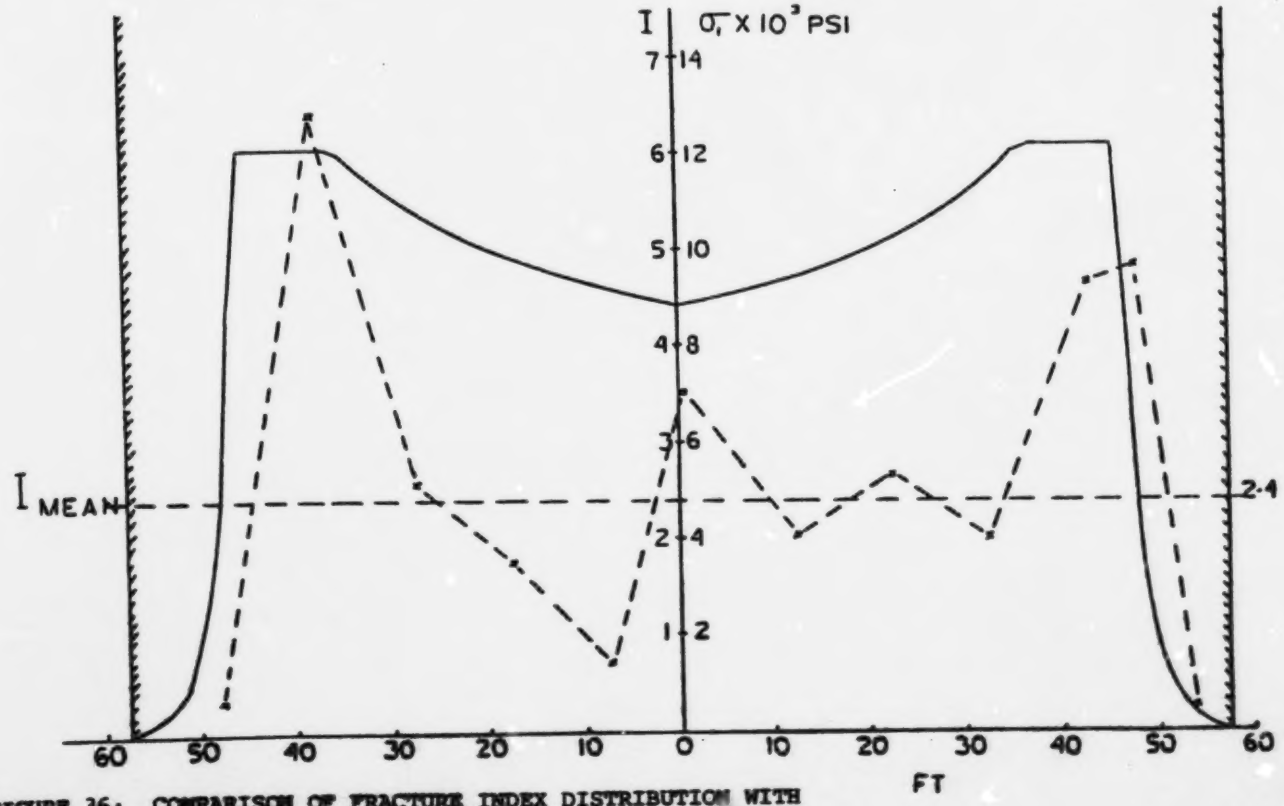

FIGURE 36: COMPARISON OF FRACTURE INDEX DISTRIBUTION WITH ANALYTICALLY DETERMINED STRESS DISTRIBUTION

tributary area theory and a square pillar, the extraction ratio R = 25.2% and the mean pillar stress concentration factor is $\gamma = 1.34$. i.e. the mean pillar stress is 884 psi. The pillar height is 10 ft.

Now Barron and Couetdic (25) conducted plate load tests on pillars in this seam and derived a uniaxial compressive for coal in the Wilson seam of 500 psi. Hence A will be put equal to $\sigma_c/2 = 250$ psi in this example. These authors also carried out tests on specimens of re-compacted broken coal to derive the angle of friction, ϕ_B, for the broken coal. These tests yielded a mean value of $\phi_B = 33^\circ \pm 0.8^\circ$. The value of P_B was varied in the model solutions until a reasonable agreement was obtained between the fracture zone depths. This occured when $P_B = 5$ psi. Table 14 lists the model input data and resulting calculations. Figure 36 plots the resulting stress distribution across the pillar and compares it to the fracture index distribution.

It is seen from this figure that the pillar is stable with a central elastic core, there is a fracture zone and a yield zone around the periphery of the pillar. The peak stress abutment areas coincide fairly well with those indicated by the fracture indices and the coal is yielding in this abutment zone. The fracture zones also coincide fairly well.

However it should be noted that the results are very sensitive to the value of P_B, which is unknown. Thus the only conclusion that may be legitimately drawn is that it is possible to explain the field results very well with the model solution provided that a judicous choice of the value of P_B is made.

6.3 Case History #12: Fracture Zone in Three Pillars at McIntyre #2 Mine, #4 Seam

Barron (24) also carried out air injection tests in three pillars in the #2 mine, #4 seam at McIntyre Mines, Grande Cache, Alberta. Figure 37 shows the location of the three test pillars, A, B, and C in the mine. Figure 38 shows the results of air injection tests in these three pillars.

The total overburden in the area of these pillars is 1400 ft. giving an overburden stress of 1540 psi. The pillars are all 10 ft. high and the rooms are 20 ft. wide.

TABLE 14: MODEL RESULTS FOR CANMORE TEST PILLAR

```
)CALCULATION FOR RECTANGULAR OPENING
)
)
)VIRGIN STRESS= 660.0         EXTRACTION RATIO-0.0
)LENGTH OF SPAN=    0.0       SEMI-WIDTH OF PILLAR= 57.5
)SEMI-HEIGHT OF PILLAR= 5.0  OVERBURDEN DEPTH=  600
)DISTANCE "X"=  0.0             SEMI-ROOM WIDTH=  9.0
)RATIO "SH/SV"=0.330          NUMBER OF PILLARS IN SPAN= 0
)COMPRESSIVE STRENGTH OF BROKEN COAL=  5.
)MOHR CONSTANT "A"=  250.00
)ANGLE OF INTERNAL FRICTION OF BROKEN COAL=33.
)POISSONS RATIO FOR SURROUNDING ROCK=0.0
)POISSONS RATIO FOR PILLAR ROCK=0.0
)COEFFICIENT OF SLIDING FRICTION FOR BROKEN COAL=0.65
)YOUNGS MODULAS FOR SURROUNDING ROCK=         0
)YOUNGS MODULAS FOR PILLAR ROCK=         0
)STRESS REDISTRIBUTION COEFFICIENT=0.50
)TOTAL NUMBER OF SLICES=   460
)SLICE INTERVAL IN PRINTOUT=   4
)


)HE RESULTS ARE
)
)MEAN STRESS CONCENTRATION=1.340
)MEAN PILLAR STRESS:LHS= 884.
)MAXIMUM STRESS CONCENTRATION=    2.11
)THE PILLAR IS STABLE
)THE FAILURE MODE WILL BE ULTIMATE YIELD
)THE PILLAR STRENGTH =   1016.26
)THE SAFETY FACTOR   =      1.15
)THE CRITICAL PILLAR DIMENSION TO AVOID
)        A) CATASTROPHIC YIELD IS  12.77
)        B) ULTIMATE YIELD IS  34.63
)             K1=               2.2731
)             K2=               0.7176
)             K3=               0.7879
)
)
)  SLICE   (90-0)  TAUS/F   TAU    STATUS     PONE   PTHREE ACCUM STRESS
)  -----   ------  ------   ---    ------     ----   ------ ------------
)  1( 0.3)  30.00   216.5  600.4   FAILED      5.4     0.2     0.0
)  8( 2.0)  30.05   219.3  650.5   FAILED     14.1     3.0   204.1
) 12( 3.0)  30.11   222.1  662.9   FAILED     23.1     5.7   276.1
) 16( 4.0)  30.19   226.3  672.6   FAILED     37.0    10.1   338.0
) 20( 5.0)  30.31   232.6  680.7   FAILED     58.6    16.8   393.2
) 24( 6.0)  30.49   241.9  687.1   FAILED     92.3    27.3   442.7
) 28( 7.0)  30.77   255.2  691.3   FAILED    144.5    43.6   486.8
) 32( 8.0)  31.19   273.9  691.8   FAILED    225.7    68.8   524.2
) 36( 9.0)  31.82   299.4  686.0   FAILED    351.7   108.1   552.8
) 40(10.0)  32.75   333.5  668.9   FAILED    547.6   169.1   560.4
) 44(11.0)  34.11   378.1  631.8   FAILED    851.9   263.9   564.2
) 48(12.0)  36.75   422.2  563.3  YIELDED   1215.9   368.1   529.1
) 52(13.0)  36.75   422.2  537.2  YIELDED   1215.9   368.1   492.1
) 56(14.0)  36.75   422.2  517.0  YIELDED   1215.9   368.1   466.1
) 60(15.0)  36.75   422.2  499.5  YIELDED   1215.9   368.1   444.8
) 64(16.0)  36.75   422.2  483.7  YIELDED   1215.9   368.1   426.1
) 68(17.0)  36.75   422.2  469.2  YIELDED   1215.9   368.1   409.0
) 72(18.0)  36.75   422.2  455.5  YIELDED   1215.9   368.1   393.0
) 76(19.0)  36.75   422.2  442.5  YIELDED   1215.9   368.1   377.7
) 80(20.0)  36.75   422.2  430.0  YIELDED   1215.9   368.1   362.8
) 84(21.0)  36.75   422.2  417.3 NOT FAILED 1230.4   368.1   346.8
) 88(22.0)  36.75   422.2  405.1 NOT FAILED 1213.0   368.1   331.3
) 92(23.0)  36.75   422.2  394.5 NOT FAILED 1191.0   368.1   318.8
) 96(24.0)  36.75   422.2  385.1 NOT FAILED 1171.3   368.1   308.0
)100(25.0)  36.75   422.2  376.4 NOT FAILED 1153.1   368.1   298.4
)104(26.0)  36.75   422.2  368.4 NOT FAILED 1136.4   368.1   289.7
)108(27.0)  36.75   422.2  360.9 NOT FAILED 1120.9   368.1   281.9
)112(28.0)  36.75   422.2  353.9 NOT FAILED 1106.3   368.1   274.7
)116(29.0)  36.75   422.2  347.4 NOT FAILED 1092.7   368.1   268.1
)120(30.0)  36.75   422.2  341.2 NOT FAILED 1079.8   368.1   262.0
)124(31.0)  36.75   422.2  335.4 NOT FAILED 1067.7   368.1   256.3
)128(32.0)  36.75   422.2  329.9 NOT FAILED 1056.2   368.1   250.9
)132(33.0)  36.75   422.2  324.7 NOT FAILED 1045.3   368.1   245.9
)136(34.0)  36.75   422.2  319.7 NOT FAILED 1034.9   368.1   241.2
)140(35.0)  36.75   422.2  315.0 NOT FAILED 1025.1   368.1   236.8
)144(36.0)  36.75   422.2  310.5 NOT FAILED 1015.6   368.1   232.6
)148(37.0)  36.75   422.2  306.1 NOT FAILED 1006.6   368.1   228.6
)152(38.0)  36.75   422.2  302.0 NOT FAILED  998.0   368.1   224.9
)156(39.0)  36.75   422.2  298.1 NOT FAILED  989.8   368.1   221.3
)160(40.0)  36.75   422.2  294.3 NOT FAILED  981.9   368.1   217.9
)164(41.0)  36.75   422.2  290.6 NOT FAILED  974.3   368.1   214.6
)168(42.0)  36.75   422.2  287.1 NOT FAILED  967.0   368.1   211.5
)172(43.0)  36.75   422.2  283.8 NOT FAILED  960.0   368.1   208.5
)176(44.0)  36.75   422.2  280.5 NOT FAILED  953.2   368.1   205.7
)180(45.0)  36.75   422.2  277.4 NOT FAILED  946.7   368.1   202.9
)184(46.0)  36.75   422.2  274.4 NOT FAILED  940.5   368.1   200.3
)188(47.0)  36.75   422.2  271.5 NOT FAILED  934.4   368.1   197.8
)192(48.0)  36.75   422.2  268.7 NOT FAILED  928.5   368.1   195.3
)196(49.0)  36.75   422.2  266.0 NOT FAILED  922.9   368.1   193.0
)200(50.0)  36.75   422.2  263.4 NOT FAILED  917.4   368.1   190.7
)204(51.0)  36.75   422.2  260.8 NOT FAILED  912.1   368.1   188.5
)208(52.0)  36.75   422.2  258.4 NOT FAILED  907.0   368.1   186.4
)212(53.0)  36.75   422.2  256.0 NOT FAILED  902.0   368.1   184.4
)216(54.0)  36.75   422.2  253.7 NOT FAILED  897.2   368.1   182.4
)220(55.0)  36.75   422.2  251.4 NOT FAILED  892.5   368.1   180.5
)224(56.0)  36.75   422.2  249.2 NOT FAILED  888.0   368.1   178.7
)228(57.0)  36.75   422.2  247.1 NOT FAILED  883.5   368.1   176.9
)
)BRITTLE/DUCTILE TRANSITION POINT:TAUF=    422.2
)FRACTURE ZONE ENDED ON  48TH SLICE AND EXTENDED 12.0 FT INTO THE PILLAR.
)YEILD ZONE ENDED ON  83TH SLICE AND EXTENDED 20.8 FT INTO THE PILLAR.
)DEPTH OF FRACTURE ZONE JUST AT FAILURE 11.60
```

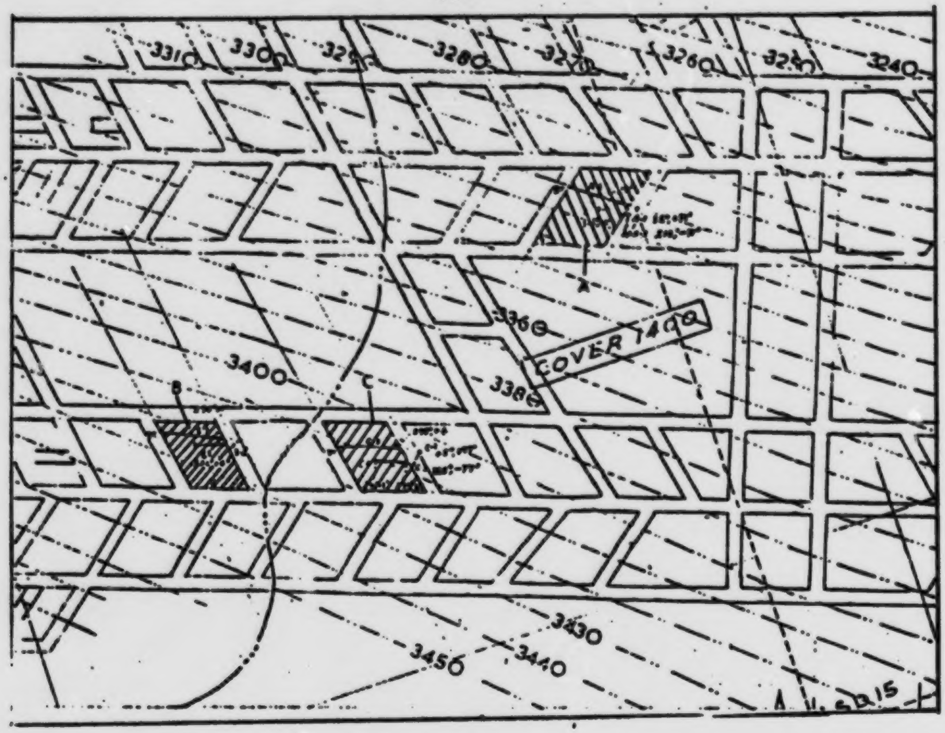
3310
3300
3290
3280
3270
3260
3250
3240
A
3360
COVER 1400
3380
3400
B
C
3430
3440
3450

FIGURE 37: LOCATION OF THE TEST PILLARS, #2 MINE, #4 SEAM, McINTYRE MINES

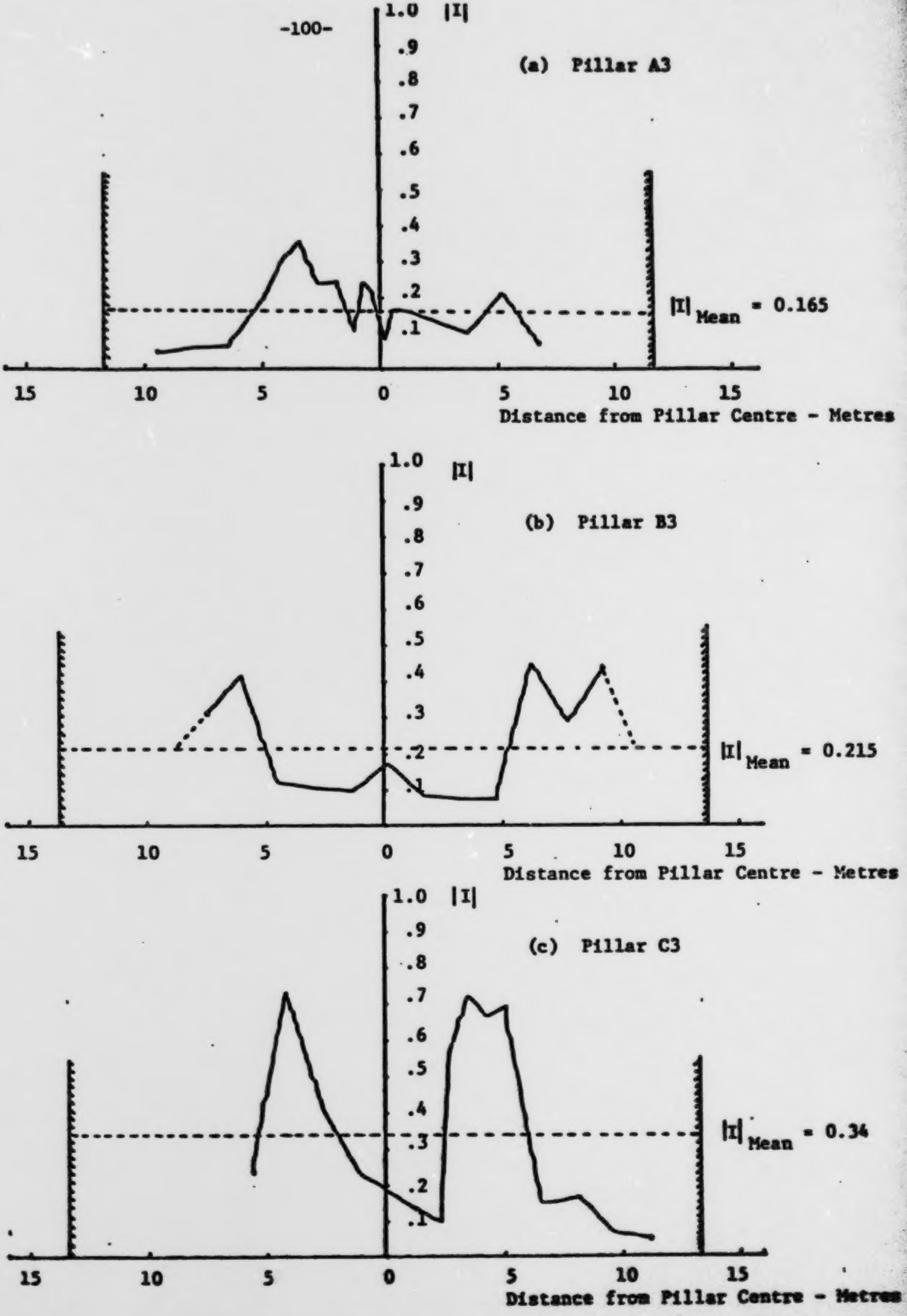

FIGURE 38: FRACTURE INDEX DISTRIBUTION ACROSS PILLARS, A, B, AND C

Barron et al (26) estimated the uniaxial cube strength for a 120" cube of this coal as 1070 ± 295 psi. i.e. $\sigma_c = 1070$, hence $A = 535$ psi. The values of ϕ_B and P_B were varied to obtain the best fit to the fracture index curves. A value of $\phi_B = 24^o$ seemed to apply for all pillars but P_B was slightly different for each coal (20 psi, 10 psi, and 35 psi respectively for pillars A, B, and C). In this case, Coates pillar stress formula was used to determine the mean applied pillar stress. Table 15 lists the input data and results for these model runs.

Figures 39, 40 and 41 show the resulting stress distribution for pillars A, B, and C together with a comparison to the fracture index distribution. It is seen from these figures that the model results appear to fit the experimental data quite well, with the depth of the fracture zones and peak abutment zones coinciding fairly well.

However, although it was possible to use the same ϕ_B, μ_B values for each of these pillars it was necessary to vary P_B over the range 10-35 psi in order to obtain the good fit to the experimental data for each of the three pillars. Although this is not a particularly wide range of P_B, its value has a significant influence on the depth of the fracture zone in the pillar.

6.4 Conclusions

These two case histories have shown that:-

(i) It is possible to obtain a good agreement between the analytic model solution and the field data, provided that a judicous choice of the coal and broken coal strength parameters, A, ϕ_B, μ_B and P_B is made.

(ii) A can be estimated from data within the literature, as can ϕ_B and μ_B (= tan ϕ_B). However P_B is not known and not easily determined, and thus its' evaluation probably poses the major impediment to the application of the analytic model.

TABLE 15: MODEL RESULTS FOR McINTYRE TEST PILLARS

A

```
CALCULATION FOR RECTANGULAR OPENING

VIRGIN STRESS=1540.0           EXTRACTION RATIO=0.287
LENGTH OF SPAN= 616.0          SEMI-WIDTH OF PILLAR= 38.0
SEMI-HEIGHT OF PILLAR= 5.0  OVERBURDEN DEPTH= 1400
DISTANCE "X"=228.00              SEMI-ROOM WIDTH= 10.0
RATIO "SH/SV"=0.330            NUMBER OF PILLARS IN SPAN=13
COMPRESSIVE STRENGTH OF BROKEN COAL= 20.
MOHR CONSTANT "A"= 330.00
ANGLE OF INTERNAL FRICTION OF BROKEN COAL=34.
POISSONS RATIO FOR SURROUNDING ROCK=0.30
POISSONS RATIO FOR PILLAR ROCK=0.30
COEFFICIENT OF SLIDING FRICTION FOR BROKEN COAL=0.45
YOUNGS MODULUS FOR SURROUNDING ROCK= 3000000
YOUNGS MODULUS FOR PILLAR ROCK= 1000000
STRESS REDISTRIBUTION COEFFICIENT=0.50
TOTAL NUMBER OF SLICES=   304
SLICE INTERVAL IN PRINTOUT=   4

THE RESULTS ARE

MEAN STRESS CONCENTRATION=1.387
MEAN PILLAR STRESS(LHS)=2136.
MAXIMUM STRESS CONCENTRATION=      2.19
THE PILLAR IS STABLE
THE FAILURE MODE WILL BE ULTIMATE YIELD
THE PILLAR STRENGTH =    2270.33
THE SAFETY FACTOR    =       1.06
THE CRITICAL PILLAR DIMENSION TO AVOID
       A) CATASTROPHIC YIELD IS  21.90
       B) ULTIMATE YIELD IS  35.24
            K1=              1.0000
            K2=             -0.2250
            K3=              0.0073

  SLICE    (90-Q)   TAUB/F     TAU      STATUS        FONE    PTHREE  ACCUM
  ------   ------   ------    ---      ------        ----    ------  ------
  1( 0.3)  30.00    463.3   1449.8     FAILED          20.1      0.0      0
  8( 2.0)  30.05    470.7   1500.6     FAILED          35.0      7.7    613
 12( 3.0)  30.10    475.3   1587.7     FAILED          46.9     12.9    831
 16( 4.0)  30.15    482.9   1619.4     FAILED          63.0     19.4   1023
 20( 5.0)  30.22    490.9   1645.1     FAILED          82.2     27.3   1179
 24( 6.0)  30.29    500.6   1677.4     FAILED         105.0     37.2   1357
 28( 7.0)  30.38    512.0   1712.6     FAILED         133.1     49.4   1530
 32( 8.0)  30.48    525.6   1748.0     FAILED         167.0     64.4   1690
 36( 9.0)  30.60    541.6   1789.9     FAILED         210.7     83.0   1849
 40(10.0)  30.73    560.3   1831.7     FAILED         263.7    105.9   2008
 44(11.0)  30.90    582.2   1874.7     FAILED         329.1    134.2   2166
 48(12.0)  31.10    607.5   1918.3     FAILED         409.9    169.2   2326
 52(13.0)  31.35    636.6   1961.8     FAILED         509.6    212.4   2482
 56(14.0)  31.64    670.0   2002.7     FAILED         632.9    265.0   2638
 60(15.0)  31.97    708.0   2046.3     FAILED         785.1    331.7   2798
 64(16.0)  32.38    751.2   2071.8     FAILED         973.1    413.1   2936
 68(17.0)  32.85    800.0   2092.1     FAILED        1205.3    513.6   3071
 72(18.0)  33.39    855.0   2099.0     FAILED        1492.0    637.0   3190
 76(19.0)  33.98    916.0   2085.7     FAILED        1846.2    781.2   3285
 80(20.0)  34.76    985.0   2061.0     FAILED        2293.7    980.6   3347
 84(21.0)  35.64   1053.5   1986.3     FAILED        2834.0   1214.8   3368
 88(22.0)  36.73   1130.1   1812.6     FAILED        3491.3   1383.8   3353
 92(23.0)  38.04   1244.7   1587.9     FAILED        4318.8   1858.4   3148
 96(24.0)  39.00   1250.6   1443.8    YIELDED        4301.1   1858.4   2939
100(25.0)  39.00   1250.6   1334.8    YIELDED        4301.1   1858.4   2774
104(26.0)  39.00   1250.6   1274.1    YIELDED        4301.1   1858.4   2623
108(27.0)  39.00   1250.6   1196.3  NOT FAILED       4306.6   1858.4   2477
112(28.0)  39.00   1250.6   1134.3  NOT FAILED       4175.8   1858.4   2363
116(29.0)  39.00   1250.6   1081.9  NOT FAILED       4072.8   1858.4   2260
120(30.0)  39.00   1250.6   1036.5  NOT FAILED       3979.3   1858.4   2186
124(31.0)  39.00   1250.6    996.0  NOT FAILED       3896.6   1858.4   2114
128(32.0)  39.00   1250.6    959.3  NOT FAILED       3821.8   1858.4   2049
132(33.0)  39.00   1250.6    926.1  NOT FAILED       3754.0   1858.4   1991
136(34.0)  39.00   1250.6    890.7  NOT FAILED       3691.8   1858.4   1938
140(35.0)  39.00   1250.6    857.7  NOT FAILED       3634.9   1858.4   1889
144(36.0)  39.00   1250.6    841.7  NOT FAILED       3581.6   1858.4   1844
148(37.0)  39.00   1250.6    817.8  NOT FAILED       3531.9   1858.4   1803
152(38.0)  39.00   1250.6    784.9  NOT FAILED       3485.7   1858.4   1764

BRITTLE/DUCTILE TRANSITION POINT:TAUF=   1250.6
FRACTURE ZONE ENDED ON  93TH SLICE AND EXTENDED 23.3 FT INTO THE P
YIELD ZONE ENDED ON 105TH SLICE AND EXTENDED 26.3 FT INTO THE PILL
DEPTH OF FRACTURE ZONE JUST AT FAILURE 23.90
```

B

```
CALCULATION FOR RECTANGULAR OPENING


VIRGIN STRESS=1540.0           EXTRACTION RATIO=0.254
LENGTH OF SPAN= 315.0          SEMI-WIDTH OF PILLAR= 43.5
SEMI-HEIGHT OF PILLAR= 5.0  OVERBURDEN DEPTH= 1400
DISTANCE "X"=148.00              SEMI-ROOM WIDTH= 10.0
RATIO "SH/SV"=0.330            NUMBER OF PILLARS IN SPAN= 5
COMPRESSIVE STRENGTH OF BROKEN COAL= 10.
MOHR CONSTANT "A"=  330.00
ANGLE OF INTERNAL FRICTION OF BROKEN COAL=34.
POISSONS RATIO FOR SURROUNDING ROCK=0.30
POISSONS RATIO FOR PILLAR ROCK=0.30
COEFFICIENT OF SLIDING FRICTION FOR BROKEN COAL=0.45
YOUNGS MODULUS FOR SURROUNDING ROCK= 3000000
YOUNGS MODULUS FOR PILLAR ROCK= 1000000
STRESS REDISTRIBUTION COEFFICIENT=0.50
TOTAL NUMBER OF SLICES=   348
SLICE INTERVAL IN PRINTOUT=   4


THE RESULTS ARE

MEAN STRESS CONCENTRATION=1.263
MEAN PILLAR STRESS(LHS)=1945.
MAXIMUM STRESS CONCENTRATION=      2.19
THE PILLAR IS STABLE
THE FAILURE MODE WILL BE ULTIMATE YIELD
THE PILLAR STRENGTH =    2211.75
THE SAFETY FACTOR    =       1.14
THE CRITICAL PILLAR DIMENSION TO AVOID
       A) CATASTROPHIC YIELD IS  25.06
       B) ULTIMATE YIELD IS  30.73
            K1=              0.6331
            K2=             -0.4051
            K3=              0.5334


  SLICE    (90-Q)   TAUB/F     TAU      STATUS        FONE    PTHREE  ACCUM STRESS
  ------   ------   ------    ---      ------        ----    ------  ------------
  1( 0.3)  30.00    462.3   1430.4     FAILED          10.5      0.6      0.0
  8( 2.0)  30.03    467.1   1470.0     FAILED          18.4      3.0    588.3
 12( 3.0)  30.06    469.9   1472.0     FAILED          24.4      6.4    735.0
 16( 4.0)  30.09    473.3   1481.6     FAILED          31.9      9.7    894.0
 20( 5.0)  30.12    477.5   1496.3     FAILED          41.1     13.7   1039.9
 24( 6.0)  30.16    482.6   1515.9     FAILED          52.5     18.6   1176.9
 28( 7.0)  30.21    488.7   1539.9     FAILED          66.5     24.7   1309.1
 32( 8.0)  30.27    496.1   1567.5     FAILED          83.9     32.2   1438.0
 36( 9.0)  30.34    505.0   1599.3     FAILED         105.3     41.5   1567.4
 40(10.0)  30.43    515.7   1631.9     FAILED         131.8     52.9   1690.9
 44(11.0)  30.53    528.3   1667.7     FAILED         164.5     67.1   1825.1
 48(12.0)  30.65    543.3   1706.8     FAILED         204.5     84.6   1959.2
 52(13.0)  30.79    560.9   1744.6     FAILED         254.9    106.2   2086.3
 56(14.0)  30.96    581.5   1784.8     FAILED         316.4    132.9   2218.4
 60(15.0)  31.16    606.4   1824.3     FAILED         392.5    165.0   2350.9
 64(16.0)  31.39    633.8   1863.5     FAILED         486.5    205.5   2483.1
 68(17.0)  31.67    664.8   1900.2     FAILED         602.6    256.0   2613.6
 72(18.0)  32.00    701.1   1932.9     FAILED         746.0    318.9   2740.5
 76(19.0)  32.38    742.6   1959.1     FAILED         923.1    398.6   2861.3
 80(20.0)  32.84    789.2   1975.7     FAILED        1141.0    498.3   2972.1
 84(21.0)  33.38    842.1   1970.2     FAILED        1412.0    607.3   3067.9
 88(22.0)  34.02    901.6   1960.9     FAILED        1745.7    731.0   3141.0
 92(23.0)  34.78    968.6   1915.0     FAILED        2137.7    938.2   3184.7
 96(24.0)  35.68   1043.2   1832.2     FAILED        2666.7   1138.6   3183.0
100(25.0)  36.76   1126.9   1695.6     FAILED        3290.4   1422.0   3122.5
104(26.0)  38.08   1220.4   1486.6     FAILED        4071.8   1730.0   2977.7
108(27.0)  39.00   1250.6   1291.3    YIELDED        4381.1   1854.7   2782.2
112(28.0)  39.00   1250.6   1195.1  NOT FAILED       4290.3   1854.7   2564.0
116(29.0)  39.00   1250.6   1122.5  NOT FAILED       4149.8   1854.7   2425.0
120(30.0)  39.00   1250.6   1063.9  NOT FAILED       4038.1   1854.7   2313.9
124(31.0)  39.00   1250.6   1014.4  NOT FAILED       3920.9   1854.7   2226.1
128(32.0)  39.00   1250.6    971.4  NOT FAILED       3841.0   1854.7   2139.5
132(33.0)  39.00   1250.6    933.3  NOT FAILED       3763.1   1854.7   2068.6
136(34.0)  39.00   1250.6    899.3  NOT FAILED       3693.3   1854.7   2005.4
140(35.0)  39.00   1250.6    868.2  NOT FAILED       3630.0   1854.7   1948.4
144(36.0)  39.00   1250.6    840.0  NOT FAILED       3572.2   1854.7   1898.0
148(37.0)  39.00   1250.6    814.0  NOT FAILED       3519.0   1854.7   1849.0
152(38.0)  39.00   1250.6    789.9  NOT FAILED       3469.0   1854.7   1805.3
156(39.0)  39.00   1250.6    767.6  NOT FAILED       3424.1   1854.7   1764.0
160(40.0)  39.00   1250.6    746.7  NOT FAILED       3381.5   1854.7   1727.1
164(41.0)  39.00   1250.6    727.2  NOT FAILED       3341.6   1854.7   1691.0
168(42.0)  39.00   1250.6    708.8  NOT FAILED       3304.0   1854.7   1658.0
172(43.0)  39.00   1250.6    691.5  NOT FAILED       3268.7   1854.7   1627.0

BRITTLE/DUCTILE TRANSITION POINT:TAUF=   1250.6
FRACTURE ZONE ENDED ON 105TH SLICE AND EXTENDED 26.3 FT INTO THE PILLAR.
YIELD ZONE ENDED ON 110TH SLICE AND EXTENDED 27.5 FT INTO THE PILLAR.
DEPTH OF FRACTURE ZONE JUST AT FAILURE 26.22
```

C

```
CALCULATION FOR RECTANGULAR OPENING


VIRGIN STRESS=1540.0           EXTRACTION RATIO=0.248
LENGTH OF SPAN= 440.0          SEMI-WIDTH OF PILLAR= 44.5
SEMI-HEIGHT OF PILLAR= 5.0  OVERBURDEN DEPTH= 1400
DISTANCE "X"=270.00              SEMI-ROOM WIDTH= 10.0
RATIO "SH/SV"=0.330            NUMBER OF PILLARS IN SPAN= 5
COMPRESSIVE STRENGTH OF BROKEN COAL= 30.
MOHR CONSTANT "A"=  330.00
ANGLE OF INTERNAL FRICTION OF BROKEN COAL=34.
POISSONS RATIO FOR SURROUNDING ROCK=0.30
POISSONS RATIO FOR PILLAR ROCK=0.30
COEFFICIENT OF SLIDING FRICTION FOR BROKEN COAL=0.45
YOUNGS MODULUS FOR SURROUNDING ROCK= 3000000
YOUNGS MODULUS FOR PILLAR ROCK= 1000000
STRESS REDISTRIBUTION COEFFICIENT=0.50
TOTAL NUMBER OF SLICES=   356
SLICE INTERVAL IN PRINTOUT=   4


THE RESULTS ARE

MEAN STRESS CONCENTRATION=1.380
MEAN PILLAR STRESS(LHS)=2125.
MAXIMUM STRESS CONCENTRATION=      2.19
THE PILLAR IS STABLE
THE FAILURE MODE WILL BE ULTIMATE YIELD
THE PILLAR STRENGTH =    2832.71
THE SAFETY FACTOR    =       1.33
THE CRITICAL PILLAR DIMENSION TO AVOID
       A) CATASTROPHIC YIELD IS  18.60
       B) ULTIMATE YIELD IS  30.60
            K1=              1.4313
            K2=              0.0700
            K3=              0.0000


  SLICE    (90-Q)   TAUB/F     TAU      STATUS        FONE    PTHREE  ACCUM STRESS
  ------   ------   ------    ---      ------        ----    ------  ------------
  1( 0.3)  30.00    463.3   1447.6     FAILED          35.6      1.6      0.0
  8( 2.0)  30.10    476.2   1557.8     FAILED          54.4     12.6    586.6
 12( 3.0)  30.18    485.6   1596.3     FAILED          82.5     22.6    750.3
 16( 4.0)  30.27    496.8   1621.5     FAILED         111.6     33.9    931.9
 20( 5.0)  30.38    510.0   1645.6     FAILED         143.9     47.0   1088.3
 24( 6.0)  30.51    525.7   1669.1     FAILED         182.7     63.1   1234.3
 28( 7.0)  30.66    543.9   1692.7     FAILED         232.9     86.4   1371.3
 32( 8.0)  30.84    565.2   1715.8     FAILED         293.7    112.7   1503.0
 36( 9.0)  31.05    589.9   1737.9     FAILED         368.7    145.2   1630.1
 40(10.0)  31.32    618.2   1758.1     FAILED         461.4    188.3   1767.2
 44(11.0)  31.63    650.6   1775.0     FAILED         573.9    234.9   1899.6
 48(12.0)  32.00    687.3   1786.9     FAILED         717.2    296.1   1963.0
 52(13.0)  32.44    729.4   1791.6     FAILED         891.9    371.7   2087.0
 56(14.0)  32.98    776.7   1785.4     FAILED        1107.5    468.1   2138.0
 60(15.0)  33.57    830.0   1764.0     FAILED        1373.9    588.4   2201.7
 64(16.0)  34.29    895.8   1724.8     FAILED        1702.9    722.9   2241.5
 68(17.0)  35.16    966.0   1630.5     FAILED        2109.2    898.0   2251.7
 72(18.0)  36.18   1031.7   1549.7     FAILED        2611.1   1116.1   2221.2
 76(19.0)  37.41   1115.4   1383.7     FAILED        3230.9   1384.3   2137.7
 80(20.0)  38.88   1208.7   1170.9  NOT FAILED       4022.8   1626.5   1984.5
 84(21.0)  39.17   1208.7   1079.4  NOT FAILED       3838.7   1626.5   1815.0
 88(22.0)  39.30   1208.7   1015.3  NOT FAILED       3696.6   1626.5   1702.2
 92(23.0)  39.50   1208.7    963.4  NOT FAILED       3580.3   1626.5   1613.1
 96(24.0)  39.74   1208.7    919.3  NOT FAILED       3486.6   1626.5   1541.0
100(25.0)  39.89   1208.7    880.9  NOT FAILED       3416.6   1626.5   1479.0
104(26.0)  40.03   1208.7    846.6  NOT FAILED       3348.6   1626.5   1424.7
108(27.0)  40.15   1208.7    815.8  NOT FAILED       3281.7   1626.5   1376.7
112(28.0)  40.25   1208.7    787.7  NOT FAILED       3223.7   1626.5   1333.0
116(29.0)  40.37   1208.7    762.0  NOT FAILED       3170.6   1626.5   1298.0
120(30.0)  40.47   1208.7    738.2  NOT FAILED       3121.6   1626.5   1259.6
124(31.0)  40.57   1208.7    716.3  NOT FAILED       3076.3   1626.5   1227.2
128(32.0)  40.66   1208.7    695.7  NOT FAILED       3034.0   1626.5   1197.4
132(33.0)  40.74   1208.7    676.5  NOT FAILED       2994.6   1626.5   1169.7
136(34.0)  40.83   1208.7    658.5  NOT FAILED       2957.6   1626.5   1144.0
140(35.0)  40.90   1208.7    641.5  NOT FAILED       2922.8   1626.5   1119.9
144(36.0)  40.98   1208.7    625.5  NOT FAILED       2889.7   1626.5   1097.4
148(37.0)  41.06   1208.7    610.4  NOT FAILED       2858.9   1626.5   1076.3
152(38.0)  41.12   1208.7    596.0  NOT FAILED       2829.0   1626.5   1056.3
156(39.0)  41.19   1208.7    582.4  NOT FAILED       2801.6   1626.5   1037.8
160(40.0)  41.25   1208.7    569.4  NOT FAILED       2775.0   1626.5   1019.7
164(41.0)  41.31   1208.7    557.0  NOT FAILED       2749.7   1626.5   1002.0
168(42.0)  41.37   1208.7    545.2  NOT FAILED       2725.6   1626.5    985.7
172(43.0)  41.43   1208.7    533.8  NOT FAILED       2703.5   1626.5    971.4
176(44.0)  41.49   1208.7    523.0  NOT FAILED       2680.4   1626.5    956.0

BRITTLE/DUCTILE TRANSITION POINT:TAUF=   1208.6
FRACTURE ZONE ENDED ON  80TH SLICE AND EXTENDED 20.0 FT INTO THE PILLAR.
DEPTH OF FRACTURE ZONE JUST AT FAILURE 20.31
```

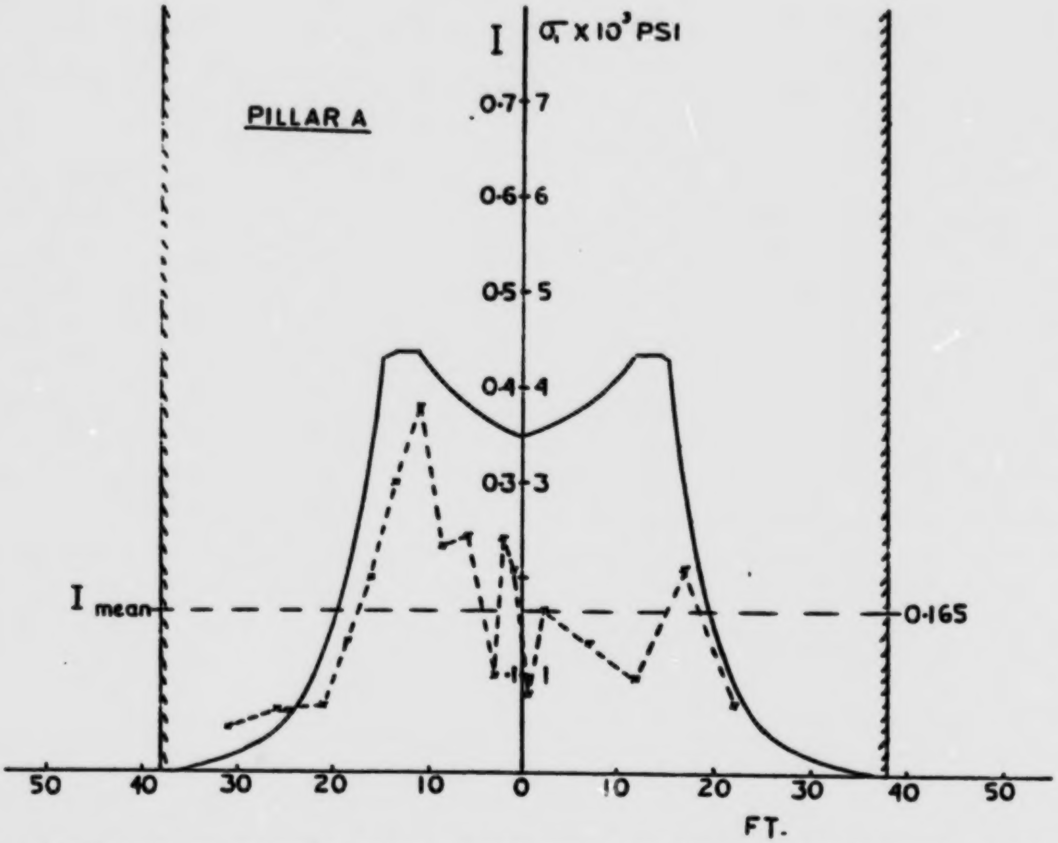

FIGURE 39: COMPARISON OF FRACTURE INDEX DISTRIBUTION AND STRESS DISTRIBUTION ACROSS PILLAR A

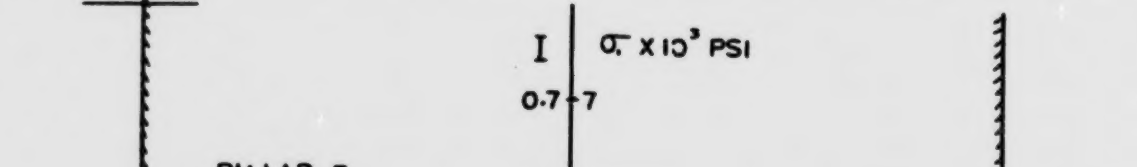

IGURE 40: COMPARISON OF FRACTURE INDEX DISTRIBUTION AND STRESS DISTRIBUTION ACROSS PILLAR B

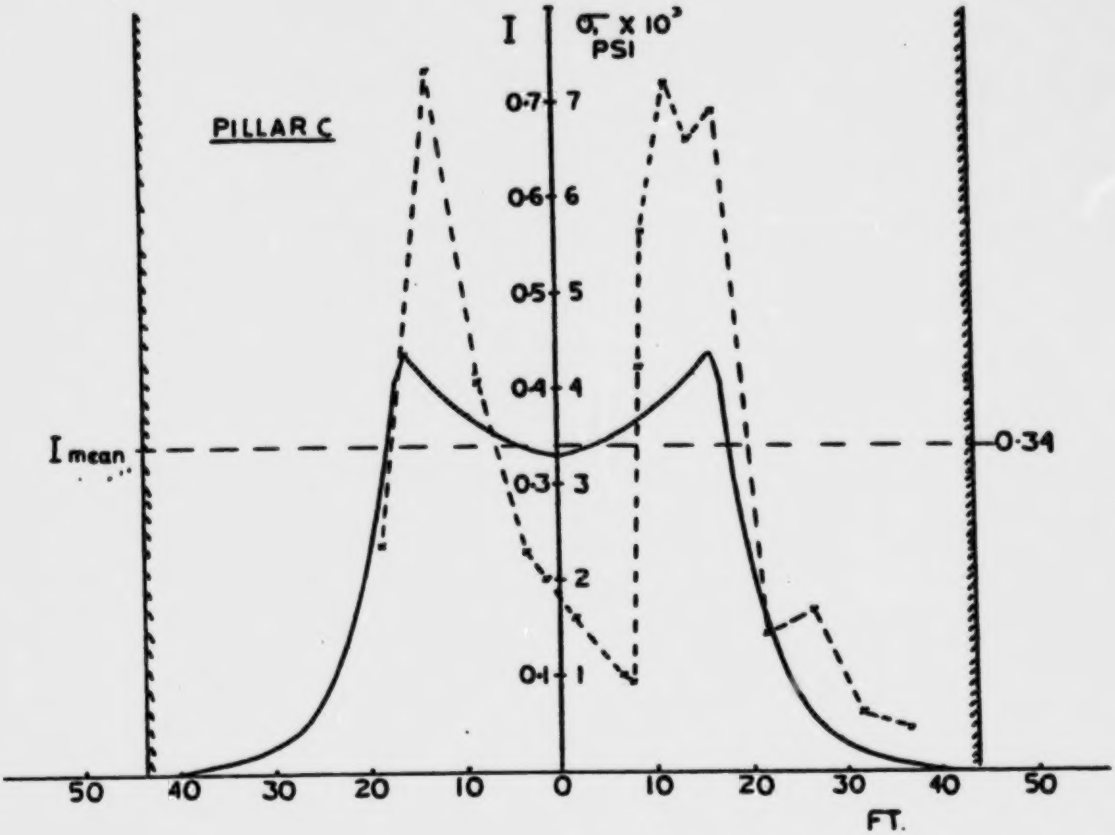

FIGURE 41: COMPARISON OF FRACTURE INDEX DISTRIBUTION AND STRESS DISTRIBUTION ACROSS PILLAR C

7. CASE HISTORIES OF RELEVANCE TO PILLAR YIELDING

7.1 Case History #13: A Coal Pillar Strength Determination

7.1.1 Case Background

Skelly, Wolgamott and Wang (27) presented the results of a study of the measurement of pillar strength in situ, as well as laboratory tests of small coal specimens. The field work was carried out in the Keystone No. 1 Mine, West Virginia in the Pocohontos #3 seam.

The test pillars were located in an active production section of the mine, where the depth of overburden was approximately 800 ft. They assumed an overburden load of 1.16 psi per foot to give $S_V = 930$ psi. The pillars were 80 ft. square with an average height of 5.8 ft. The test pillars were blocked out on 100 ft. centres, giving 20 ft. wide rooms. The test pillars were instrumented with vibrating wire stressmeters.

Test pillar E was instrumented prior to being blocked out, in order to determine the average pillar stress increase resulting from the adjacent entry development. The average stress change measured was about 110 psi compared to an expected change of 520 psi from tributary area calculation. From these measurements and calculations the average stress in test pillar A prior to instrumentation was estimated to be within the range 1040 to 1450 psi.

Test pillar A was loaded to failure by sequential reduction of its cross section dimensions as illustrated in Figure 42 (A to D). A total of 17 cuts were taken from the test pillar over the course of the experiment. Average changes in vertical stress and deformation are plotted in Figure 43 (the author has inserted cut numbers and pillar dimensions onto this figure). The minimum and maximum values of the pillar strength so determined are 2900 and 3310 psi. These limits were computed from the sum of (a) the estimated average pillar stress prior to instrumentation (1040-1450 psi) and (b) the average change in pillar stress measured between the time of stressmeter installation and pillar failure (1860 psi).

In addition these authors carried out a detailed laboratory testing program on

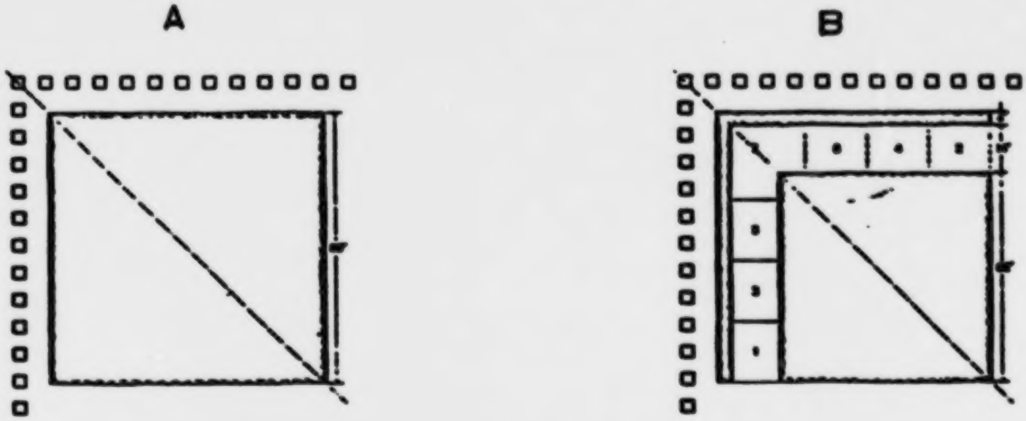

. Original configuration of Test Pillar A, with crib supports placed on 8-ft centers along the gob line.

After seven cuts had been taken, the pillar had been reduced to 62 ft on a side, with a 4-ft fender of coal left standing.

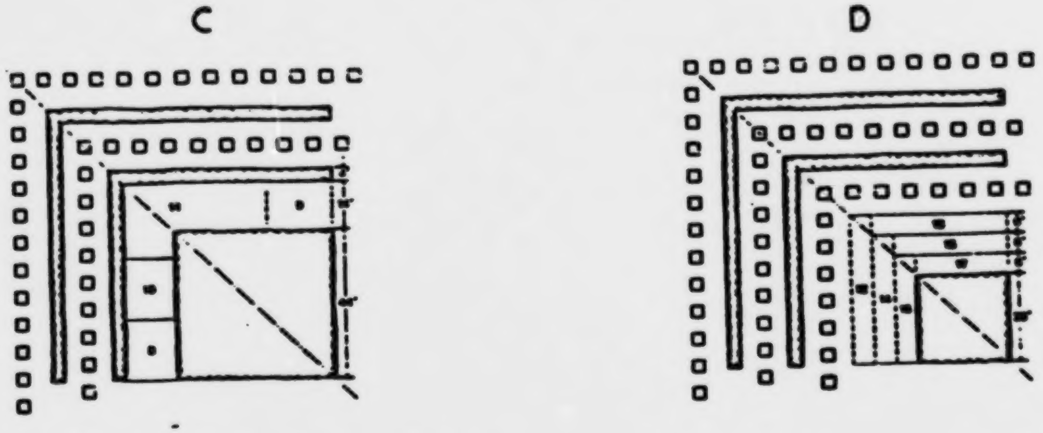

A second set of splits was driven in four cuts, after additional crib supports were set in place. The pillar was reduced to 44 ft on a side.

The final cuts were taken in pairs, decreasing the pillar side length to 38, 32, and 26 ft.

FIGURE 42: MINING SEQUENCE WHEN REDUCING TEST PILLAR SIZE

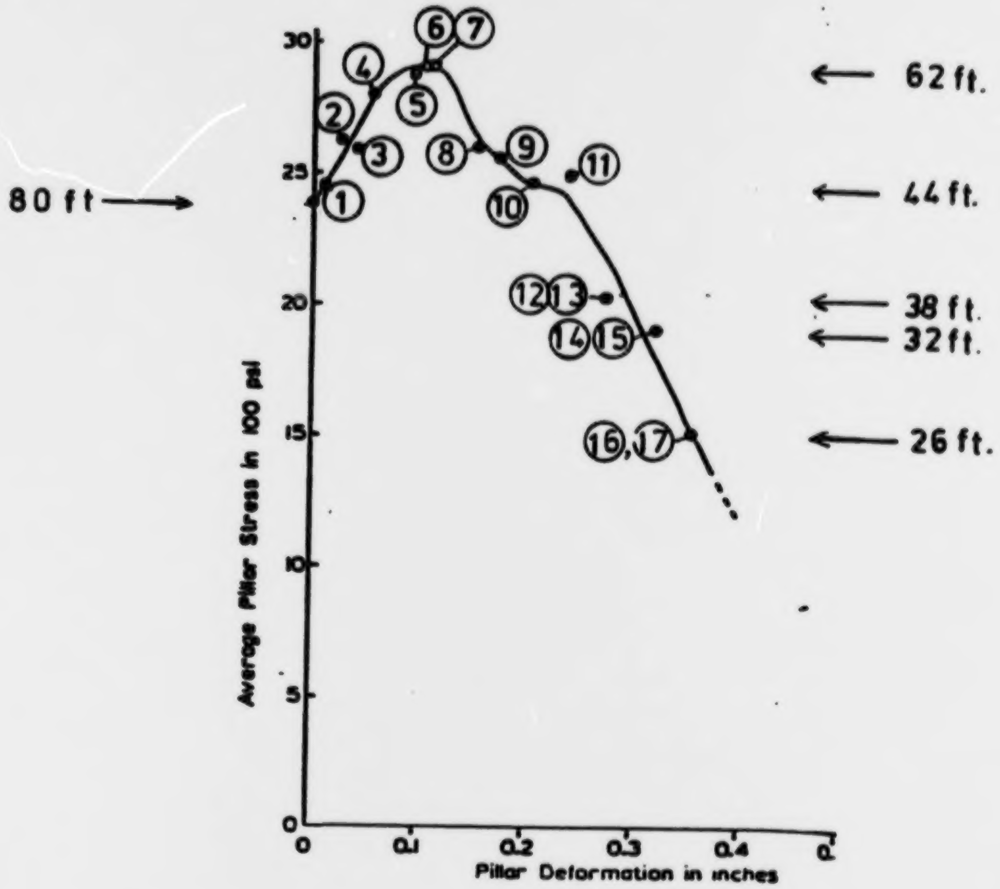

Stress-deformation curve for Test Pillar A. The initial stress level in the figure was based on the minimum estimate of average pillar stress at the time of instrumentation.

FIGURE 43: STRESS CHANGES IN TEST PILLARS AS SIZE IS REDUCED

specimens of this coal and determined the following size/strength relationship:-

$$\sigma_C = 2360\ D^{-0.21}\ \text{psi} \qquad \text{(D in inches)}$$

7.1.2 Discussion

It is seen from Figure 43 that the pillar was stable at 80 ft. square but failed at 62 ft. square. Thereafter the residual stress capacity of the pillar reduced with diminishing size. As given in the table below.

B Ft.	Mean Stress on the pillar, psi.
80	2420
62	2950
44	2500
38	2052
32	1921
26	1500

It is speculated that the analytic model should not only be able to fit the failure of this pillar (at B = 62ft.) but, if the model is correct, after failure the pillar should be yielding and the model should correctly predict the residual mean stress capacities after failure. This will be attempted.

7.1.3 Model Solution

Skelly et al's relationship $\sigma_C = 2360\ D^{-0.21}$ was used to determine the cube strength of height equal to the pillar height (70 inches). However Barron's limit of 64 inches was imposed, giving:

$$\sigma_H = 2360\ (64)^{-0.21} = 985\ \text{psi}$$

Hence the A value for the model input = 985/2 = 492.5 psi

Values of ϕ_B and P_B were varied until the failure stress at 62 ft. pillar size was matched to to observed results. This occurred for $\phi_B = 24^\circ$ and $P_B = 44$ psi. The strengths and stress distribution were then determined for all the other pillar sizes. Table 16 gives the input data and results for each of these six cases. Figure 44 shows the resulting stress distributions.

7.1.4 Discussions and Conclusions

The table below summarises and compares the analytically determined strengths with those measured.

B ft.	Mean Stress on Pillar measured psi.	Pillar Strength (residual capacity when failed)
80	2420	3198 (not failed)
62	2950	2955 (matched by choice of input)
44	2500	2513 (residual cap.)
38	2052	2272 (residual cap.)
32	1921	1942 (residual cap.)
26	1500	1459 (residual cap.)

It is seen from this comparison that the agreement between the calculated and measured residual mean stress capacities of the pillar as the size is reduced is amazingly good. This is therefore probably the strongest evidence we have to date that the mode of failure of the pillar is by yielding as explained by pseudo-ductile yield.

In addition, these authors plotted and compared the strength ratio (σ_p/σ_c) variation with B/H ratio using their data in conjunction with various pillar strength formulae. These are shown in Figure 45, together with the analytical model results over the same range of B/H ratios. The following give the relationships compared:-

Curve 1: $\frac{\sigma_p}{\sigma_c} = 0.78 + 0.22\ (\frac{B}{H})$

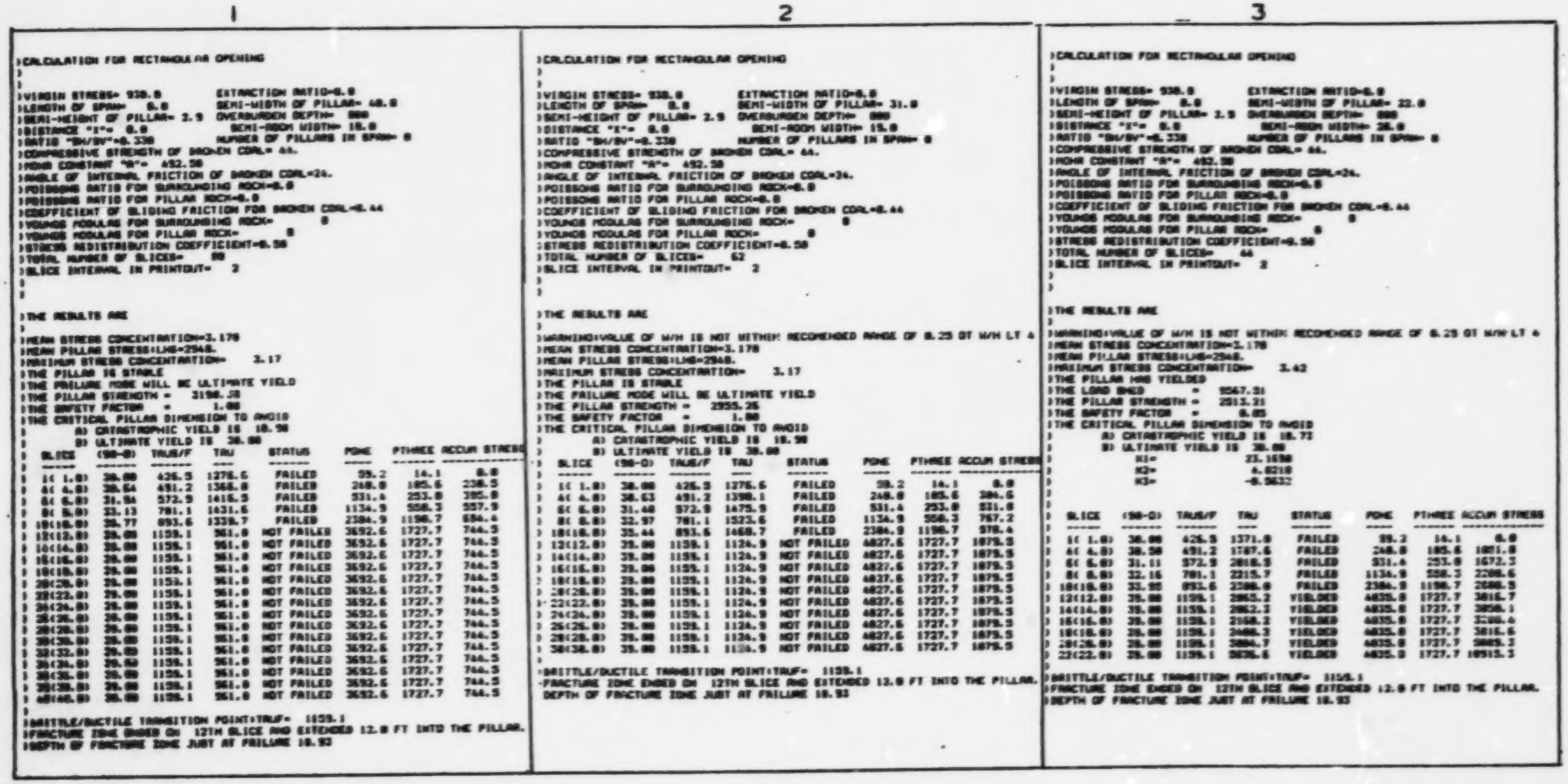

1

```
)CALCULATION FOR RECTANGULAR OPENING
)
)
)VIRGIN STRESS= 930.0          EXTRACTION RATIO=0.0
)LENGTH OF SPAN=    0.0        SEMI-WIDTH OF PILLAR= 40.0
)SEMI-HEIGHT OF PILLAR= 2.5  OVERBURDEN DEPTH=  800
)DISTANCE "X"=  0.0              SEMI-ROOM WIDTH= 10.0
)RATIO "SH/SV"=0.330           NUMBER OF PILLARS IN SPAN= 0
)COMPRESSIVE STRENGTH OF BROKEN COAL= 44.
)MOHR CONSTANT "A"=  452.50
)ANGLE OF INTERNAL FRICTION OF BROKEN COAL=24.
)POISSONS RATIO FOR SURROUNDING ROCK=0.0
)POISSONS RATIO FOR PILLAR ROCK=0.0
)COEFFICIENT OF SLIDING FRICTION FOR BROKEN COAL=0.44
)YOUNGS MODULAS FOR SURROUNDING ROCK=        0
)YOUNGS MODULAS FOR PILLAR ROCK=        0
)STRESS REDISTRIBUTION COEFFICIENT=0.50
)TOTAL NUMBER OF SLICES=     80
)SLICE INTERVAL IN PRINTOUT=   2
)
)

)THE RESULTS ARE
)
)MEAN STRESS CONCENTRATION=3.170
)MEAN PILLAR STRESS:LHS=2948.
)MAXIMUM STRESS CONCENTRATION=     3.17
)THE PILLAR IS STABLE
)THE FAILURE MODE WILL BE ULTIMATE YIELD
)THE PILLAR STRENGTH =    3198.38
)THE SAFETY FACTOR    =        1.08
)THE CRITICAL PILLAR DIMENSION TO AVOID
)        A) CATASTROPHIC YIELD IS  18.58
)        B) ULTIMATE YIELD IS  30.00
)  SLICE     (90-0)   TAUS/F     TAU       STATUS       PONE    PTHREE ACCUM STRESS
)  ------    ------   ------     ---       ------       ----    ------ ------------
)  1( 1.0)   30.00    426.5    1276.6      FAILED        59.2     14.1      0.0
)  4( 4.0)   30.64    491.2    1366.0      FAILED       248.0    185.6    238.5
)  6( 6.0)   31.94    572.9    1416.5      FAILED       531.4    253.0    395.0
)  8( 8.0)   33.13    781.1    1431.6      FAILED      1134.9    558.3    557.9
) 10(10.0)   35.77    893.6    1339.7      FAILED      2384.9   1190.7    684.4
) 12(12.0)   39.00   1159.1     961.0   NOT FAILED     3692.6   1727.7    744.5
) 14(14.0)   39.00   1159.1     961.0   NOT FAILED     3692.6   1727.7    744.5
) 16(16.0)   39.00   1159.1     961.0   NOT FAILED     3692.6   1727.7    744.5
) 18(18.0)   39.00   1159.1     961.0   NOT FAILED     3692.6   1727.7    744.5
) 20(20.0)   39.00   1159.1     961.0   NOT FAILED     3692.6   1727.7    744.5
) 22(22.0)   39.00   1159.1     961.0   NOT FAILED     3692.6   1727.7    744.5
) 24(24.0)   39.00   1159.1     961.0   NOT FAILED     3692.6   1727.7    744.5
) 26(26.0)   39.00   1159.1     961.0   NOT FAILED     3692.6   1727.7    744.5
) 28(28.0)   39.00   1159.1     961.0   NOT FAILED     3692.6   1727.7    744.5
) 30(30.0)   39.00   1159.1     961.0   NOT FAILED     3692.6   1727.7    744.5
) 32(32.0)   39.00   1159.1     961.0   NOT FAILED     3692.6   1727.7    744.5
) 34(34.0)   39.00   1159.1     961.0   NOT FAILED     3692.6   1727.7    744.5
) 36(36.0)   39.00   1159.1     961.0   NOT FAILED     3692.6   1727.7    744.5
) 38(38.0)   39.00   1159.1     961.0   NOT FAILED     3692.6   1727.7    744.5
) 40(40.0)   39.00   1159.1     961.0   NOT FAILED     3692.6   1727.7    744.5
)
)BRITTLE/DUCTILE TRANSITION POINT:TAUF=   1159.1
)FRACTURE ZONE ENDED ON  12TH SLICE AND EXTENDED 12.0 FT INTO THE PILLAR.
)DEPTH OF FRACTURE ZONE JUST AT FAILURE 10.93
```

2

```
)CALCULATION FOR RECTANGULAR OPENING
)
)
)VIRGIN STRESS= 930.0          EXTRACTION RATIO=0.0
)LENGTH OF SPAN=    0.0        SEMI-WIDTH OF PILLAR= 31.0
)SEMI-HEIGHT OF PILLAR= 2.5  OVERBURDEN DEPTH=  800
)DISTANCE "X"=  0.0              SEMI-ROOM WIDTH= 15.0
)RATIO "SH/SV"=0.330           NUMBER OF PILLARS IN SPAN= 0
)COMPRESSIVE STRENGTH OF BROKEN COAL= 44.
)MOHR CONSTANT "A"=  452.50
)ANGLE OF INTERNAL FRICTION OF BROKEN COAL=24.
)POISSONS RATIO FOR SURROUNDING ROCK=0.0
)POISSONS RATIO FOR PILLAR ROCK=0.0
)COEFFICIENT OF SLIDING FRICTION FOR BROKEN COAL=0.44
)YOUNGS MODULAS FOR SURROUNDING ROCK=        0
)YOUNGS MODULAS FOR PILLAR ROCK=        0
;STRESS REDISTRIBUTION COEFFICIENT=0.50
)TOTAL NUMBER OF SLICES=     62
)SLICE INTERVAL IN PRINTOUT=   2
)
)

)THE RESULTS ARE
)
)WARNING:VALUE OF W/H IS NOT WITHIN RECOMENDED RANGE OF 0.25 GT W/H LT 4
)MEAN STRESS CONCENTRATION=3.170
)MEAN PILLAR STRESS:LHS=2948.
)MAXIMUM STRESS CONCENTRATION=     3.17
)THE PILLAR IS STABLE
)THE FAILURE MODE WILL BE ULTIMATE YIELD
)THE PILLAR STRENGTH =    2955.25
)THE SAFETY FACTOR    =        1.00
)THE CRITICAL PILLAR DIMENSION TO AVOID
)        A) CATASTROPHIC YIELD IS  18.58
)        B) ULTIMATE YIELD IS  30.00
)  SLICE     (90-0)   TAUS/F     TAU       STATUS       PONE    PTHREE ACCUM STRESS
)  ------    ------   ------     ---       ------       ----    ------ ------------
)  1( 1.0)   30.00    426.5    1276.6      FAILED        59.2     14.1      0.0
)  4( 4.0)   30.63    491.2    1390.1      FAILED       248.0    185.6    304.6
)  6( 6.0)   31.48    572.9    1475.9      FAILED       531.4    253.0    531.0
)  8( 8.0)   32.97    781.1    1523.6      FAILED      1134.9    558.3    757.2
) 10(10.0)   35.44    893.6    1460.7      FAILED      2384.9   1190.7    970.4
) 12(12.0)   39.00   1159.1    1124.9   NOT FAILED     4827.6   1727.7   1079.5
) 14(14.0)   39.00   1159.1    1124.9   NOT FAILED     4827.6   1727.7   1079.5
) 16(16.0)   39.00   1159.1    1124.9   NOT FAILED     4827.6   1727.7   1079.5
) 18(18.0)   39.00   1159.1    1124.9   NOT FAILED     4827.6   1727.7   1079.5
) 20(20.0)   39.00   1159.1    1124.9   NOT FAILED     4827.6   1727.7   1079.5
) 22(22.0)   39.00   1159.1    1124.9   NOT FAILED     4827.6   1727.7   1079.5
) 24(24.0)   39.00   1159.1    1124.9   NOT FAILED     4827.6   1727.7   1079.5
) 26(26.0)   39.00   1159.1    1124.9   NOT FAILED     4827.6   1727.7   1079.5
) 28(28.0)   39.00   1159.1    1124.9   NOT FAILED     4827.6   1727.7   1079.5
) 30(30.0)   39.00   1159.1    1124.9   NOT FAILED     4827.6   1727.7   1079.5
)
·BRITTLE/DUCTILE TRANSITION POINT:TAUF=   1159.1
-FRACTURE ZONE ENDED ON  12TH SLICE AND EXTENDED 12.0 FT INTO THE PILLAR.
 DEPTH OF FRACTURE ZONE JUST AT FAILURE 10.93
```

3

```
)CALCULATION FOR RECTANGULAR OPENING
)
)
)VIRGIN STRESS= 930.0          EXTRACTION RATIO=0.0
)LENGTH OF SPAN=    0.0        SEMI-WIDTH OF PILLAR= 22.0
)SEMI-HEIGHT OF PILLAR= 2.5  OVERBURDEN DEPTH=  800
)DISTANCE "X"=  0.0              SEMI-ROOM WIDTH= 20.0
)RATIO "SH/SV"=0.330           NUMBER OF PILLARS IN SPAN= 0
)COMPRESSIVE STRENGTH OF BROKEN COAL= 44.
)MOHR CONSTANT "A"=  452.50
)ANGLE OF INTERNAL FRICTION OF BROKEN COAL=24.
)POISSONS RATIO FOR SURROUNDING ROCK=0.0
)POISSONS RATIO FOR PILLAR ROCK=0.0
)COEFFICIENT OF SLIDING FRICTION FOR BROKEN COAL=0.44
)YOUNGS MODULAS FOR SURROUNDING ROCK=        0
)YOUNGS MODULAS FOR PILLAR ROCK=        0
)STRESS REDISTRIBUTION COEFFICIENT=0.50
)TOTAL NUMBER OF SLICES=     44
)SLICE INTERVAL IN PRINTOUT=   2
)
)

)THE RESULTS ARE
)
)WARNING:VALUE OF W/H IS NOT WITHIN RECOMENDED RANGE OF 0.25 GT W/H LT 4
)MEAN STRESS CONCENTRATION=3.170
)MEAN PILLAR STRESS:LHS=2948.
)MAXIMUM STRESS CONCENTRATION=     3.42
)THE PILLAR HAS YIELDED
)THE LOAD SHED        =    9567.31
)THE PILLAR STRENGTH =    2513.21
)THE SAFETY FACTOR    =        0.85
)THE CRITICAL PILLAR DIMENSION TO AVOID
)        A) CATASTROPHIC YIELD IS  18.73
)        B) ULTIMATE YIELD IS  30.00
)              K1=                23.1650
)              K2=                 4.0210
)              K3=                -0.5632
)
)
)  SLICE     (90-0)   TAUS/F     TAU       STATUS       PONE    PTHREE ACCUM STRESS
)  ------    ------   ------     ---       ------       ----    ------ ------------
)  1( 1.0)   30.00    426.5    1371.0      FAILED        59.2     14.1      0.0
)  4( 4.0)   30.50    491.2    1787.6      FAILED       248.0    185.6   1071.0
)  6( 6.0)   31.11    572.9    2018.5      FAILED       531.4    253.0   1672.3
)  8( 8.0)   32.16    781.1    2215.7      FAILED      1134.9    558.3   2200.6
) 10(10.0)   33.95    893.6    2300.0      FAILED      2384.9   1190.7   2600.5
) 12(12.0)   39.00   1159.1    2865.2     YIELDED      4835.0   1727.7   3016.7
) 14(14.0)   39.00   1159.1    2862.3     YIELDED      4835.0   1727.7   3050.1
) 16(16.0)   39.00   1159.1    2168.2     YIELDED      4835.0   1727.7   3300.4
) 18(18.0)   39.00   1159.1    2408.3     YIELDED      4835.0   1727.7   3816.6
) 20(20.0)   39.00   1159.1    3004.7     YIELDED      4835.0   1727.7   3005.3
) 22(22.0)   39.00   1159.1    5036.6     YIELDED      4835.0   1727.7  10515.3
)
)BRITTLE/DUCTILE TRANSITION POINT:TAUF=   1159.1
)FRACTURE ZONE ENDED ON  12TH SLICE AND EXTENDED 12.0 FT INTO THE PILLAR.
)DEPTH OF FRACTURE ZONE JUST AT FAILURE 10.93
```

TABLE 16: MODEL SOLUTIONS FOR CASE HISTORY #13

TABLE 16/ CONTINUED

4

```
)CALCULATION FOR RECTANGULAR OPENING
)
)
)VIRGIN STRESS= 930.0         EXTRACTION RATIO=0.0
)LENGTH OF SPAN=    0.0       SEMI-WIDTH OF PILLAR= 15.0
)SEMI-HEIGHT OF PILLAR= 2.9  OVERBURDEN DEPTH=  800
)DISTANCE "X"=  0.0             SEMI-ROOM WIDTH= 31.0
)RATIO "SH/SV"=0.330          NUMBER OF PILLARS IN SPAN= 0
)COMPRESSIVE STRENGTH OF BROKEN COAL= 44.
)MOHR CONSTANT "A"=  492.50
)ANGLE OF INTERNAL FRICTION OF BROKEN COAL=24.
)POISSONS RATIO FOR SURROUNDING ROCK=0.0
)POISSONS RATIO FOR PILLAR ROCK=0.0
)COEFFICIENT OF SLIDING FRICTION FOR BROKEN COAL=0.44
)YOUNGS MODULAS FOR SURROUNDING ROCK=       0
)YOUNGS MODULAS FOR PILLAR ROCK=       0
)STRESS REDISTRIBUTION COEFFICIENT=0.50
)TOTAL NUMBER OF SLICES=     30
)SLICE INTERVAL IN PRINTOUT=   2
)
)

)THE RESULTS ARE
)
)WARNING:VALUE OF W/H IS NOT WITHIN RECOMENDED RANGE OF 0.25 GT W/H LT 4
)MEAN STRESS CONCENTRATION=3.170
)MEAN PILLAR STRESS:LHS=2940.
)MAXIMUM STRESS CONCENTRATION=    3.63
)THE PILLAR HAS YIELDED
)THE LOAD SHED        =  12838.63
)THE PILLAR STRENGTH =   2272.00
)THE SAFETY FACTOR    =       0.77
)THE CRITICAL PILLAR DIMENSION TO AVOID
)        A) CATASTROPHIC YIELD IS  10.55
)        B) ULTIMATE YIELD IS  30.00
)              K1=               5.2811
)              K2=               0.6686
)              K3=               0.5124
)
)
)  SLICE    (90-D)   TAUS/F    TAU      STATUS     PONE   PTHREE ACCUM STRESS
)  -----    ------   ------    ---      ------     ----   ------ ------------
)  1( 1.0)   30.00    426.5   1451.1    FAILED      59.2    14.1       0.0
)  4( 4.0)   30.47    491.2   1907.0    FAILED     240.0   105.6    1232.5
)  6( 6.0)   31.03    572.9   2174.2    FAILED     531.4   253.0    1908.2
)  8( 8.0)   31.99    781.1   2627.7    FAILED    1134.9   558.3    2769.9
) 10(10.0)   33.68    893.6   2597.0    FAILED    2384.9  1198.7    3323.6
) 12(12.0)   39.00   1159.1   2306.9   YIELDED    4835.0  1727.7    4002.9
) 14(14.0)   39.00   1159.1   2678.4   YIELDED    4835.0  1727.7    4418.1
) 16(16.0)   39.00   1159.1   3147.7   YIELDED    4835.0  1727.7    5433.6
) 18(18.0)   39.00   1159.1   4637.4   YIELDED    4835.0  1727.7    8563.1
)
)BRITTLE/DUCTILE TRANSITION POINT:TAUF=  1159.1
)FRACTURE ZONE ENDED ON  12TH SLICE AND EXTENDED 12.0 FT INTO THE PILLAR.
)DEPTH OF FRACTURE ZONE JUST AT FAILURE 10.93
```

5

```
)CALCULATION FOR RECTANGULAR OPENING
)
)
)VIRGIN STRESS= 930.0         EXTRACTION RATIO=0.0
)LENGTH OF SPAN=    0.0       SEMI-WIDTH OF PILLAR= 16.0
)SEMI-HEIGHT OF PILLAR= 2.9  OVERBURDEN DEPTH=  800
)DISTANCE "X"=  0.0             SEMI-ROOM WIDTH= 34.0
)RATIO "SH/SV"=0.330          NUMBER OF PILLARS IN SPAN= 0
)COMPRESSIVE STRENGTH OF BROKEN COAL= 44.
)MOHR CONSTANT "A"=  492.50
)ANGLE OF INTERNAL FRICTION OF BROKEN COAL=24.
)POISSONS RATIO FOR SURROUNDING ROCK=0.0
)POISSONS RATIO FOR PILLAR ROCK=0.0
)COEFFICIENT OF SLIDING FRICTION FOR BROKEN COAL=0.44
)YOUNGS MODULAS FOR SURROUNDING ROCK=       0
)YOUNGS MODULAS FOR PILLAR ROCK=       0
)STRESS REDISTRIBUTION COEFFICIENT=0.50
)TOTAL NUMBER OF SLICES=     32
)SLICE INTERVAL IN PRINTOUT=   2
)
)

)THE RESULTS ARE
)
)WARNING:VALUE OF W/H IS NOT WITHIN RECOMENDED RANGE OF 0.25 GT W/H LT 4
)MEAN STRESS CONCENTRATION=3.170
)MEAN PILLAR STRESS:LHS=2940.
)MAXIMUM STRESS CONCENTRATION=    3.94
)THE PILLAR HAS YIELDED
)THE LOAD SHED        =  16853.75
)THE PILLAR STRENGTH =   1942.24
)THE SAFETY FACTOR    =       0.66
)THE CRITICAL PILLAR DIMENSION TO AVOID
)        A) CATASTROPHIC YIELD IS  10.33
)        B) ULTIMATE YIELD IS  30.00
)              K1=               2.0939
)              K2=              -0.3370
)              K3=               0.7033
)
)
)  SLICE    (90-D)   TAUS/F    TAU      STATUS     PONE   PTHREE ACCUM STRESS
)  -----    ------   ------    ---      ------     ----   ------ ------------
)  1( 1.0)   30.00    426.5   1339.7    FAILED      59.2    14.1       0.0
)  4( 4.0)   30.43    491.2   2052.4    FAILED     240.0   105.6    1492.0
)  6( 6.0)   30.93    572.9   2370.6    FAILED     531.4   253.0    2450.7
)  8( 8.0)   31.00    781.1   2722.2    FAILED    1134.9   558.3    3524.1
) 10(10.0)   33.15    893.6   3074.0    FAILED    2384.9  1198.7    4737.4
) 12(12.0)   39.00   1159.1   3372.3   YIELDED    4835.0  1727.7    5949.3
) 14(14.0)   39.00   1159.1   4312.0   YIELDED    4835.0  1727.7    7970.6
) 16(16.0)   39.00   1159.1   9826.9   YIELDED    4835.0  1727.7   17715.4
)
)BRITTLE/DUCTILE TRANSITION POINT:TAUF=  1159.1
)FRACTURE ZONE ENDED ON  12TH SLICE AND EXTENDED 12.0 FT INTO THE PILLAR.
)DEPTH OF FRACTURE ZONE JUST AT FAILURE 10.93
```

6

```
)CALCULATION FOR RECTANGULAR OPENING
)
)
)VIRGIN STRESS= 930.0         EXTRACTION RATIO=0.0
)LENGTH OF SPAN=    0.0       SEMI-WIDTH OF PILLAR= 13.0
)SEMI-HEIGHT OF PILLAR= 2.9  OVERBURDEN DEPTH=  800
)DISTANCE "X"=  0.0             SEMI-ROOM WIDTH= 37.0
)RATIO "SH/SV"=0.330          NUMBER OF PILLARS IN SPAN= 0
)COMPRESSIVE STRENGTH OF BROKEN COAL= 44.
)MOHR CONSTANT "A"=  492.50
)ANGLE OF INTERNAL FRICTION OF BROKEN COAL=24.
)POISSONS RATIO FOR SURROUNDING ROCK=0.0
)POISSONS RATIO FOR PILLAR ROCK=0.0
)COEFFICIENT OF SLIDING FRICTION FOR BROKEN COAL=0.44
)YOUNGS MODULAS FOR SURROUNDING ROCK=       0
)YOUNGS MODULAS FOR PILLAR ROCK=       0
)STRESS REDISTRIBUTION COEFFICIENT=0.50
)TOTAL NUMBER OF SLICES=     26
)SLICE INTERVAL IN PRINTOUT=   2
)
)

)THE RESULTS ARE
)
)WARNING:VALUE OF W/H IS NOT WITHIN RECOMENDED RANGE OF 0.25 GT W/H LT 4
)MEAN STRESS CONCENTRATION=3.170
)MEAN PILLAR STRESS:LHS=2940.
)MAXIMUM STRESS CONCENTRATION=    4.44
)THE PILLAR HAS YIELDED
)THE LOAD SHED        =  19356.86
)THE PILLAR STRENGTH =   1439.11
)THE SAFETY FACTOR    =       0.49
)THE CRITICAL PILLAR DIMENSION TO AVOID
)        A) CATASTROPHIC YIELD IS  10.65
)        B) ULTIMATE YIELD IS  30.00
)              K1=               0.9585
)              K2=              -0.7291
)              K3=               0.6964
)
)
)  SLICE    (90-D)   TAUS/F    TAU      STATUS     PONE   PTHREE ACCUM STRESS
)  -----    ------   ------    ---      ------     ----   ------ ------------
)  1( 1.0)   30.00    426.5   1721.2    FAILED      59.2    14.1       0.0
)  4( 4.0)   30.40    491.2   2229.6    FAILED     240.0   105.6    1093.9
)  6( 6.0)   30.86    572.9   2637.4    FAILED     531.4   253.0    3192.5
)  8( 8.0)   31.33    781.1   3214.4    FAILED    1134.9   558.3    4867.4
) 10(10.0)   32.46    893.6   4121.6    FAILED    2384.9  1198.7    7392.1
) 12(12.0)   39.00   1159.1   6466.7   YIELDED    4835.0  1727.7   12520.5
)
)BRITTLE/DUCTILE TRANSITION POINT:TAUF=  1159.1
)FRACTURE ZONE ENDED ON  12TH SLICE AND EXTENDED 12.0 FT INTO THE PILLAR.
)DEPTH OF FRACTURE ZONE JUST AT FAILURE 10.93
```

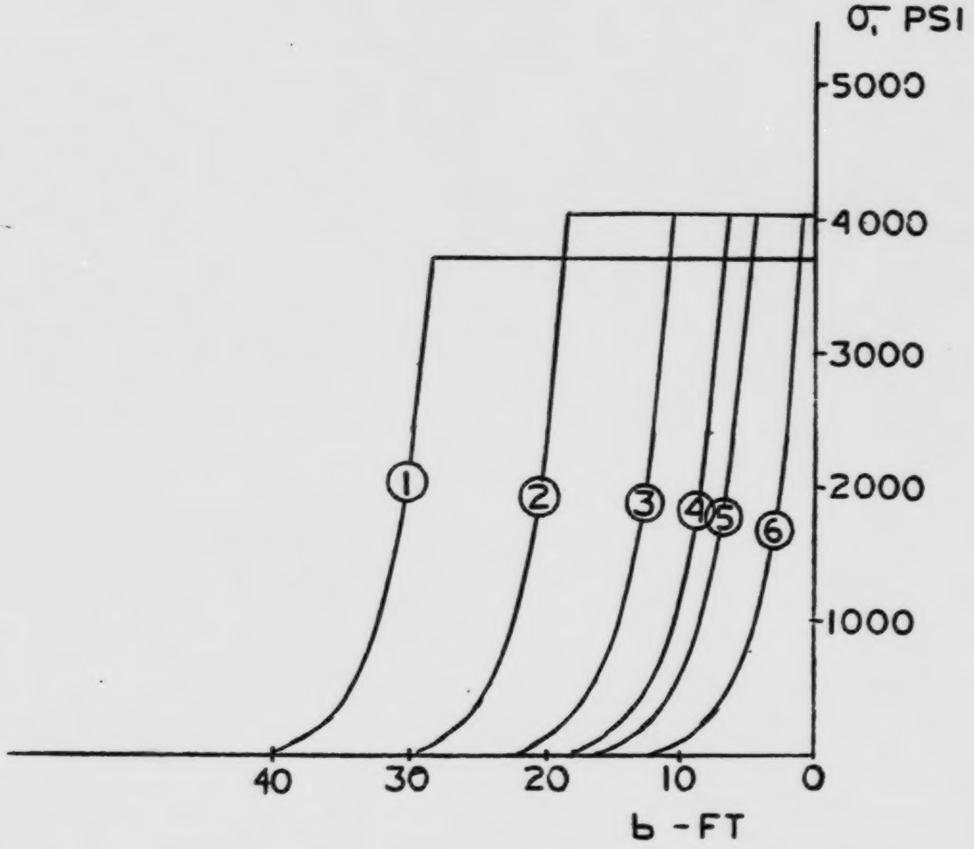

FIGURE 44: MODEL STRESS DISTRIBUTIONS IN THE TEST PILLAR AT DIFFERENT SIZES

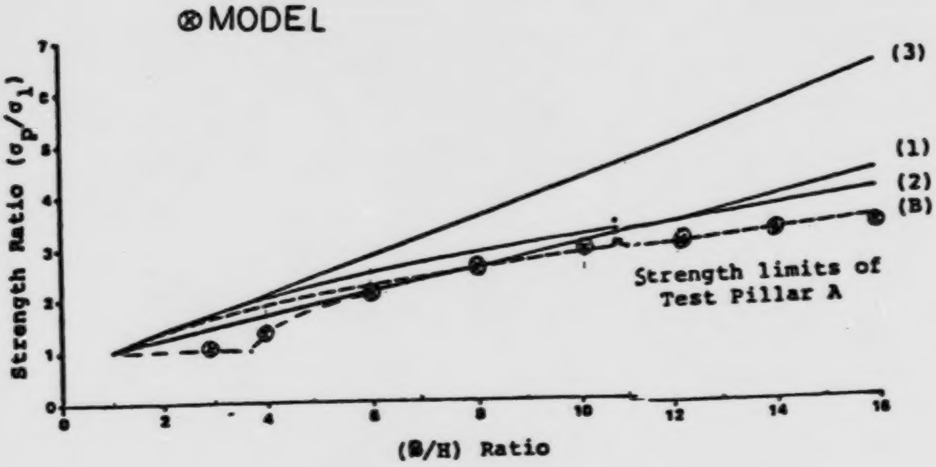

Comparisons between variations of pillar strength and (W/H) ratio obtained using equations 1-3 and the limits of data obtained in the present study. Equation B determined from laboratory results is presented for comparison (dashed curve).

FIGURE 45: COMPARISON OF VARIOUS PILLAR STRENGTH VS B/H RELATIONSHIPS

Curve 2: $\frac{\sigma_p}{\sigma_c} = (\frac{B}{H})^{½}$

Curve 3: $\frac{\sigma_p}{\sigma_c} = 0.64 + 0.36 (\frac{B}{H})$

Curve B: $\frac{\sigma_p}{\sigma_c} = (\frac{B}{H})^{0.45}$ (derived from their laboratory study)

It is seen that the model results are in excellent agreement with Curve B and Curve 2 for large B/H ratios. However, at low B/H ratios the model results deviate significantly from the other formulae.

7.2 Case History #14: Stress Measurements in Coal Pillars

7.2.1 Case Background

Hazen and Artler (28) carried out a field and laboratory test program in which they tested coal specimens from the Pittsburgh No. 8 seam from the Powhatan No. 4 mine, Ohio and made measurements of the stress distribution across the diagonals of pillars during primary and secondary mining.

From a comprehensive (96 specimen) study of size and shape effects on the strength of specimens of this coal they derived the following relationship:-

$$\sigma_s = 2747 \sqrt{\frac{B}{H}}$$

as shown in their results in Figure 46.

i.e. k (for a 1 inch cube) = 2747.

In the field study two locations were selected to measure the additional load carried by a coal pillar during mining in a block pillar system with secondary mining. The first site was under 710 to 780 ft. of cover and the second site under 600 to 640 ft. of cover. The pillars were located on 80 ft. square centres with the initial pillars designed to be 62 ft. square and the final pillars after secondary

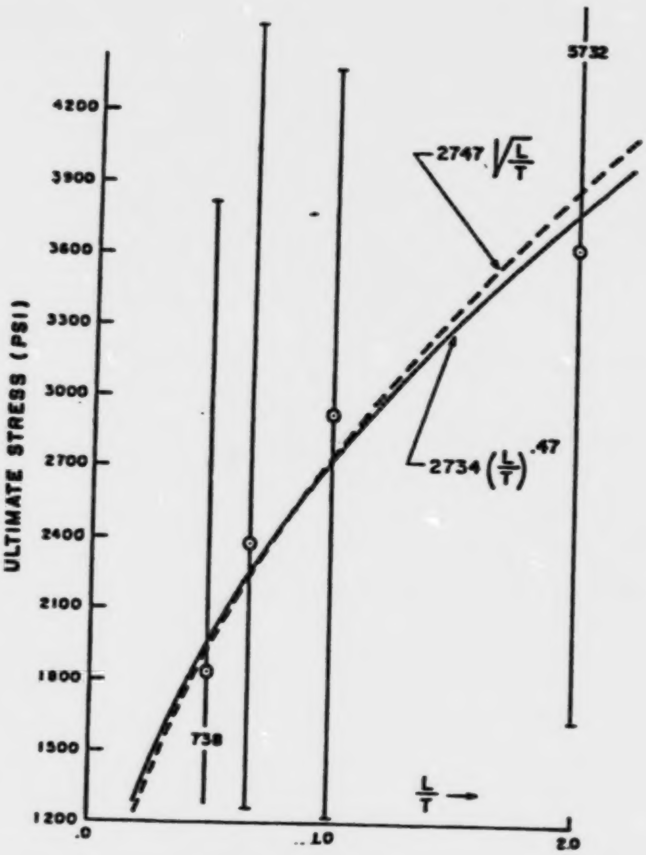

FIGURE 46: SPECIMEN STRENGTH/SHAPE RESULTS FOR CASE HISTORY #14

mining were designed to be 47 ft. square. The pillars were instrumented with stress measuring cells at seven points along the pillar diagonal from the corners to the pillar centre. In addition 3 load cells were located to measure the stress at the centre of the side, at the corner and spaced between these locations. The overburden stress was taken as 1 psi per foot and the initial stress on the pillar was obtained by tributary area theory.

Unfortunately this paper does not give all the results in detail. However, Hazen and Artler noted that all of the pillars displayed the same general trend. The higher stresses were found in the pillar core with lower stresses at the periphery. The stress distribution was assumed symetrical about the centre of the pillar, Figure 47 shows the stress profile across a pillar diagonal under 1000 psi overburden stress during initial and secondary mining. They noted that the zone of high stress becomes smaller as the pillar is reduced in area and the ratio of high to low stresses becomes larger with secondary mining and that there is a highly stressed inner core with less stress in a region extending in 10 ft. from the pillar surface.

From the in situ measurements, the average stress found in the initial pillars was 950 psi whereas the average stress in the final pillar was 860 psi.

The fact that the average pillar stress has dropped with decrease in pillar size suggests to the author that the pillars may have failed by yielding. The model will be used to examine this possibility.

7.2.2 Model Solution

The pillars were 78 inches high. Thus using k (1 inch cube) equal to 2747; and assuming a 64 inch upper strength limit gives the cube strength σ_H for a cube of this height as:-

$$\sigma_H = 2747 \times \frac{1}{\sqrt{64}} = 344 \text{ psi}$$

Hence A for input in the model is 172 psi.

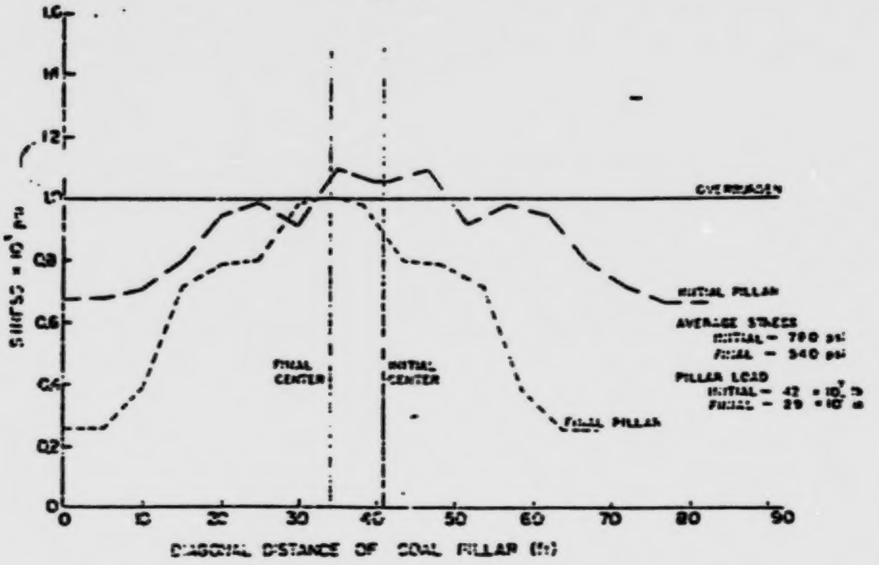

FIGURE 47: AVERAGE STRESS PROFILE OF A COAL PILLAR SUBJECTED TO 1000 PSI OVERBURDEN STRESS DURING INITIAL AND SECONDARY MINING

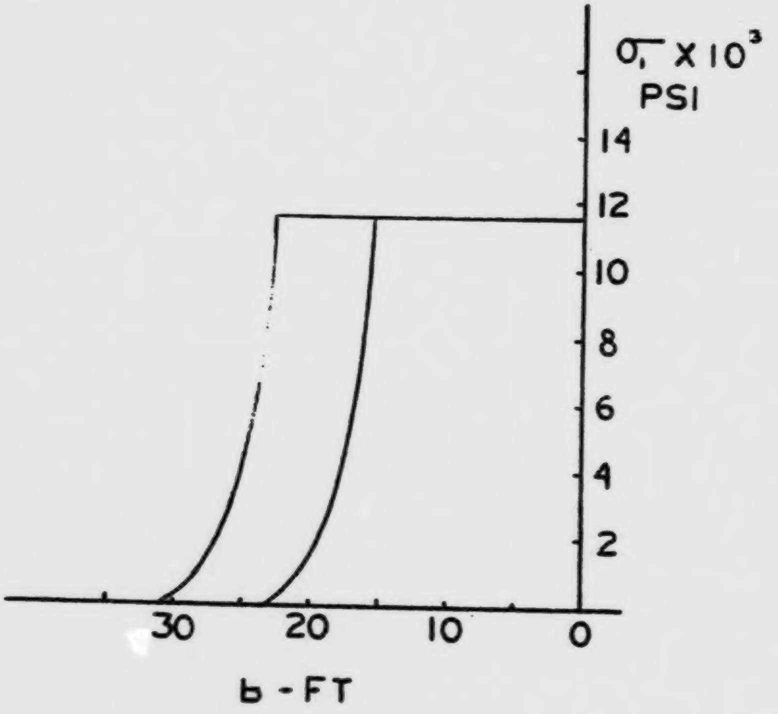

FIGURE 48: MODEL STRESS DISTRIBUTION FOR CASE HISTORY #14

Values of $\phi_B = 27^{\circ}$, $\mu_B = \tan \phi_B = 0.5095$ and $P_B = 30$ psi were assumed. Table 17 shows the model results for the initial pillar (62 ft. square) and the final pillar (47 ft. square). Figure 48 shows the resulting stress distribution across the pillar.

It is seen from these model solutions that the pillar has yielded at both sizes; the residual mean pillar stress capacities being 954 psi and 889 psi respectively; which is close to the mean values of 950 and 860 reported by Hazen and Artler. In addition, the vertical stress at yield (P_{1T}) from the model is 1157 psi. It will be noted that, from Figure 47, the stress distribution at the pillar centres observed by Hazen and Artler are almost flat, corresponding to what might be expected in a yielding situation and that the magnitude of this "yield stress" for the two pillars approximately 1080 psi and 1000 psi respectively, close to that predicted by the model.

Hence it may be concluded that, with a judicous choice of the ϕ_B, μ_B and P_B values, the results of Hazen and Artler can be explained by the model solution. i.e. the pillars have failed by pseudo-ductile yield.

7.3 Conclusion

It is seen from the two case histories given in this section that:-

(i) There appears to be good evidence in the literature that pillars can fail by yielding and that the residual stress capacity of the yielded pillar may be predicted by the analytic model.

(ii) The study by Skelly, Walgomott and Wang is particularly satistying since, the residual stress capacity is accurately predicted by the model for four different pillar sizes after failure has occurred.

(iii) As always, a judicous choice has had to be made for the input parameters, which cannot be confirmed. Nonetheless, these studies show that the model will explain these results.

```
1CALCULATION FOR RECTANGULAR OPENING

  VIRGIN STRESS= 836.0          EXTRACTION RATIO=0.0
  LENGTH OF SPAN=    0.0        SEMI-WIDTH OF PILLAR= 31.0
  SEMI-HEIGHT OF PILLAR= 3.3  OVERBURDEN DEPTH=  760
  DISTANCE "X"=  0.0              SEMI-ROOM WIDTH= 10.0
  RATIO "SH/SV"=0.330           NUMBER OF PILLARS IN SPAN= 0
  COMPRESSIVE STRENGTH OF BROKEN COAL= 30.
  MOHR CONSTANT "A"=  172.00
  ANGLE OF INTERNAL FRICTION OF BROKEN COAL=27.
  POISSONS RATIO FOR SURROUNDING ROCK=0.0
  POISSONS RATIO FOR PILLAR ROCK=0.0
  COEFFICIENT OF SLIDING FRICTION FOR BROKEN COAL=0.51
  YOUNGS MODULAS FOR SURROUNDING ROCK=         0
  YOUNGS MODULAS FOR PILLAR ROCK=         0
  STRESS REDISTRIBUTION COEFFICIENT=0.50
  TOTAL NUMBER OF SLICES=    62
  SLICE INTERVAL IN PRINTOUT=    1

0THE RESULTS ARE

  MEAN STRESS CONCENTRATION=1.160
  MEAN PILLAR STRESS:LHS= 970.
  MAXIMUM STRESS CONCENTRATION=     2.46
  THE PILLAR HAS YIELDED
  THE LOAD SHED          =    482.20
  THE PILLAR STRENGTH =    954.20
 THE SAFETY FACTOR    =      0.98
  THE CRITICAL PILLAR DIMENSION TO AVOID
         A) CATASTROPHIC YIELD IS    6.33
         B) ULTIMATE YIELD IS   33.57
              K1=               0.1642
              K2=              -0.8885
              K3=               0.9820

   SLICE    (90-D)   TAUS/F    TAU      STATUS       PONE   PTHREE ACCUM
   -----    ------   ------    ---      ------       ----   ------ ------
   1( 1.0)   30.00    149.0   723.6     FAILED        41.2     9.3      0
   2( 2.0)   30.20    159.1   655.0     FAILED        71.0    23.5    178
   3( 3.0)   30.52    172.0   634.8     FAILED       118.4    45.1    273
   4( 4.0)   30.97    190.6   629.0     FAILED       189.1    77.0    353
   5( 5.0)   31.62    213.5   628.4     FAILED       296.4   127.4    419
   6( 6.0)   32.53    242.4   622.9     FAILED       459.3   202.8    472
   7( 7.0)   33.70    270.7   604.5     FAILED       706.6   317.3    509
   8( 8.0)   35.50    323.7   560.3     FAILED      1082.1   491.0    522
   9( 9.0)   38.25    358.2   471.5    YIELDED      1157.5   491.0    497
  10(10.0)   38.25    358.2   453.8    YIELDED      1157.5   491.0    474
  11(11.0)   38.25    358.2   440.3    YIELDED      1157.5   491.0    457
  12(12.0)   38.25    358.2   429.6    YIELDED      1157.5   491.0    444
  13(13.0)   38.25    358.2   420.7    YIELDED      1157.5   491.0    434
  14(14.0)   38.25    358.2   413.2    YIELDED      1157.5   491.0    426
  15(15.0)   38.25    358.2   406.0    YIELDED      1157.5   491.0    418
  16(16.0)   38.25    358.2   401.2    YIELDED      1157.5   491.0    412
  17(17.0)   38.25    358.2   396.5    YIELDED      1157.5   491.0    407
  18(18.0)   38.25    358.2   392.4    YIELDED      1157.5   491.0    403
  19(19.0)   38.25    358.2   388.9    YIELDED      1157.5   491.0    400
  20(20.0)   38.25    358.2   386.0    YIELDED      1157.5   491.0    397
  21(21.0)   38.25    358.2   383.7    YIELDED      1157.5   491.0    395
  22(22.0)   38.25    358.2   382.1    YIELDED      1157.5   491.0    395
  23(23.0)   38.25    358.2   381.1    YIELDED      1157.5   491.0    395
  24(24.0)   38.25    358.2   380.9    YIELDED      1157.5   491.0    397
  25(25.0)   38.25    358.2   381.9    YIELDED      1157.5   491.0    401
  26(26.0)   38.25    358.2   384.3    YIELDED      1157.5   491.0    408
  27(27.0)   38.25    358.2   388.0    YIELDED      1157.5   491.0    420
  28(28.0)   38.25    358.2   397.0    YIELDED      1157.5   491.0    438
  29(29.0)   38.25    358.2   412.1    YIELDED      1157.5   491.0    471
  30(30.0)   38.25    358.2   443.4    YIELDED      1157.5   491.0    537
  31(31.0)   38.25    358.2   535.0    YIELDED      1157.5   491.0    726

BRITTLE/DUCTILE TRANSITION POINT:TAUF=    358.2
 FRACTURE ZONE ENDED ON    9TH SLICE AND EXTENDED   9.0 FT  INTO THE P
 DEPTH OF FRACTURE ZONE JUST AT FAILURE   7.66
1CALCULATION FOR RECTANGULAR OPENING
```

```
  VIRGIN STRESS= 836.0          EXTRACTION RATIO=0.0
  LENGTH OF SPAN=    0.0        SEMI-WIDTH OF PILLAR= 23.5
  SEMI-HEIGHT OF PILLAR= 3.3  OVERBURDEN DEPTH=  760
  DISTANCE "X"=  0.0              SEMI-ROOM WIDTH= 10.0
  RATIO "SH/SV"=0.330           NUMBER OF PILLARS IN SPAN= 0
  COMPRESSIVE STRENGTH OF BROKEN COAL= 30.
  MOHR CONSTANT "A"=  172.00
  ANGLE OF INTERNAL FRICTION OF BROKEN COAL=27.
  POISSONS RATIO FOR SURROUNDING ROCK=0.0
  POISSONS RATIO FOR PILLAR ROCK=0.0
  COEFFICIENT OF SLIDING FRICTION FOR BROKEN COAL=0.51
  YOUNGS MODULAS FOR SURROUNDING ROCK=         0
  YOUNGS MODULAS FOR PILLAR ROCK=         0
  STRESS REDISTRIBUTION COEFFICIENT=0.50
  TOTAL NUMBER OF SLICES=    47
  SLICE INTERVAL IN PRINTOUT=    1

0THE RESULTS ARE

  MEAN STRESS CONCENTRATION=1.160
  MEAN PILLAR STRESS:LHS= 970.
  MAXIMUM STRESS CONCENTRATION=     2.48
  THE PILLAR HAS YIELDED
  THE LOAD SHED          =   1090.42
  THE PILLAR STRENGTH =    889.32
 THE SAFETY FACTOR    =      0.92
  THE CRITICAL PILLAR DIMENSION TO AVOID
         A) CATASTROPHIC YIELD IS    6.32
         B) ULTIMATE YIELD IS   33.57
              K1=               0.1190
              K2=              -0.9203
              K3=               0.9869

   SLICE    (90-D)   TAUS/F    TAU      STATUS       PONE   PTHREE ACCUM
   -----    ------   ------    ---      ------       ----   ------ ------
   1( 1.0)   30.00    149.0   689.5     FAILED        41.2     9.3      0
   2( 2.0)   30.21    159.1   627.1     FAILED        71.0    23.5    193
   3( 3.0)   30.53    172.0   619.0     FAILED       118.4    45.1    313
   4( 4.0)   30.98    190.6   627.5     FAILED       189.1    77.0    418
   5( 5.0)   31.60    213.5   638.2     FAILED       296.4   127.4    495
   6( 6.0)   32.45    242.4   644.4     FAILED       459.3   202.8    567
   7( 7.0)   33.63    270.7   637.1     FAILED       706.6   317.3    622
   8( 8.0)   35.24    323.7   602.6     FAILED      1082.1   491.0    651
   9( 9.0)   38.25    358.2   522.2    YIELDED      1157.5   491.0    632
  10(10.0)   38.25    358.2   509.5    YIELDED      1157.5   491.0    617
  11(11.0)   38.25    358.2   502.1    YIELDED      1157.5   491.0    610
  12(12.0)   38.25    358.2   498.5    YIELDED      1157.5   491.0    610
  13(13.0)   38.25    358.2   497.9    YIELDED      1157.5   491.0    615
  14(14.0)   38.25    358.2   500.3    YIELDED      1157.5   491.0    625
  15(15.0)   38.25    358.2   505.0    YIELDED      1157.5   491.0    641
  16(16.0)   38.25    358.2   515.0    YIELDED      1157.5   491.0    664
  17(17.0)   38.25    358.2   529.0    YIELDED      1157.5   491.0    696
  18(18.0)   38.25    358.2   549.5    YIELDED      1157.5   491.0    741
  19(19.0)   38.25    358.2   579.9    YIELDED      1157.5   491.0    807
  20(20.0)   38.25    358.2   626.0    YIELDED      1157.5   491.0    906
  21(21.0)   38.25    358.2   704.9    YIELDED      1157.5   491.0   1069
  22(22.0)   38.25    358.2   857.0    YIELDED      1157.5   491.0   1384
  23(23.0)   38.25    358.2  1284.1    YIELDED      1157.5   491.0   2264

BRITTLE/DUCTILE TRANSITION POINT:TAUF=    358.2
 FRACTURE ZONE ENDED ON    9TH SLICE AND EXTENDED   9.0 FT  INTO THE P
 DEPTH OF FRACTURE ZONE JUST AT FAILURE   7.66
```

TABLE 17: MODEL SOLUTIONS FOR CASE HISTORY #14

8. CONCLUSIONS AND RECOMMENDATIONS

8.1 Conclusions

The objective of the studies reported in this Phase 2 report was to evaluate the applicability of the analytical approach to the design of coal pillars, developed in the Phase 1 report, by testing the model against experimental data derived from the literature.

This was done in a series of steps, the first of which was a detailed consideration of the meaning and values of the coal properties required for input into the model.

8.1.1 With respect to the input parameters it was concluded that:-

1. Coal strength/size effects must be taken into account when deriving the value of A, the "Mohr constant", to be used in the model equations. The value to be used is that given by the relationship:-

$$A = \frac{\sigma_H}{2}$$

where σ_H is the uniaxial compressive strength of a cube of coal of side length equal to the pillar height.

2. This value of σ_H can be determined from small scale tests on coal cubes in the laboratory using the relationship:-

$$\sigma_H = k\,D^{\alpha}$$

where D is the cube dimension in inches and k is numerically equal to the 1 inch cube strength. Ideally α should be derived for each specific coal from laboratory tests on a range of conveniently sized coal cubes. However, if such data is unavailable than a value of $\alpha = -0.5$ gives an acceptable first approximation.

3. It appears that there is an upper size limit to this variation of cube strength with size dimension. It is shown that this limit occurs when D is approximately 64

inches. i.e. for pillar heights of greater than 64 inches, the cube strength is given by that for the 64 inch cube:-

$$\text{i.e.} \quad \sigma_H = k.\, 64^{\alpha}$$

which, if $\alpha = -0.5$ gives:-

$$\sigma_H = 0.125\ k$$

4. No modification of the coal strength input parameters are required to take into account the size/shape relationships for coal strength. Such effects are taken into account in the model.

5. It is assumed in the case histories studied that μ_B, the coefficient of sliding friction of coal on coal equals tan ϕ_B, where ϕ_B is the angle of internal friction for broken coal. There is no evidence in the literature to verify or deny this assumption; this should be experimentally investigated (see recommendations)

6. It is also assumed in the model that μ_B is a constant and does not vary with normal stress. This appears to be a reasonable first approximation for coal within the range of normal stresses encountered in coal pillars. However, caution should be exercised since there is evidence in the literature that μ_B may vary with normal stress at very low and very high normal stresses.

7. There is no evidence in the literature to establish whether or not μ_B and ϕ_B are size affected. They are assumed not to be; however this should also be examined experimentally (see recommendations). Assuming that $\mu_B = \tan \phi_B$ and that they are not size affected then they can be determined from small scale laboratory tests on broken coal specimens, on recompacted broken coal specimens and/or by shear box tests.

8. The determination of the cohesion, and hence the uniaxial compressive strength, P_B, of broken coal is most unsatisfactory. At best laboratory results from tests on broken coal yield only a maximum possible value for P_B. In reality a value of perhaps 1/10th of this maximum value may be a better estimate.

This lack of certainty in the determination of P_B is unfortunate since the model solutions are quite sensitive to the magnitude of P_B. In practice it may be better to back analyse field results to determine the effective P_B value for that coal at that site and then use the value so determined for further design analysis at that site.

9. It is not known whether P_B is size affected.

The second step of this study comprised an evaluation of specimen testing data from the literature to seek verification of the proposed brittle/pseudo-ductile transition point on the Mohr envelope.

8.1.2 With respect to brittle/pseudo-ductile transition it was concluded that:-

10. There is excellent evidence in the literature to show that, for some coals and coal measure rocks at least, the brittle/pseudo-ductile transition point does exist within the stress ranges that may be expected in coal pillars.

11. The fact that this transition point does exist means that a change in the mode of failure must occur beyond this transition point. This is taken as being very strong indirect evidence that the proposed failure theory can and does apply to coal.

12. The analytical model solution gives the first rational explanation of the failure mechanism taking place when Holland reported test results in which wide specimens did not fail abruptly. It is shown that there is a critical (B/H) ratio above which the specimen cannot fail abruptly but fails gradually by pseudo-ductile yield. The physical description of the failure of these specimens given by Holland is markedly similar to that which would be expected from the failure theory developed in the Phase 1 report.

13. It is also shown that the use of the uniaxial compressive strength (σ_H) to determine the "Mohr constant" A and give a Mohr envelope expressed by:-

$$\tau = A\sigma + \frac{A^2}{4}$$

gives only a first approximation to the curvilinear Mohr envelope for failure. This can lead to significant errors in the exact determination of the transition point. This form should only be used if the only strength data available is a uniaxial compressive strength.

14. It is shown that, if a full set of triaxial strength data for the coal is available, it is better to express the Mohr envelope in Balmer's parametric form; this leads to a much more accurate determination of the transition point.

However, at present, the model computer program deals only with the single parameter, A form, of Mohr envelope. To deal with Balmers form of Mohr envelope the equations for failure used in the model must be re-stated and programmed. This has not yet been done. (see recommendations).

Finally a series of case histories based on field measurements in coal pillars were examined and model solutions to fit these results were sought. Unfortunately, but inevitably, all of the necessary coal input parameters were not available for each of these case histories. This lead to assumptions being mark for the missing values; the assumed values were within the ranges that might be expected for these coals but nevertheless some doubt must remain because of this. These field study case histories were split into four groups and the conclusions were as follows.

8.1.3 Field case histories related to stress distributions across pillars

There were two case studies in this group.

15. In the first case it was shown that the model solution gave a much better fit to the field data than did the original author's elastic solution.

16. In the second case, the model solution could not be made to fit the field data; indeed the model predicted a very different stress distribution. No explanation can be offered for the difference.

8.1.4 Field case histories related to pillar strength formulae

The pillar strength formulae developed in the Phase 1 report were compared to four different pillar stress formulae developed by different authors and given in the literature. The conclusions were:-

17. The shape or form of the model equations differ totally from the empirical formulae given in the literature. In particular, the model predicts that, for each specific pillar height there is a minimum pillar width below which the pillar strength remains constant ($\sigma_{p\ min}$) whereas all the empirical formulae suggest that strength continually decreases with decreasing pillar width.

18. However, if the analytically derived strengths were treated as "real data" (field data) then it was shown that they correlated to the width and height relationships used by each of the other formulae with an acceptable correlation coefficient of > 0.9. i.e. in the following forms:-

(i) $\bar{\sigma}_p \propto \frac{B^{0\cdot46}}{H^{0\cdot66}}$

(ii) $\bar{\sigma}_p \propto (\frac{B}{H})$

(iii) $\bar{\sigma}_p \propto \frac{\sqrt{B}}{H}$

(iv) $\bar{\sigma}_p \propto \sqrt{\frac{B}{H}}$

These correlations coefficients are no worse than those obtained by the original workers in establishing their empirical formulae.

Hence it may be concluded that when viewed in this manner the analytical equations give results which are totally compatible with each of these previous studies. Clearly this does not prove the validity of the analytical approach but does indicate that the analytical model yields strengths compatible with other studies.

8.1.5 Field case histories related to fracture zone development in pillars

Two case histories were concluded in this group. It was concluded that:-

19. For both cases it was possible to obtain a good agreement between the analytical model solution and the field data, provided that a judicous choice is made for the coal and broken coal strength properties. (A, μ_B, ϕ_B and P_B).

20. The values of A, μ_B, ϕ_B can be reasonably estimated. However P_B is unknown and was adjusted until the model solution fitted the field data. The results are, unfortunately, sensitive to these assumed P_B values.

8.1.6 Field case histories related to pillar yielding

There were two case histories in this group. It was concluded that:-

21. Both of these sets of field results could be well fitted by the concept of the pillar failing by pseudo-ductile yielding. In one of these cases the prediction by the model solution of the residual mean pillar stress at different sizes was surprisingly accurate. These results were thus concluded to give additional strong indirect evidence in favour of the analytical model concepts, particularly with respect to the yielding of wide coal pillars.

Thus, with one exception, each of the field case histories could be well fitted by the analytic model solution provided that a judicous choice were made for the input parameters for the coal properties required by the model. Unfortunately the case histories did not give sufficient information to define all of the required input parameters, this lead to intelligent estimates being made for some of these properties. In these circumstances, although the model may give a good "prediction" of the field data, some doubt must remain with respect to the model validity because of this use of "typical estimated" proporties rather than actual values.

8.2 Recommendations

A number of questions remain unanswered or unproved particularly with respect to the determination and use of coal properties in the model. It is therefore recommended that a comprehensive coal specimen testing program be carried out with the aim of determining:-

(i) Size/shape effects on coal strength; are they applicable to triaxial conditions? The basic coal strength parameter used by most workers is the uniaxial 1 inch cube strength. Coal strength is very dependent on the specimen size and shape and much work is reported in the literature establishing accepted coal strength/size/shape relationships for uniaxially loaded specimens. The value for the uniaxial strength used in the model is that given by these relationships for a cube of size equal to the pillar height.

However, the model takes into account the triaxial loading conditions generated in the pillar. The question therefore arises as to whether the size/shape effects established for uniaxial conditions can be assumed to apply under triaxial conditions? If the uniaxial size effects apply to triaxial conditions without modification then this will result in parallel Mohr envelopes. However, a good case could be made to suggest that, once pseudo-ductile yielding commences then the strengths may be size independent. In such a case the Mohr envelopes would converge.

There are no previous studies that address this question, but it must be answered if full benefit is to be obtained from this model capability. It is essential to use the correct size adjusted Mohr envelope in inputting the coal parameters in the model.

(ii) Frictional properties of coal The model also requires the input of two other coal parameters namely μ the sliding coefficient of friction on a fractured coal surface and ϕ_B the angle of internal friction of broken coal. An argument could be made that $\mu = \tan \phi_B$ but there is insufficient evidence in the literature to confirm or deny this. An investigation should therefore be carried out to determine these two parameters and to determine whether or not μ is related in any way to ϕ_B.

In addition, it is assumed in the model that the coefficient of sliding friction, μ, is a constant independent of the applied normal stress. Whilst this is a reasonable first approximation there is evidence in the literature that μ varies with normal stress (see Phase 1 report, Page 68). This could easily be investigated during experiments aimed at determining μ and ϕ_B.

(iii) Brittle/pseudo-ductile transition point The failure criterion developed in Phase 1 of the study and used in the model defines a brittle/pseudo-ductile transition point on the Mohr envelope as being that point on the Mohr envelope where the shear resistance to sliding exceeds the shear resistance to fracture. This failure criterion has been used successfully to predict hard rock behaviour at exceptionally high confining pressures; it has not previously been applied to coal or at such relatively low confining pressures. At least one reputable reviewer has questioned the application of this failure criterion to coal at the relatively low stress levels experienced in coal pillars. Some significant evidence backing the use of this failure criterion has been obtained from the case histories; however this evidence is indirect and, in view of the fundamental nature of this query to the whole conceptional approach, it is believed that a test program should be specifically designed and carried out to prove or disprove the application of this failure criterion to coal.

(iv) Standard tests to determine the coal property parameters As seen above the model requires the input of coal property parameters that have not usually been measured in past studies. Hence there is a need to develop standardized test procedures to determine these parameters and, if possible, to develop a single simple laboratory test from which all these parameters might be obtained.

Appendix E gives a detailed coal testing program which should establish answers to these outstanding questions.

Finally it is recommended that the failure equations be re-stated and the computer model adjusted to allow the program to deal with a Mohr envelope when expressed in the Balmer parametric form. This should be introduced as a user option so that, if a full suite of triaxial strength data is available, then the user may choose the more accurate Balmer form of Mohr envelope to describe the failure envelope. However, if only uniaxial compressive strength is available, then the user must be able to use the single parameter parabolic form of approximate Mohr envelope that is currently in the program.

9. REFERENCES

1. Barron, K.
"An Analytical Approach to the Design of Coal Pillars. Part I: The Analytical Method", DSS Contract Report, ISQ 80-00161, January 1982

2. Hustrulid, W.A.
"A Review of Coal Pillar Strength Formulae", Rock Mechanics, V.8, pp. 115-145, 1976

3. Bieniawski, Z.T.
"In-Situ Large Scale Testing of Coal", Proc. Conf. on In-Situ Investigation Rock and Soil, British Geotechnical Society, London, pp. 44-49, 1969

4. Orawin, E.
"Mechanism of Seismic Faulting", Rock Deformation, Geological Soc. Am, Mem. 79, pp. 323-345, 1960

5. Byerlee, J.D.
"Frictional Characteristics of Granite under High Confining Pressure", J. Geophysical Research, 14, pp. 3634-3648, July 1967

6. Kripakov, N.P.
"Analysis of Pillar Stability on Steeply Pitching Seams using the Finite Element Method", U.S. Bureau of Mines, Report of Investigation 8579, 1981

7. Balmer, G.
"A General Analytic Solution for Mohr's Envelope" A.S.T.M Proc, 52, June 1952

8. Atkinson, R.H. and Ko, H.Y.
"Strength Characteristics of U.S. Coals", Proc. 18th Symposium on Rock Mechanics, Keystone, Colorado, pp. 282-1:6, 1977

9. Hobbs, D.W.
"The Behavious of Broken Rock under Triaxial Compression", Int. J. Rock Mechanics and Min. Sci., V.7, pp. 125-148, 1970

10. Lowall, C.E. and Holland, C.T.
"Some Physical Characteristics of West Virginia Coal", Research Bulletin of Engineering Experimental Station, West Virginia University, Bulletin 17, 1937

11. Holland, C.T.
"The Strength of Coal in Mine Pillars", Proc. 6th Symposium on Rock Mechanics, Univerisity of Missouri, Rolla, pp. 450-466, 1964

12. Holland, C.T.
"Physical Properties of Coal and Associated Rock as Related to Causes of Bumps in Coal Mines", Trans. AIME, V. 149, pp. 75-93, 1942

13. Leeman, E.R. and van Heerden, W.L.
"Stress Measurements in Coal Pillars, Parts I and II", Colliery Engineering, pp. 517-519, Dec. 1963, and pp. 26-31, January 1964

14. van Heerden, W.L.
"Stress Measurements in Coal Pillars", Proc. 2nd Int. Congress on Rock Mechanics, Paper 4-16, pp. 497-501, 1970

15. Salamon, M.D.G. and Oravecz, K.I.
"Displacement and Strains Induced by Bord and Pillar Mining in South African Collieries", Proc. 1st Congress Int. Soc. Rock Mechanics, Lisbon, V. 2, pp. 227-231, 1966

16. Bieniawski, Z.T.
"The Effect on Specimen Size on Compressive Strength of Coal", Int. J. Rock Mechanics and Min. Sci., Vol. 5, No. 4, pp 325-335, 1968

17. Salamon, M.D.G. and Munro, A.H.
"A Study of the Strength of Coal Pillars", J. S. African Inst. Min. and Met., pp. 55-67, 1967

18. Bieniawski, Z.T.
"Contribution to the Discussion of 'A Study of the Strength of Coal Pillars' and 'A Method of Designing Bond and Pillar Workings", J. S. African Inst. Min. and Met., pp 185-187, November 1967

19. Sowry, C.G.
"Contribution to the Discussion of 'A Study of the Strength of Coal Pillars' and 'A Method of Designing Bond and Pillar Workings", J. S. African Inst. Min. and Met., pp 187-192, November 1967

20. Bieniawski, Z.T.
"In-Situ Strength and Deformation Characteristics of Coal", Engineering Geology, V. 2, No. 5, pp. 325-340, 1968

21. Holland, C.T. and Gaddy, F.L.
"Some Aspects of Permanent Support of West Virginia Coals", Proc. West Virginia Mining Institute, pp 54-55, 1956

22. Steart, F.A.
"Strength and Stability of Pillars in Coal Mines", J. Chemical, Metallurgical and Mining Soc. of S. Africa, pp 309-325, 1954

23. Wagner, H.
"Determination of the Complete Load-Deformation Characteristics of Coal Pillars", Proc. 3rd Int. Congress Rock Mechanics, Denver, 11-B, pp 1076-1087, 1974

24. Barron, K.
"An Air Injection Technique for Investigation of the Integrity of Pillars and Ribs in Coal Mines", Int. J. Rock Mechanics, Min. Sci. and Geomech. Abstr., Vol. 16, pp. 69-76, April 1978

25. Barron, K. and Couetdic, J.M.
"Plate Load Testing as a Method of Assessing the In-Situ Strength Properties of Western Canadian Coal", Int. J. Rock Mechanics Min. Sci. and Geomech. Abstr., Vol. 12, No. 10, pp. 303-310, October 1975

26. Barron, K., Wright, P.L., and Smales, T.
"Guidelines for the Design of Coal Pillars in the #4 Seam at McIntyre Mines Ltd., Grande Cache, Alberta", Proc. 1st Inst. Conf. on Stability in Underground Mining, Aug. 16-18, 1982, Vancouver; Soc. Min. Eng. A.I.M.E., New York, pp. 559-578, 1983

27. Skelly, W.A., Wolgamott, J., and Wang, F.D.
"Coal Mine Pillar Strength and Deformation Prediction through Laboratory Sample Testing", Proc. 18th U.S. Symposium on Rock Mechanics, Keystone, Po., June 23-24, Paper #2B5-1, 1977

28. Hazen, G. and Artler, L.
"Practical Coal Pillar Design Problems", Mining Congress Journal, pp. 86-92, June 1976

10. ACKNOWLEDGEMENTS

The author gratefully acknowledges the funding received for this project from the Canada Centre for Mineral and Energy Technology, Dept. Energy Mines and Resources, Canada via the Department of Supply and Services. Gilles Mongeau and Maureen Brock acted successively as Science Procurement Manager for D.S.S. during this contract, their efforts were much appreciated. Dr. D.F.G. Hedley acted as Scientific Authority on behalf of CANMET; his constructive comments during progress of this work were of great help.

Mr. Stephen Thornton, CMRC, contributed valuable assistance via computer program development, literature searches and case history analyses. Finally the author would like to thank Mrs. Christine Urquhart for deciphering the authors' writing and typing the text.

APPENDIX A: ERRATA AND CHANGES TO PART 1 REPORT

Errata

Page 57, line 15, line 20 and line 25

$\sigma_{P.b}$ should read $\sigma_p \cdot b$

Page 78, Figure 26: Flow diagram for revised failure criteria

Wrong figure reproduced. Replace this figure with correct Figure 26 attached.

Page 95 - Figure 33

Line 6, first block $\quad \bar{\sigma}_p \text{ (min)} = \frac{\bar{Y}}{Y_{m.m}} \cdot 2A \qquad -(39)$

add qualifer: if $Y_{mm} < \bar{Y}$ put $Y_{mm} = \bar{Y}$

Second block, right hand side, equation 88

First term of this equation is given as: $\frac{P_B \,(1-\text{Sin}\ \phi_B)}{2\ b\ \underline{\tan\ \phi_B}} \bigg\{$

correct this item to read: $\frac{P_B \,(1-\text{Sin}\,\phi_B)}{2\ b\ \underline{\text{Sin}\ \phi_B}} \bigg\{$

Page 147, Reference 16 Fractional should read Frictional

Page A15: Correlation coefficient should be negative since a' decreases as k increases.

Page A20, one line from bottom: $\frac{\sigma_p}{S_v} = \bar{Y}$ is average pillar stress concentration not average pillar stress.

Page A23, (c), (ii) should read:-

$$\text{when } k > 0.0985 + \underline{1.271} \log_e \left(\frac{W}{H}\right)$$

Page A26, last paragraph, 5th line

$\frac{\sigma_p}{S_v} = \bar{Y}$ is average pillar stress concentration not average pillar stress

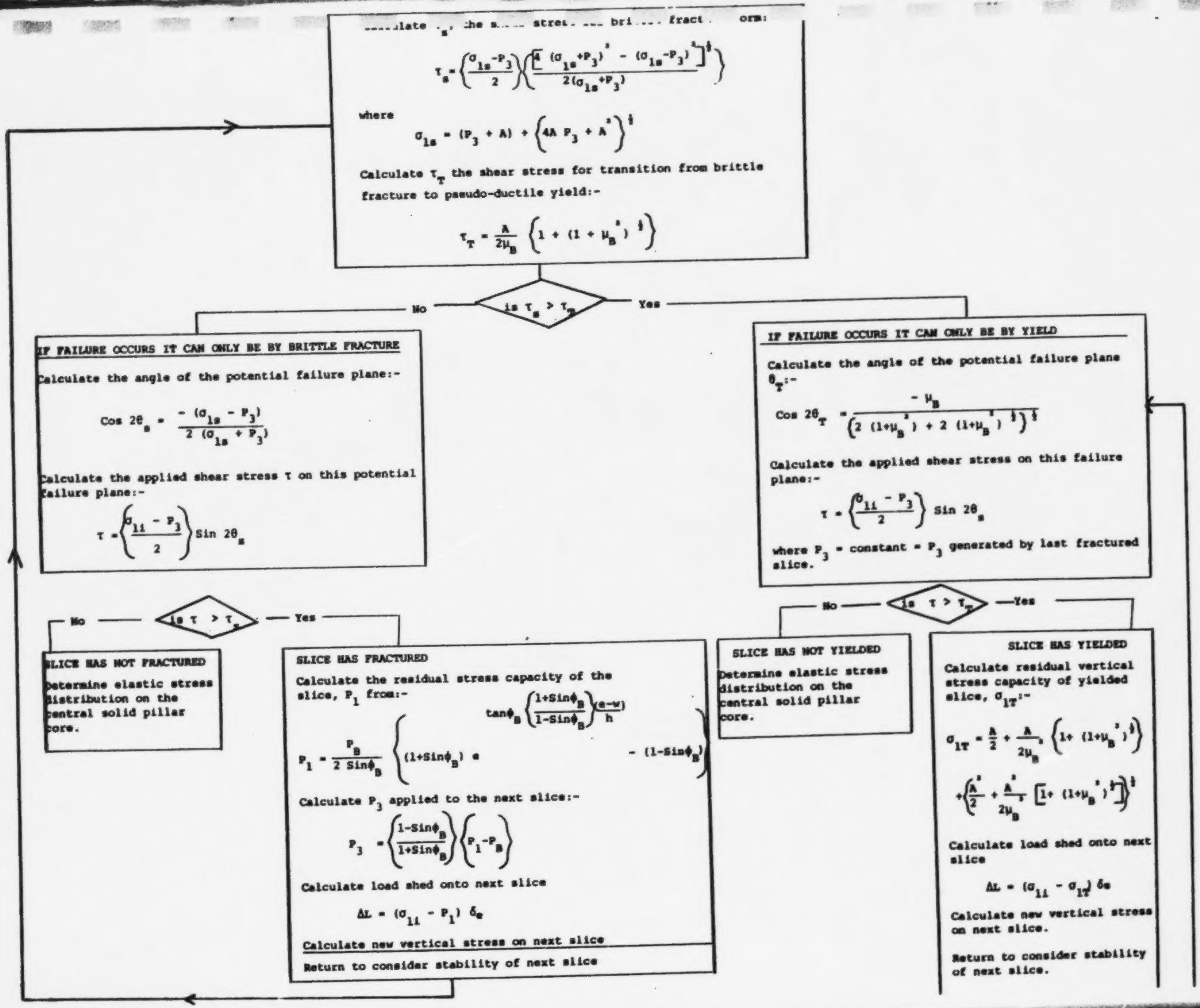

[illegible]late τ_s, the s[illegible] stre[illegible] [illegible] bri[illegible] fract[illegible] [illegible]orm:

$$\tau_s = \left\{\frac{\sigma_{1s} - P_3}{2}\right\}\left\{\frac{\left[4(\sigma_{1s}+P_3)^2 - (\sigma_{1s}-P_3)^2\right]^{\frac{1}{2}}}{2(\sigma_{1s}+P_3)}\right\}$$

where

$$\sigma_{1s} = (P_3 + A) + \left\{4A\,P_3 + A^2\right\}^{\frac{1}{2}}$$

Calculate τ_T the shear stress for transition from brittle fracture to pseudo-ductile yield:-

$$\tau_T = \frac{A}{2\mu_B}\left\{1 + (1 + \mu_B^2)^{\frac{1}{2}}\right\}$$

IF FAILURE OCCURS IT CAN ONLY BE BY BRITTLE FRACTURE

Calculate the angle of the potential failure plane:-

$$\text{Cos } 2\theta_s = \frac{-(\sigma_{1s} - P_3)}{2(\sigma_{1s} + P_3)}$$

Calculate the applied shear stress τ on this potential failure plane:-

$$\tau = \left\{\frac{\sigma_{1i} - P_3}{2}\right\}\text{Sin } 2\theta_s$$

IF FAILURE OCCURS IT CAN ONLY BE BY YIELD

Calculate the angle of the potential failure plane θ_T:-

$$\text{Cos } 2\theta_T = \frac{-\mu_B}{\left(2(1+\mu_B^2) + 2(1+\mu_B^2)^{\frac{1}{2}}\right)^{\frac{1}{2}}}$$

Calculate the applied shear stress on this failure plane:-

$$\tau = \left\{\frac{\sigma_{1i} - P_3}{2}\right\}\text{Sin } 2\theta_s$$

where P_3 = constant = P_3 generated by last fractured slice.

SLICE HAS NOT FRACTURED

Determine elastic stress distribution on the central solid pillar core.

SLICE HAS FRACTURED

Calculate the residual stress capacity of the slice, P_1 from:-

$$P_1 = \frac{P_B}{2\,\text{Sin}\phi_B}\left\{(1+\text{Sin}\phi_B)\,e^{\tan\phi_B\left\{\frac{1+\text{Sin}\phi_B}{1-\text{Sin}\phi_B}\right\}\frac{(e-w)}{h}} - (1-\text{Sin}\phi_B)\right\}$$

Calculate P_3 applied to the next slice:-

$$P_3 = \left\{\frac{1-\text{Sin}\phi_B}{1+\text{Sin}\phi_B}\right\}\left\{P_1 - P_B\right\}$$

Calculate load shed onto next slice

$$\Delta L = (\sigma_{1i} - P_1)\,\delta_e$$

Calculate new vertical stress on next slice

Return to consider stability of next slice

SLICE HAS NOT YIELDED

Determine elastic stress distribution on the central solid pillar core.

SLICE HAS YIELDED

Calculate residual vertical stress capacity of yielded slice, σ_{1T}:-

$$\sigma_{1T} = \frac{A}{2} + \frac{A}{2\mu_B^2}\left\{1 + (1+\mu_B^2)^{\frac{1}{2}}\right\} + \left\{\frac{A^2}{2} + \frac{A^2}{2\mu_B^2}\left[1 + (1+\mu_B^2)^{\frac{1}{2}}\right]\right\}^{\frac{1}{2}}$$

Calculate load shed onto next slice

$$\Delta L = (\sigma_{1i} - \sigma_{1T})\,\delta_e$$

Calculate new vertical stress on next slice.

Return to consider stability of next slice.

FIGURE A1: FLOW DIAGRAM FOR REVISED FAILURE CRITERIA

Page A41, second paragraph, line 7 then
second paragraph, line 10 peripheries
5th line from bottom symmetry

Page A61, Equation I.33

$$\frac{\tau}{(\underline{\sigma} - \sigma_3)} = \qquad \text{not} \quad \frac{\tau}{(\sigma_1 - \sigma_3)} =$$

Page A63, Table I.2, row 2, column 5 σ_{12} not σ_{21}

Program Changes

Due to the need for some specific corrections and changes to the main Pillar Program, the following procedures have been inserted:-

(a) A square pillar calculation for the local extraction ratio has been added to the rib pillar calculation. By specifying the variable "TYPE", in the second read statement, to be either "0" for rib pillars or "1" for square pillars this addition can be implemented. This change has been inserted into lines 95 and 113.

(b) Corrections have been made to lines 95 and 113. The symbol ".EQ." should have been ".NE.".

(c) The method for calculating the value of K2 has been changed. Originally the method used came from Chapter 3. This has since been dropped and the method outlined in Chapter 4 has been inserted. Both functions FC3 and DO3 have totally been rewritten for this reason. Due to the need for increased input the call statement had to also be altered.

(d) Due to the rounding off error which was detected in the results of the program, a variable "FAILT" has been introduced. This variable compares the results of the "STRETH SUBROUTINE" with the final pillar slice calculation to ensure a pillar is within the same failure mode. A warning is printed out if the failure modes differ. This has been inputted into the end of the main section of the pillar program.

(e) An error was noted regarding the value of "QUI" not being set to yield when the pillar went through the "NOT FAILED" section of the program.

This has been corrected by the insertion of "QUI = YES" at line 234.

(f) The section of the program which sent results to be graphed to a file has been removed. These included all lines between 389 and 398.

A new version of the pillar program has been written for use on the "Floating Point System's Array Processor 190L". The array processor (AP) is a dedicated number crunching device which is being used with the University of Alberta's AMDAHL 470 V/8. Using the AP for large numbers of slices was initially suggested by Denise Thornton and Ron Torgerson of the University's Numerical Analysis Department. As a result the AP has been found to be the quickest and most inexpensive method for evaluting pillars in the 500 to 4000 slice range.

The changes which were made to the program consisted of removing lines 165 to 325 and placing them into their own subroutine. This subroutine must then be compiled separately and finally run as part of the original program. The new run command is:-

```
RUN AP.RUN+*FPSLIB 5=datafile 6=outputfile t=3
```

The time specified is the AMDAHL time. The AP has a maximum time of 5 minutes. At this time the charge for the AP is $1.00 per minute and the AMDAHL is $54.00 per minute.

APPENDIX B: SIZE/SHAPE RELATIONSHIPS FOR THE UNIAXIAL COMPRESSIVE STRENGTH OF COAL SPECIMENS

One of the prime input parameters for this computer analysis of coal pillar stability is the uniaxial compressive strength of coal. However, it is well known that the uniaxial compressive strength of coal is dependent on both the size and shape of the coal specimen tested. Consequently it is necessary to review and evaluate these effects before deciding on the value to be used in the program input.

B.1 Size/strength relationships for cubical test specimens

B1.1 Review of Previous work

Daniels and Moore (B1), Rice (B2), Lowall and Holland (B3), Greenwald et al (B4), and others have found from experimental tests on cubical coal specimens that the larger is the edge dimension the lower is the uniaxial compressive strength of the cube. Steart (B5), from small specimen tests and mine observation, concluded that the uniaxial compressive strength of cubical specimens varied inversely as the square root of the edge dimension, D.

$$\text{ie. } \sigma_c \propto D^{-\frac{1}{2}} \qquad \text{(B.1)}$$

Millard et al (B.6) tested cubes of Llandebie anthracite and determined that σ_c varied with the specimen weight, G, according to the power relationship $\sigma_c \propto G^{-0.52}$; this can be expressed in terms of the edge dimensions of the cube as:-

$$\sigma_c \propto D^{-0.44} \qquad \text{(B.2)}$$

Test by Millard et al on two other coals (Betteshanger and Langwith) gave values of the exponent as -0.47 and -0.53 respectively.

Gaddy (B.7) tested a wide range of different coals and concluded that, considering the variability of coal, for all practical purposes the cube strength was universely proportional to the square root of the edge dimension. These tests included specimens up to 64 inches edge dimension.

Evans et al (B.8) tested two coals, Deep Duffryn and Barnsley Hards, and although confirming that the uniaxial cube strength was dependent on a power function of D, obtained the exponents -0.32 and -0.17 respectively. Hustrulid (B.9) noted that Evans et al tested cubes down to ⅛ inch edge dimension and suggested that such cubes would be difficult to prepare and thus that the meaning of the results was questionable. He then showed that a reasonable fit could be obtained for the Evans data in the form $\sigma_c = kD^{-0.5}$ if only the 1 inch and greater cubes were considered. Whether or not Hustrulids criticism of the experimental technique for the very small specimens is justified is questionable; however, it does appear to the author that testing of cubes of much less than 1 inch is somewhat academic.

Bieniawski (B10, B11, B12, B13, and B14) has reported the results of both laboratory and in-situ tests on cubical specimens from the Witbank colliery, ranging in size from a 1 inch to 79 inch edge dimension. On the basis of these tests Bieniawski concluded that:-

(a) for samples less than D = 60 inches

$$\sigma_p = 2899 \frac{B^{0.16}}{H^{0.55}} \text{ where B and H are in inches}$$

which for cubical specimens reduces to

$$\sigma_c = 2899 \ D^{-0.39} \qquad \text{(B.3)}$$

(b) for specimens with D > 60 inches

$$\sigma_p = 400 + 220 \frac{B}{H}$$

ie. for a cube, B/H = 1, σ_c = 620 psi ie. a constant (B.4)

Evans (B.15) in discussing Bieniawski's results pointed out that the results could be divided into three groups:

(i) A size range from 0.75 to 3 inches: no significant variation with size
(ii) 6 inches to 18 inches: marked strength variation with size
(iii) 34 inches to 60 inches: little size variation

Further, these size ranges coincided with the three different test methods used and that, since all other investigators had observed marked size effects in the small size range, Evans questioned the validity of the small size range method and results.

Hustrulid (B.9) demonstrated that a curve, based on the 6 inch cube size results, and assuming a $D^{-½}$ relationship could also given an acceptable fit to Bieniawski's data even including the data for the small cube sizes. Hustrulid also noted that it was difficult to discern any significant difference in Bieniawski's cube strengths for cubes of 24 inches or larger; the reduction in strength with D varying from 24 inches to 79 inches was only 23%, and from 36 inches to 79 inches it was only about 9%. He therefore considered that, for all practical purposes, the cube strengths for cubes larger than 36 inches could be considered as equal to that for a 36 inch cube.

B.1.2 Conclusions with respect to cube strengths

In summary therefore it may be concluded that the bulk of cube strength data may be expressed in the form:-

$$\sigma_c = kD^{-½} \qquad (B.5)$$

where k is a constant for the coal (and is numerically but not dimensionally equal to the strength of a 1 inch cube).

There is some doubt as to whether this equation applies for specimens much less than 1 inch in edge dimension; however this is not seen to be a major practical consideration since usually k is derived from testing of convenient size coal cubes, usually in the 1-4 inch size range.

Logically there should be an upper size limit to this equation since clearly the strength will not reduce with size ad infinitum. There appears to be some minor disagreement between various authors on the upper limit beyond which the cube strength is for all practical purposes a constant. Hustrulid suggests 36 inches, Bieniawski suggests 60 inches whilst Gaddy indicates a continuing reduction even at 64 inches. This aspect will be further, later in this Appendix.

B.2Shape/Strength Relationships for Prismatic Test Specimens

In this section the effect of varying the width/height ratio, (B/H), on specimen strength will be considered. For the most part prismatic specimens having square cross section will be considered, but some data from specimens having rectangular sections and circular sections will also be included. For rectangular sections the width, B, will be considered to be the minimum lateral dimension.

B.2.1 Review of previous work

In a number of cases the results of previous work have been expressed in "nomalised" form to assist in comparisons, that is the prism strength σ_p has been divided by the cube strength σ_c to produce an equation in dimensionless form. However it should be noted, as pointed out by Hustrulid (B.9), that previous investigators have been inconsistent in their choice of sample dimensions (height or width) used to specify the comparative cube strength; this has resulted in some inconsistencies between results when the specimen height is varied and the width is kept constant and vice-versa. Care should be taken to bear this in mind when reviewing previous work.

In this discussion H is the specimen height and B is the minimum lateral dimension.

Griffith and Conners (B.16) determined that the strength of anthracite specimens was inversely proportional to the square root of the height, all other things being equal (ie. constant B).

Holland (B.17) showed experimentally that for small laboratory specimens of bituminous coal the prism strength is proportional to $\sqrt{B/H}$; this was also confirmed by later work by the same author. (It should be noted that Holland placed a requirement that $B/H < 1$ for this form, and he noted that it did not apply if the specimen did not fail abruptly (some specimens, but not all, did not fail abruptly at high B/H ratios).

Hustrulid (B.9) later re-interpretted this data to derive the nomalised equation (for constant height)

$$\frac{\sigma_p}{\sigma_c} = 0.775 + 0.225\ (\frac{B}{H})$$

Greenwald et al (B.4) concluded from tests on large specimens of Pittsburgh coal that

$$\sigma_p = k\ \frac{B}{\sqrt[6]{H^5}}$$

Hustrulid (B.9) later showed that, normalising Greenwald et al's data by dividing by the cube compressive strength, the following equation also also gave a reasonable fit to their data

$$\frac{\sigma_p}{\sigma_c} = 0.778 + 0.222\ (\frac{B}{H})$$

Steart (B.5), from experiment and from observations in mines, formulated the following "rules":-

(i) The strength of pillars of the same width varies in inverse ratio to their height

i.e. if B is constant, $\sigma_p \propto (\frac{1}{H})$

(ii) The strength of pillars of square cross sections of the same height varies as the square root of their width

ie. if H is constant, $\sigma_p \propto \sqrt{B}$

(iii) The strength of pillars of cube form vary in inverse ratio to the square root of their edge dimensions

ie. when B=H=D, $\sigma_p \propto \frac{1}{\sqrt{D}}$

Hustrulid (B.9) later demonstrated that, assuming a cube strength based on 9 inch cubes from another S. African mine, Steart's data could be expressed in nomalised form by:-

$$\frac{\sigma_p}{\sigma_c} = 0.778 + 0.222\ (\frac{B}{H})$$

Bauschinger(B.18, B.19) presented tests on sandstone prisms and derived the nomalised equation:-

$$\frac{\sigma_p}{\sigma_c} = 0.778 + 0.222 \left(\frac{B}{H}\right)$$

(This was the original derivation of this equation which was later so much used by Hustrulid and others).

Bunting (B.20), from small specimen tests, derived the following equation for the strength of anthracite specimens:-

$$\sigma_p = 1750 + 750 \left(\frac{B}{H}\right)$$

which, using his mean value of 2500 psi for the strength of cubes of 2 to 6 inch size, nomalises to give:-

$$\sigma_p = 0.70 + 0.30 \left(\frac{B}{H}\right)$$

In addition Bunting plotted the "squeezing loads" (based on overburden depth and extraction ratio) for a number of failing pillars and derived:-

$$\sigma_p = 700 + 300 \left(\frac{B}{H}\right)$$

which, taking 1000 psi as the cube strength for a cube of side equal to the seam height gives:-

$$\frac{\sigma_p}{\sigma_c} = 0.70 + 0.30 \left(\frac{B}{H}\right)$$

Holland (B.22) also noted that if Bunting's results are considered for the cubical specimens and those where B/H >1, then they can also be represented quite closely by the $\sqrt{B/H}$ form.

Holland and Gaddy (B.21) developed a general pillar strength formula given by:-

$$\sigma_p = k \left\{\sqrt{\frac{B}{H}}\right\}$$

which follows from a logical application of Steart's rules.

Evan et al (B.8) conducted experiments on the strength of coal prisms where the two dimensions (width B and height H) were held constant and the depth, L, was varied. It was considered that when the height remains constant the prism strength was controlled by the least lateral dimension.

Salamon and Munro (B.23) surveyed mine pillars in S. Africa and obtained the following relationship:

$$\sigma_p = 1322 \frac{B^{0.46}}{H^{0.66}} \text{ where B and H are in inches}$$

This is quite similar to Hollands (B.17) form $\propto\sqrt{B/H}$.

Hustrulid (B.9) showed that this equation, over a range B/H from 1 to 9, was not greatly different from:-

$$\sigma_p = 1028 + 294 \left(\frac{B}{H}\right)$$

or, in nomalised form:-

$$\frac{\sigma_p}{\sigma_c} = 0.778 + 0.222 \left(\frac{B}{H}\right)$$

Bieniawski (B.10, B.11, B.12, B.13, B.14) concluded from his studies that the strength of cubes of edge length greater than 60 inches was constant. From his data for prisms with a square base of 60 inches or less he derived:-

$$\sigma_p = 400 + 220 \left(\frac{B}{H}\right)$$

and gave (B.11) the nomalized form of this equation as:-

$$\frac{\sigma_p}{\sigma_c} = 0.645 + 0.355\ (\frac{B}{H})$$

However, it was noted by Hustrulid (B.9) that this nomalised form given by Bieniawski had been constructed for the situation in which the width was held constant and the height varied from 24 inches to 60 inches; it was therefore only because the cube strengths at 24 inches and 60 inches differed by relatively little that this nomalised form of Bieniawski's equation was similar to previous results. However, Hustrulid then plotted Bieniawskis results in which the sample heights were kept constant and the widths varied; the nomalising cube strength being that of a cube of size equal to the height, and showed that these results were closely fitted by:-

$$\frac{\sigma_p}{\sigma_c} = 0.778 + 0.222\ (\frac{W}{H})$$

B.2.2 Summary and Discussion of strength/shape relationships

In summary, the results of past work on prism strength - shape relationships have been expressed in one of three different basic forms:-

(i) The power form

$$\sigma_p = k \sqrt{\frac{B}{H}}$$

(Salamon and Munro's relationship $\sigma_p = k\left\langle \frac{B^{0.46}}{H^{0.66}} \right\rangle$ can be regarded as a variation of this power form).

(ii) The linear form

$$\sigma_p = a + b\ (\frac{B}{H})$$

and (iii) The "general" form

$$\sigma_p = k\left\{\sqrt{\frac{B}{H}}\right\}$$

Consider these in turn.

The power curve form of Salamon and Munro has been criticised by Bieniawski (B.11) on the grounds that, for a constant height, the strength of the pillar increases as the width of the pillar increases, and further, for a constant width, the strength of the pillar decreases with increasing height - both these trends continuing to infinity. Bieniawski argues, with good justification, that there must be some limits to these trends. This criticism is, however, equally applicable to the other forms given above unless such limits are set. Bieniawski and Hustrulid introduce such limits by limiting the maximum cube strength, in Bieniawski's case to 60 inches, in Hustrulid's case to 24 inches.

Much emphasis has been placed by Hustrulid and others on the fact that the nomalised linear form, $\frac{\sigma_p}{\sigma_c} = a' + b'\left(\frac{B}{H}\right)$, is dimensionally correct.

Hustrulid states, when comparing with the Salamon and Munro equation, the "The attractiveness of this equation is that it is dimensionally correct and provides the opportunity to introduce the various coal cube strengths". In the author's opinion this is a fallicious statement since, although this equation is dimensionally correct, the introduction of "various coal cube strengths" by the relationship

$$\sigma_c = \frac{k}{\sqrt{D}}$$

defeats this alleged advantage. The constant k cannot have the dimensions of strength and therefore is no better than or worse than the direct use of k in the Salamon/Munro equation which he criticizes as being dimensionally incorrect!

Hustrulid (B.9) concludes that the size/shape effects from all data may be expressed by two equations, one for the size effect on cubes and the other for the shape effect:-

(a) a cube size compressive strength relationship given by:-

$$\sigma_c = \frac{k}{\sqrt{H}} \quad \text{when } H < 36 \text{ inches}$$

$$\text{and } \sigma_c = \frac{k}{\sqrt{36}} \quad \text{when } H > 36 \text{ inches}$$

This is in general agreement with all other work, except that he puts on an upper limit on this size effect of 36 inches whereas Bieniawski puts an upper limit of 60 inches in this effect. Other author's put no limit due primarily to a lack of data in the upper size ranges. It would seem logical that there is some upper limit to the size effect but, in the author's opinion there is insufficient data to specify this upper limit exactly.

The percentage difference between these limits can be expressed as follows:-

$$\Delta\% = \frac{\frac{k}{\sqrt{36}} - \frac{k}{\sqrt{60}}}{\frac{k}{\sqrt{36}}} \times 100 = 22.5\%$$

This is not an insignificant percentage difference in the strengths of large cubes; however there is insufficient data to ascertain the true "upper" limit of size effects. Since Bieniawski's limit will yield lower coal strengths it is suggested by the author that this would lead to more conservative design and should therefore be used.

(b) Compressive strength - shape relationship

$$\frac{\sigma_p}{\sigma_c} = 0.778 + 0.222 \left(\frac{B}{H}\right)$$

(This equation applies only to cases where H is kept constant and B varied)

There is no doubt that these two sets of equations developed by Hustrulid give a reasonable fit to most of the experimental data reported in the literature. However, the author is none too happy with the conclusion that it requires two separate equations to define the combined size/shape effects and the consequent difference in shape effects when B is varied and H is kept constant or vice versa. A cube is only a special case of a prism and thus intuitively it would be expected that the combined size/shape effects ought to be able to be expressed in a single relationship which reduces to the cube equation in that special case.

The relationship developed by Holland and Gaddy, the "general form", based on Stearts' rules does in fact satisfy these requirements:-

$$\sigma_p = k \frac{\sqrt{B}}{H}$$

because (i) when B=~~H~~=D for a cube $\sigma_c = \frac{k}{\sqrt{D}}$ (Stearts third rule)

(ii) when B is constant and H varied $\sigma_p \propto \frac{1}{H}$ (Stearts first rule)

(iii) when H is constant and B varied $\sigma_p \propto \sqrt{B}$ (Stearts second rule)

Consequently, in the author's opinion a relationship in this form has a much greater basic appeal. However, to date no worker has done a comprehensive evaluation of all the data with respect to this form of relationship. This is rectified in the next section by the author.

B.3 Evaluation of the "General" Form of The Size/Shape Relationship

B.3.1 Statistical analysis

The author undertook to re-evaluate the available strength size/shape data with the object of checking whether or not the single equation in the "general" form can adequately express all of this data. The available uniaxial coal compressive strength data from as many sources as possible have been compiled in Tables B1 - 4.

This data has been statistically analysed as follows:-

TABLE B1: U.K COAL DATA

Coal Location	Sample Number	Sample Dimensions - inches H	B	W	σ_f p.s.i.	$\sqrt{B}/H$	$\sigma_f = a_o + b_o(\sqrt{B}/H)$ a_o	b_o	correlation coeff. r	k (p.s.i.)	σ_f/k	$1/(\sqrt{B}/H)$	$1/(\sigma_f/k)$	[illegible] $\sigma_f = a_o' + b_o'(\sqrt{B}/H)$ a_o'	b_o'	r'	k'	σ_f/k'	Notes
OAKDALE BED // 2	23/29	2	.866	.866	320	.47	-185	1075	1	890	.36	2.12	2.77	-	-	-	590	.36	1" dia
CLEAT //		1	1	1	890	1.0					1.0	1	1					1.0	
OAKDALE BED // 3	23/29	2	.866	.866	925	.47	-	-	-	-	-	-	-	-	-	-	-	-	1" dia
CLEAT ⊥											-	-	-					-	
OAKDALE BED ⊥	B 29	2	.866	.866	770	.47	433	717	1	1150	.67	2.12	1.49	-	-	-	1150	.67	1" dia
CLEAT //		1	1	1	1150	1					1.0	1	1					1	
PENTREMAWR BED //	B 29	2	.866	.866	2630	.47	280	5000	1	5280	.498	2.12	2.0	-	-	-	5280	.498	1" dia
CLEAT //		1	1	1	5290	1					1	1	1					1	
PENTREMAWR BED ⊥	B 29	2	.866	.866	4590	.47	3720	1830	1	5550	.825	2.12	1.21	-	-	-	5550	.825	1" dia
CLEAT //		1	1	1	5550	1.0					1	1	1					1	
DEEP DUFFRYN BED //	B 29	2	.866	.866	1020	.47	-150	2490	1	2349	.43	2.12	2.32	-	-	-	2349	.43	1" dia
CLEAT //		1	1	1	2390	1					1	1	1					1	
DEEP DUFFRYN BED ⊥	B 29	2	.866	.866	1000	.47	618.6	1629	.956	2243	.446	2.12	2.25	-257.8	2795	.983	2539	.394	1" dia
CLEAT //		1	1	1	2650	1					1.18	1	.85					1.04	
	B 8	0.25	.25	.25	3700	2					1.65	-	-					-	
		.5	.5	.5	2860	1.41					1.27	-	-					-	
		1	1	1	2380	1					1.06	1	.94					.937	
		2	2	2	1820	.707					0.81	1.41	1.23					.717	
CWMTILLERY BED //	B 29	2	.866	.866	1010	.47	3537	1396	1	1750	.577	2.12	1.73	-	-	-	1750	.577	1" dia
CLEAT //		1	1	1	1750	1					1	1	1					1	
CWMTILLERY BED ⊥	B 29	2	.866	.866	1920	.47	1270	1339	1	2630	.73	2.12	1.37	-	-	-	2630	.73	1" dia
CLEAT //		1	1	1	2630	1					1	1	1					1	
[illegible] BED //	B 29	2	.866	.866	4390	.47	3902	1037	1	4990	.888	2.12	1.13	-	-	-	4990	.888	1" dia
[illegible] CLEAT //		1	1	1	4990	1					1	1	1					1	
BARNSLEY BED ⊥	B 29	2	.866	.866	7450	.47	6929	1659	.795	8078	.92	2.12	1.09	7003	952		7955	.936	1" dia
HARDS CLEAT //		1	1	1	8080	1					1	1	1					1.02	
	A 6	.125	.125	.125	11730	2.83					1.45	-	-					-	
		.25	.25	.25	10820	2.0					1.34	-	-					-	
		.75	.75	.75	9030	1.15					1.12	.87	.89					1.135	
		1	1	1	8930	1					1.10	1	.91					1.12	
		1.3	1.3	1.3	7870	.877					.97	1.14	1.03					.989	
		1.44	1.44	1.44	7090	.833					.877	1.2	1.14					.891	
		1.6	1.6	1.6	7530	.790					.93	1.27	1.07					.946	
		.5	.5	.5	9580	1.41					1.18	-	-						
		.5	.5	1	9410	1.41					1.16	-	-					-	
		.5	.5	2	9590	1.41					1.19	-	-					-	
		.5	1	1	10120	2					1.25	-	-					-	
		.5	1	2	9910	2					1.23	-	-					-	
		2	2	4	10890	2.83					1.35	-	-					-	
		1	.5	.5	8290	.707					1.03	1.41	.97					1.04	
		1	.5	1	7650	.707					.95	1.41	1.05					.965	
		1	.5	2	8260	.707					1.02	1.41	.98					1.03	
		1	1	1	8040	1					.995	1	1.005					1.01	
		1	1	2	8100	1					1	1	1					1.02	
		1	2	2	7590	1.41					.94	.707	1.06					.954	
		2	.5	.5	7060	.353					.87	2.83	1.149					.887	
		2	.5	1	6960	.353					.86	2.83	1.16					.875	
		2	.5	2	7170	.353					.89	2.83	1.12					.901	
		2	1	1	7850	.5					.97	2	1.03					.986	
		2	1	2	7460	.5					.92	2	1.08					.935	
		2	2	2	6630	1					.82	1	1.22					.833	
[illegible] BED //	B 29	2	.866	.866	3420	.47	3079	734	1	3810	.897	2.13	1.11	-	-	-	3810	.897	1" dia
[illegible] CLEAT //		1	1	1	3810	1					1	1	1					1	
BARNSLEY BED ⊥	B 29	2	.866	.866	[illegible]	.47	1837	3452	1	5290	[illegible]	2.13	[illegible]	-	-	-	5290	[illegible]	
BRIGHTS CLEAT //		1	1	1	5290	1					1	1	1					1	
[illegible] BED //	B 29	2	.866	.866	1960	.47	-	-	-	-	-	-	-	-	-	-	-	-	
CLEAT //		-	-	-	-	-					-	-	-					-	
[illegible] BED ⊥	B 29	2	.866	.866	[illegible]	.47	-	-	-	-	-	-	-	-	-	-	-	-	
[illegible]		-	-	-	-	-					-	-	-					-	

TABLE I (CONT.)

COAL / LOCATION	SOURCE OF MATERIAL	SAMPLE DIMENSIONS - INCHES H	B	W	σ_f p.s.i.	$\frac{\sqrt{B}}{H}$	$\sigma_f = a_0 + b_0(\sqrt{B}/H)$ a_0	b_0	corr. coeff. r	k_0 (lb/in²)	σ_f/k_0	$\frac{1}{(\sqrt{B}/H)}$	$\frac{1}{(\sigma_f/k_0)}$	[illegible] $\sigma_f = a_0' + b_0'(\sqrt{B}/H)$ a_0'	b_0'	r'	k_0'	σ_f/k_0'	NOTES
MARKHAM BED //	B 29	2	[illegible]	[illegible]	[illegible]	.47	287	4283	1	4570	.5	2.13	2	–	–	–	4570	.5	[illegible]
CLEAT //		1	1	1	4570	1					1	1	1					1	
[illegible] BED ⊥	B 29	2	[illegible]	.96	3160	.47	1791	3019	1	4760	.663	2.13	1.91	–	–	–	4760	[illegible]	[illegible]
CLEAT //		1	1	1	4760	1					1	1	1					1	
LINBY BED ⊥	B 29	2	[illegible]	[illegible]	1510	.47	-831	4981	1	4150	.364	2.13	2.75	–	–	–	4150	[illegible]	[illegible]
CLEAT //		1	1	1	4150	1					1	1	1					1	
LINBY BED ⊥	B 29	2	[illegible]	[illegible]	3150	.47	-1115	9075	1	7960	.40	2.13	2.5	–	–	–	7960	.4[illegible]	[illegible]
CLEAT //		1	1	1	7960	1					1	1	1					1	
ANTHRACITE BED ⊥		4	4	4	2330	.5	2072	2891	.725	4913	.47	2	2.12	-286	5690	.977	535·1	.435	
		2	2	2	4030	.707					.82	1.41	1.21					.756	
		1	1	1	5210	1					1.06	1	.94					.973	
		.5	.5	.5	8600	1.41					1.75	–	–					–	
		.25	.25	.25	6130	2.0					1.23	–	–					–	

ALL DATA $\frac{\sigma_f}{k_0} = 0.574 + 0.389\frac{\sqrt{B}}{H}$ $r = 0.77$

PRISMS ONLY $\frac{\sigma_f}{k_0} = 0.568 + 0.329\frac{\sqrt{B}}{H}$ $r = 0.71$

TABLE B2: US COAL DATA

COAL / LOCATION	SOURCE REFERENCE	SAMPLE DIMENSIONS - INCHES			σ_f p.s.i	$\frac{\sqrt{B}}{H}$	$\sigma_f = a_o + b_o(\sqrt{B}/H)$			h_o [illegible]	σ_f / h_o	$\frac{1}{(\sqrt{B}/H)}$	$\frac{1}{(\sigma_f/h_o)}$	[illegible] H ≤ [illegible] Data					NOTES
		H	B	W			a_o	b_o	COR. COEFF r					$\sigma_f = a_o' + b_o'(\sqrt{B}/H)$ a_o'	b_o'	r'	h_o'	σ_f / h_o'	
ANTHRACITE (VARIOUS SEAMS)	B 1	2	2	2	2369	.707	1138	2314	0.65	3452	.686	1.41	1.46	-	-	-	3452	.686	
		3	3	3	3390	.577					.982	1.73	1.02					.982	
		4	4	4	1999	.50					.579	2	1.72					.579	
		6	6	6	1549	.41					.450	2.45	2.22					.450	
		4	2	2	2321	.353					.670	2.83	1.49					.670	
		8	4	4	1801	.25					.52	4	1.92					.52	
		12	4	4	1405	.167					.41	5.98	2.43					.41	
ANTHRACITE DIFFERENT BEDS.	B 16	1	2	2	5750	1.41	2018	2687	.999	4705	1.22	.71	.82	-	-	-	4705	1.22	
		2	2	2	4087	.707					.87	1.41	1.15					.87	
		4	2	2	2854	.353					.61	2.83	1.64					.61	
WEST VIRGINIA SEAMS AS NOTED	B 3																		
PITTSBURG ⊥	B 3	3	3	3	2710	.577	-3144	10146	1	7001	.387	1.73	2.58	-	-	-	7001	.387	
		2	2	2	4029	.707					.575	1.41	1.74					.575	
POCAHONTAS #3 ⊥	B 3	3	3	3	1432	.577	542	1757	.839	2299	.622	1.73	1.61	-	-	-	2299	.622	
		3	3	3	1680	.577					.730	1.73	1.37					.730	
		6.5	1.5	6.5	1231	.392					.535	2.55	1.87					.535	
BAKERSTON ⊥	B 3	3	3	3	2420	.577	-534	5119	1	4585	.527	1.73	1.90	-	-	-	4585	.527	
		8.5	10.25	10.75	1391	.376					.303	2.66	3.30					.303	
ISLAND CREEK ⊥	B 3	3	3	3	4734	.577	3275	2[illegible]7	1	5803	.815	1.731	1.23	-	-	-	5803	.815	
		1.5	1.5	1.5	5338	.816					.919	1.22	1.09					.919	
STOCKTON ⊥	B 3	3	3	3	6844	.577	1700	8915	1	10615	.645	1.73	1.55	-	-	-	10615	.645	
		7.75	7	7	4740	.341					.446	2.93	2.24					.446	
PITTSBURG COAL BED	B 7	30	30	30	817	.182	-195	6411	.966	6216	.131	5.49	7.63	-	-	-	6216	.131	
		31	31	31	920	.179					.148	5.60	6.75					.148	
		32	32	32	885	.177					.142	5.65	7.04					.142	
		54	54	54	306	.136					.049	7.35	20.4					.049	
		64	64	64	695	.125					.112	8	8.9					.112	
		2	2	2	4043	.707					.65	1.41	1.53					.65	
		3	3	3	2969	.577					.477	1.73	2.09					.477	
		4	4	4	3297	.50					.530	2	1.88					.530	
		5	5	5	3266	.447					.525	2.23	1.90					.525	
		6	6	6	2663	.408					.428	2.45	2.34					.425	
		7	7	7	2571	.378					.413	2.64	2.42					.413	
		9	9	9	1832	.333					.295	3.0	3.39					.295	
CLINTWOOD	B 7	2	2	2	3033	.707	898	2948	.969	3847	.788	1.41	1.27	-	-	-	3847	.788	
		3	3	3	2449	.577					.636	1.73	1.57					.636	
		4	4	4	2445	.50					.635	2	1.57					.635	
		5	5	5	2302	.447					.598	2.23	1.67					.598	
		7	7	7	1962	.378					.509	2.64	1.96					.509	
POCAHONTAS #4	B 7	2	2	2	3050	.707	1953	1454	.794	3048	.899	1.41	1.12	-	-	-	3048	.899	
		3	3	3	2743	.577					.805	1.73	1.24					.805	
		4	4	4	2478	.50					.727	2	1.37					.727	
		5	5	5	2780	.447					.815	2.23	1.23					.815	
		7	7	7	2511	.378					.736	2.64	1.36					.736	
HARLAN	B 7	2	2	2	6688	.707	252	8826	.880	9078	.736	1.41	1.36	-	-	-	9078	.736	
		3	3	3	5138	.577					.566	1.73	1.77					.566	
		4	4	4	3958	.50					.436	2	2.29					.436	
		5	5	5	5106	.447					.562	2.23	1.78					.562	
		7	7	7	3396	.378					.374	2.64	2.67					.374	
MARKER	B 7	2	2	2	7156	.707	587	9231	.993	9908	.722	1.41	1.38	-	-	-	9905	.722	
		3	3	3	5862	.577					.591	1.73	1.69					.591	
		4	4	4	5479	.50					.553	2	1.81					.553	
		5	5	5	4741	.447					.478	2.23	2.09					.475	
		7	7	7	4015	.378					.405	2.64	2.46					.408	

TABLE B2 (CONT)

Coal / Location	Sample Number	Sample Dimensions - inches			σ_f p.s.i.	$\sqrt{B}/H$	$\sigma_f = a_0 + b_0(\sqrt{B}/H)$			k_0 (1" cube)	σ_f/k_0	$1/(\sqrt{B}/H)$	$1/(\sigma_f/k_0)$	[illegible]					Notes
		H	B	W			a_0	b_0	corr. coeff. r					$\sigma_f = a_0' + b_0'(\sqrt{B}/H)$			k_0'	σ_f/k_0'	
														a_0'	b_0'	r'			
PITTSBURGH #8 SEAM	B 26	1.75	.875	.875	2000	.539	—				.696	1.87	1.43					.613	[illegible]
		1.3	.875	.875	2000	.719					.696	1.39	1.43					[illegible]	
		.875	.875	.875	2350	1.069					.818	.935	1.22					.720	
		.44	.875	.875	2650	2.135					.923	-	-					-	
		4.25	2.125	2.125	1450	.343					.510	2.91	1.96					.44	
		3.17	2.125	2.125	2600	.459					.905	2.17	1.10					.80	
		2.13	2.13	2.13	2600	.685					.905	1.46	1.10					.80	
		1.06	2.13	2.13	4200	1.37					1.46	.73	.68					1.29	
		6	3	3	1900	.289	2156	716	.446	2872	.661	3.46	1.51	1643	1617	.176	3261	.58	
		4.47	3	3	2300	.387					.80	2.58	1.25					.71	
		3	3	3	3550	.577					1.236	1.73	.81					1.09	
		1.5	3	3	3500	1.154					1.29	.87	.81					1.07	
		8	4	4	1950	.25					.68	4	1.47					.60	
		6	4	4	2500	.335					.87	2.98	1.15					.77	
		4	4	4	3500	.5					1.22	2	.82					1.07	
		2	4	4	3900	1.0					1.36	1	.74					1.19	
PITTSBURGH COAL BED	B4 AND B27	62	31.8	31.8	500	.091					.119	10.98	8.77					.119	k_0'' [illegible]
		63.25	45.4	45.4	600	.1065					.136	9.38	7.35					.136	
		63.6	63.8	63.8	695	.126					.158	7.93	6.32					.155	$a_0'' = 277$
		30.9	31.8	31.8	920	.182					.209	5.49	4.78					.209	$b_0'' = 3769$
		31.9	32.2	32.2	885	.178					.201	5.61	4.97					.201	$r = .913$
		30.3	42	42	1050	.213	197.6	4199	.94	4397	.239	4.69	4.18	-	-	-	4397	.239	$b_0'' = 4093$
		29.7	20.5	20.5	900	.152					.205	6.57	4.88					.205	
		29.8	20.5	20.5	950	.152					.216	6.57	4.63					.216	
		30.4	51	51	1200	.235					.273	4.25	3.66					.273	
		29.1	11.8	11.8	800	.118					.182	8.47	5.49					.182	

TABLE B3: S. AFRICAN COAL DATA

COAL / LOCATION	SOURCE REFERENCE	CUBE DIMENSIONS - INCHES			σ_f	$\sqrt{B}$	$\sigma_f = a_0 + b_0(\sqrt{B}/H)$				$\sigma_f/$	$1/$	$1/$	MODIFIED - [illegible] Data $\sigma_f = a_0' + b_0'(\sqrt{B}/H)$				$\sigma_f/$	NOTES
		H	B	W	p.s.i.	H	a_0	b_0	r	k_0	k_0	$(\sqrt{B}/H)$	(σ_f/k_0)	a_0'	b_0'	r'	k_0'	k_0'	
WITBANK [illegible]	B12	48	24	24	582	.102	—	—	—	—	.114	9.8	8.77					[illegible]	
		48	24	24	[illegible]	.102					.118	9.8	8.47					.115	
		[illegible]	24	24	630	.136					.123	7.35	8.13					.123	
		36	24	24	656	.136					.129	7.35	7.75					.129	
		24	24	24	774	.204					.152	4.9	6.58					.152	
		24	24	24	800	.204					.157	4.9	6.37					.157	
		36	36	36	708	.167					.139	6.0	7.19					.134	
		36	36	36	710	.167					.169	6.0	5.92					.169	
		24	36	36	861	.250					.176	4.0	5.18					.176	
		24	36	36	894	.250					.175	4.0	5.71					.175	
		48	48	48	641	.144					.129	6.9	7.75					.129	
		48	48	48	661	.144					.129	6.9	7.75					.129	
		36	48	48	717	.192					.140	5.2	7.14					.140	
		36	48	48	756	.192					.148	5.2	6.75					.148	
		24	48	48	955	.288					.187	3.5	5.34					.157	
		24	48	48	964	.288					.189	3.5	5.29					.157	
		60	60	60	635	.129					.125	7.75	8					.125	$a_0'' = -26$
		60	60	60	652	.129					.128	7.75	7.81					.128	
		48	60	60	645	.161					.127	6.21	7.87					.127	$b_0'' = 538$
		48	60	60	678	.161					.133	6.21	7.52					.133	
		36	60	60	729	.215					.143	4.65	6.99					.143	$k_0'' = 512$
		36	60	60	749	.215					.147	4.65	6.80					.147	
		24	60	60	938	.323					.184	3.09	5.43					.184	$r = 0.931$
		24	60	60	950	.323					.186	3.09	5.37					[illegible]	
		80	80	80	647	.112	-217	5306	.931	5090	.127	8.92	7.87	—	—	—	5090	.127	
		80	80	80	649	.112					.127	8.92	7.87					.127	
		48	80	80	740	.186					.146	5.4	6.84					.145	
		48	80	80	806	.186					.158	5.4	6.33					.158	
		36	80	80	859	.248					.169	4.03	5.91					.169	
		36	80	80	862	.248					.169	4.03	5.91					.169	
		24	80	80	1324	.373					.260	2.7	3.84					.260	
		24	80	80	1324	.373					.260	2.7	3.84					.260	
		.75	.75	.75	4260	1.155					.836	.865	1.19					.836	
		1	1	1	4760	1					.935	1	1.07					.935	
		2	2	2	4880	.707					.959	1.41	1.04					.959	
		2.7	2.7	2.7	4575	.608					.899	1.64	1.11					.899	
		3	3	3	4070	.577					.799	1.73	1.25					.749	
		6	6	6	1850	.408					.363	2.45	2.75					.363	
		12	12	12	1158	.288					.227	3.47	4.41					.227	
		18	18	18	910	.236					.179	4.23	5.58					.179	
		28	28	28	779	.189					.152	5.29	6.58					.153	
		1	1	1	5700	1					1.12	1	0.89					1.12	
		17.7	17.7	17.7	[illegible]	.238					.118	4.2	8.47					.118	
		17.7	17.7	17.7	697	.238					.127	4.2	7.3					.137	
		17.7	17.7	17.7	639	.238					.126	4.2	7.93					[illegible]	
		9.05	17.7	17.7	2440	.465					.479	2.15	2.08					.479	
		9.05	17.7	17.7	2615	.465					.514	2.15	1.95					.514	

TABLE B 3 (CONT).

COAL LOCATION	SOURCE [illegible]	CORE DIMENSIONS - INCHES			σ_f p.s.i.	$\sqrt{B}/H$	$\sigma_f = a_0 + b_0(\sqrt{B}/H)$			k_0 (1" cube)	σ_f/k_0	$1/(\sqrt{B}/H)$	$1/(\sigma_f/k_0)$	[illegible]					NOTES
		H	B	W			a_0	b_0	[illegible] r					$\sigma_f = a_0' + b_0'(\sqrt{B}/H)$			k_0'	σ_f/k_0'	
														a_0'	b_0'	r'			
NATAL - DURBAN NAVIGATION	B5	9	9	9	4600	[illegible]	—				·753	1.33	1.32					·753	[illegible]
		9	9	9	1990	·333					·317	3.0	3.15					·317	
		18	9	9	1000	·167	-27.6	6135	·999	6108	·163	5.98	6.13	–	–	–	6108	·163	
		27	9	9	700	·111					·115	9.0	8.69					·115	
NEW LARGO		49.3	55.2	55.2	2153	·152					·252	6.55	2.12					·252	
		45.9	55.7	55.7	2129	·159					·431	6.49	2.32					·431	
		43.9	49.1	49.1	2066	·157					·367	6.28	2.72					·367	
		41.5	55.9	55.9	2199	·177					·391	5.69	2.56					·391	
		29.7	55.9	55.9	2763	·251					·491	3.98	2.01					·491	
		25.6	54.9	54.9	2672	·255	1564	4363	·765	5528	·475	3.97	2.10	·	·	–	5528	·475	
		19.9	54.0	54.0	2743	·371					·523	2.69	1.91					·523	
		20	55.3	55.3	2990	·372					·531	2.69	1.88					·531	
		11.8	55.2	55.2	3309	[illegible]					·587	2.26	1.70					·557	
		16.1	54.7	54.7	3649	·459					·646	·218	1.55					·646	

TABLE B 4: MISCELLANEOUS COAL DATA

COAL LOCATION	SOURCE [illegible]	CORE DIMENSIONS - INCHES			σ_f p.s.i.	$\sqrt{B}/H$	$\sigma_f = a_0 + b_0(\sqrt{B}/H)$			k_0 (1" cube)	σ_f/k_0	$1/(\sqrt{B}/H)$	$1/(\sigma_f/k_0)$	[illegible]					NOTES
		H	B	W			a_0	b_0	[illegible] r					$\sigma_f = a_0' + b_0'(\sqrt{B}/H)$			k_0'	σ_f/k_0'	
														a_0'	b_0'	r'			
[illegible] - CLOVER [illegible] [illegible]	B28	·5	·5	·5	2320	1·41	—				1.307	–	–					–	
		1	1	1	2075	1					1.169	1	·855					1.15	
		1	1	1	1570	1					·855	1	1.129					·866	
		2	2	2	1325	·707					·746	1.41	1.34					·731	
		3	3	3	1150	·577	338	1436	0·957	1779	·648	1.73	1.59	273	1577	0·92	1812	·634	
		4	4	4	1030	·50					·58	2	1.72					·559	
		5	5	5	1000	·447					·563	2.23	1.77					·551	
STARKEY - CLOVER BAR ZONE UNCONFINED	B28	·9	·9	·9	5000	1·05					1.175	·95	·85					1.175	
		1.05	1.05	1.05	4070	·975					·957	1.02	1.05					·957	
		1.18	1.18	1.15	2740	·920					·879	1.08	1.13					·879	
		1.56	1.56	1.56	2900	·800					·682	1.25	1.47					·682	
		2	2	2	2750	·707					·647	1.41	1.55					·647	
		2.2	2.2	2.2	2420	·674	-518	4771	0·96	4252	·579	1.48	1.73	–	–	–	4252	·578	
		3	3	3	2190	·577					·515	1.73	1.44					·515	
		4	4	4	1960	·50					·461	2	2.17					·461	
		5	5	5	2135	·477					·502	2.09	1.99					·502	

(i)For each set of results for any one coal a linear correlation between σ_p and $\sqrt{B}/H$ was performed, giving an equation in the form:

$$\sigma_p = a_0 + b_0 \left\{\frac{\sqrt{B}}{H}\right\}$$

together with the correlation coefficient, where B and H are in inches. From this equation the uniaxial cube strength, $\sigma_c = k_0$, for a 1 inch cube was determined and the data was then normalised by dividing each individual σ_p value by the k_0 value for that coal.

(ii) A linear correlation was then performed on this nomalised data in the form:-

$$\frac{\sigma_p}{k_0} = a_0^1 + b_0^1 \left\{\frac{\sqrt{B}}{H}\right\}$$

for

(a) all U.K. coals - giving $\frac{\sigma_p}{k_0} = 0.574 + 0.389 \left\{\frac{\sqrt{B}}{H}\right\}$, $r = 0.77$

(b) all U.S. coals - giving $\frac{\sigma_p}{k_0} = 0.247 + 0.693 \left\{\frac{\sqrt{B}}{H}\right\}$, $r = 0.73$

(c) all S. African coals - giving $\frac{\sigma_p}{k_0} = 0.055 + 1.009 \left\{\frac{\sqrt{B}}{H}\right\}$, $r = 0.88$

(d) all coals - giving $\frac{\sigma_p}{k_0} = 0.235 + 0.664 \left\{\frac{\sqrt{B}}{H}\right\}$, $r = 0.82$

Figures B1, B2, B3, B4 and B5 show these results.

Considering the wide range of coals, the variance in testing techniques etc., these correlations are relatively good.

(iii) Because the $1/\sqrt{D}$ form is fairly well established, and because the cube strength data dominates the total number of measurements available, it was decided to investigate the applicability of this equation to the non-cubic

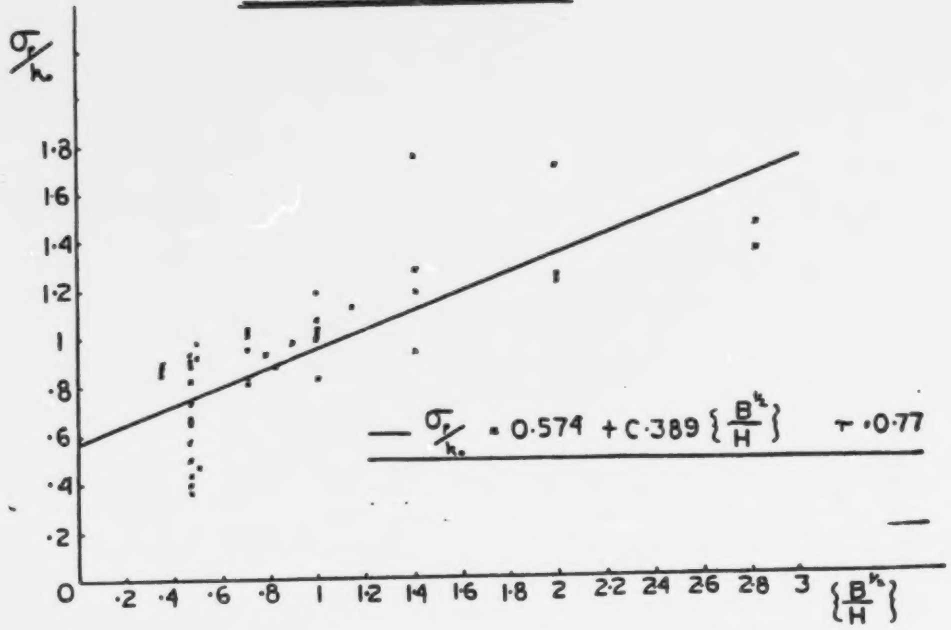

U.K COALS - ALL DATA

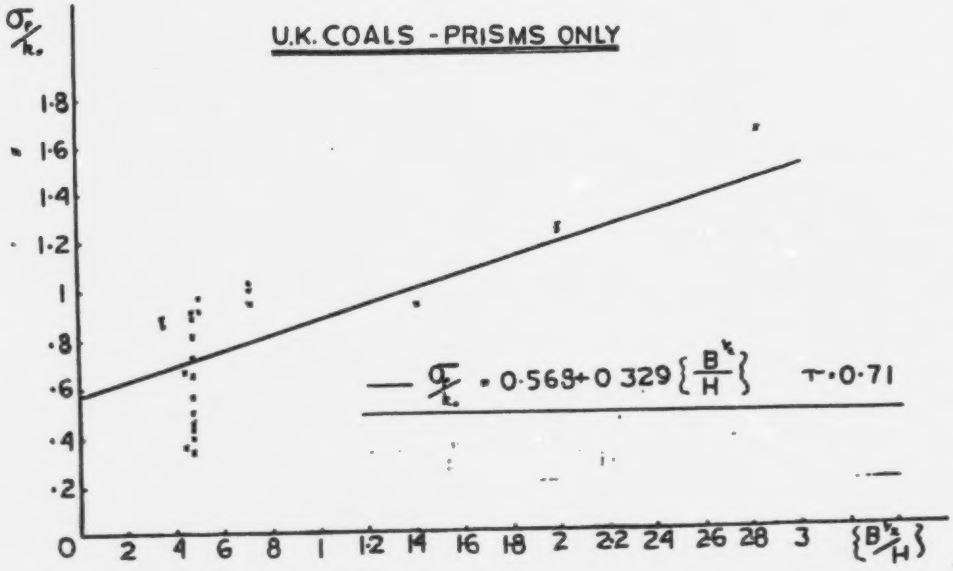

U.K. COALS - PRISMS ONLY

FIGURE B1: UNIAXIAL COMPRESSIVE STRENGTH CORRELATIONS - U.K. COALS

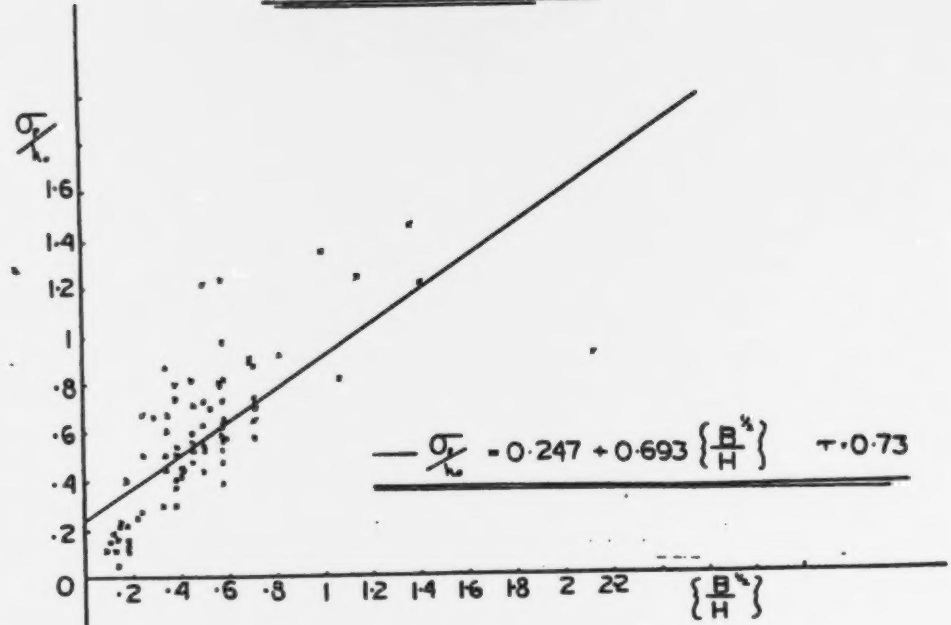

U.S. COALS - ALL DATA

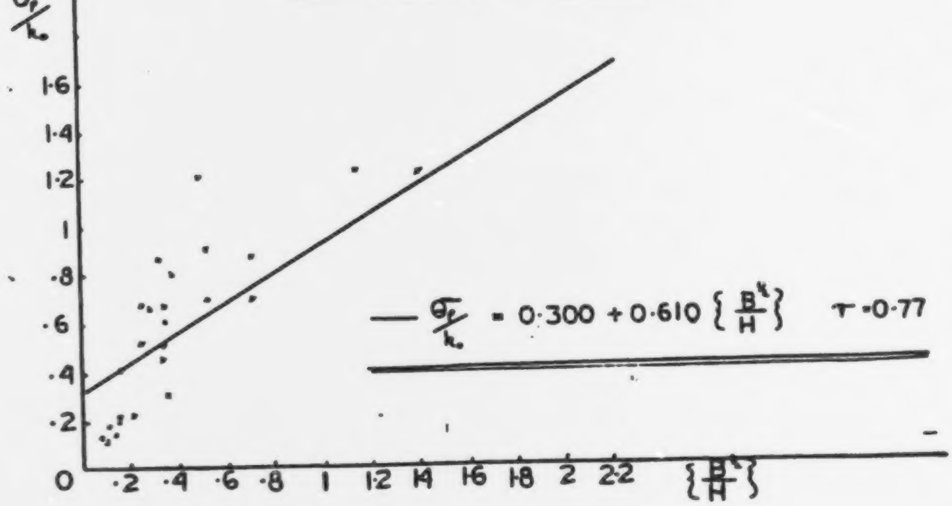

US COALS - PRISMS ONLY

FIGURE B2: UNIAXIAL COMPRESSIVE STRENGTH CORRELATIONS - U.S. COALS

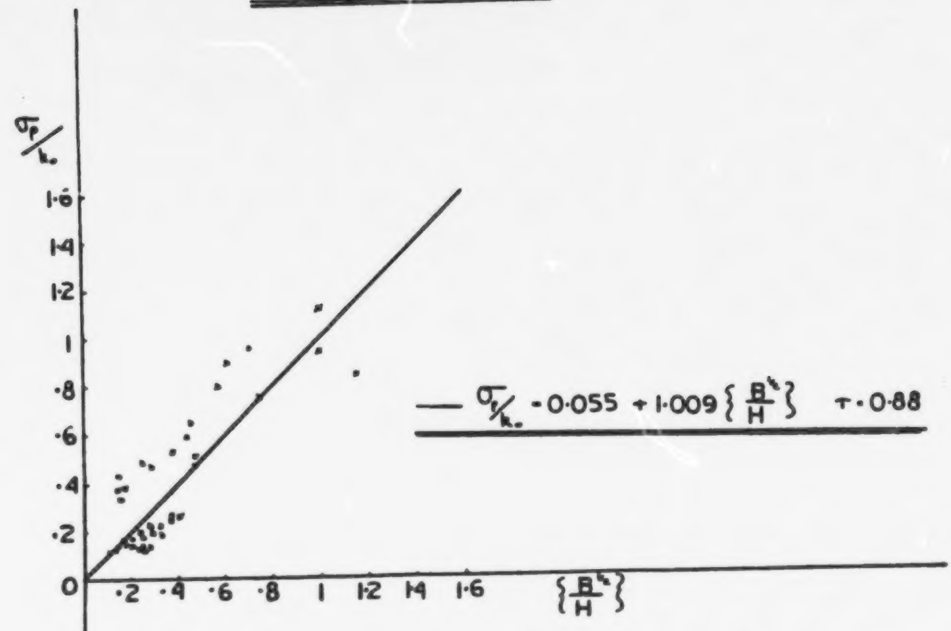
S.A COALS - ALL DATA

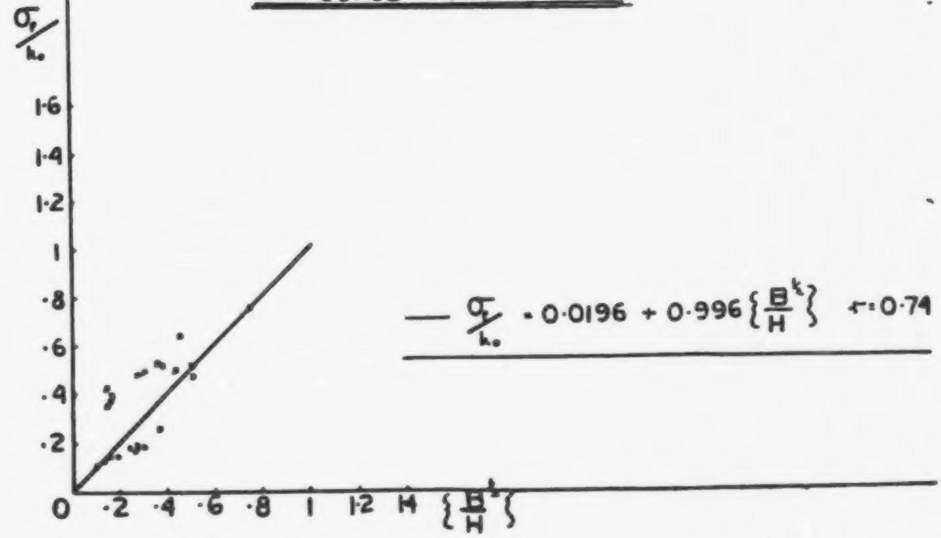
S.A. COALS - PRISMS ONLY

FIGURE B3: UNIAXIAL COMPRESSIVE STRENGTH CORRELATIONS - S. AFRICAN COALS

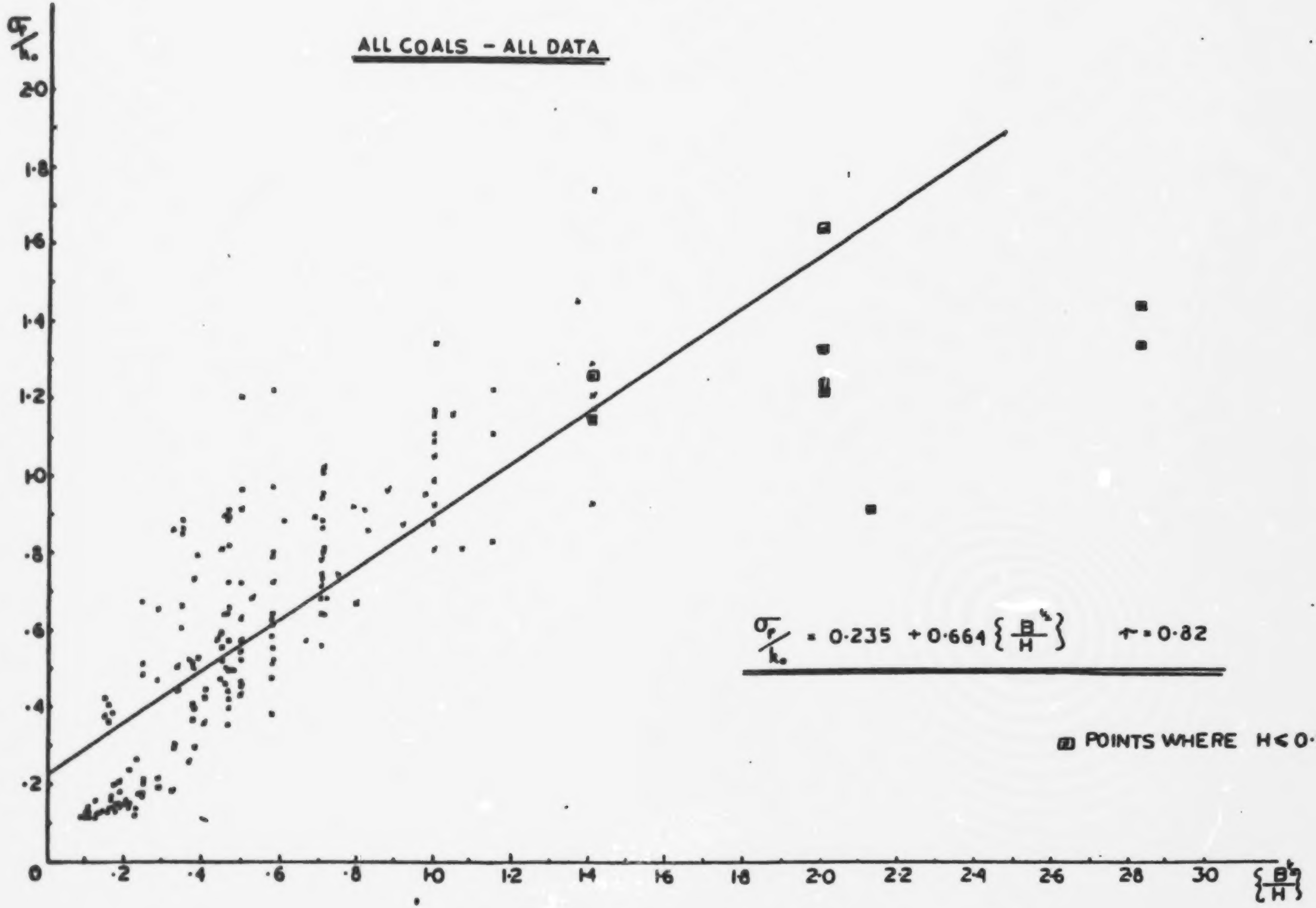

FIGURE B4: UNIAXIAL COMPRESSIVE STRENGTH CORRELATIONS - ALL COALS - ALL DATA

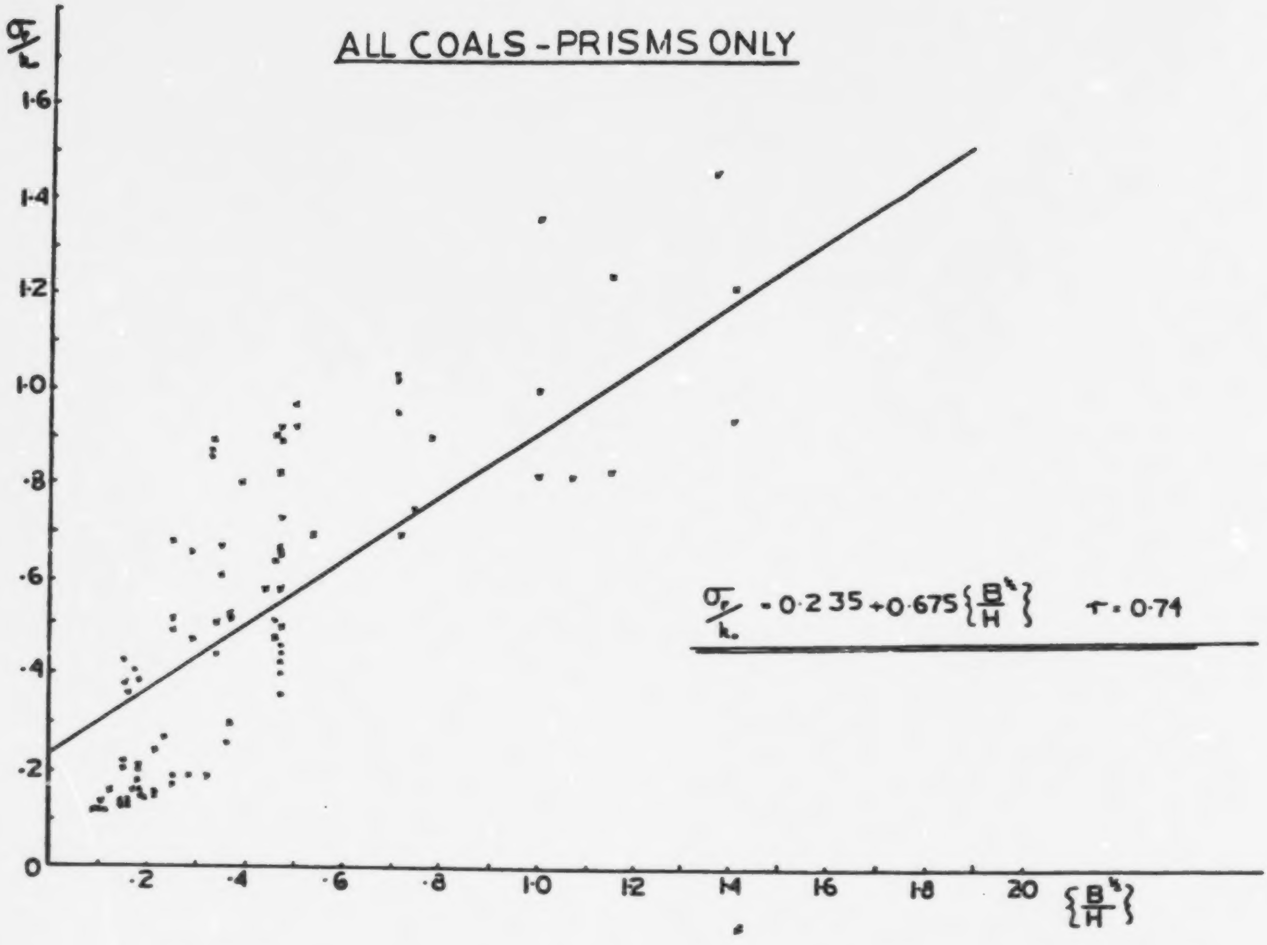

FIGURE B5: UNIAXIAL COMPRESSIVE STRENGTH CORRELATIONS - ALL COALS - PRISMS ONLY

(prism) specimens only. (ie. eliminating the cube data) The following results were obtained and the comparison with the total data given:-

(a) U.K. Coals

all data $\frac{\sigma_p}{k_0} = 0.574 + 0.389 \left\{\frac{\sqrt{B}}{H}\right\}$, $r = 0.77$

non cubic specimens $\frac{\sigma_p}{k_0} = 0.568 + 0.329 \left\{\frac{\sqrt{B}}{H}\right\}$, $r = 0.71$

(b) U.S. Coals

all data $\frac{\sigma_p}{k_0} = 0.247 + 0.693 \left\{\frac{\sqrt{B}}{H}\right\}$, $r = 0.73$

non cubic specimens $\frac{\sigma_p}{k_0} = 0.300 + 0.610 \left\{\frac{\sqrt{B}}{H}\right\}$, $r = 0.77$

(c) S. African Coals

all data $\frac{\sigma_p}{k_0} = 0.055 + 1.009 \left\{\frac{\sqrt{B}}{H}\right\}$, $r = 0.88$

non cubic specimens $\frac{\sigma_p}{k_0} = 0.0196 + 0.996 \left\{\frac{\sqrt{B}}{H}\right\}$, $r = 0.74$

(d) All Coals

all data $\frac{\sigma_p}{k_0} = 0.235 + 0.664 \left\{\frac{\sqrt{B}}{H}\right\}$, $r = 0.82$

non cubic specimens $\frac{\sigma_p}{k_0} = 0.235 + 0.675 \left\{\frac{\sqrt{B}}{H}\right\}$, $r = 0.74$

These additional correlations are also shown in Figure B1 - 5.

Comparison of the correlations for the total data and the non-cube data shows that they are not substantially different. It follows therefore that the general form equation appears to fit all of the data, both cubes and prisms, quite well and thus that it is not necessary to use the two expressions of Hustrulid to describe the size/shape effects.

(iv) On examining Figure B4 it was noted that a disproportionate number of points at high $\sqrt{B}/H$ values appeared to deviate from this correlation line. Further examination showed that most of these points were associated with tests where the specimen height was less than or equal to 0.5 inches. Apparently at small sizes the general form of equation appears to breakdown; this appears from Figure B4 to occur $\sqrt{B}/H > 1.4$.

Thus for cubes where B=H=D then the general form appears to breakdown when

$$\sqrt{D} > 1.4\,D \qquad \text{i.e.}\quad D < \left(\frac{1}{1.4}\right)^2 = 0.51 \text{ inches}$$

This is in accordance with Hustrulid's comments on the doubtfullness of the application of his equations to Evans results for cube specimens below 1" size.

It will therefore be assumed that the general form of the size/shape relationship breaksdown and does not apply to specimens where $\sqrt{B}/H > 1.4$. What does this mean in practical terms? The table below shows the B_b and B_b/H values at breakdown for a range of H values.

H inches	$B_b = (1.4\,H)^2$	(B_b/H)
0.5	0.49	1.02
1	1.96	1.96
10	196	19.6
120	28,224	235.0

It is seen from this that, in practice, such a breakdown in the general equation will only likely occur in the testing of small size specimens. At very large sizes the B_b/H ratio becomes very large and such specimens (or pillars) are unlikely to occur. eg. with H = 120 inches (10 ft) the equation would apply up to values of B_b = 2352 ft.

Consequently the data for all coals was re-analysed, eliminating all test data when $\sqrt{B}/H > 1.4$. This required re-evaluation of k_0 to derive the new, k_o', values for those data sets from which data was eliminated, followed by redetermination of the ${}^{\sigma}p/k_o'$ values and the new correlation. This yielded :-

for all coals $\left(\frac{\sqrt{B}}{H} < 1.4\right)$ $\qquad \frac{\sigma_p}{k_o'} = 0.103+0.917 \left\{\frac{\sqrt{B}}{H}\right\}$ $\qquad r = 0.87$

Figure B6 shows this correlation.

Comparing this correlation curve to that obtained previously:-

$$\frac{\sigma_p}{k_o} = 0.235 + 0.664 \left\{\frac{\sqrt{B}}{H}\right\} \qquad r = 0.82$$

indicates that the curve has steepened and that a better correlation coefficient has been obtained.

(v) It was then decided to examine the data to see if there was an lower limit to the value of $\sqrt{B}/H$ for which the general form of the relationship applies. On Figure B4 all points for the small values of $\sqrt{B}/H$ are clustered close to the origin and it is difficult to see whether or not there is a deviation from the correlation curve. Consequently the "inverse" correlation of k_o/σ_c was plotted against $H/\sqrt{B}$. This correlation is seen in Figure B7 and yielded:-

$$\frac{k_o}{\sigma_c} = - 0.0770 + 1.005 \left\{\frac{H}{\sqrt{B}}\right\}, \qquad r = 0.832$$

Now from examination of Figure B7 it is seen that all data points for $H/\sqrt{B} > 8$ fall on one side of the curve only. ie. it appears that the general form of the relationship breaksdown when

$$\frac{H}{\sqrt{B}} > 8 \quad \text{ie. when } \frac{\sqrt{B}}{H} < 0.125$$

For cube specimens, when H=B=D, then this breakdown occurs when $\sqrt{D} = 8$ ie. when D = 64 inches.

This is very close to the limit of 60 inches observed by Bieniawski beyond which

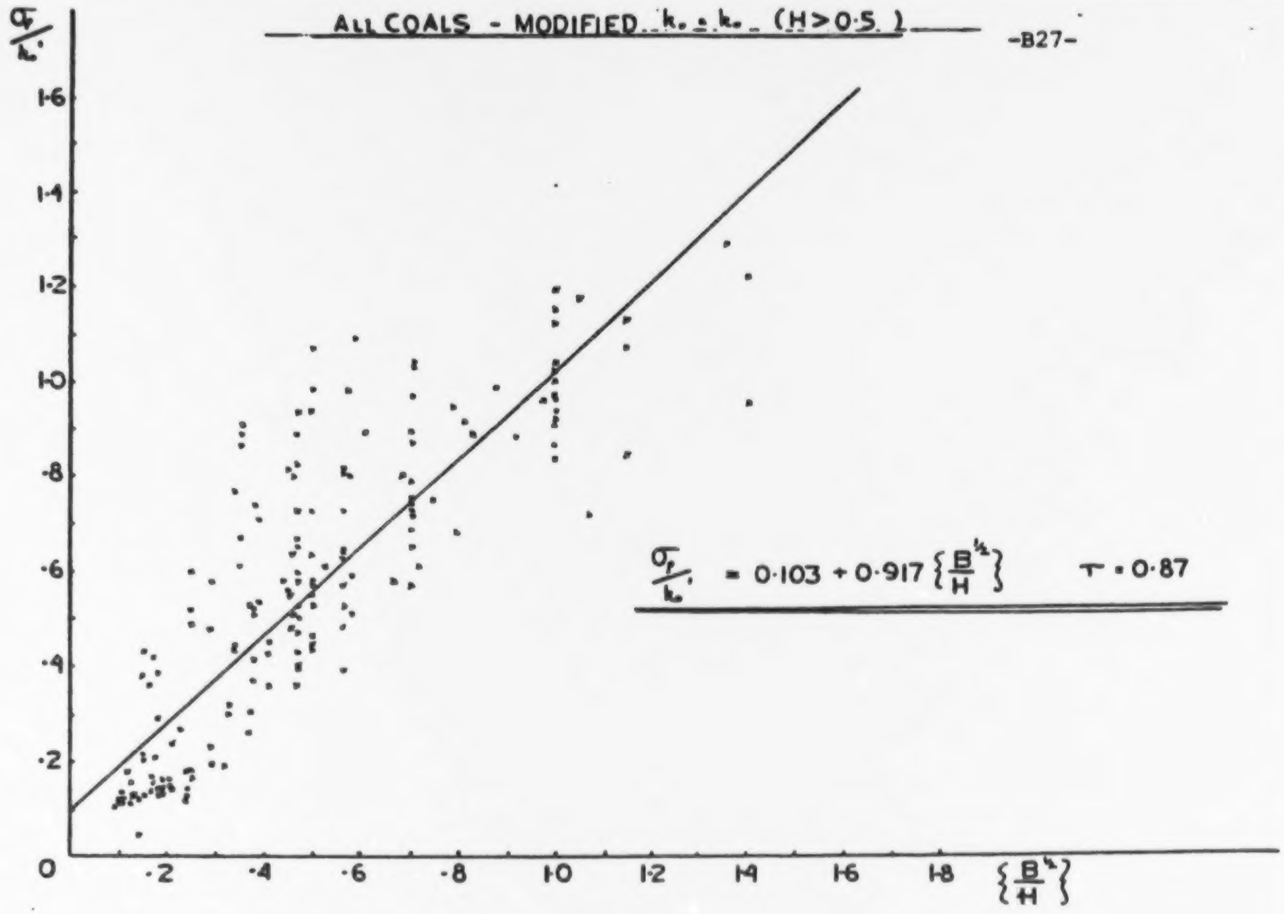

FIGURE B6: CORRELATIONS - ALL COALS WHEN H > 0.5 INCHES

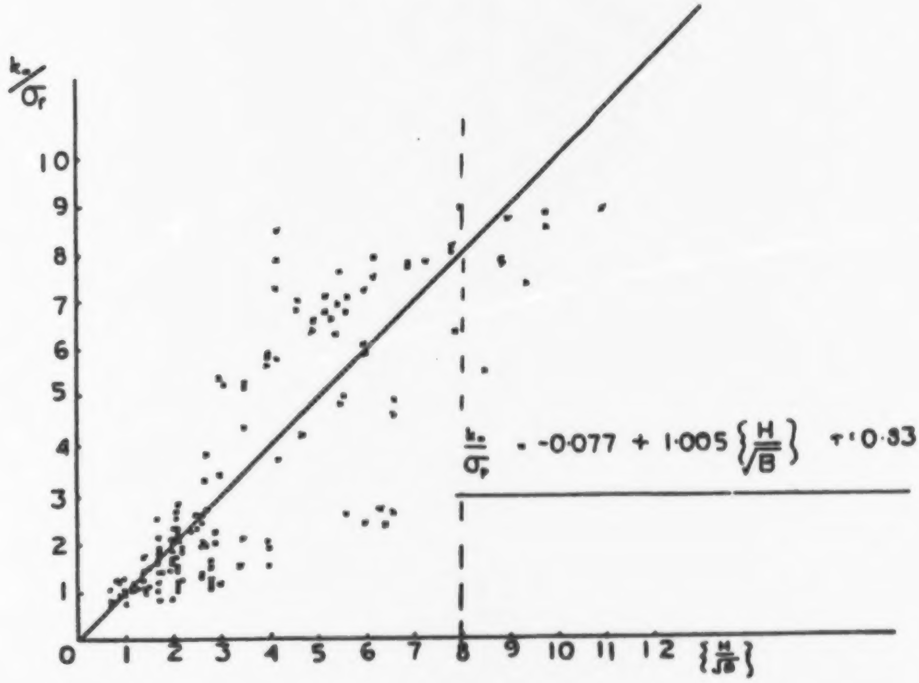

FIGURE B7: CORRELATIONS - ALL COALS IN INVERSE (H/√B) FORM (√B/H < 1.4)

the cube strength is regarded as being constant. We may therefore also conclude that when $\sqrt{B}/H < 0.125$ there will be a constant specimen (pillar) strength given by that at which $\sqrt{B}/H = 0.125$.

What does this mean in practice? The table below shows the B_b'/H and B_b' values at breakdown for a range of H values.

H inches	$B_b' = (.125\ H)^2$	B_b'/H
0.5	.0039	128
1	.0156	64
10	1.56	6.4
120	225	1.875

It is seen from this that for small specimens this limit is unlikely to be reached because the width/height ratios at breakdown are so high. However, once we reach "pillar dimensions" it is clearly seen that a such breakdown is possible and that beyond certain dimensions the pillar will achieve a constant strength given by that for $\sqrt{B}/H = 0.125$.

B.3.2 Summary and Conclusions

(i) The re-examination of all the experimental test data on prisms and cubes has shown that the general form of the strength/shape relationships given by:-

$$\sigma_p = k \frac{\sqrt{B}}{H}$$

gives a good fit to the data provided that the following limits are imposed

$$0.125 < \frac{\sqrt{B}}{H} < 1.4$$

(ii) In practice the upper limit ($\sqrt{B}/H < 1.4$) will only be experienced with the testing of small specimens. For cubes the relationship breaksdown when B=H=D= 0.5 inches. This agrees with the comments of Hustrulid on Evans tests of small cubes.

(iii) In practice the lower limit ($\sqrt{B}/H > 0.125$) will only be experienced for large specimens (pillars) and means that at sizes where this limit is exceeded the pillar will have a constant strength equal to that when $\sqrt{B}/H = 0.125$.

For cubes, when B=H=D, this occurs when D=64 inches. This is in close agreement to Bieniawski's maximum cube size of 60 inches beyond which the cube has a constant strength.

(iv) The use of this "general" form relationship does not give a significantly better fit to the data than do Hustrulid's two equation form. However, the use of a single relationship is intrinsically more satisfying since a cube is after all only a special case of a prism. Further the use of the general form eliminates the need to be concerned about the differences between tests where B is varied and H held constant or vice-versa; the general form relationship automatically allows data from a either set of tests to be lumped together.

B.4 Comparison of The Three Strength/Shape Relationships For a Typical Pillar Size

Finally the strength/shape relationships in the power, linear and general forms will be compared when applied to a typical pillar size, where the pillar height H = 120 inches. A value of the uniaxial 1 inch cube strength of 6000 psi will be used in this example. Table B5 gives the calculations and Figure B8 shows the results. It will be noted that when used in this manner the three forms give significantly different results for the shape effect although they are in excellent agreement for the cube size. (B/H = 1)

The application of these equations to pillars will be discussed in more detail in the case histories on pillar strength formulae given in the main text.

TABLE B5: COMPARISON OF SHAPE RELATIONSHIPS FOR H = 120", σ_c FOR 1 INCH CUBE = 6000 psi (k = 6000)

B/H	B inches	Power Curve Form $\sigma_p = k' \sqrt{B}/H$	Linear Form $\sigma_p = k' (.778+.222\ (B/H))$	General Form $\sigma_p = k \sqrt{B}/H$	
		$k' = \frac{k}{\sqrt{60}} = 775$	$k' = \frac{k}{\sqrt{60}} = 775$	k = 6000	
		σ_p	σ_p	$\frac{\sqrt{B}}{H}$	σ_p
0.25	30	387	645	.0456	750 *
0.5	60	548	688	.0645	750 *
0.75	90	671	732	.0791	750 *
1.0	120	775	775	.091	750 *
2.0	240	1096	947	.129	774
3.0	360	1342	1119	.158	948
4.0	480	1550	1291	.1826	1096
5.0	600	1732	1463	.204	1224
10.0	1200	2450	2323	.289	1734

* $\frac{\sqrt{B}}{H} < 0.125$ thus $\sigma_p = 6000 \times .125$

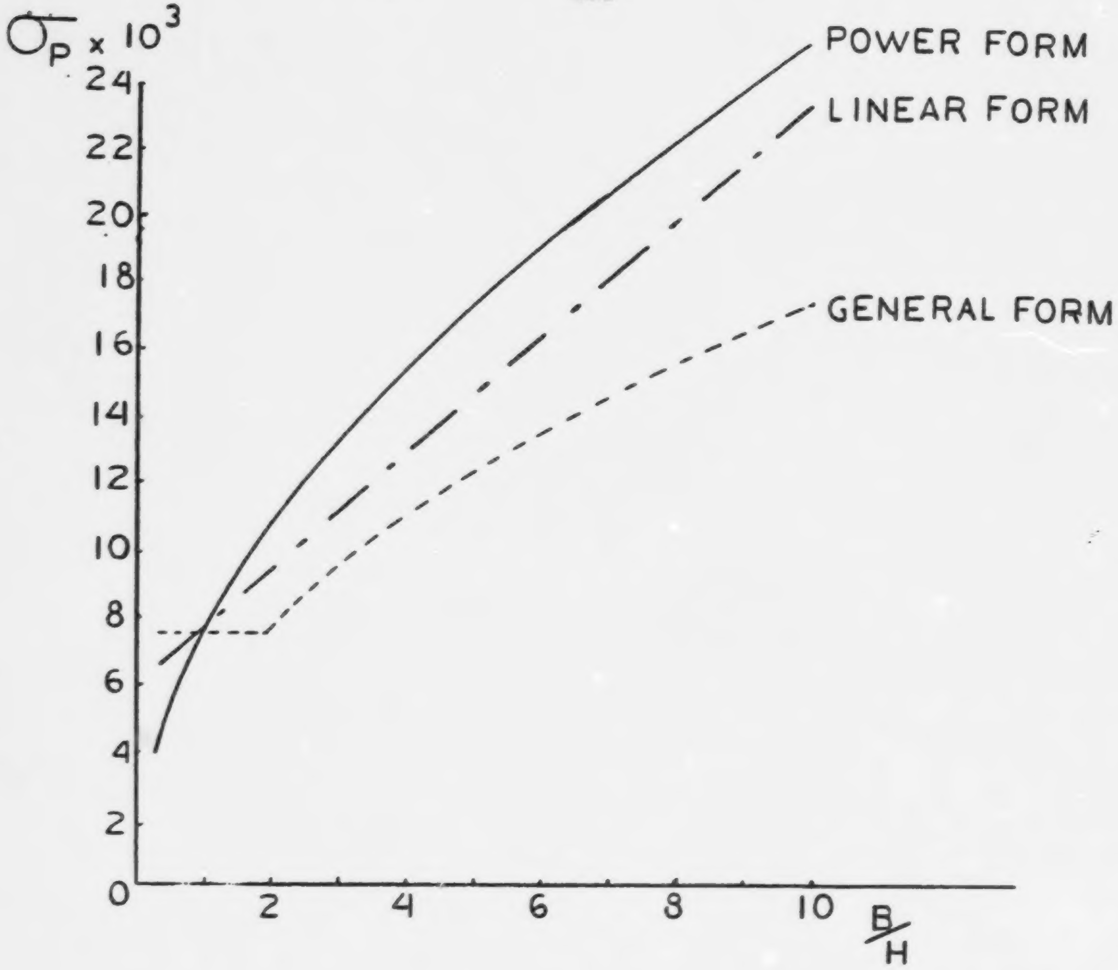

FIGURE B8: 3 FORMS OF STRENGTH SHAPE RELATIONSHIPS FOR SPECIMENS OF PILLAR SIZE

B.5 Conclusion

1. Past studies have indicated significant size and shape influences on the uniaxial strength of coal specimens. It is shown that these effects may be described by a single equation of the form:-

$$\sigma_p = k \frac{\sqrt{B}}{H}$$

where k is numerically (but not dimensionally equal to the uniaxial strength of a 1 inch cube), B is the minimum specimen width (inches) and H is the specimen height (inches).

2. This equation gives a reasonable fit to the experimental data in the literature provided that upper and lower limits are set to its' use. These limits are:-

$$0.125 < \frac{\sqrt{B}}{H} < 1.4$$

3. The lower limit implies that for large specimens the prism strength becomes a constant. For cubes this occurs when B=H=D = 64 inches which is close to that given by Bieniawski of 60 inches.

4. This "general" form of the relationship gives no better fit to the data than the "two equation" relationship advocated by Hustrulid. However it is preferred because it satisfies both the cube data and non cube data by a single relationship and avoids (unlike Hustrulid) the necessity of separating data in which the height is varied and width constant from that in which the width is varied and the height kept constant.

REFERENCES FOR APPENDIX B

B.1 Daniels, J. and Moore, L.D. "The Ultimate Crushing Strength of Coal", Engineering and Mining Journal, p. 263-268, 1907

B.2 Rice, G.S. "Test of the Strength of Roof Supports used in Anthracite Mines of Pennsylvania", Bulletin 303, U.S. Bureau of Mines, p. 1-44, 1929

B.3 Lowall, C.E. and Holland, C.T. "Some Physical Characteristics of West Virginia Coal", Research Bulletin of Engineering Experimental Station, West Virginia University, Bulletin 17, 1937

B.4 Greenwald, H.P, Howarth, H.C., and Hartmann, I "Experiments on the Strength of Small Pillars of Coal in the Pittsburgh Bed", U.S. Bureau of Mines, Technical Paper 605, 1939

B.5 Steart, F.A. "Strength and Stability of Pillars in Coal Mines", Journal Chemical, Metallurgical and Mining Society of S. Africa, p. 309-325, 1954

B.6 Millard, D.J., Newman, P.C., and Phillips, J.W. "The Apparent Strength of Extensively Cracked Materials", Proc. of the Physical Society, B. Volume LXVIII, p. 723-728, 1955

B.7 Gaddy, F.L. "A Study of the Ultimate Strength of Coal as Related to the Absolute Size of the Cubical Specimens Tested", Bulletin 112, Virginia Engineering Experimental Station, Virginia Polytechnic Institute, 1956

B.8 Evans, I, Pomeray, C.D. and Berenbaum "The Compressive Strength of Coal", Colliery Engineering, Vol. 38, p. 75-80, p. 123-127, and p. 172-178, 1961

B.9 Hustrulid, W.A. "A Review of Coal Pillar Strength Formulae", Rock Mechanics, V. 8, p. 115-145, 1976

B.10 Bieniawski, Z.T. "Contribution to the Discussion of 'A Study of the Strength of Coal Pillars' and 'A Method of Designing Bord and Pillar Workings'", Journal S. African Institute of Mining and Metallurgy, pp 187-192, November 1967

B.11 Bieniawski, Z.T. "In-Situ Strength and Deformation Characteristics of Coal", Engineering Geology, V. 2, No. 5, p. 325-340, 1968

B.12 Bieniawski, Z.T. "The Effect of Specimen Size on the Compressive Strength of Coal", Int. Journal of Rock Mechanics and Mining Sciences, V. 5, No. 4, p. 325-335, July 1968

B.13 Bieniawski, Z.T. "In-Situ large Scale Testing of Coal", Proc. Conf. on In-situ Investigations of Rock and Soils, British Geotechnical Society, London, p. 44-49, 1969

B.14 Bieniawski, Z.T. "Note on In-Situ Testing of the Strength of Coal Pillars", Journal S. African Inst. Mining and Metallurgy, p. 445-465, May 1968

B.15 Evans, I "Discussion on 'The Effect of Specimen Size on the Compressive Strength of Coal'", International Journal on Rock Mechanics and Mining Sciences, V. 7, No. 2, p 230, March 1970

B.16 Griffith, W. and Conner, E.T. "Mining Conditions Under the City of Scramton, Pa", Bulletin 25, U.S. Bureau of Mines, p. 77-82, 1912

B.17 Holland, C.T. "The Physical Properties of Coal and Associated Rock on Related to the Causes of Baups in Mines", Trans. AIME, Vol. 149, p. 75-93, 1942

B.18 Bauschinger, J "Mitteilungen aus dem Mechanisch-Technischen Laboratorium der K. Technischen Hockschule in Munchen", Vol. 6, 1876

B.19 M.O. Withey, and Aston, J. "Johnson's Materials of Construction", 7th Edition, John Wiley, p. 112-114, 1930

B.20 Bunting, D. "Chamber Pillars in Deep Anthracite Mines", Trans. AIME, p. 739-748, 1911

B.21 Holland, C.T. and Gaddy, F.L. "Some Aspects of Permanent Support of Overburden on Coal Beds", Proc. West Virginia Coal Mining Institute, p. 43-66, 1957

B.22 Holland, C.T. "The Strength of Coal Mine Pillars", Proc. 6th Symposium on Rock Mechanics, University of Missouri, Rolla, p. 450-466, 1964

B.23 Salamon, M.D.G. and Munro, A.H. "A Study of the Strength of Coal Pillars", Journal of S. African Inst. Mining and Metallurgy, p. 55-67, September 1967

B.24 Hobbs, D.W. "The Strength and Stress Strain Characteristics of Oakdale Coal under Triaxial Compression", Geol. Mag., Vol. 97, p. 422-435, 1960

B.25 Hobbs, D.W. "The Strength and Stress Strain Characteristics of Coal in Triaxial Compression", J. Geol., Vol. 72, p. 214-231, 1964

B.26 Hazen, G. and Artler, L. "Practical Coal Pillar Design Problem", Mining Congress Journal, pp. 86-92, June 1976

B.27 Greenwald, H.P., Howorth, H.C., and Hartmann, I "Progress Report: Experiments on Strength of Small Pillars of Coal in the Pittsburgh Bed", Report of Investigation 3575, USBM, June 1941

B.28 Jeramec, M.L., and Cruden, D.M. "Strength of Coal from the Star-Key Mine near Edmonton, Alberta", CIM Bulletin, p. 94-99, February 1979

APPENDIX C: VALUES FOR THE ANGLE OF FRICTION OF BROKEN COAL AND FOR THE UNIAXIAL COMPRESSIVE STRENGTH OF BROKEN COAL

C.1 For a Selection of Western Canadian Coals

Patching (C.1 and C.2) carried out triaxial compression tests on a number of fragmented Western Canadian Coals. Each group has a straight line Mohr envelope of failure and the values obtained for the angle of internal friction, ϕ_B, for these broken coals are listed below.

TEST #	ϕ_B	TEST#	ϕ_B	TEST#	ϕ_B	TEST#	ϕ_B
38	33.17	60	45.50	81	37.17	102	34.87
39	34.67	61	42.00	82	39.00	103	35.87
40	34.50	61-B	41.87	83	39.50	104	35.33
41	34.50	62	40.87	84	34.87	105	33.17
42	-	63	40.17	85	35.33	106	34.17
43	-	64	40.17	86	39.00	107	-
44	-	65	39.00	87	-	108	33.87
45	35.67	66	33.50	88	40.50	109	34.00
46	37.17	67	34.17	89	39.17	110	34.87
47	36.50	68	34.00	90	39.17	111	33.87
48	36.17	69	36.33	91	38.67	112	33.67
49	35.17	70	36.33	92	40.00	113	32.67
50	36.50	71	34.22	93	38.17	114	32.5
51	37.00	72	33.87	94	39.87	115	32.33
52	36.67	73	38.50	95	38.67	116	34.17
53	39.00	74	38.87	96	36.50	117	34.33
54	40.83	75	37.17	97	35.17	118	35.17
55	40.00	76	37.33	98	35.17		
56	38.83	77	38.00	99	36.50		
57	39.00	78	38.17	100	37.00		
58	37.17	79	40.50	101	36.50		
59	-	80	40.17				

Mean = 36.8°

Standard Deviation = 3.0°

Range 32.3° to 45.5°

The author also took Patchings results and correlated σ_1 vs σ_3 in straight line form to yield

$$\sigma_1 = 1.94 + 3.319\,\sigma_3, \quad r = 0.990 \text{ in kg/cm}^2$$

ie. when $\sigma_3 = 0$ $\quad \sigma_1 = P_B = 1.94 \text{ kg/cm}^2 = \underline{27.5 \text{ psi}}$

C.2 For Canmore Coal

Barron and Couetdic (C.3) tested re-compacted crushed coal from the Wilson seam at Canmore, Alberta. Three different re-compaction loads were used to check the variation of the angle of friction ϕ_B with recompaction pressure. All specimens were approximately 2 inches high by 1 inch diameter. Three specimens for each re-compaction pressure were tested at each of the following confining pressures: 250 psi, 500 psi, 750 psi, 1000 psi. The Mohr failure envelope for each re-compaction pressure closely approximated straight lines. The slope of the Mohr failure envelope was determined to yield ϕ_B. Straight line correlations between σ_1 and σ_3 in the form $\sigma_1 = a + b\,\sigma_3$ were used to determine this uniaxial strength of the broken coal.

Test Group	Recompaction load (lbs)	ϕ_B	$a = P_B$ psi.	Specific/gravity ρ
A	5,000	$29.7^{\circ}+0.4$	225	1.119
B	25,000	$33.0^{\circ}+0.8$	737	1.180
C	25,000	$34.6^{\circ}+0.8$	725	1.230
Mean	All Specimens	$33.0^{\circ}+0.8$	560	1.180

C.3 For U.K. Coals

Wilson (C.4) reported results of triaxial tests on granulated coals, for a range of different size of particles. He determined the "triaxial stress factor", k', for these results. The triaxial stress factor is related to the angle of friction for these broken coals by:-

$$k' = \frac{1 + \sin\phi_B}{1 - \sin\phi_B}$$

if it is assumed that the Mohr envelope of failure is a straight line. His results showed that a straight line approximation for the Mohr envelope was valid for these cases. Unfortunately he reports no data on the cohesion intercept and hence P_B cannot be evaluated. Wilson results are summarized below:-

COAL	SIZE RANGE mm	AVERAGE k	ϕ_B
Dawdon Coal (# 331 B)	0-0.5	3.3	32.3°
	0.5-1.59	3.0	30°
	1.6-3.2	2.9	29.1°
Markham Coal Barnsley Hards (#743)	0-0.5	2.9	29.1°
	0.5-1.59	2.6	26.4°
	1.59-3.2	2.6	26.4°
Parkgate top coal Hickleton 569A	0.5-1.59	2.8	28.3°
Parkgate bottom coal Hickleton 569B	0.5-1.59	2.8	28.3°
Hwch anthracite Cwmgwilli 514B	0.5-1.59	2.3	23.2°
Stanllyd anthracite Cwngwilli 514C	0.5-1.59	2.6	26.4°
		Mean	28.0°
		Standard Deviation	2.5°
		Range	23.2° 32.3°

C.4 U.S. Coals

Atkinson and Ko (C.5) carried out triaxial tests on solid coal samples and continued the tests after failure to determine the residual stress after failure. The residual stress envelope should therefore give a measure of the angle of friction for the broken (failed) specimen.

They plotted their results in the form:-

$$(\frac{\sigma_1 - \sigma_3}{2}) = a + (\frac{\sigma_1 + \sigma_3}{2}) \tan \alpha$$

The angle of internal friction, ϕ, and the cohesion, S_o are obtained from:-

$$\text{Sin}\phi = \tan\alpha \qquad \text{and } S_o = \frac{a}{\text{Cos }\phi}$$

They showed that a straight line relationship applied for all of these residual stress results. The table below summarises their results and evaluates the values of ϕ_B and P_B (= $\frac{2\ S_o\ \text{Cos}\phi_B}{1\ \text{-Sin}\phi_B}$) obtained by them.

Coal	Residual a psi	tanα (=Sinϕ_B)	ϕ_B	$S_o = \frac{a}{\text{Cos}\phi_B}$	$P_B = \frac{2\ S_o\ \text{Cos}\phi_B}{1 - \text{Sin}\phi_B}$
Beehive	213	.6246	38.6^o	272	1130
Bruceton	177	.6789	42.8^o	241*	1103
Decker	372	.4749	28.3^o	422*	1413
Federal #2	325	.6137	37.8^o	411	1678
		Mean	36.9^o	337	1331
		Standard Deviation	6.1^o	93	270
		Range	28.3^o— 42.8^o	240-420	1100-1680

*Note: there is an error in calculation of these values in Atkinson and Ko's paper.

C.5 Discussion

It is seen from the above results that the range of "angle of friction" values for broken coal is quite large; from a minimum of 23.2^o to a maximum of 45.5^o. The average of the mean values for each coal is 31.8^o with a standard deviation of 6.0^o.

Atkinson and Ko noted that:-

(i) U.S. Coals have a higher angle of friction than the U.K. coals (it would appear that the Canadian coals tested lie somewhere between these values).

(ii) The ratio of the residual angle of friction (i.e. broken specimens) to the peak angle of friction (i.e. solid specimens at failure) for the U.S. Coals was approximately 0.8 for the coals tested.

(Note: this assumes that the Mohr envelope of peak stress is a straight line, which was proven by Atkinson and Ko to be the case for their test coals, over the confining pressure range tested. This will be discussed further in the text, section 3.2).

Hence, for use in the model for case history studies, if a value of the angle of internal friction for the solid coal is known then ϕ_B for broken coal (if unknown) might be estimated approximately as 0.8 times the solid coal value.

With respect to the results for the cohesion of broken coal, S_o, (and hence for P_B), it is seen that the values are significantly greater than zero. Since these data represent tests on broken coal the available cohesion would be expected to be very low or equal to zero. Hobbs (C.6) reports the results of triaxial tests on broken coal measure rocks (but not on coal itself) that have a marked curvature at low levels of confining pressure and that have a zero cohesion intercept. If the test data were available at low confining pressure levels it might also indicate a curved envelope in this area resulting in low values of cohesion (and thus P_B) for the above results. Hence, at best, the values of P_B calculated from the above results can only be considered as maximum possible values of P_B which in all liklihood are in fact considerably lower (but not necessarily zero). The range of "maximum" P_B values given by the above results is:-

25 psi to 1680 psi

Bearing in mind that a zero value for P_B is unacceptable for the model (it does not allow confining pressure to be built up in the pillar) it might perhaps be better to assume P_B values of perhaps 1/10 those of the maximum range given above:-

P_B range 1 - 200 psi

Conclusion

(i) The angle of friction for broken coals can have a wide variation from as low as 23° to as high as 45°. A "typical" mean value is around 30°.

(ii) Where ϕ_B is unknown, but the angle of internal friction for solid coal is known (ϕ_s), then ϕ_B can be approximated by putting $\phi_B = 0.8\ \phi_s$.

(iii) All the broken coal tests reported above give linear Mohr envelopes and hence a constant angle of friction for broken coal, within the confining pressure ranges tested. Hence the assumption in the model that ϕ_B (and μ_B) are constant is a reasonable first approximation. However it should be remembered (see note, page 68, Phase 1 Report) that there is evidence in the literature (C.7, C.8) that μ_B may vary with normal stress at higher confining pressures.

(iv) The determination of the cohesion of broken coal, and hence the uniaxial compressive strength, P_B, of broken coal is unsatisfactory. At best, the results give an overestimate of the value and can be considered is the "maximum possible" value. In reality a value of perhaps 1/10th of this maximum value is probably more realistic, giving a range for coals of approximately 1-200 psi. An unfortunate implication of this lack of knowledge of P_B, and the difficulty of determining P_B, is that the depth of the fracture zone as calculated by the model is very sensitive to the value of P_B. Likewise, the strength of the pillar when failure occurs in the fracture mode is also sensitive to P_B. When failure of the pillar occurs in the yield mode then the strength is much less sensitive to P_B. In practice, if all other parameters are known, then it may be better to "back analyse" field results to determine an effective P_B value for further application in any one mine.

(v) There is no evidence in the literature to indicate whether or not ϕ_B and P_B are influenced by specimen size. It will continue to be assumed that they are size independent until proved to the contrary.

REFERENCES FOR APPENDIX C

C.1 Patching, T. "Triaxial Compression Tests on Fragmented Coal", Dept. E.M.R., Canada. Fuels & Mining Practice Div., Report FMP 60/68 - MIN, 1960

C.2 Patching, T. "Triaxial Compression Tests on Fragmented Coal, Report #2", Dept. E.M.R., Canada. Fuels & Mining Practice Div., Report FMP 61/33 - MIN, 1961

C.3 Barron, K. and Couetdic, J.M. "Plate-load Testing as a Method of Assessing the In-Situ Strength Properties of Western Canadian Coals", Int. J. Rock Mech. and Min. Science and Geomech. Abstracts, Vol. 12, No. 10, pp. 303-310, October 1975

C.4 Wilson, A.H. "A Study of Yield Zones Around Roadways", National Coal Board, London, Final Report on ECSC Research Project 6220-AB/8/802, December 1975

C.5 Atkinson, R.H. and Ko, H.Y. "Strength Characteristics of U.S. Coals", Proc. 18th Symp. on Rock Mechanics, Keystone, Colorado, pp. 283-1:6, 1977

C.6 Hobbs, D.W. "The Behaviour of Broken Rock under Triaxial Compression", Int. J. Rock Mech and Min Sci., Vol. 7, pp. 125-148, 1970

C.7 Byerlee, J.D. "Frictional Characteristics of Granite under High Confining Pressure", J. Geophysical Research, 14, pp. 3634-3648, July 1967

C.8 Maurer, W.C. "Shear Failure of Rock Under Compression", Soc. Pet. Eng. Journal, 5, pp. 167-175, 1965

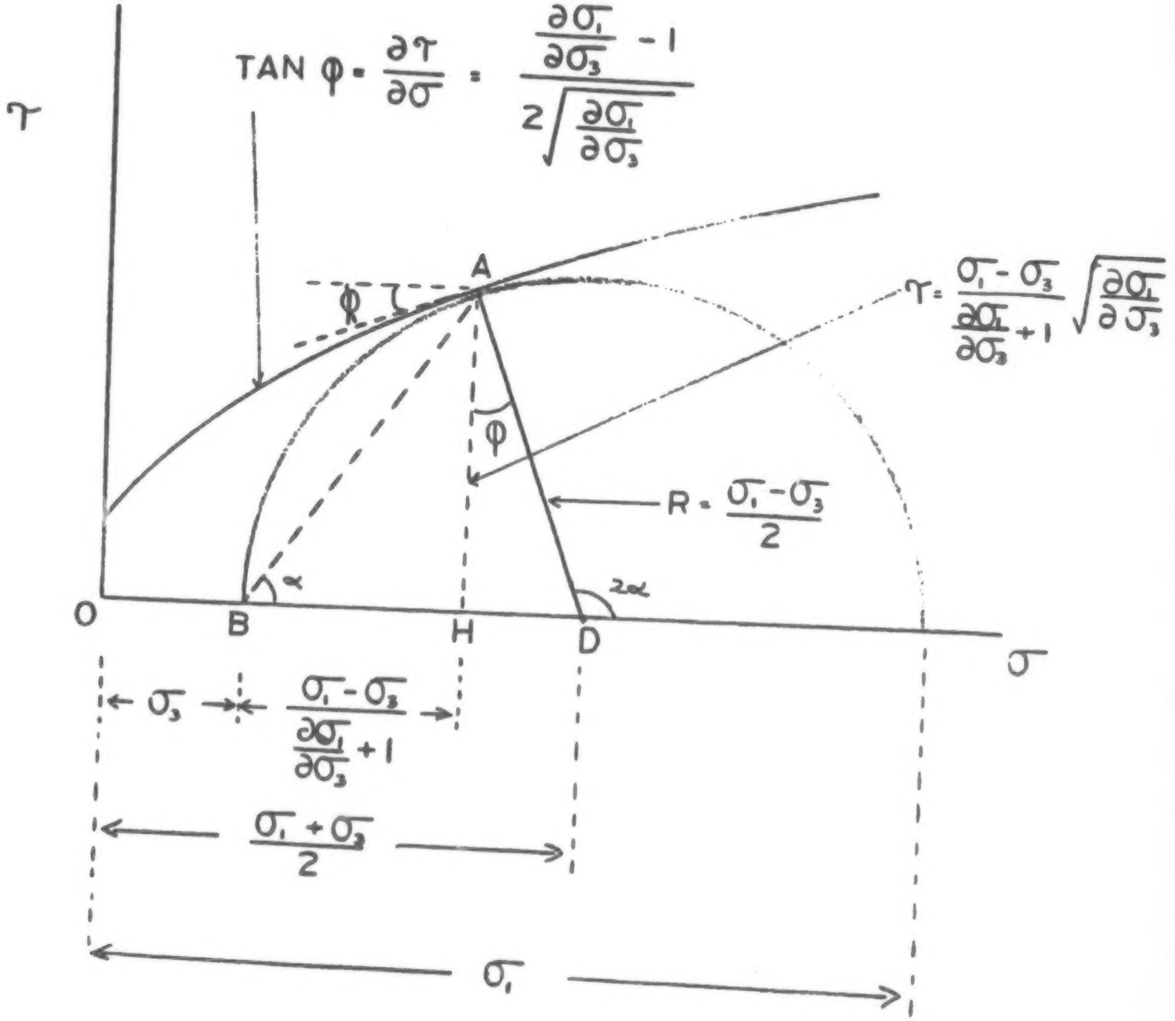
$\tan\varphi = \frac{\partial\tau}{\partial\sigma} = \frac{\frac{\partial\sigma_1}{\partial\sigma_3} - 1}{2\sqrt{\frac{\partial\sigma_1}{\partial\sigma_3}}}$
τ
A
φ
$\tau = \frac{\sigma_1 - \sigma_3}{\frac{\partial\sigma_1}{\partial\sigma_3} + 1}\sqrt{\frac{\partial\sigma_1}{\partial\sigma_3}}$
φ
$R = \frac{\sigma_1 - \sigma_3}{2}$
α
2α
O
B
H
D
σ
σ_3
$\frac{\sigma_1 - \sigma_3}{\frac{\partial\sigma_1}{\partial\sigma_3} + 1}$
$\frac{\sigma_1 + \sigma_3}{2}$
σ_1

FIGURE D1: MOHR'S DIAGRAM

$$\tan \propto = \sqrt{\frac{\partial\sigma_1}{\partial\sigma_3}} \qquad (5)$$

Also, by geometry:-

$$2 \propto = 90 + \phi \qquad (6)$$

where ϕ is the inclination of Mohr's envelope (the angle of internal friction). Hence from equation 5 and 6:-

$$\frac{\partial\tau}{\partial\sigma} = \tan \phi = \left\{ \frac{\frac{\partial\sigma_1}{\partial\sigma_3} - 1}{2 \sqrt{\frac{\partial\sigma_1}{\partial\sigma_3}}} \right\} \qquad (7)$$

D.2 Application to a Curved Envelope

Balmer applied the above to the consideration of a curvelinear envelope when the relationship between the principal stresses is given by:-

$$\sigma_3 = a + b\ \sigma_1{}^c \qquad (8)$$

The arbitrary constants, a, b and c can be determined from the data by the method of least squares, as follows:-

The equation is considered in two steps. The first step is to evaluate c. If the derivative of equation 8 is approximated by using finite increments in order to apply it to discrete data, then:-

$$\frac{\Delta\sigma_1}{\Delta\sigma_3} = \frac{1}{b\ c\ \sigma_1{}^{c-1}} \qquad (9)$$

In logarithnic form this equation can be written as:-

$$\log_e \left\{ \frac{\Delta\sigma_1}{\Delta\sigma_3} \right\} = -\log (bc) - (c-1) \log_e \sigma_1 \qquad (10)$$

Equation 10 is linear if $\log\left\{\frac{\Delta\sigma_1}{\Delta\sigma_3}\right\}$ and $\log \sigma_1$ are considered the variables with log (bc) and (c-1) arbitary constants. Hence the numerical value of c can be determined by the conventional method of least squares.

Since the value of c is now known, the method of least squares can now be applied to equation 8 to determine a and b.

By substitution of equations 8 and 9, using

$\frac{\Delta\sigma_1}{\Delta\sigma_3}$ equal to $\frac{\partial\sigma_1}{\partial\sigma_3}$, in equations 2 and 3, σ_3 is eliminated and the following parametric relationships are determined:-

$$\sigma = \left\{\frac{b\ (c+1)\ \sigma_1{}^{c}}{1+\ bc\ \sigma_1{}^{c-1}}\right\} + a \qquad (11)$$

and

$$\tau = \left\{\frac{\sigma_1 - a - b\sigma_1{}^{c}}{1 + bc\ \sigma_1{}^{c-1}}\right\} \sqrt{bc\ \sigma_1{}^{c-1}} \qquad (12)$$

also from equations 7 and 9:-

$$\frac{\partial\tau}{\partial\sigma} = \left\{\frac{1 - bc\ \sigma_1{}^{c-1}}{2\ \sqrt{bc\ \sigma_1{}^{c-1}}}\right\} \qquad (13)$$

A computer program has been written to evaluate the constants, a, b and c by this method; it also evaluates the parametric relationships (11) and (12) allowing the envelope to be plotted. The program plots both the Mohr's circles and the resulting parametric envelope.

D.3 Application to Triaxial Data for Coal

Table D.1 gives Hobbs (D.2) triaxial stress data for a number of U.K. coals. This

TABLE D.1: TRIAXIAL FRACTURE STRENGTH DATA FOR COALS (FROM HOBBS D.2)

Orientation of Weakness Planes	Confining Pressure σ_3 P.S.I.	Axial Fracture Strength - σ_1 P.S.I. Coal/1	Coal/2	Coal/3	Coal/4	Coal/5	Coal/6	Coal/7	Coal/8	Coal/9
Bedding planes parallel, main cleat planes parallel.	0	2630	1020	320	1010	4390	3420	1960	2300	1510
	500	-	5080	3680	5810	7590	8780	7940	8480	5590
	1000	9650	6590	4480	7330	9770	10060	10190	10090	8250
	2000	13520	9460	6940	-	13940	-	-	11970	-
	3000	14280	12580	9980	14490	14380	15460	15890	14480	13360
	4000	19.930	15110	13780	-	18920	-	-	16200	-
	5000	22540	16140	15330	18850	20130	19480	21010	18230	16570
Parabolic Parameter	A	3859.8	2952.2	1853.2	3072.4	3357.1	3808.8	3900.6	3560.6	2791.9
Balmer Form Parameters	a	-143.1	-166.3	-34.96	-195.39	+25.01	-258.37	-297.51	-404.84	-296.16
	b	.000701	.000922	.02064	.001175	.000001	.000003	.000122	.000016	.000262
	c	1.578	1.598	1.285	1.552	2.266	2.158	1.767	2.001	1.727
Bedding planes perpendicular main cleat planes parallel.	0	4580	1000	770	1920	7450	3460	2280	3160	3150
	500	-	5010	5990	6210	9320	7340	6730	7560	8780
	1000	11100	7350	6160	8520	14020	10460	9220	8350	11600
	2000	14200	9970	8160	-	14930	-	-	12060	-
	3000	18630	11620	11110	13690	16430	15710	15420	14350	17140
	4000	22920	14460	12670	-	17930	-	-	15300	-
	5000	29710*	16040	17000	18160	20030	19820	18910	17900	21230
Parabolic Parameter	A	4913.5	2545.1	1769.4	3043.6	4387.3	3790.0	3494.2	3184.8	4352.8
Balmer Form Parameters	a	-927.4	-277.76	-61.85	-272.45	-483.06	-309.11	-258.06	-274.37	-327.96
	b	.200885	-.001114	.001755	.000269	$2.05x10^{-8}$	.000025	.000073	.000016	.000010
	c	1.0	1.585	1.535	1.712	2.658	1.935	1.834	2.004	2.020

*σ_3 = 4750 in this case.

COAL 1 - PENTEMAWR
COAL 2 - DEEP DUFFRYN
COAL 3 - OAKDALE
COAL 4 - CWMTILLERY
COAL 5 - BARNSLEY HARDS
COAL 6 - BARNSLEY BRIGHTS
COAL 7 - TEVERSAL
COAL 8 - MARKHAM
COAL 9 - LINBY

data was used in the Phase 1 Report to illustrate the single parameter parabolic form of Mohr envelope was in that report. The parameters A (for single parameter parabolic envelope) and a, b and c (for the Balmer solution) are also given in this table. Figure D.2 to D.19 show the Balmer envelopes determined from this data.

If these Balmer envelopes are compared with the envelopes for the same data given in Figures I.4 to I.21 in the Phase 1 Report, then it is seen that in all cases the Balmer form of envelope gives a much superior fit to the coal data.

It may be concluded therefore that:-

(i) if a full set of triaxial strength data is available, then the use of the Balmer parametric form of Mohr envelope is much superior.

(ii) However, the use of this form of envelope will require that the equations for the fracture criteria used in the model be re-stated in a modified form and the appropriate changes then be made in the model program. Whilst this is not difficult, it has not been done as part of this contract; consequently the case histories considered in this report all use the single parameter form of parabolic envelope.

(iii) Where the only strength data for the coal is a uniaxial compressive strength then it is not possible to derive, a, b and c, but it is possible to obtain A. Hence in such cases the single parameter parabolic form of Mohr envelope:-

$$\tau^2 = A\sigma + \frac{A^2}{4}$$

is probably the best approximation for a curvilinear envelope. Differences in the stress conditions at the transition point when using one or other envelope are discussed and illustrated in Section 3.1 of the text.

NOTE: The parameter c in the Balmer form of Mohr envelope is a measure of the curvature of the envelope. If c is > 1, then the envelope curves over quite rapidly. If c = 1 the equation reverts to that of a straight line. In practice, any solution in which $1 < c < 1.1$ is probably acceptably fitted as a straight line relationship. It should also be noted that, with a poor set of input data, it is possible for c to be < 1. This indicates the envelope would curve in the opposite direction; such a curvature is deemed to be physically unacceptable. Hence in such cases the

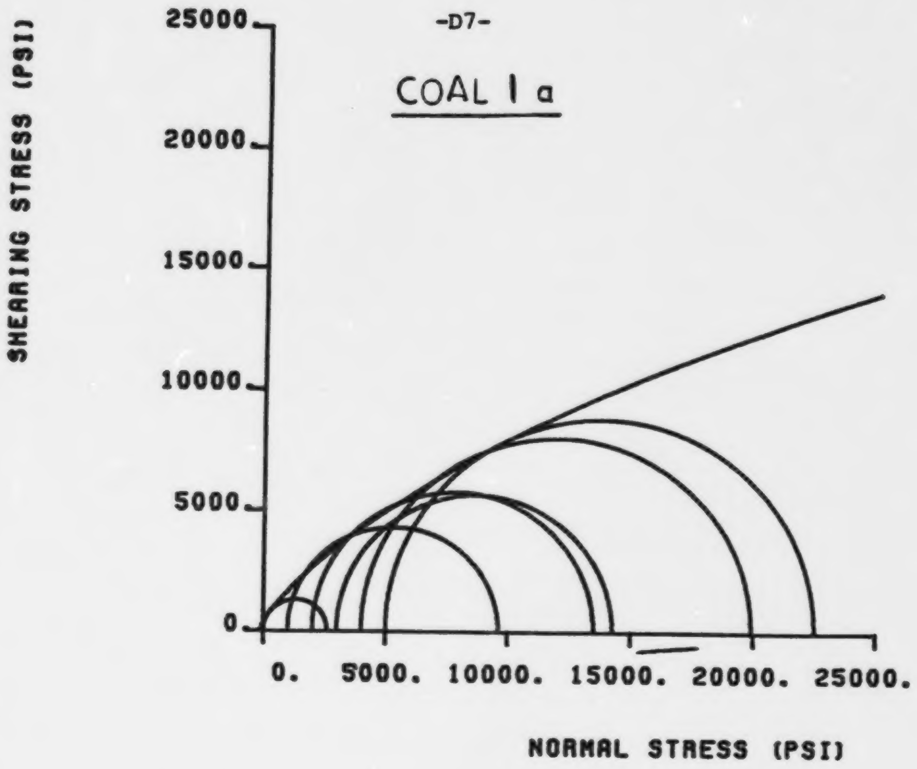

FIGURE D2

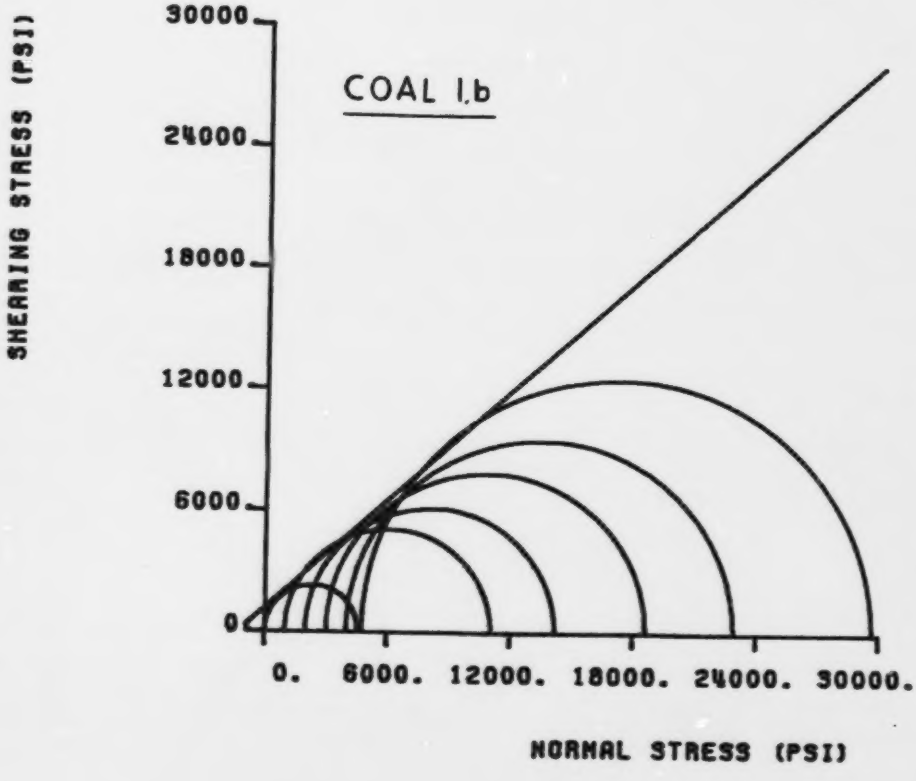

FIGURE D3

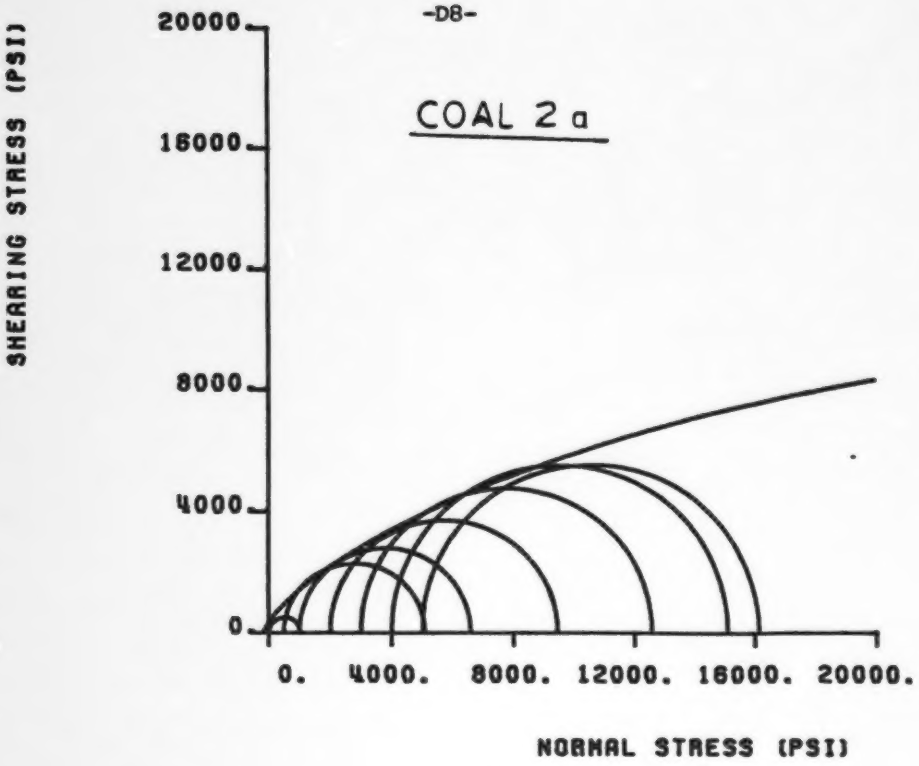

FIGURE D4

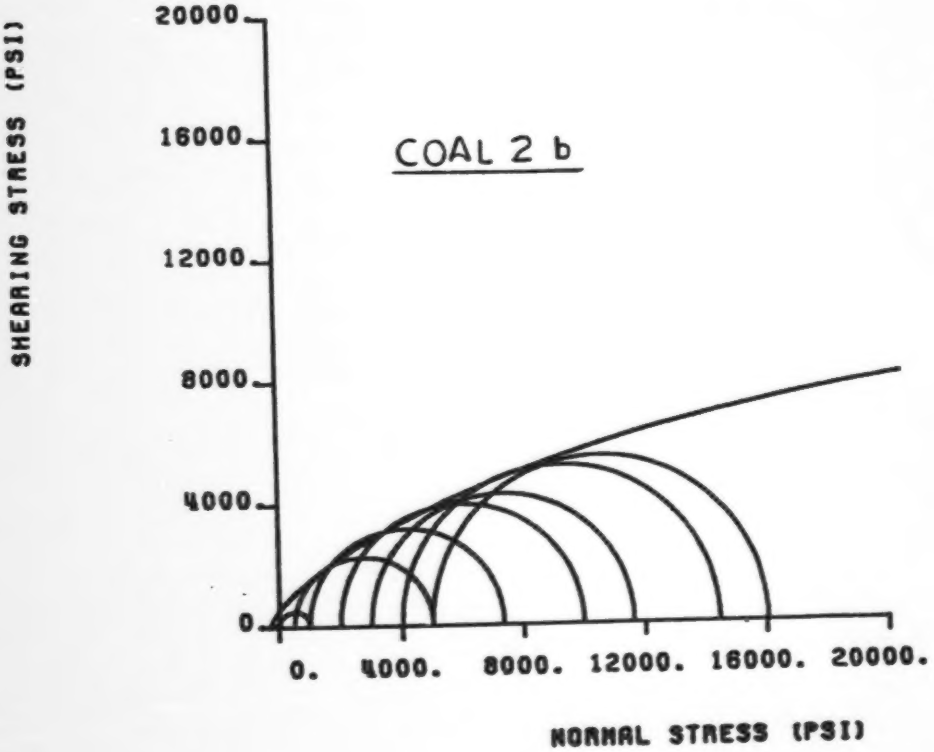

FIGURE D5

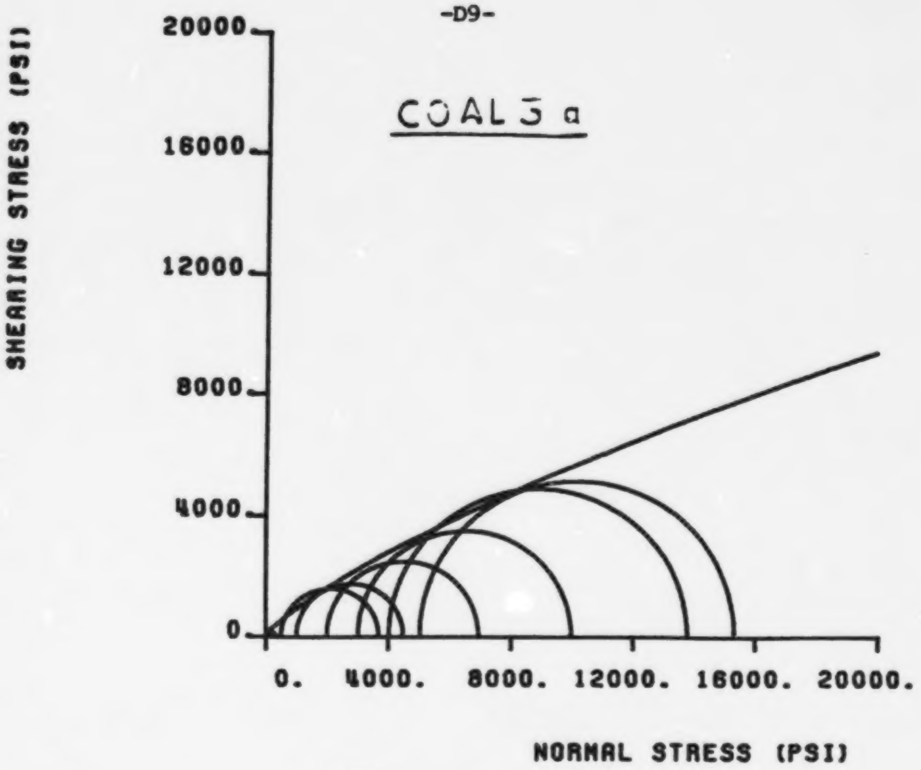

FIGURE D6

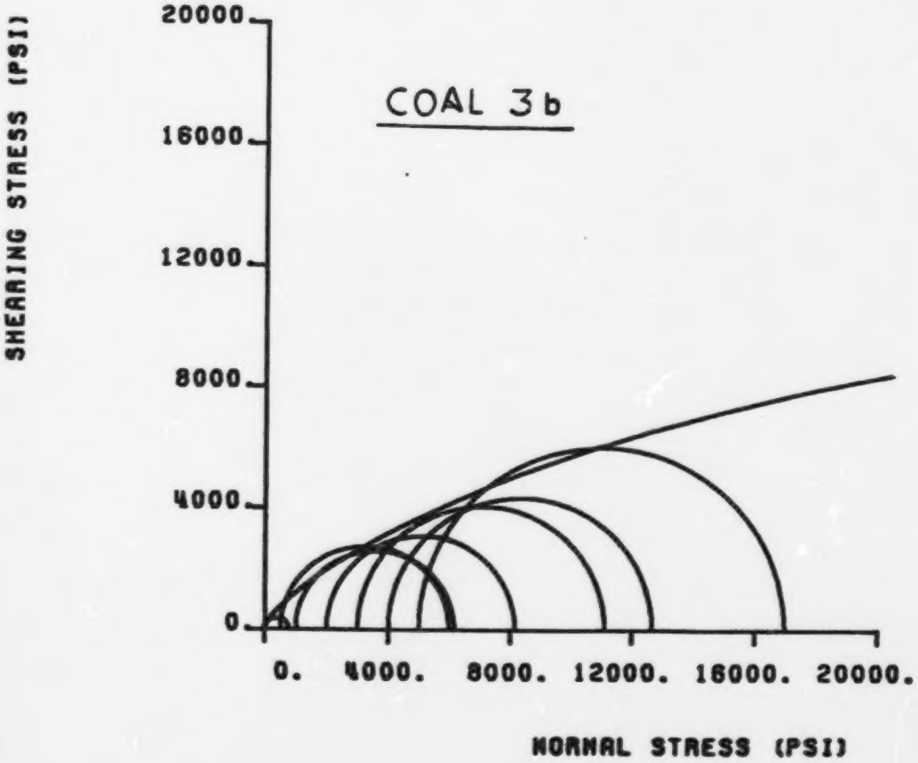

FIGURE D7

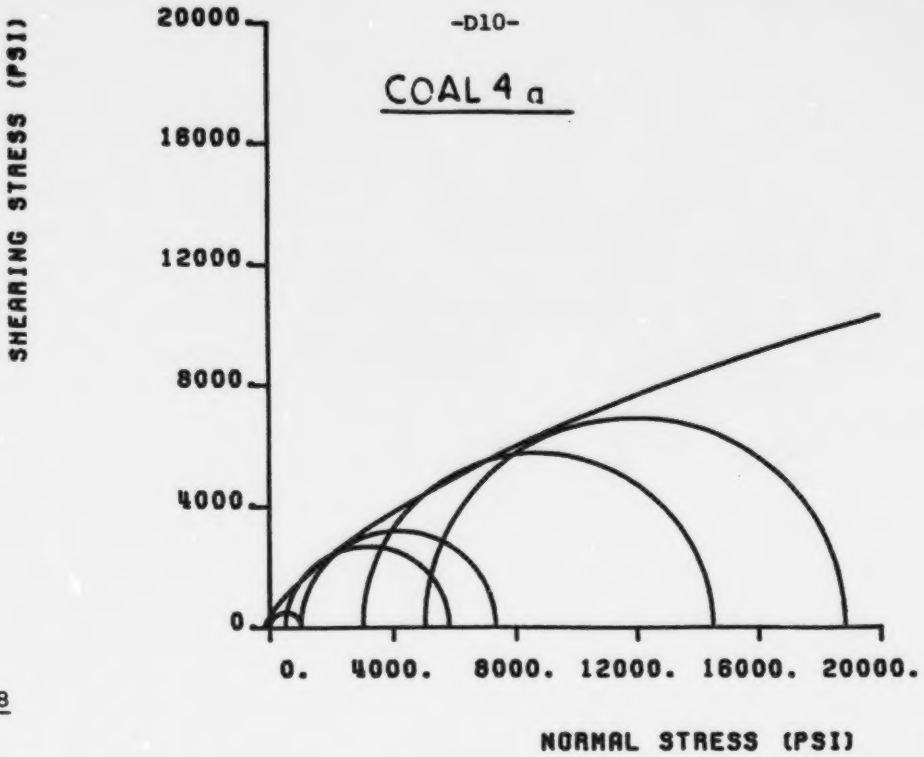

FIGURE D8

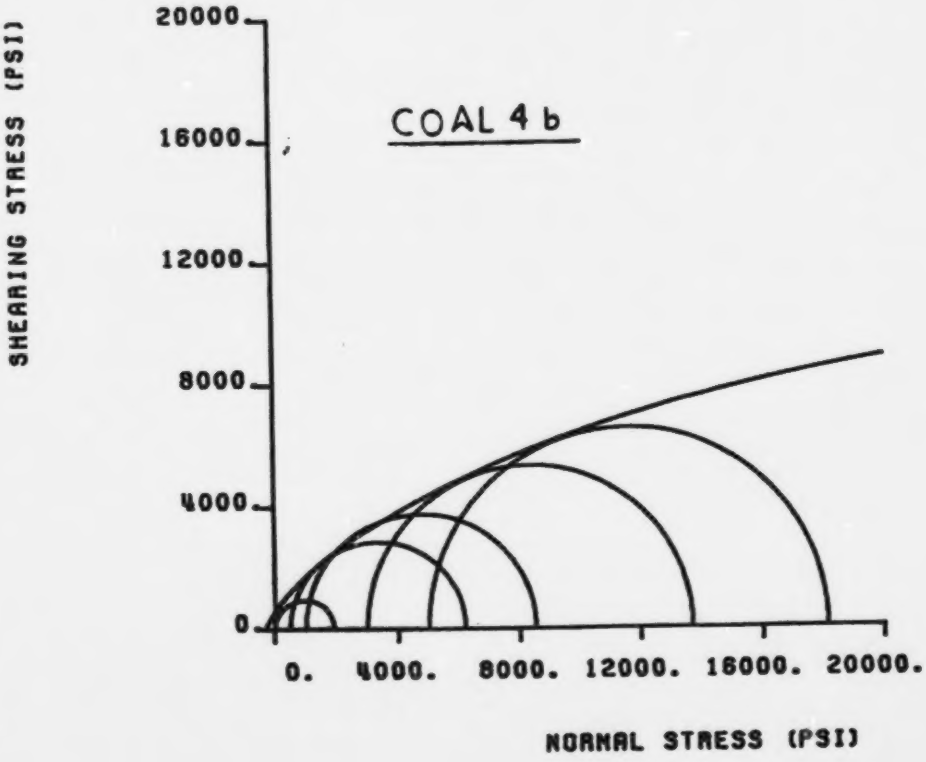

FIGURE D9

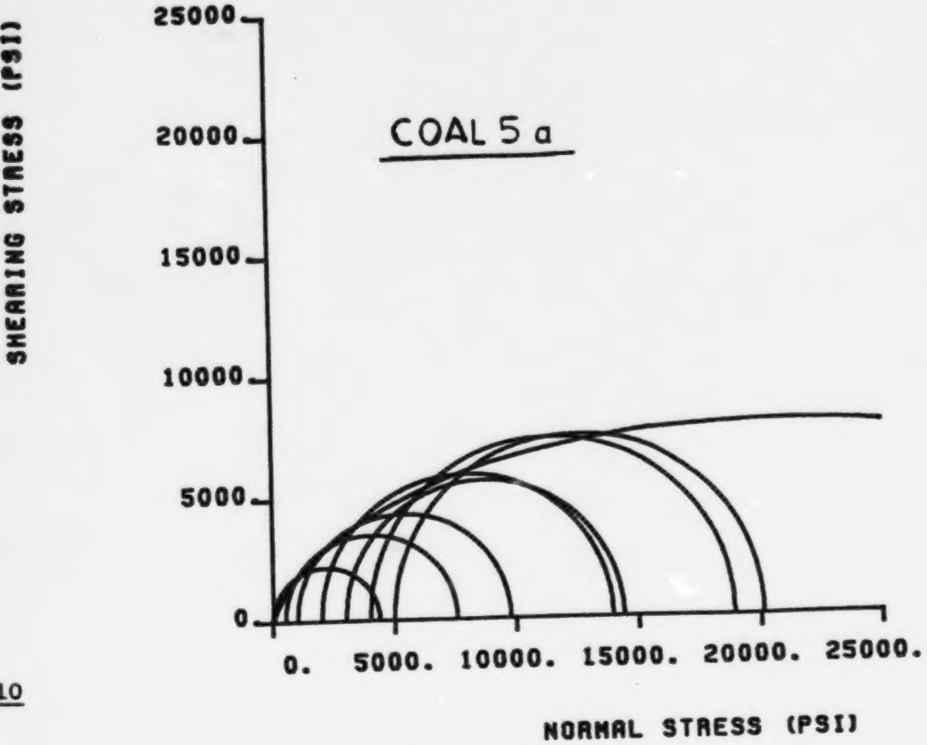

FIGURE D10

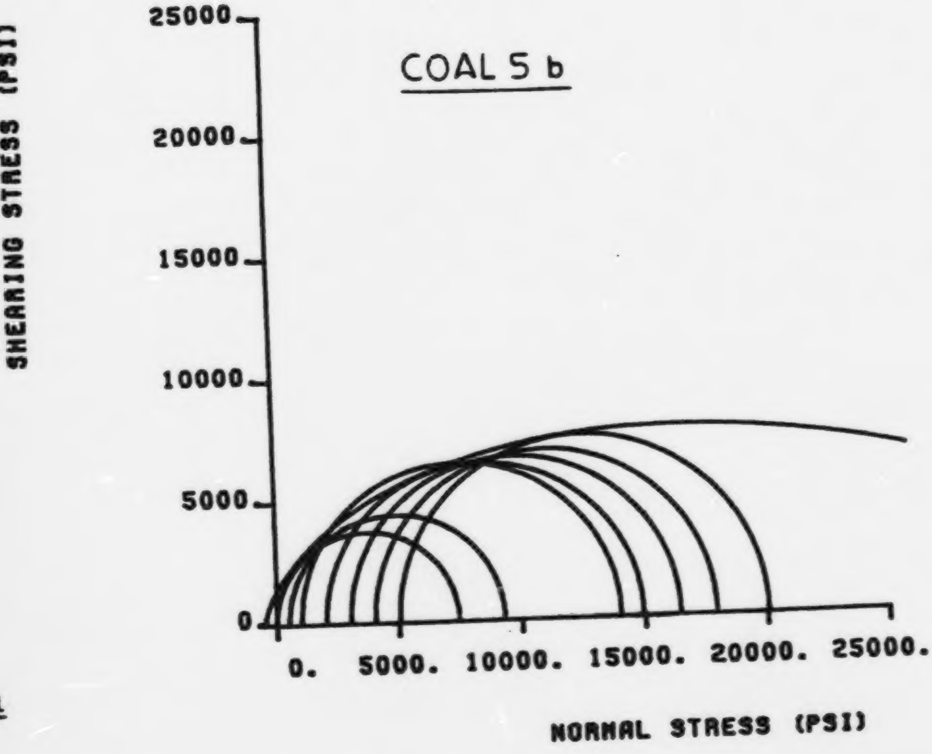

FIGURE D11

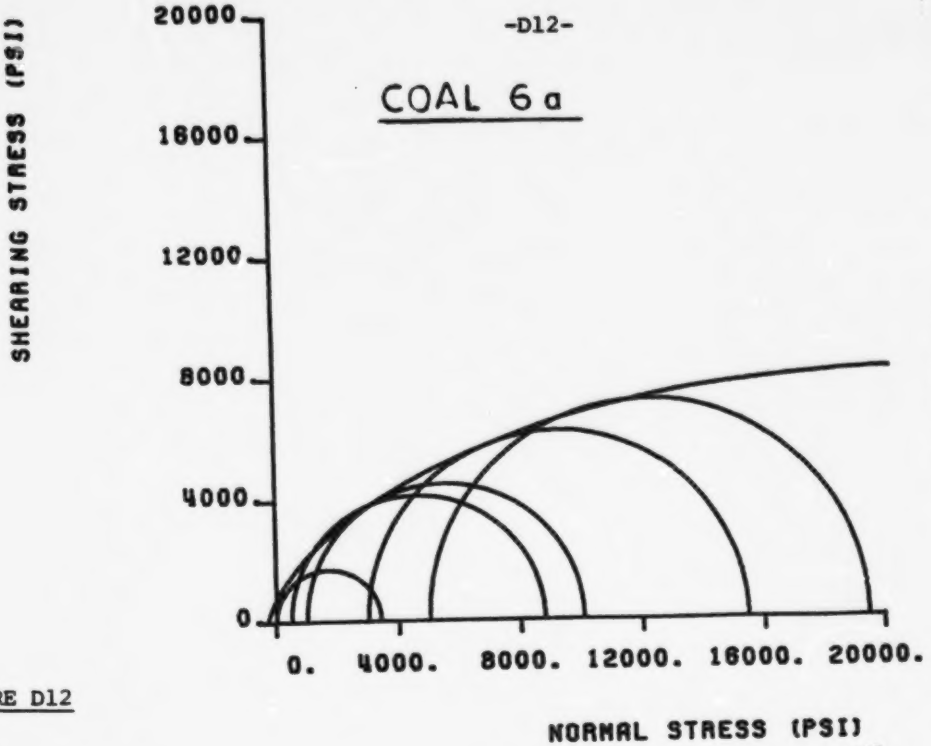

FIGURE D12

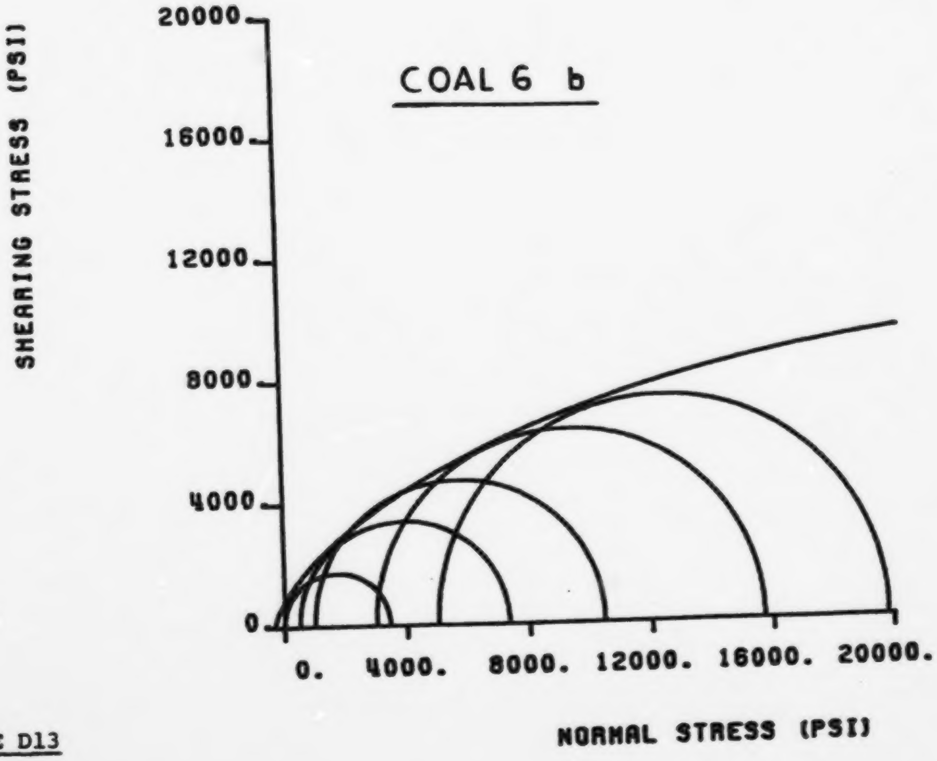

FIGURE D13

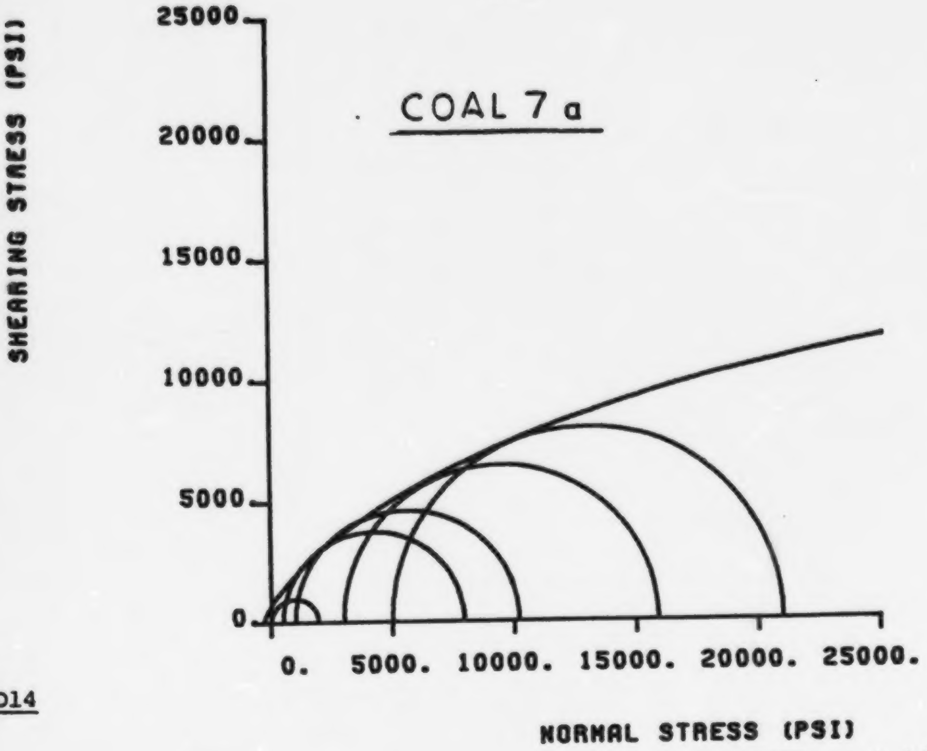

FIGURE D14

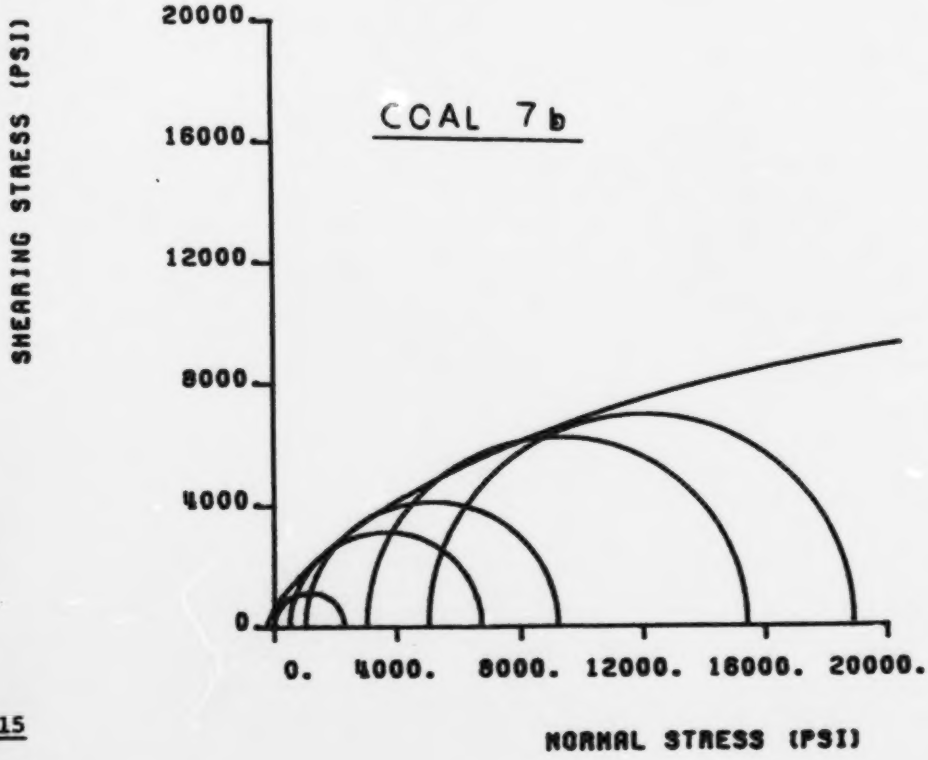

FIGURE D15

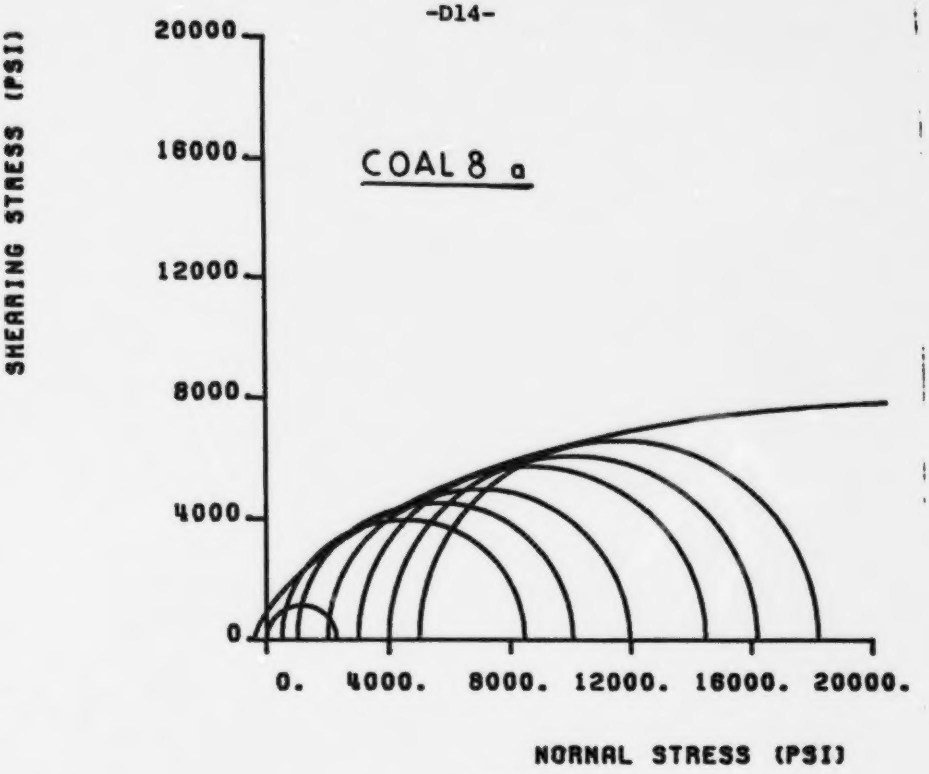

FIGURE D16

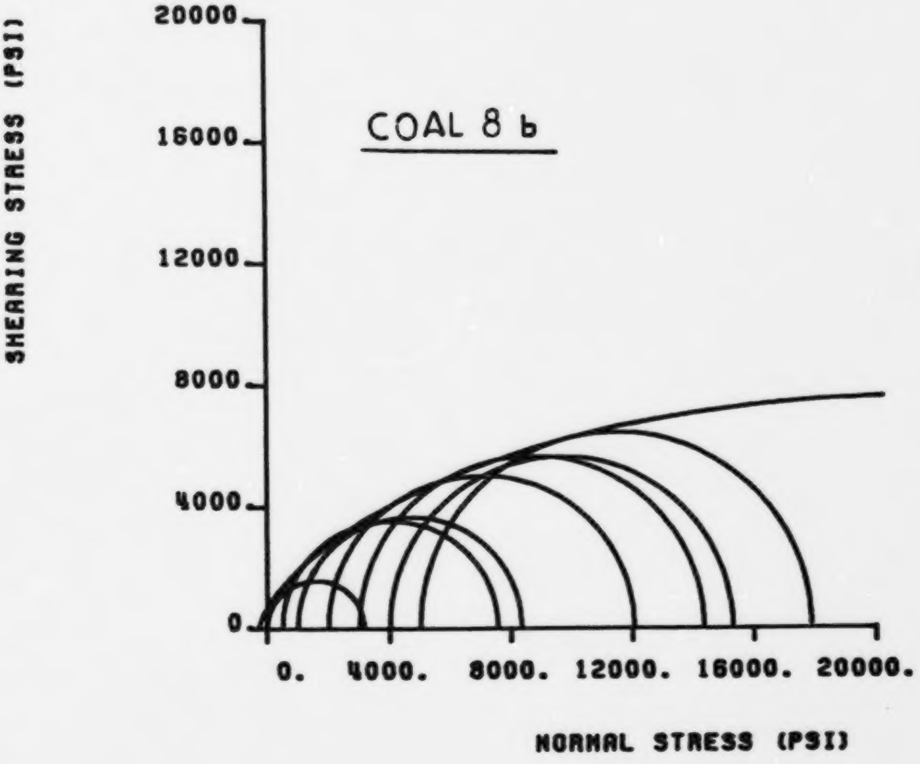

FIGURE D17

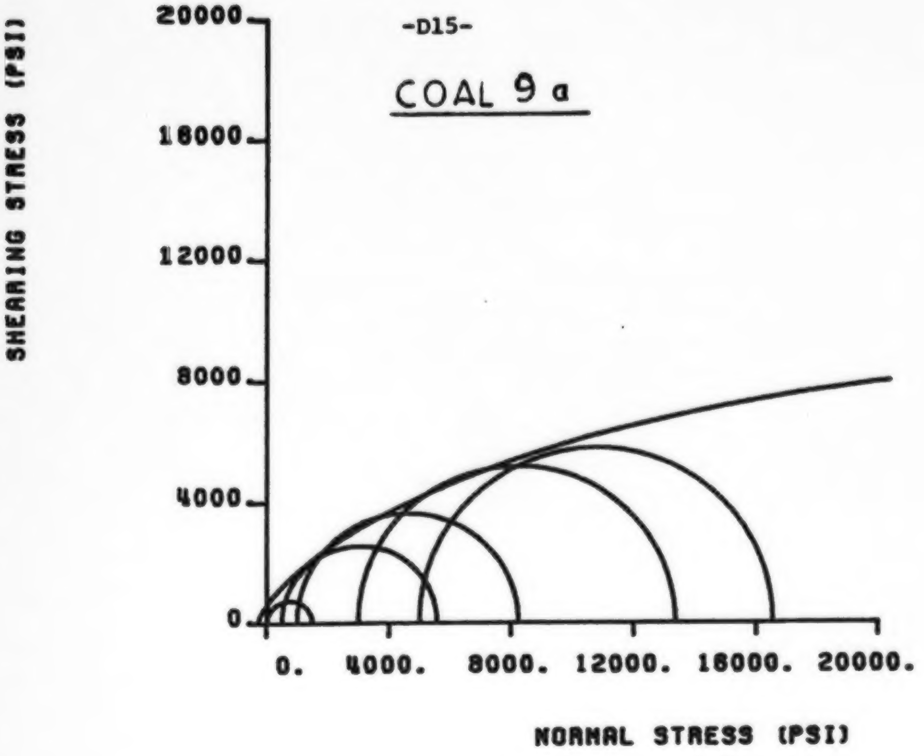

FIGURE D18

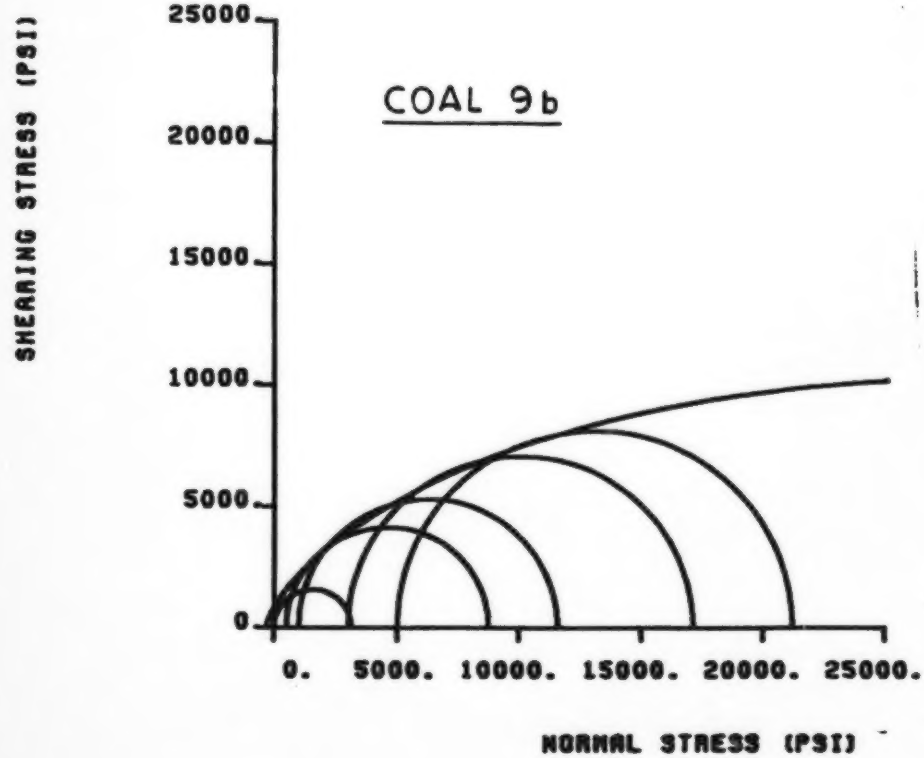

FIGURE D19

program automatically reverts to a c=1 solution as the "next best" fit.

D.4 Appendix D References

D.1 Balmer, G. "A General Analytic Solution of Mohr's Envelope", A.S.T.M., Proc 52, June 1952

D.2 Hobbs, D.W. "The Strength and Stress/Strain Characteristics of Coal in Triaxial Compression", J. Geol., Vol. 72, pp. 214-231, 1964

APPENDIX E: A PROPOSED COAL TESTING PROGRAM

E.1 Introduction

The case histories studied in this Phase 2 Report lead to, amongst others, the following conclusions:-

(i) Provided that the case history allows a good calculation to be made of the mean pillar stress (unfortunately not always possible) then a judicious choice of the input parameters for the coal properties enables the model results to be fitted closely to the field results.

(ii) The model results are very sensitive to the input values for the coal properties. Unfortunately, in most cases, the case histories from the literature being examined give insufficient data on the coal properties to adequately define the required input data. This has lead to intelligent estimates being made for some of these properties in order to complete a specific case history. In these circumstances, although the model may give a good "prediction" of the field data, some doubt must remain with respect to the model validity because of this use of "typical estimated" properties rather than actual values.

Hence the results of Phase 2 of this study are inconclusive; the model developed still appears to be qualitatively sound and will give a good quantitative prediction of field results if the input properties are judiciously chosen. Verification of these input parameters is however lacking and thus some doubt must remain with respect to the model applicability and validity. A number of questions still remain to be answered before this model may be accepted or rejected; these questions are discussed below.

E.2 UNANSWERED QUESTIONS

The main questions remaining to be answered all relate to the determination and use of the coal properties in the model:-

(i) Size/shape effects on coal strength; are they applicable to triaxial conditions? The basic coal strength parameter used by most workers is the uniaxial 1 inch cube strength. Coal strength is very dependent on the specimen size and shape and much work is reported in the literature establishing accepted coal strength/size/shape relationships for uniaxially loaded specimens. The value for the uniaxial strength used in the model is that given by these relationships for a cube of size equal to the pillar height.

However, the model takes into account the triaxial loading conditions generated in the pillar. The question therefore arises as to whether the size/shape effects established for uniaxial conditions can be assumed to apply under triaxial conditions? This is illustrated in Figure E.1 where the Mohr circles (1) and (2) are the uniaxial strength of a large and a small specimen respectively. If the uniaxial size effects apply to triaxial conditions without modification then this will result in parallel Mohr envelopes as illustrated in curves A and B of Figure E1A. However, a good case could be made to suggest that, once pseudo-ductile yielding commences then the strengths may be size independent. In such a case the Mohr envelopes would converge, as illustrated in Figure E1B. There are no previous studies that address this question, but it must be answered if full benefit is to be obtained from this model capability. It is essential to use the correct size adjusted Mohr envelope in inputting the coal parameters in the model.

(ii) Frictional properties of coal The model also requires the input of two other coal parameters namely μ_B the sliding coefficient of friction on a fractured coal surface and ϕ_B the angle of internal friction of broken coal. An argument could be made that $\mu_B = \tan \phi_B$ but there is insufficient evidence in the literature to confirm or deny this. An investigation should therefore be carried out to determine these two parameters and to determine whether or not μ_B is related in any way to ϕ_B.

In addition, it is assumed in the model that the coefficient of sliding friction, μ_B, is a constant independent of the applied normal stress. Whilst this is a reasonable first approximation there is evidence in the literature that μ_B varies with normal stress (see Phase 1 report, Page 68). This could easily be investigated during experiments aimed at determining μ_B and ϕ_B.

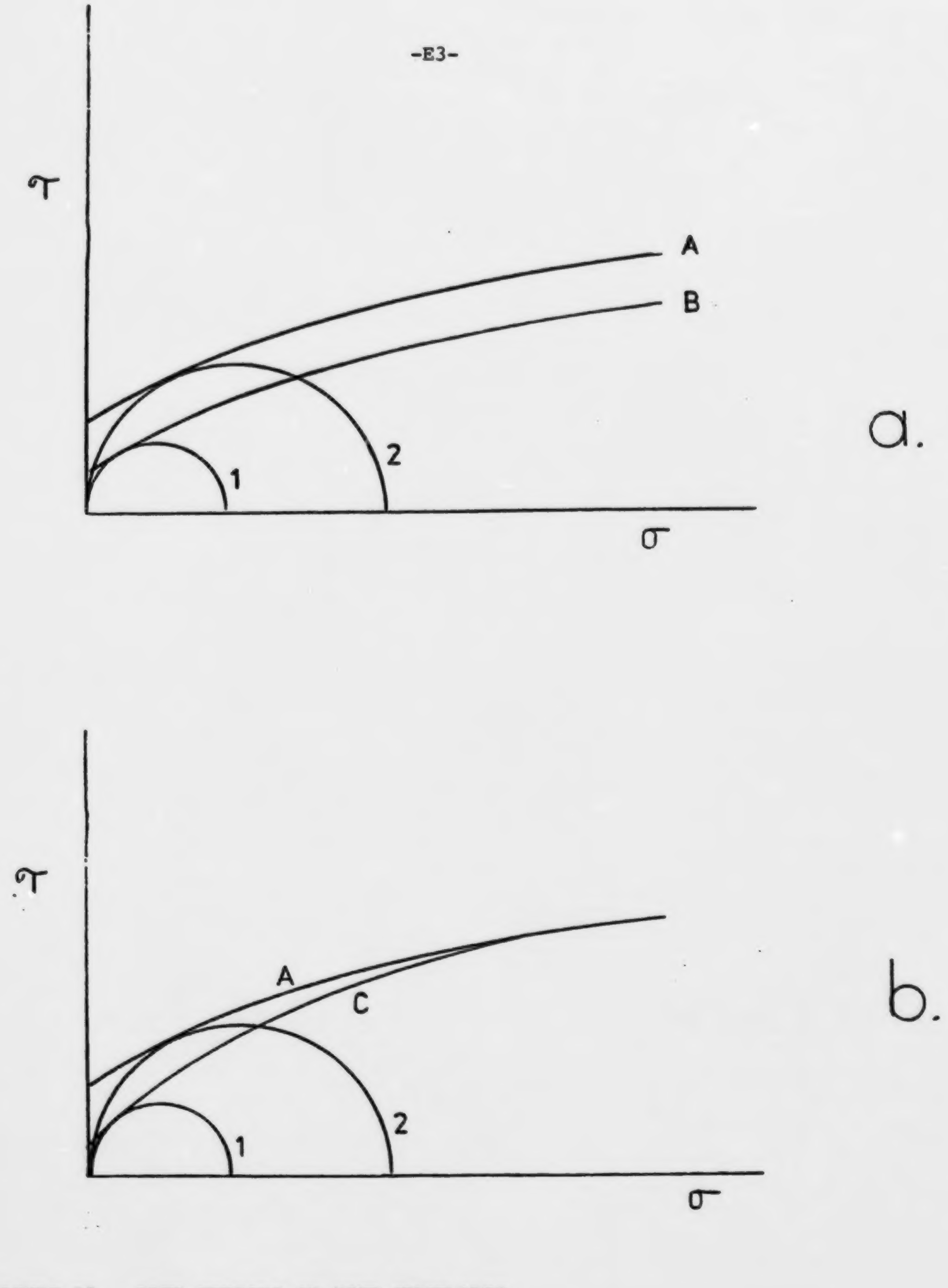
τ
A
B
a.
1
2
σ
τ
A
C
b.
1
2
σ

FIGURE E1: SIZE EFFECTS ON MOHR ENVELOPES

(iii) Brittle/pseudo-ductile transition point The failure criterion developed in Phase 1 of the study and used in the model defines a brittle/pseudo-ductile transition point on the Mohr envelope as being that point on the Mohr envelope where the shear resistance to sliding exceeds the shear resistance to fracture. This failure criterion has been used successfully to predict hard rock behaviour at exceptionally high confining pressures; it has not previously been applied to coal or at such relatively low confining pressures. At least one reputable reviewer has questioned the application of this failure criterion to coal at the relatively low stress levels experienced in coal pillars. Some significant evidence backing the use of this failure criterion has been obtained from the case histories; however this evidence is indirect and, in view of the fundamental nature of this query to the whole conceptional approach, it is believed that a test program should be specifically designed and carried out to prove or disprove the application of this failure criterion to coal.

(iv) Standard tests to determine the coal property parameters As seen above the model requires the input of coal property parameters that have not usually been measured in past studies. Hence there is a need to develop standardized test procedures to determine these parameters and, if possible, to develop a single simple laboratory test from which all these parameters might be obtained.

E.3 PHASE 3 - STUDY PROPOSAL

E3.1 Objectives

The objectives of Phase 3 of this pillar study are to carry out a laboratory testing program on one coal to obtain the following answers and information.

1. To determine if the coal strength/size/shape relationships established for uniaxially loaded specimens are applicable to triaxial conditions or if they require modification for triaxial conditions.

2. To measure the frictional properties of fractured surfaces and broken coal (μ_B and tan ϕ_B respectively) and to determine what, if any, relationship exists between these parameters.
3. To determine the solid coal Mohr envelope and the shear resistance to sliding on a fractured surface in order to prove or disprove the postulated existence of the brittle/pseudo-ductile transition point and thus validate or disprove the application of this failure criterion to coal.

4. To develop standardized tests to obtain the coal properties required by the model and to attempt to develop a single test from which all this data might be obtained.

E3.2 Proposal Approach

A detailed laboratory testing program is outlined in the next section which is aimed at achieving the objectives outlined above. All of these tests will be carried out on one coal with the axis of the major principal stress perpendicular to the bedding planes. The tests have been restricted to one coal only since it is believed that it is essential to verify these concepts by a meticulous and comprehensive program on a single coal; clearly if the concepts are verified for one coal then they are potentially applicable to other coals. The testing of specimens perpendicular to the bedding planes will eliminate complications that might arise by specimen anisotropy.

The planned tests have been grouped into 5 categories:-

Group A: These tests are aimed at establishing the uniaxial strength/size/shape relationships for this coal.

Group B: These tests are aimed at investigating the applicability of the uniaxial size/shape relationships to triaxial conditions, and at determining the frictional characteristics on fractured surfaces.

Group C: These tests on recompacted coal are aimed at investigating and determining the internal frictional angle and the cohesion of the broken coal.

Group D: These tests are aimed at verifying the frictional characteristics of fractured surfaces obtained from the triaxial tests by an alternative shear box test method.

Group E: The uniaxial tests on specimens with large width/height ratios are in fact "model pillar" tests. Hence using the results of the above tests together with the analytical model it should be possible to predict these test results and thereby confirm or deny the concepts developed. If successful, then clearly this test could be potentially used as a "single test" to determine all the parameters required by the model.

E.4 Detailed Coal Testing Program

E4.1 Group A - Uniaxial Tests on Solid Coal Specimens. (all tests carried out perpendicular to the bedding planes).

Objective: To define the effects of size and shape on the uniaxial strength of the test coal.

Group A.1: Cube Strength/Size Effect

1. Prepare 3 specimens each of cubes of edge dimensions 1", 2", 3", and 6" respectively ----- 12 specimens.
2. Measure and weigh specimens - determine coal density.
3. Load cubes to failure, measure applied load and deformation between plattens.

   Plot - Stress - Strain curves — determine modulus.
4. Correlate uniaxial crushing strength, σ_c with edge dimension D inches in form:-

$$\sigma_c = \frac{k}{D^{\alpha}} \text{ ; determine } k \text{ and } \alpha \text{ for this coal}$$

Group A.2: Rectangular prisms (square base), H/W $\geq$ 1. - shape effects

1. Range of H/W ratios to be considered --- (1, 1½, 2)
2. Range of W, 1", 2", and 3"
3. Prepare 3 specimens of each following sizes

   (1x1); (2x2); (3x3) - already done in Group A above

(1½x1); (3x2); (4½x3) 18 additional specimens
(2x1); (4x2); (6x3)

4. Measure and weigh all specimens - determine density.
5. Load prisms to failure, measure applied load and deformation between plattens

   Plot stress/Strain curves — determine modulus.
6. Correlate uniaxial prism crushing strength, σ_p, with height and width in form:

$$\text{(i)}\quad \sigma_p = \sigma_c\,(A + B\,(W/H)) \quad \text{where } \sigma_c = \text{cube strength}$$

$$\text{and/or}\quad \text{(ii)}\quad \sigma_p = \sigma_c \frac{W^{\beta}}{H^{\gamma}} \quad \text{determine } \beta \text{ and } \gamma$$

7. Derive general expression for rectangular specimen strengths relating all results to "k" for this coal.

Group A.3: Circular prisms (circular section), (H/W > 1)

1. Range of H/W ratios to be considered — (1, 1½, 2)
2. Range of W - 1", 2", and 3"
3. Prepare 3 specimens of each of the following sizes

   (1x1); (2x2); (3x3)
   (1½x1); (3x2); (4½x3)
   (2x1); (4x2); (6x3) 27 specimens
4. Measure and weigh all specimens - determine density.
5. Load prisms to failure, measure applied load and deformation between plattens.

   Plot stress/Strain curves — determine modulus.
6. Correlate uniaxial circular prism crushing strength, σ_{pc}, width/height and width in form

$$\text{(i)}\quad \sigma_{pc} = \sigma_{cc}\,(A_1 + B_1\,(W/H)) \quad \text{where } \sigma_{cc} \text{ is strength of circular prism } H/W = 1$$

$$\text{and/or}\quad \text{(ii)}\quad \sigma_{pc} = \sigma_{cc} \frac{W^{\beta_1}}{H^{\gamma_1}} \quad \text{determine } \beta_1 \text{ and } \gamma_1$$

7. Compare β_1 and γ_1, with β and γ from Group A.2. Compare A_1, and B_1 with A & B from Group A.2.
8. Derive correction factors, if any, for translating circular section results to be equivalent to rectangular section results.
9. Derive general expression for circular and rectangular strengths in terms of k for coal. Plot all results from groups A1, A2, and A3 in this form to demonstrate applicability of general expression.

E4.2 Group B - Triaxial Tests on Solid Coal Specimens. (all tests carried out perpendicular to the bedding planes)

Objectives:

(i) To evaluate the applicability of uniaxial size/shape effects to triaxial conditions.

(ii) To determine Mohr envelope for peak stress for solid coal.

(iii) To determine Mohr envelope for residual stress for solid coal.

(iv) To determine Mohr envelope for sliding on fractured coal specimens.

Group B.1: Triaxial tests on circular prisms, H/W = 2, W = 1"

1. Prepare 3 specimens for testing at each of 6 confining pressures.
2. Use 6 confining pressures ranging from 0 psi to maximum of apparatus capacity. Note: uniaxial (0 psi) tests already completed with Group A3. Hence require 15 specimens.
3. Measure and weigh all specimens — determine density.
4. Test procedure - for each specimen.
   (i) Apply confining pressure - load to failure at constant confining pressure measuring the load and specimen deformation. Continue load after peak stress at failure until arrive at "residual stress" for specimen. - Plot stress/Strain curve as as illustrated in Figure E2. Determine modulus.
   (ii) If possible, after residual stress established, unload specimen and conduct "slip tests" at incremental confining pressure steps - as illustrated in Figure E3.

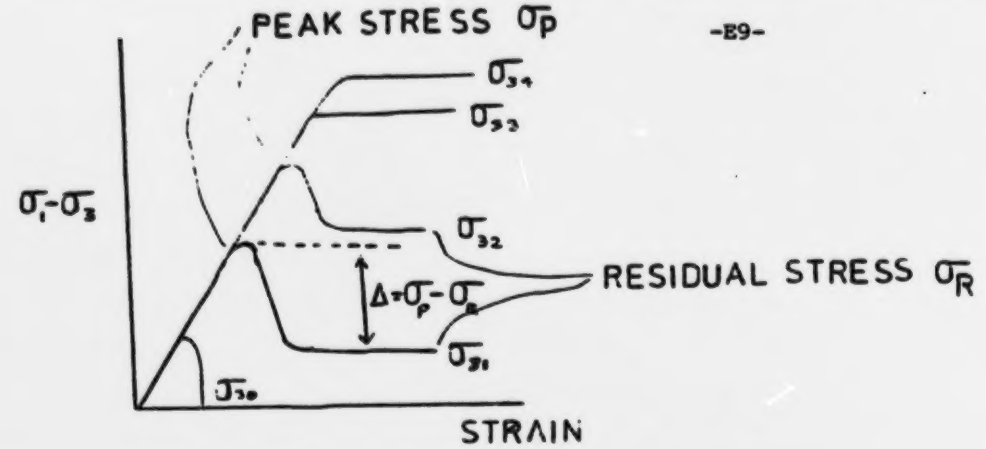

FIGURE E2: STRESS/STRAIN CURVES FOR TRIAXIAL TESTS - VARYING CONFINING PRESSURE

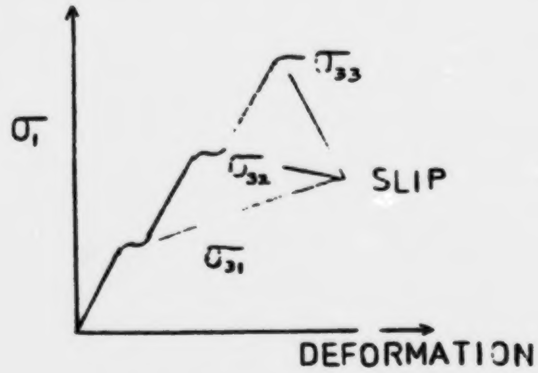

FIGURE E3: STRESS/DEFORMATION CURVES FOR SLIP TESTS ON BROKEN SPECIMENS

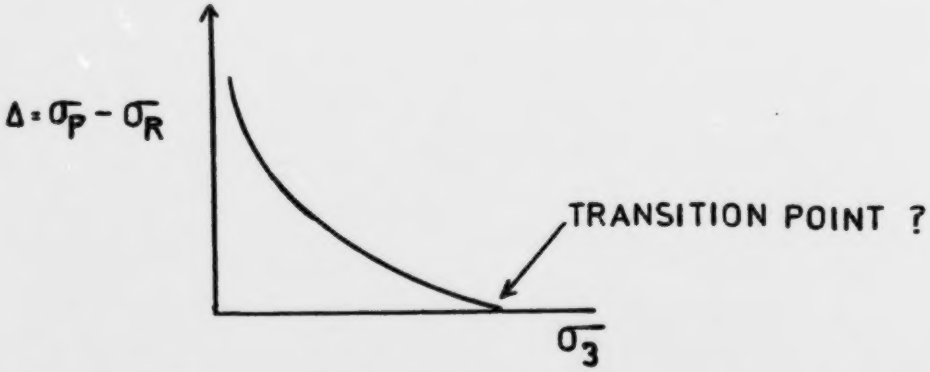

FIGURE E4: POSSIBLE ESTIMATE OF TRANSITION POINT BY DIFFERENCES BETWEN PEAK AND RESIDUAL STRESSES

(iii) On completion of test, examine specimen
  - has specimen failed on shear plane? -if so measure angle of failure
  - has specimen "bulged" during failure?
  - make notes on failure mode for each specimen

5. Analysis
   (i) Plot Mohr envelope of peak stresses - derive equation of Mohr envelope in Balmers form. Is this envelope curvilinear?
   (ii) Plot Mohr envelope of residual stress - derive equation of Mohr envelope in Balmers form. Is this envelope curvilinear?
   (iii) Do the two envelopes intersect at some point. Determine the stresses at the point of intersection.
   (iv) Plot the difference between the peak and residual stresses for each specimen against confining pressure, as shown in Figure E4. At what stress does this differential reach zero? Do these stresses coincide with the point of intersection of the Mohr envelopes?
   (v) Plot Mohr envelope for the "slip test" results; derive equation of Mohr envelope in Balmers form. Does this envelope coincide with that for the residual stress envelope?
   (vi) What is the "cohesion" given by the residual stress envelope and by the slip test envelope? Are they the same?

Group B2: Triaxial Tests on Circular Prisms, H/W = 2, W = 2"

Prepare specimens and repeat tests as in Group B1 for these 2" diameter specimens. — 15 specimens
Repeat analysis given in Group B1

Additional analysis required:

(i) Do size effects determined from uniaxial tests apply to the triaxial tests?
(ii) Is the intersection point of Mohr envelope for peak & residual stress affected by size?
(iii) Are the residual envelope and the "slip test envelope" affected by size?
(iv) Is the cohesion given by the residual and slip test envelopes affected by size?

E4.3 Group C: Triaxial Tests on Recompacted Broken Coal

Objectives

(i) To determine Mohr envelope for broken coal; does this change with degree of re-compaction (density)

(ii) To determine if there is a "residual" stress for recompacted broken coal

(iii) To determine variation of cohesion of broken coal with degree of compaction

(iv) Is the cohesion given by the residual and slip test envelopes affected by size?

Group C1: Triaxial tests on recompacted broken coal (H/W = 2, W = 1")

(i) Crush and sieve coal to a particle size < 0.1".

(ii) Prepare 2" high by 1" diameter specimens by recompacting the coal by loading in steel cylinders. Prepare 18 specimens at each of 3 different re-compaction loads. - groups C1.1; C1.2; and C1.3; —— 54 specimens

(iii) Measure and weigh all specimens - determine density

For each sub-group, C1.1, C1.2, C1.3 carry out following tests

(i) Triaxial tests at 6 different confining pressures from 0 psi to maximum capacity of apparatus.

(ii) Apply confining pressure - load to failure at constant confining pressures measuring the load and specimen deformation. Continue to load after peak stress has been reached and determine whether there is a "residual stress" for the specimen. Plot stress/ strain curves and determine modulus.

(iii) If possible, after "residual stress" established, unload specimen and conduct "slip tests" at incremental confining pressure steps.

(iv) On completion of test, examine specimen - note mode of failure, angle of shear, bulging, etc.

Analysis

(i) Determine Mohr envelope for each of re-compacted broken coal groups, deriving equation in Balmers form. Is Mohr envelope curvilinear?

(ii) Determine Mohr envelopes for residual stresses and slip tests and compare with envelope above, at the three re-compaction densities.

(iii) Attempt to correlate Mohr envelope constants for broken coal results and solid coal results by relating to density variation.

(iv) Examine variation in "cohesion" with density.

(v) Examine variation of modulus with density.

Group C2: Triaxial tests on re-compacted broken coal (H/W = 2, W = 2")

(i) Prepare specimens as with group C1 but this time prepare 2" diameter specimens. - 54 specimens

(ii) Repeat Group C1 tests for sub groups, C2.1; C2.2; C2.3

(iii) Examine results to see if there is a size effect for recompacted broken coal.

E4.4 Group D: Shear Box Tests - Cut Coal Specimens

Objective:

(i) To determine envelope for slip on cut surfaces by shear box tests.

(ii) To compare this envelope with Mohr envelope for "residual stress" and "slip tests" for solid and recompacted broken coal.

Test Procedure

(i) Prepare test specimens of size to fit shear box.

(ii) Run each specimen at 6 normal stresses from 0.1 x maximum normal stress capacity to 1 x maximum stress capacity of shear box. Repeat for 6 specimens.

(iii) Apply first normal load, increase shear load until slip occurs, apply second normal load, etc.

Analysis

Plot τ, σ, envelope and compare to residual stress and slip test envelope from solid and re-compacted broken coal.

E4.5 Group E: Uniaxial Model Pillars (H/W < 1)

Objectives:

(i) To test specimen with low H/W ratios and compare with analytical model predictions.

(ii) To determine, if possible, stresses at brittle/pseudo ductile transition point.

(iii) To determine if maximum brittle fracture zone depth remains constant with varying width for constant height.

(iv) To determine if maximum brittle fracture zone depth varies with height for constant width, in accordance with analytical model.

Specimens Use, if possible 3 H/W ratios of 1/3, 1/6, 1/10

(i) Prepare following specimens (a) 1" high W = 3", 6", and 10"
(b) 1½" high W = 4½, 9", and 15"
(c) 2" high W = 4, 12, and 20"

3 specimens of each —— 27 specimens

(ii) **Test procedures**

1. Load specimen uniaxially and measure specimen deformation between plattens.
2. Each specimen loaded until failure occurs, either by sudden failure or by "yield" as indicated by the stress - strain curve. Attempt to distinguish between catastrophic and non catastrophic failure.
3. After failure, examine specimen. If possible, measure depth of brittle fracture zone.

(iii) Analysis

1. For each set of same height. Determine depth of fracture zone -is this constant?
2. For each set at same height, by difference between the yield loads, determine the vertical stress at yield.
3. Examine vertical stress at yield for the 3 sets and determine the size effect relationship.
4. Use results from previous groups to predict stress distribution, fracture zone and strength of specimen, using analytical model.

POOR

QUALITY

ORIGINAL